The University Of Sheffield.

Identifying novel immune modulating factors in a genome-wide *Staphylococcus aureus* screen in human neutrophils

Dingyi Yang

The University of Sheffield

Department of Infection, Immunity, and Cardiovascular Diseases

Thesis submitted for the degree of Doctor of Philosophy

Sept 2017

Abstract

The multi-antibiotic resistant *Staphylococcus aureus* continues to be a worldwide clinical burden and there is an urgent need for novel therapeutic strategies. Neutrophils are essential during the innate immune response to *S. aureus*, yet this pathogen uses multiple evasion mechanisms to survive or even replicate within neutrophils. In addition, *S. aureus* induces rapid and profound neutrophil cell death, which further subverts the immune response.

The aim of this project was to identify novel immune modulating genes of *S. aureus* through the screening of a genome-wide *S. aureus* mutant library of 1,920 strains in a neutrophil cell death assay. The mutant library was constructed by transposon insertion in the clinically relevant community acquired methicillin-resistant *S. aureus* (USA300) background. Individual *S. aureus* strains were co-incubated with primary human neutrophils isolated from healthy subjects, at an MOI of 10 for 3 hours before ToPro-3 staining and assessment of cell loss via flow cytometry.

A number of internal controls with known pro-death functions including *lukGH, agrA* and *saeS* were among the 34 strains that resulted in attenuated cell death. Four gene mutations not previously associated with cell death*: purB, lspA, clpP* and *pfo* were also identified and subsequently verified by genetic transduction. The *clpP* and *lspA* were further validated by gene complementation. The purine synthesis pathway (*purB*) was found to be important for bacterial replication and pathogenesis in a zebrafish embryo model, yet this *in vivo* phenotype was proved to be neutrophil-independent. Lack of *lspA* led to significantly reduced phagocytosis, indicating the necessity of lipoproteins in bacterial recognition and regulation of neutrophil lysis. Pyruvate metabolism (*pfo*) was required for neutrophil cell lysis *in vitro*. Yet no attenuated phenotype of *pfo* or *lspA* was found *in vivo,* possibly due to host-dependent effects. The *clpP* mutant failed to grow or induce host mortality in wild type

zebrafish embryos, but virulence was restored in a phagocyte-depleted model, suggesting the importance of *clpP* in bacterial survival and pathogenesis, possibly via Clp ATPase regulated post-phagocytosis stress tolerance and *clpP* modulated expression of secreted toxins. This thesis identified novel gene functions and suggests possible mechanisms of *S. aureus* induced neutrophil cell lysis, which may aid the design of future antibiotic-independent therapeutic strategies to restore failures of innate immunity.

Acknowledgement

I would like to thank Dr. Lynne Prince and Professor Simon Foster for their guidance, encouragement, and support throughout my PhD. It has been a privilege to work in their groups and continue my passion in learning more about the host pathogen interaction study. I would also like to thank all members, past and present, from the Prince Group and the department of IICD who have aided me in accomplishing this work. I would like to express my gratitude to the blood donors for their generous contribution that makes this work possible. I would like to show my thanks to Ms. Susan Clark and Ms. Kay Hopkinson for their patient assistance with all things flow cytometer related. It also has been a pleasure working with so many fantastic people in Foster laboratory. Many thanks to John, Rebecca, Bartek, Kasia for technical advice and assistance in fish and genetic works. Also Mark, much appreciated.

My special thanks go to my parents and sister for their support, encouragement, and love throughout my PhD. This work would not have been possible without our WeChat chats. I am also grateful for their understanding that my home visits were so rare.

Finally, I would like to thank all my friends outside of the laboratory, both in Sheffield and worldwide. I would like to express my profound gratitude for them supporting my study, listening to my difficulties, offering great helps when needed, reminding me to focus my mind, and sharing my pain and joy. Separate thanks go to Libby and Louise for supporting me in bad and in very bad times.

This project was funded by the University of Sheffield. I would also like to thank the Florey Institute Scholarship for financing my tuition fees and living costs.

Table of contents

Abbreviations

AI	Adenine and inosine
AICAR	5-amino-1-(5-phospho-D-ribosyl) imidazole-4-carboxamide
Amp	Ampicillin
AMP	Adenosine-monophosphate
AMPs	Antimicrobial peptides
ARG	Antibiotic resistance genes
Aur	Aureolysin
BAX	Bcl-2-associated X protein
BIP	Bactericidal-increasing protein
CA-MRSA	Community-associated MRSA
CFU	Colony forming unit
CGD	Chronic granulomatous disease
CHIPS	Chemotaxis inhibitory protein of staphylococcus
Clf	Clumping factors
Cm	Chloramphenicol
COPD	Chronic obstructive pulmonary disease
Dpf	Day post fertilisation
EAP	Extraceullular adherence protein
ECB	Extracellular complement-binding protein
EFB	Extracellular fibrinogen-binding protein
Ery	Erythromycin
FBS	Fetal bovine serum

FPR	Flormyl peptide receptor
FSC	Forward scatter
F/T	Freeze-thawed
GMP	Guanosine monophosphate
GPCR	G protein couple receptor
HA-MRSA	Hospital-associated MRSA
HBSS	Hank's Balanced Salt Solution
HIE	Hyperimmunoglobulin E-recurrent infections
Hpf	Hour post ferterlisation
ICAM-1	Intercellular adhesion molecule 1
Ig	Immunoglobulins
IMP	Inosine monophosphate, Adenylo-succ, N6-(1,2-dicarboxyethyl)-AMP
Kan	Kanamycin
LAD	Leukocyte adhesion deficiencies
Lin	Lincomycin
LWT	London wild type
MLKL	Mixed lineage kinase domain-like
MOI	Multiplicity of infection
MPO	Myeloperoxidase
MprF	Multiple peptide resistance factor
MRSA	Methicillin resistant *S. aureus*
MSCRAMMs	Microbial surface components recognising adhesive matrix molecules

NE	Neutrophil elastase
NETs	Neutrophil extracellular traps
NK	Natural-killer
NLRP3	A pyrin domain containing protein
NTML	Nebraska transposon mutant library
PBS	Phosphate buffered saline
PFOR	Pyruvate ferredoxin oxidoreductase
PICD	Phagocytosis-induced cell death
PMA	Phorbol myristaste acetate
PPP	Platelet-poor plasma
PRP	Platelet-rich plasma
PSGL-1	P-selectin glycoprotein ligand-1
PSMs	Phenol-soluble modulins
PVL	Panton-valentine leukocidin
RIPK3	Receptor interacting protein kinase-3
ROS	Reactive oxygen species
RT	Room temperature
SAICAR	5'-phosphoribosyl-4-(N-succinocarboxamide)-5-aminoimidazole
Sak	Staphylokinase
SBI	Staphylococcal binder of immunoglobulin
SCIN	Staphylococcal complement inhibitor
ScpA	Staphopain A
SD	Standard deviation
SERAMs	Secretable expanded repertoire adhesive molecules

SpA	Staphylococcal protein A
SPIN	Staphylococcal peroxidase inhibitor
SSC	Side scatter
SSL	Staphylococcal superantigen-like protein
SSTI	Skin and soft tissue infections
TCA	Tricarboxylic acid
Tet	Tetracycline
TIR	Terminal inverted repeats
TLR	Toll-like receptor
vWbp	Von Willebrand factor-binding protein
WT	Wild type

CHAPTER 1

Introduction

1.1 Staphylococcus aureus

S. aureus is a Gram-positive human pathogenic bacterium. This highly adaptive microorganism is capable of generating uncomplicated skin and soft tissue infections as well as a number of life-threatening and often fatal diseases through two main mechanisms: the production of toxins or direct infection of tissues (Lowy, 1998, Tenover and Gaynes, 2000).

1.1.1 Epidemiology of *S. aureus*

Staphylococci include more than 40 ubiquitous species which infect humans, mammals and birds through skin, glands or mucous membranes. Compared with other major pathogenic staphylococci such as *S. hemolyticus, S. saprophyticus, and S. lugdunensis*, *S. aureus* plays the most predominant role in causing human infection and diseases (Kloos and Bannerman, 1999).

Approximately 30% to 50% of healthy adults are colonised with *S. aureus* in their anterior nares, which is mainly transmitted through hand contact (Lowy, 1998, Casewell and Hill, 1986). The reason why anterior nares are frequently colonised is because *S. aureus* is capable of adhering to nasal epithelial cells (Aly *et al*., 1980). Nasal carriage of *S. aureus* depends on both host genetics and microbial factors, although their relative roles remain unclear (Johannessen *et al*., 2012). Patients with intravenous drug addiction, type 1 diabetes, haemodialysis therapy, recent surgical procedures, and impaired leukocytes are at higher risk of colonisation with *S. aureus* (Tuazon *et al*., 1975, Tuazon and Sheagren, 1974).

Furthermore, the risk of infection increases along with colonisation of *S. aureus* (Tuazon and Sheagren, 1974, Tuazon *et al*., 1975, Wenzel and Perl, 1995, Yu *et al*., 1986).

As the leading threat of a range of infections including upper and lower respiratory tracts, bloodstream, skin and soft tissues, bone and joints, the spreading of *S. aureus* has been reported throughout the world, primarily in China, United States (US), Europe, Canada, and parts of the Western Pacific (Chuang and Huang, 2013, Diekema *et al*., 2001). Although the initial outbreak of CA-MRSA in the US was attributed to USA400, it was soon replaced by PVL positive USA300 which was reported from each continent except for Antarctica (Liu *et al*., 2008, David and Daum, 2010). Unlike the predominance in North America, Europe has comparatively lower prevalence but higher genetic diversity of CA-MRSA (Mediavilla *et al*., 2012). A range of MRSA clones including ST1, ST8, ST30, ST59, ST80, and ST152 were identified on the Europe continent, as well as ST93 from UK (Sowash and Uhlemann, 2014). The *S. aureus* epidemiology study reveals generally lower burden of CA-MRSA in Europe comparing to the US (Otter and French, 2010). The rate of MRSA in invasive isolates in Europe differs from <1% in Norway and Denmark, <5% in Netherlands, to >40% in UK and Greece (Otter and French, 2010). More than 12,000 cases of *S. aureus* were reported in England during the financial year of 2016/2017, which represents a 24.5% and 7.7% increase from 2011/2012 and 2015/2016 respectively (PHE, 2017).

1.1.2 Clinical significance of *S. aureus*

1.1.2.1 Infections of skin and soft tissue

Cutaneous invasion of *S. aureus* mostly occurs at open wounds, follicles or skin glands, which further causes skin and soft tissue infections (SSTI) including abscesses and cellulitis (Seeleang *et al*., 2013). Atopic dermatitis is an inflammatory skin condition closely related with *S. aureus* infection since 90% of atopic dermatitis patients were found to be colonized with *S. aureus* (Abeck and Mempel, 1998). *S. aureus* enterotoxin B, hemolysin invasion of

T cells and monocytes, together with family history of atopy were revealed as the pathogenic factors involved in *S. aureus*-triggered atopic dermatitis (Abeck and Mempel, 1998, Manders, 1998, Prince *et al*., 2012). *S. aureus* colonisation of wound infections was widely found among patients after surgery where elongated surgical time, extended surgical procedures, and presence of foreign material could all increase the risk of *S. aureus* infection (Nichols and Raad, 1999). In addition, nasal carriage of *S. aureus* increases the possibility of infection in wound patients (Kluytmans *et al*., 1997).

1.1.2.2 Bone and joint infections

S. aureus bone infections can arise as a complication of septicaemia in a haematogenous manner, or as a result of wound infection or surgery. Haematogenous spread of *S. aureus* is usually derived from skin infections to long bones, particularly at the metaphyseal area where a highly vascularized environment provides ideal spreading channels for *S. aureus* (Cunningham *et al*., 1996, Dhanoa *et al*., 2012, Lipsky, 1997).

Septic arthritis refers to infection of joints by pathogenic bacteria which degrade cartilage via production of pro-inflammatory cytokines and proteolytic enzymes. *S. aureus* is the most prevalent aetiological agent in this context, leading to notable morbidity and mortality (Carreno Perez, 1999, Sharff *et al*., 2013). This joint infection can also arise as a result of both surgical infection and haematogenous spread of *S. aureus* (Goldenberg, 1998). Subsequently *S. aureus*-induced inflammation causes chronic damage to the cartilage, which leads to joint destruction (Goldenberg, 1998). The panton-valentine leukocidin (PVL) is a major *S. aureus* pathogenic factor in this context, which can make the infection fatal with complications of multiorgan failure (Rafai *et al*., 2013).

1.1.2.3 Respiratory Diseases

Pneumonia is a lung disease primarily caused by viruses, fungi and bacteria. Infection of alveoli in pneumonia prevents efficient gaseous exchange and leads to increased respiratory

burden and often death (McLuckie A, 2009). *S. aureus* infection counts for 500,000 hospitalisations and 20,000 deaths among pneumonia patients in the US during 2005 (Klein *et al*., 2007). The morbidity of *S. aureus*-induced pneumonia has increased along with various risk factors, such as surgery, old age, and immunosuppressive treatment. *S. aureus* associated pneumonia is also highly life threatening in patients with lung diseases like chronic obstructive pulmonary disease (COPD), where lung capacity is already impaired (Lowy, 1998). Post-influenza necrotizing pneumonia caused by *S. aureus* superinfection leads to 50% mortality among infections in Europe (Kumar *et al*., 2009), identifying *S. aureus* as a major risk factor in this disease. The secreted cytotoxins such as PVL enhance bacterial virulence and are closely associated with staphylococcal pneumonia. Bacterial multiplication following colonisation induces expression of PVL and newly synthesized toxins contribute to neutrophil cell death, particularly in a pneumonia model (Yoong and Pier, 2012, Loffler *et al*., 2010).

1.1.3 Treatment and antibiotic resistance of *S. aureus*

Antibiotics have been widely applied for clinical use since the discovery of penicillin in the 1940's. This important therapeutic breakthrough was short lived for *S. aureus*, when a penicillin resistant strain emerged in the presence of selective pressure (Lambert, 2005). A number of *S. aureus* antibiotic resistance genes (ARG) such as *mecA, femA, erm, msrA,* and *blaZ* have since been identified (Duran *et al*., 2012). Spreading of ARG through horizontal gene transfer mechanisms gives rise to rapidly increasing numbers of *S. aureus* with multiple ARG (Lambert, 2005, Chambers and Deleo, 2009). The emergence of *S. aureus* ARG kept in step with the development of novel antibiotics including penicillin, flucloxacillin, gentamicin, and vancomycin (Brumfitt and Hamilton-Miller, 1989, Charles *et al*., 2004), significantly disabling anti-*S. aureus* therapeutic strategies. The methicillin resistant *S. aureus* strain, also known as MRSA, emerged in 1959 and was first seen in

hospitals, and given the name of hospital-associated MRSA (HA-MRSA) (Jevons, 1961). Worryingly, community-associated MRSA (CA-MRSA) strains emerged in the early 1980's, illustrating the rapid dissemination of ARG and significantly increasing the chance of contracting MRSA infection (Estivariz *et al*., 2007, Hill *et al*., 2001, Baggett *et al*., 2003). By 2012, MRSA was widespread throughout the world. The rates of HA-MRSA strains among total HA-*S. aureus* strains were found to be higher than 50% in US and South Korea (Stefani *et al*., 2012). Meanwhile a dramatic increase of CA-MRSA infections in US was reported from 50/year in 1996 to 1100/year in 2004 (King *et al*., 2006), indicating a new infective environment at risk of MRSA.

With the existence of prevalent multiple ARG, treatments of MRSA infections have become limited. Even though some prescribed novel anti-MRSA agents such as glycopeptides, linezolid, quinuristin-dalfopristin and ceftobiprole were developed, many shortcomings of these approaches have been reported including insufficient MRSA killing, relatively high incidence of severe or even fatal side effects, and antibiotic resistance (Charles *et al*., 2004, Longworth, 2001, Lentino *et al*., 2008, Tsiodras *et al*., 2001).

1.1.4 Community-acquired *S. aureus*

Unlike HA-MRSA which more commonly invades individuals at risk of infections such as immune-defective patients or individuals with preconditions, CA-MRSA is capable of causing infections in healthy people (Seeleang *et al*., 2013). CA-MRSA accounts for 26% of pneumonia cases and data indicate that CA-MRSA leads to a higher pneumonia mortality than HA-MRSA (Valour *et al*., 2013, Wunderink, 2013), although it is not clear why this is so. A study of 139 *S. aureus* isolates revealed that PVL was detected in approximately 94% of CA-MRSA strains, while only 7% of HA-MRSA are PVL positive (Bhatta *et al*., 2016). A possible explanation therefore of enhanced virulence of CA-MRSA is PVL gene

expression, which is also associated with 62% of pneumonia cases (Morgan, 2007, Tsuji *et al*., 2007).

PVL production enables CA-MRSA attachment onto exposed collagen which is more commonly found on injured bronchial mucosa (Vaitkus *et al*., 2013). As a consequence of this, PVL makes chronic lung disease patients more vulnerable to CA-MRSA. Furthermore, PVL causes haemorrhage, infarction and necrotising vasculitis, which can result in fatal consequences (Morgan, 2007). To achieve this, PVL modifies immune cell function in ways such as neutrophil priming and cytokine release, as well as inducing neutrophil lysis (Naimi *et al*., 2003). It seems that PVL is very likely to be the reason why CA-MRSA has higher host cell killing efficiency than HA-MRSA.

USA300, the most abundant CA-MRSA strain in Europe and US (97% of total CA-MRSA), has developed resistance against gentamincin, clindamycin, doxycycline and trimoxazole; and can lead to SSTI, necrotizing pneumonia and septic arthritis (Vardakas *et al*., 2013, Francis *et al*., 2005, McDougal *et al*., 2010, Tietz *et al*., 2005). USA300 expresses multiple virulence factors to enhance bacterial pathogenesis. For example the lytic toxin, leukocidin (Luk) GH, which synergizes with PVL to enhance bacterial pathogenesis (Ventura *et al*., 2010). In Detroit, MI, 20% of nosocomial bloodstream infections were caused by the USA300 strain during 2005 to 2007 (Chua *et al*., 2008). More severe SSTIs and necrotizing pneumonia were found with PVL-expressing USA300 strain compared to non-PVL strains in rabbit models (Diep *et al*., 2010, Lipinska *et al*., 2011). Another pore-forming toxin, α-toxin, is known to be produced significantly by USA300 strain, with regulation by accessory gene regulator (*agr*) system (Kobayashi and DeLeo, 2009). In a murine model, reduced production of α-toxin led to fewer skin lesions (Weiss *et al*., 2009). The *agr* quorum sensing system mediates gene expression via the *agrBDCA* operon and plays an essential role in staphylococcal production of other neutrophil-lytic toxins in USA300 clones such as α-

hemolysin (Thurlow *et al*., 2012). Consistently, the *Δagr* USA300 mutants resulted in attenuated sepsis, pneumonia and skin abscess formation in murine models (Cheung *et al*., 2011, Kobayashi *et al*., 2011, Montgomery *et al*., 2010). The expression level of *S. aureus* exoprotein regulator/sensor kinase genes *saeRS* was found higher in USA300 than USA400 strains in a mice model (Montgomery *et al*., 2008). The *sae* system senses changes environmental signals including hydrogen peroxide and regulates structural compounds of the cell envelope (Geiger *et al*., 2008). Active *saeRS* enhances the expression of virulence genes such as *hla, sbi,* and *lukFS* (PVL) (Nygaard *et al*., 2010). In summary, it is evident that there is a strikingly high mortality of various diseases caused by widespread CA and HA-MRSA, among them USA300 has proven to be particularly successful to become the dominant strain in the western world, and that there is a worrying lack of effective therapies.

1.1.5 Current strategies for treatment

All MRSA strains are widely considered to possess resistance against β-lactam antibiotics. There is a general consensus that these antibiotics do not warrant clinical use due to their ineffective killing of MRSA. However, the degree of resistance against β-lactam antibiotics or other antimicrobial agents varies among different MRSA strains.

Glycopeptides were first used against MRSA. Many limitations of this approach have been reported however, such as insufficient tissue penetration, low oral bioavailability, a requirement for monitoring of drug levels in serum, and limited therapeutic window (Ratnaraja and Hawkey, 2008). Vancomycin was provided as an empirical treatment for patients with CA-MRSA infections. However, vancomycin-resistant MRSA (VRSA, MIC > 16μg/mL) generated by gaining *vanA* ARG have been identified (Charles *et al*., 2004). Even though it is challenging to treat VRSA infection, there is limited cases reported to date (14 in the US) (McGuinness *et al*., 2017). An additional group of strains known as vancomycin intermediate-resistant *S. aureus* (VISA, MIC = 4-8μg/mL) brings relatively high burden and

the resistance mechanisms remains undefined (McGuinness *et al*., 2017). VISA are typically associated with heterogeneous VISA (hVISA), a mixed population consisting majority of little or no resistant *S. aureus* and a sub-population of VISA (Howden *et al*., 2010). To date hVISA has been reported worldwide from countries such as Japan, India, Korea, China, Thailand, Spain, Greece, Germany, Italy, and the UK (Ariza *et al*., 1999, Kim *et al*., 2000, Marchese *et al*., 2000, Trakulsomboon *et al*., 2001, Wong *et al*., 2000). The hVISA phenotypes include persistent infection, prolonged vancomycin uptake, and treatment failure (Liu and Chambers, 2003, Howden *et al*., 2006). Linezolid is one of the synthetic oxazolidinones used in MRSA treatments based on the principle of inhibiting MRSA protein synthesis by binding with the 23S subunit of ribosome to inhibit translation (Charles *et al*., 2004). As the most prescribed anti-MRSA agent, linezolid use was approved in many countries including the US and UK. The drug has an impressive 100% bioavailability, which makes it an effective agent against MRSA either via oral or intravenous intake (Pfizer, 2007). However, it comes with a relatively high incidence of side effects. Approximately 3% of patients developed thrombocytopenia, and reversible bone marrow suppression is another severe side effect caused by prolonged therapy of linezolid (Longworth, 2001). Lactic acidosis is a rare but fatal side effect (Lentino *et al*., 2008). Moreover, after a few years of widespread use, MRSA isolates resistant to linezolid were reported (Tsiodras *et al*., 2001). Apart from linezolid, there were many other synthetic antimicrobial agents developed for MRSA treatment, such as dalbavancin, tigecycline, quinuristin-dalfopristin, and ceftobiprole. They all reduced MRSA pathogenesis, yet various side effects from mild headache and gastrointestinal illness, to diarrhoea, blurred vision and numbness have been described (Ratnaraja and Hawkey, 2008).

Due to the emergence of multi-resistant MRSA and lack of safe and efficient agents to overcome those bacteria, pharmaceutical companies kept developing new antimicrobial

agents like lysostaphin (Von Eiff *et al*., 2003). However, clinical trials to show the efficacy of this agent in humans are still pending (Von Eiff *et al*., 2003). In light of this, developing novel treatments of MRSA infections in an unconventional, antibiotic-independent manner is a necessary and urgent task for eliminating *S. aureus* and other bacteria. A breakthrough of using intravenous application of phage therapy for antibacterial treatment has been achieved recently, where a patient was saved from severe infection of antibiotic resistant *Acinetobacter baumannii* (Gen, 2017). Although full details of this study have not yet been disclosed, it provided an alternative natural drug development which can be potentially applied towards *S. aureus* treatment. In light of this, the development of highly-targeted and novel therapies towards enhancing human immune responses may be a way forward in the treatment of *S. aureus* infection, circumventing the problems associated with antibiotic resistance.

1.1.6 Virulence factors of *S. aureus*

A vast variety of virulence factors are expressed by *S. aureus* to achieve initial colonisation, host environmental adaptation, nutrient acquisition, host immune survival, and eventually successful infections (Lowy, 1998). Inhibition or removal of those factors, at both the genetic and molecular level, modifies the pathogenicity of *S. aureus* and leads to attenuated virulence (Casadevall and Pirofski, 1999). There are three main categories of virulence determinants: those affecting host adhesion, immune evasion, and tissue spread. Examples of these are cell-surface components including microbial surface components recognising adhesive matrix molecules (MSCRAMMs) and secretable expanded repertoire adhesive molecules (SERAMs) facilitate bacterial binding to the extracellular matrix and host cell surface (Clarke and Foster, 2006). *S. aureus* is also capable of phagocyte evasion, particularly from neutrophils, the most prominent cellular component of human innate immunity (Rigby and DeLeo, 2012). A large number of enzymes and toxins such as PVL,

leukocidins, and γ-hemolysin are secreted by *S. aureus* for resistance against host immune strategies. In addition, a range of extracellular molecules including proteases, nucleases, lipases, superantigens and collagenases have impact on generating tissue damage and promote *S. aureus* spreading (Foster, 2005).

This study focuses on staphylococcal factors modulating immune cells. A list of *S. aureus* virulence factors involved in immune evasion strategies are shown in Table 1.1. Some virulence factors assist staphylococcal infections via preventing activation of inflammatory factors. For example, the prothrombin autoactivation results in simultaneous attraction of phagocytes to immobilise bacteria, but the process can be inhibited by superantigen-like protein SSL10 which inhibits prothrombin activation (Thammavongsa *et al*., 2015). *S. aureus* also inhibit neutrophil chemotaxis via the production of chemotaxis inhibitory protein of staphylococcus (CHIPS) and formal peptide receptor-like 1 inhibitor (FLIPr) (Thammavongsa *et al*., 2015). CHIPS and FLIPr binds to human formylated peptide receptor FPR1 and FPR2 separately to inhibit the receptor signalling functions and therefore block neutrophil recruitment (Prat *et al*., 2009). C5a, another signal of *S. aureus* infection, could be recognised by complement receptor C5aR and induce neutrophil activation. CHIPS exclusively binds the C5aR N-terminus and inhibits neutrophil recruitment efficiently (Rooijakkers *et al*., 2005b).

Additionally, *S. aureus* is capable of regulating anti-opsonisation and anti-phagocytosis activities. Aureolysin (Aur) and staphylokinase (Sak) cleaves complement factor C3 to compromise opsonisation (Thammavongsa *et al*., 2015). Furthermore, Staphylococcal Binder of Immunoglobulin (Sbi) and Clumping factors (Clf) inhibit complement pathways by binding with C3 to prevent bacterial phagocytosis (Thammavongsa *et al*., 2015). An alternative mechanism protecting *S. aureus* from phagocytosis is via bacterial agglutination (Thammavongsa *et al*., 2015). The von Willebrand Factor-binding protein (vWbp), a *S.*

aureus secreted coagulase, converts prothrombin to staphylothrombin which further cleaves peptides of fibrinogen to form fibrin. The newly synthesised fibrin self-assembles and polymerises into cable structures, forming a shield-like protection around *S. aureus* to prevent phagocyte uptake. This carefully regulated, multi-step mechanism involves a number of *S. aureus* surface proteins such as ClfA and fibronectin binding protein (FnBP) (Thammavongsa *et al*., 2015). Staphylococcal complement inhibitor (SCIN) was identified as one of the most efficient complement inhibitors and inhibits neutrophil phagocytosis and killing of *S. aureus* (Rooijakkers *et al*., 2005a). It not only inhibits convertases by direct binding to the active pocket of Bb in C3bBb, but also prevents further convertase production via interaction with C3 convertases (Rooijakkers *et al*., 2005a). A similar complement inhibiting mechanism is applied by the extracellular fibrinogen biding molecule (EfB). It binds to the C3d region of C3 with a high affinity. Evidence was found that EfB blocks both classical and alternative pathways and further neutrophil phagocytosis (Lee *et al*., 2004). The *S. aureus Δefb* mutant resulted in increased mice survival and reduced abscess formation (Jongerius *et al*., 2012).

To prevent immune-mediated bacterial killing, *S. aureus* can cleave antimicrobial peptides (AMPs). MprF inhibits cationic lysozymes and AMPs such as histatin via modification of anionic phospholipids and introducing positive charges to the membrane surface (Ernst and Peschel, 2011). *S. aureus* also produce aureolysin, a major metalloproteinase, to cleave cathelicidin and thereby demolish the AMP (Sieprawska-Lupa *et al*., 2004). To promote the survival from neutrophil-mediated killing, extracellular adherence protein (Eap) of USA300 counters neutrophil serine proteases such as elastase and cathepsin G (Stapels *et al*., 2014). More recently, a novel staphylococcal peroxidase inhibitor (SPIN) was characterised with specific anti human myeloperoxidase (MPO) binding activity and enhanced USA300 survival by interfering with MPO-mediated killing (de Jong *et al*., 2017). Resistance to the

reactive oxygen species (ROS) attack provides *S. aureus* advantage within the phagosomes. All strains including USA300 produces catalase which impairs the neutrophil killing by inactivating hydrogen peroxide (Rooijakkers *et al*., 2005b). *S. aureus* also express regulator molecules to manipulate the adaptive immune responses. For example, immunoglobulins such as IgA, IgD, IgG and IgM can be modulated via staphylococcal protein A (SpA) binding (Forsgren and Nordstrom, 1974). A detailed description of known key virulence factors involved in neutrophil cell responses will be discussed in section 1.4.

The regulation of *S. aureus* virulence determinants is clearly important for expressing specific factors at the appropriate time. The gene expression of virulence factors is controlled based on environmental signals from dynamic and complex bacterial interactions with host cells. Regulators of these regulatory genes are also classified as virulence factors, since disruption of these regulators result in attenuated *S. aureus* pathogenicity. For example, the *agr* system, consists of a sensor histidine kinase and a response regulator, and plays an essential role in secreting toxins including α-toxin and down-regulating surface adhesion molecule production (Novick *et al*., 1993, Recsei *et al*., 1986). Another two-component system, the *sae* system, regulates the transcription of a range of toxins and enzymes including heamolysin and extracellular fibrinogen binding protein (Giraudo *et al*., 1994, Liang *et al*., 2006). Mutations in *sae* results in attenuation in virulence in multiple animal infection models (Liang *et al*., 2006). A number of *S. aureus* virulence genes were evolutionarily acquired from mobile genetic elements such as plasmids, phages, and pathogenicity islands (Malachowa and DeLeo, 2010). The *S. aureus* pathogenicity islands (SaPI) identified to date mainly carry toxins encoding genes and antibiotic resistant cassettes. SaPI3, for example, consists of *tst,* a toxic shock syndrome toxins encoding gene, and enterotoxins encoding genes such as *sek* and *seq* (Yarwood *et al*., 2002). Another important SaPI known as *Staphylococcus* cassette chromosome *mec* (SCC*sec*) was identified with

methicillin resistant genes such as *metA,* and *metR* (Daum *et al*., 2002). Research focused on SaPIs not only identified novel virulence factors, but also initiated comprehension of staphylococcal virulence in the light of evolution (Gal-Mor and Finlay, 2006).

1.1.7 Nebraska transposon mutant library

To promote the identification of key genetic components that play an important role in *S. aureus* biology, the Nebraska Centre for Staphylococcal Research has developed the Nebraska transposon mutant library which comprises of 1,952 CA-MRSA mutant strains. These strains are single protein coding sequence mutants in which non-essential genes in the USA300 genome have been disrupted. This sequence-defined transposon insertion library was obtained directly from the USA300_FPR3757 genome sequence (NCBI reference sequence NC_007793). The library was generated via *bursa aurealis* transposon insertions of plasmid pBursa into the genome of wild type USA300 strain (referred to as JE2) (Fey *et al*., 2013). To date, the NTML library has been applied in diverse screens to identify genes involved in polymicrobial interactions; haemolytic activity; and antimicrobial resistance of *S. aureus* (Vestergaard *et al*., 2016, Fey *et al*., 2013, Frydenlund Michelsen *et al*., 2016). Hence, this could be an appropriate approach for the identification of genes involved in immune cell responses, in order to better understand the host-pathogen interaction between *S. aureus* and the human host and also to define potential new therapeutic strategies for the treatment of *S. aureus* infections.

The genome-wide association study (GWAS) is an alternative high throughput approach for identifying the associations between single-nucleotide polymorphisms (SNPs) and varying phenotypes of a particular trait or disease (Manolio, 2010). Initially GWAS was applied for human risk-SNP identification for pathogenesis study and designing new therapy, particularly on transcriptional mutagenesis diseases (Kim and Gibson, 2010, Long *et al*., 2016, Iadonato and Katze, 2009). Methods for using GWAS to bacterial research have been

developed more recently, and have been successfully adapted to study horizontal gene transfers involved in carbapenems resistance of *Acinetobacter baumannii,* and human specific biosynthesis factor related to *Campylobacter* pathogenesis (Suzuki *et al*., 2016, Sheppard *et al*., 2013). A GWAS study conducted with 55,977 SNPs in *S. aureus* revealed association between a nonsynonymous mutation of the *rpo*B gene and increased vancomycin resistance (Alam *et al*., 2014). In a Mexican-American community from Texas, nasal swabs were collected from 858 participants for screening of *S. aureus*, 12 significant genetic regions including *KAT2B* were identified for intermittent or persistent carriage (Brown *et al*., 2015). Nelson *et al* attempted to identify genetic variants associated with acquisition of *S. aureus* bacteraemia via GWAS method, yet no common genome-wide significance was found (Nelson *et al*., 2014). Although these studies demonstrated the potential value of GWAS in the bacterial arena, no CA-MRSA GWAS studies have previously been performed, it is therefore a more time-consuming process for this project considering the demand of a large number of candidate loci screening.

Table 1.1. *S. aureus* virulence factors related to immune evasion.

Name	Gene	Function
Aureolysin	*aur*	Resistant to AMP
Catalase	*kat*	Moderation of ROS
CHIPS	*chp*	Chemotaxis inhibition
Clf	*clf*	Phagocytosis inhibition
Eap	*eap*	Phaogcytic killing inhibition
EfB	*efb*	Complement inhibition
FLIPr	*flipr*	Chemotaxis inhibition
FnBP	*fnbp*	Phagocytosis inhibition, bacterial invasion
γ-haemolysin	*hlg*	Neutrophil lysis
Leukocidin	*lukAB,*	Neutrophil lysis
MprF	*mprF*	Resistant to AMP
Phenol-soluble	*psm*	Chemotaxis inhibition, neutrophil lysis
PVL	*lukFS*	Neutrophil lysis
Staphylokinase	*sak*	Phaogocytosis inhibition
Sbi	*sbi*	Phagocytosis inhibition
SCIN	*scn*	Complement inhibition
SpA	*spa*	Phagocytosis inhibition
SPIN	*spn*	Myeloperoxidase inhibition
SSL	*ssl*	Chemotaxis inhibition, phagocytosis
Super-oxide dismutases	*sod*	Phagocytosis inhibition
vWbp	*vwb*	Phagocytosis inhibition

AMP: antimicrobial peptides; MprF: multiple peptide resistance factor; CHIPS: chemotaxis inhibitory protein of staphylococcus; vWbp: von Willebrand factor binding protein; SSL: staphylococcal superantigen-like protein; SCIN: staphylococcal complement inhibitor; SpA: staphylococcal protein A; SPIN: staphylococcal peroxidase inhibitor; Sbi: staphylococcal IgG-binding protein; Clf: clumping factor; PVL: Panton-Valentine leucocidin; ROS: reactive oxygen species.

1.2 Neutrophils as important innate immune cells in *S. aureus* infection

1.2.1 Major components of the innate immune system

The innate immune system is an evolutionarily ancient part of the host defence against microbial pathogens. It is comprised of multiple cellular and non-cellular components and is often thought of as a 'non-specific' immune response. The physical barrier includes skin, mucous membranes and cough reflex, while the chemical barrier is conferred by pH, fatty acids and enzymes secretion (Benjamini, 1988).

The innate immune system is an important defence against bacterial infection. *S. aureus* normally cannot penetrate healthy skin but can enter through hair follicles or sebaceous glands (Wang *et al*., 2009). The risks of those infection routes are minimized by acid pH of sweat and various enzymes. The high incidence of *S. aureus* infection amongst burn patients is due to the damaged skin barrier (Bang *et al*., 2002, Wang *et al*., 2009). To prevent infection of the respiratory tract, the nasal hairs and cough reflex eject invading bacteria. as part of this process, mucus traps bacteria which allows ciliated cells to drive the microorganisms upward, which are then expelled (Vareille *et al*., 2011).

Once those barriers are penetrated by invading bacteria, the cellular innate immune system comes into play. This consists of multiple specialised cells that eliminate bacteria either through phagocytosis or extracellular killing (Benjamini, 1988). Extracellular killing refers to the process of lysing target bacteria by releasing cytotoxic molecules (Benjamini, 1988). Natural-killer (NK) cells, a type of large granular lymphocyte, play a significant role in extracellular killing of infected host cells (John Clancy JR., 1998). NK cells recognise and bind to targeted bacteria, which leads to activation of intracellular signalling (Herberman, 1986). Subsequently NK cells release granules containing pore forming protein perforin and cytolytic proteases to induce bacterial lysis (Bots and Medema, 2006). Extracellular bacterial killing mechanism was also found with neutrophils, via formation of neutrophil

extracellular traps (NETs) (Papayannopoulos *et al*., 2010). Details of NETs will be disclosed in section 1.2.2.5.

Phagocytosis refers to ingestion of bacteria which is typically followed by bacterial destruction by granule-containing lysosomes and reactive oxygen species (ROS). Key phagocytic cells include monocytes macrophages, neutrophils, basophils, mast cells and eosinophils (Baggiolini, 1984). Eosinophils are granulocyte capable of releasing antimicrobial cytotoxic molecules through degranulation upon activation (Hogan *et al*., 2013). Eosinophils are recruited to the site of infection as a rapid response to pathogens (Baggiolini, 1984). They behave as protective cells in patients with *S. aureus* ventilator-associated pneumonia (Rodriguez-Fernandez *et al*., 2013). Macrophages are important for anti-*S. aureus* host defence and contribute to both the innate and adaptive immune responses by interaction with neutrophils, and presenting antigens to modulate lymphocyte immunity (Flannagan *et al*., 2015). Macrophages can phagocytose and eliminate invading pathogens through respiratory burst, reactive nitrogen intermediates, and phagolysosomal enzymes (Amer and Swanson, 2002, Fang, 2004). However, *in vivo* and *in vitro* studies evidently showed that macrophages failed to eradicate *S. aureus* (Flannagan *et al*., 2015). *S. aureus* biofilms function as a protector from macrophage phagocytosis and therefore attenuate host proinflammatory responses in a murine model (Thurlow *et al*., 2011). *S. aureus* USA300 can successfully replicate within mature macrophage phagolysosomes which leads to host cell death and bacterial escape (Flannagan *et al*., 2016).

1.2.2 Neutrophils

1.2.2.1 Neutrophil function in immunity

Neutrophils are short-lived, polymorphonuclear leukocytes containing an abundance of intracytoplasmic granules. Approximately $9x10^8$ neutrophils are produced from the bone marrow per kilogram of body weight per day (Edwards, 2005). The development of mature

neutrophils in the bone marrow is a well-characterised, strictly regulated multi-stage process, including six stages of differentiation from stem cells: myeloblast, promyelocyte, myelocyte, metamyelocyte, band (non-segmented) cell, and mature (segmented) neutrophil (Bainton, 1993). During this process, several attributes including granules and granule contents, phagocytic and chemotactic capacity and cell mobility are developed (Murphy, 1976). The mature neutrophil has a diameter of 10-12 μm, a segmented chromatin-dense nucleus, and fully functional cytoplasmic granules (Murphy, 1976). The newly produced neutrophils are in a non-activated state when released into the circulation. As well as being free in the circulation, they can loosely attach to the vascular endothelium, allowing rapid responses to local infections (Downey *et al*., 1990). After 8 to 12 hours in the circulation, a sub-population of neutrophils undergo apoptosis and are cleared by macrophages in the spleen and liver (Furze and Rankin, 2008, Sasaki *et al*., 1995). Upon signals from the site of infection or injury, neutrophils migrate into tissues and engage survival pathways which prolongs their life span (1-2 days) (Downey *et al*., 1990). The process of the neutrophilic defence against bacterial infection consists of 5 main steps, namely neutrophil recruitment, neutrophil activation, neutrophil opsonisation, phagocytosis, and killing.

1.2.2.2 Neutrophil recruitment

Neutrophils migrate from the bloodstream to the tissue, slowing down as they reach the site of infection. The P-selectin glycoprotein ligand-1 (PSGL-1) on the neutrophil cell membrane binds with P-selectin and E-selectin on activated endothelial cells via a loosely reversible interaction. The blood flow aids neutrophil rolling along the vessel wall (Moore *et al*., 1995) (Figure 1.1). When neutrophils approach the infection site, firm adhesion between intercellular adhesion molecule 1 (ICAM-1) on endothelial cells with neutrophilic β2 integrins arrests the phagocytes completely. This procedure is achieved through high-affinity interactions between β2 integrins on neutrophil surface with chemoattractants,

cytokines, selectins, and bacterial products (Ley *et al*., 2007). The infection induces and distributes various chemical signalling molecules on both neutrophils and the endothelial cell surface, which form an intricate signalling interaction network to modulate neutrophil transmigration either through endothelial junctions or through endothelial cells (Phillipson *et al*., 2006) (Figure 1.1). Potent chemotactic factors synthesized by bacteria, such as *S. aureus* produced phenol-soluble modulins (PSMs) and proteins with N-formyl-peptides, can both act on G protein couple receptor (GPCR) and therefore result in neutrophil recruitment to the site of infection (Wang *et al*., 2007, Babior, 1999).

1.2.2.3 Neutrophil chemotaxis and activation

Activation of neutrophils occurs during and following their migration to the site of infection. This primes the cells to allow them to perform effector functions when required. Microbial molecules such as Toll-like receptor (TLR) ligands and chemoattractant ligands of GPCR are the main activation stimuli. For staphylococcal infections, TLR2 recognizes conserved bacterial structures such as lipoprotein that trigger conformational changes of GPCRs which in turn primes neutrophils and stimulates the inflammatory response (Bardoel and Strijp, 2011, Bubeck Wardenburg *et al*., 2006). Known neutrophil priming agents include complement components C3a and C5a, CXCL8, granulocyte colony stimulating factor (G-CSF), TNF-α, and lipopolysaccharide (Dang *et al*., 1999, DeLeo *et al*., 1998, Guichard *et al*., 2005, Brown *et al*., 2004). Bacterially derived products such as cytolytic toxins can also prime neutrophils (Guerra *et al*., 2017). Primed neutrophil responses enhance adhesion, phagocytosis, superoxide production and degranulation (Ellis and Beaman, 2004), and therefore are more efficient at bacterial killing processes. Some priming stimuli such as lipopolysaccharide induce NADPH oxidase complex assembly via structural changes and thereby increasing the efficiency of forming reactive microbicidal products such as singlet oxygen and hypochlorous acid, accomplished by translocation of cytosolic components

from granules to the plasma or phagosome membranes (DeLeo *et al*., 1998, Rosen and Klebanoff, 1979).

1.2.2.4 Opsonisation and phagocytosis

Opsonisation is the process where invading bacteria are identified to phagocytes for destruction. Opsonisation involves the addition of complement components and/or immunoglobulins (Ig) to the target bacteria in order to facilitate a physical interaction between the particle and receptors on the immune cell (Walport, 2001). Complement is a crucial process of the innate immune system for facilitating phagocytosis of invading pathogens. Phagocytosis can then take place upon contact with opsonised *S. aureus* (Surewaard *et al*., 2013).

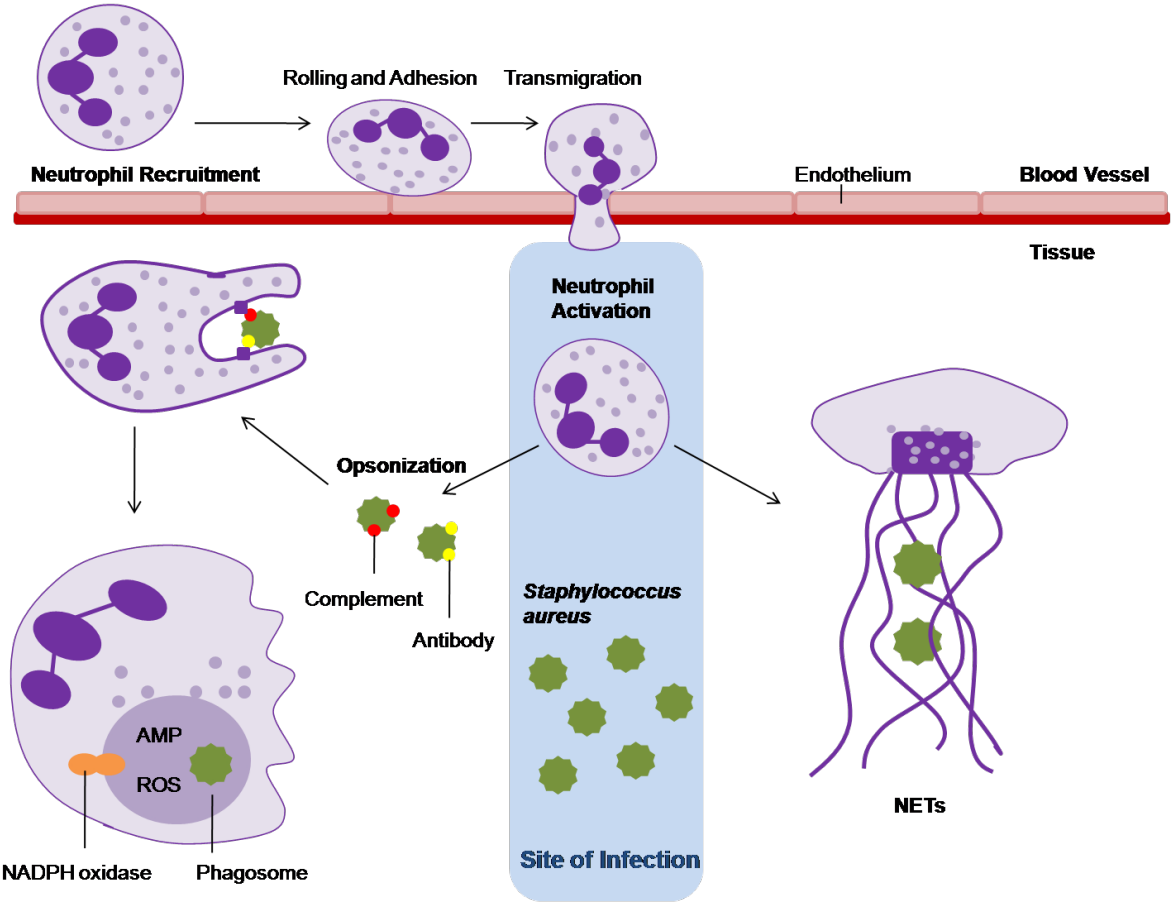

Figure 1.1 Neutrophil recruitment, activation, priming, phagocytosis and bacterial killing. AMP, antimicrobial peptides; NETs, neutrophil extracellular traps; ROS, reactive oxygen species

Three complement activation pathways namely classical, alternative, and lectin pathways can initiate the complement system (Noris and Remuzzi, 2013). Immunoglobulins like IgG and IgM activate the classical complement pathway by interacting with C1q, which causes a conformational change leading to the subsequent activation of C1r and C1s. Then C2 and C4 are cleaved into fragments by activated C1s. The fragments form C4bC2a which is an enzymatic complex that cleaves C3, an irreplaceable molecule for C3 convertases formation, into C3a and C3b (Noris and Remuzzi, 2013). The lectin pathway also results in production of C4bC2a complex. Yet instead of recognising microorganisms by antibodies, the lectin pathway relies on sugar residues on surface structures. The alternative pathway is activated by bacterial components such as toxins. Unlike the classical and lectin pathway where C4bC2a complex is formed, the alternative pathway produces C3bBb complex to generate a C3 convertase (Noris and Remuzzi, 2013). The C3 convertases sequentially produces C5 convertases when another C3b molecule is present. The C5 convertases further release C5a by cleaving C5, which is a proinflammatory molecule that primes phagocytes for bacterial intake (Bestebroer *et al*., 2010a). Meanwhile, C4b and C3b can also directly attach to bacteria or immune complexes via covalent binding (Noris and Remuzzi, 2013).

Phagocytosis is a key neutrophil defence strategy against bacterial infection, and plays an essential role in the uptake and killing of invading pathogens (Murphy, 1976). Meanwhile, many studies demonstrate a close link between phagocytosis and the acceleration of neutrophil apoptosis (Surewaard *et al*., 2013, Kobayashi *et al*., 2010, Kobayashi *et al*., 2002). Phagocytosis-induced cell death (PICD) not only helps to clear the pathogen, by disposing of neutrophils containing bacteria, but also plays a significant role in the resolution of the inflammatory response that accompanies infection (Kobayashi *et al*., 2002).

Phagocytosis is initiated when receptors on the neutrophil plasma membrane such as TLRs recognise a bacterium. This neutrophil-pathogen interaction leads to formation of

pseudopodia around the microorganism, and eventually encloses the bacterium within a phagocytic vesicle of which the membrane is derived from the plasma membrane (Klebanoff, 2005). Subsequently, a phagolysosome is generated by fusing of cytoplasmic granules with the vesicle (Figure 1.2). Then degranulation is triggered to release antimicrobial compounds into the phagolysosome, creating an inhospitable environment (Edwards, 2005). Neutrophil granule proteins are classified into four groups: azurophil (or primary) granules, specific (or secondary) granules, tertiary granules, and secretory vesicles (Lacy, 2006). The most toxic proteins such as elastase, myeloperoxidase and cathepsins are contained in primary granules (Borregaard and Cowland, 1997). Another molecule known as bactericidal-increasing protein (BIP) is capable of binding to and neutralising lipopolysaccharide (Segal, 2005). The secondary and tertiary granules are the storage sites of gelatinase, lactoferrin, lysozymes (containing acid hydrolases), and other substances (Kjeldsen *et al*., 1994, Edwards, 2005). Contents in the secretory vesicles include human serum albumin, indicating that endocytosis of the plasma membrane takes extracellular fluid into the granules (Lacy, 2006). These granule proteins assist in killing of microorganisms but are potentially harmful to host cells if released inappropriately (Borregaard *et al*., 2007). Thus, development and regulation of granulopoiesis are highly structured and complex processes. Granules are formed during all stages of neutrophil development in bone marrow (Borregaard *et al*., 2007). Primary granule proteins are synthesised during the promyelocytic stage while specific granule proteins are produced at the myelocyte stage. At the metamyelocyte stage, highly gelatinase positive granules are developed (Borregaard *et al*., 2007). Differentiation and maturation of granules are regulated by molecules such G-CSF (Dale *et al*., 1998). Granules are mobilised upon activation of cytokines, chemotactic peptide receptors, and membrane adhesion proteins (Lacy, 2006). For example, primary

granules can be selectively mobilised via Rho guanosine triphosphatese Rac2 activation induced by G protein-activated guanine nucleotide exchange factors (GEFs) (Lacy, 2006).

Understanding of conditions in the neutrophil phagocytic vacuole facilitates identification of killing mechanisms. An opsonised bacterium can be taken up into the phagocytic vacuole within 20 seconds which triggers immediate killing (Segal *et al*., 1980, Segal *et al*., 1981). Contents of numerous granules are released into the vacuole and exposed to the bacterial surface in high local concentrations (Segal *et al*., 1980). Both primary and secondary granules degranulate with similar kinetics approximately 20 seconds after bacterial phagocytosis (Segal *et al*., 1980), and it was estimated that granule enzymes occupy roughly 40% of the vacuolar volume (Hampton *et al*., 1998). About 5 minutes later, pH reaches the optimal level for the acid hydrolases and these enzymes start to enter the vacuole (Segal, 2005).

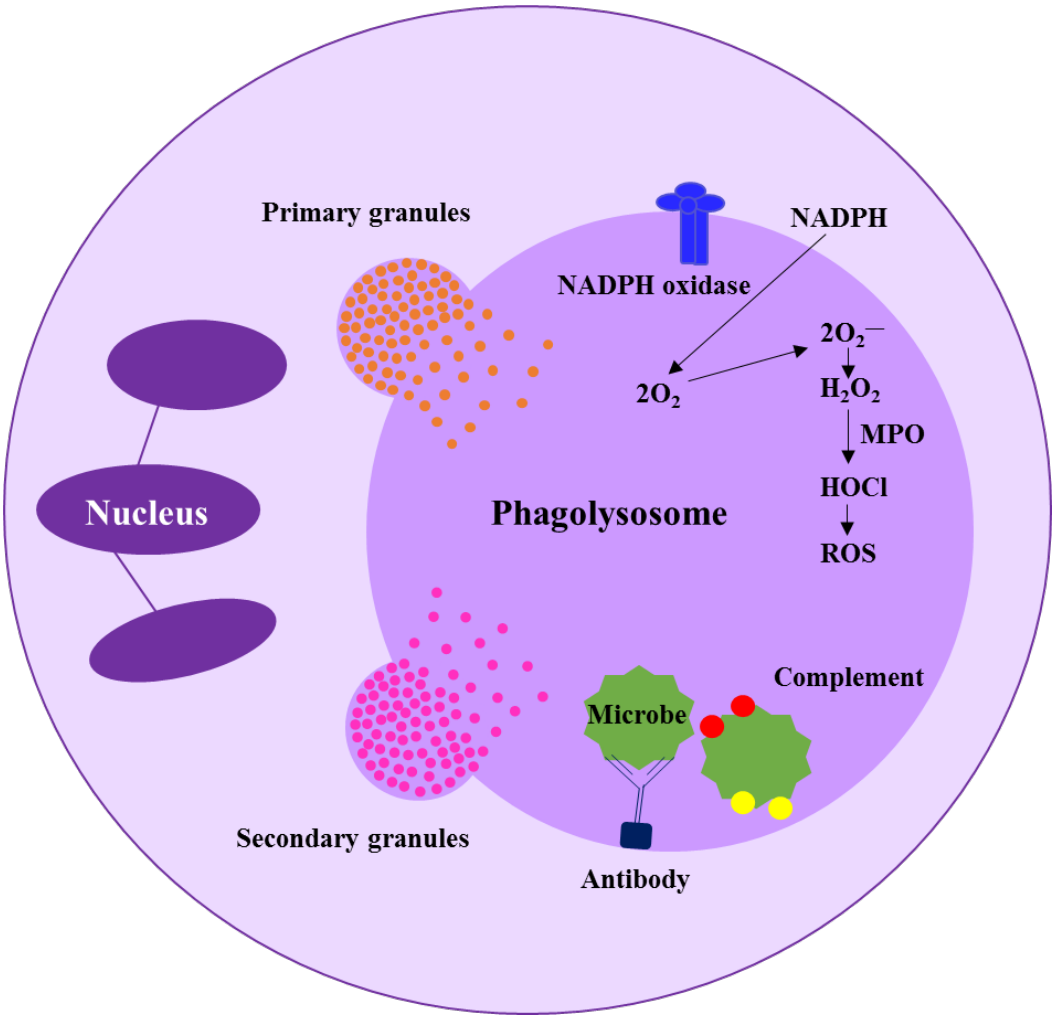

Figure 1.2 Neutrophil phagocytosis and microbicidal activity by ROS and granule proteins. MPO, myeloperoxidase; ROS, reactive oxygen species.

1.2.2.5 Pathogen killing by neutrophils

Apart from bacterial killing via the antimicrobial compounds contained within granules, there are two main strategies neutrophils use to kill bacteria like *S. aureus*. One of them is the generation of ROS which accompanies phagocytosis. ROS includes high levels of superoxide proximal to both the phagosomal and plasma membranes (Rigby and DeLeo, 2012). Specifically, electrons are transferred from cytosolic NADPH to oxygen outside of the cell or within the phagosome by NADPH-dependent oxidase, which reduces the oxygen to superoxide in between the membranes of the phagosome and engulfed *S. aureus*. By so doing, high levels of superoxide are generated, which leads to an influx of electrons into the phagosome (Babior, 1999, Klebanoff, 2005). Both superoxide and nitric oxide are potently bactericidal to *S. aureus* (Nunoshiba *et al*., 1995, Malawista *et al*., 1992), causing damage to bacterial DNA, lipids, and cellular proteins (Gaupp *et al*., 2012, Morgan *et al*., 2008). Protons are then capable of transforming superoxide to H_2O_2 which forms hypochlorous acid in the presence of the granule protein, myeloperoxidase (MPO). Subsequent secondary reactions generate a number of highly effective antimicrobial molecules, including singlet oxygen, hydroxyl radical, and chloroamines (Klebanoff, 2005) (Figure 1.2).

Recently a third neutrophil killing mechanism has been discovered whereby a novel structure is formed: neutrophil extracellular traps (NETs). NETs consist of expelled neutrophil DNA bound with histones, azurophilic granule proteins, and several cytosolic proteins (Figure 1.1). NETs possess the capability of trapping and killing various microorganisms including *S. aureus* (Brinkmann *et al*., 2004). *S. aureus* secreted PVL, LukGH, LukDE, PSMs, and γ-hemolysin can cause formation of NETs by permeabilization of the cell membranes (Kobayashi *et al*., 2015). Release of DNA and granule enzymes for NET formation was found upon stimulation with both physiological stimuli such as CXCL8 and lipopolysaccharide (Yousefi and Simon, 2016), and non-physiological agonists

including phorbol myristate acetate (PMA) (Yousefi and Simon, 2016). *In vivo,* NETs are found to be closely linked with TLR2 signalling and opsonisation (Yipp *et al*., 2012). It is also believed that NETs are tightly regulated with ROS synthesis, due to the fact that NETs cannot be formed without NADPH-oxidase (Fuchs *et al*., 2007, Yipp *et al*., 2012). NET formation is also regulated by myeloperoxidase (MPO) and neutrophil elastase (NE). The process is mediated by the release and migration of NE and MPO from granules to the nucleus, where NE degrades the linker histone H1 and regulates core histones, while chromatin decondesation is enhanced by MPO (Papayannopoulos *et al*., 2010). After clearance of infections, NETs are degraded by DNase 1 (Bratton and Henson, 2011). Increased NETs response was induced by inhibiting phagocytosis, indicating NETs might be a complementary pathogen killing mechanism when phagocytosis cannot take place.(Jablonska, 2014). As a result of the detection of histones in NETs, NETs were thought to comprise of chromosomal DNA. This came into question when it was discovered that antibodies used for the detection of histones also detected DNA, which could derive from the mitochondria (Yousefi and Simon, 2016). Subsequently, sequencing methods have established the main composition of NETs as mitochondrial DNA (Lood *et al*., 2016, Yousefi and Simon, 2016). Nevertheless, the possibility of chromosomal DNA in the formation of NETs cannot be excluded, considering nuclear DNA can be released under conditions of cell lysis. For instance, neutrophils release nuclear DNA and form NETs when encountering bacterial pore-forming toxins such as *S. aureus* secreted leukotoxin (Malachowa *et al*., 2013).

1.2.2.6 Clinical significance of neutrophils for *S. aureus* infections

Previous research has demonstrated that individuals with disorders of neutrophil functions are at high risk of *S. aureus* infection (Bogomolski-Yahalom and Matzner, 1995). Severe bacterial infections (including *S. aureus*) are often fatal among patients suffering congenital

neutrophil deficiencies (Amulic *et al*., 2012). Chronic granulomatous disease (CGD) refers to a neutrophil disorder with defective NADPH oxidase and cannot produce ROS and CGD patients present with a higher susceptibility to fungal and bacterial infections (including *S. aureus*) (Goldblatt and Thrasher, 2000, Edwards, 2005). Furthemore, neutrophils isolated from CGD patients are unable to kill *S. aureus in vitro* (Quie *et al*., 1967, Goldblatt and Thrasher, 2000). Specific-granule deficiency is an uncommon neutrophil defect, but leads to severe skin and lungs infection caused by *S. aureus*, *Candida albicans,* and *Pseudomonas aeruginosa* (Edwards, 2005). Neutrophils isolated from these patients lack specific granule compounds such as gelatinase and lactoferrin. The hyperimmunoglobulin E-recurrent infections (HIE) was first reported with *S. aureus* infection in 1966 (Edwards, 2005). The strikingly abnormal inflammatory response in HIE patients is possibly caused by delayed neutrophil recruitment to site of infection, leaving prolonged opportunity for bacterial replication (Edwards, 2005). Neutrophils in leukocyte adhesion deficiencies (LAD) patients fail to migrate to the site of infection. Skin and respiratory tract infections are commonly found among LAD patients, typically with *S. aureus* or Gram-negative bacteria (Rosenzweig and Holland, 2004). *S. aureus* bacteraemia is also a significant cause of morbidity and mortality (23%) in neutropenic patients on chemotherapy (Gonzalez-Barca *et al*., 2001). The abnormally low centration of neutrophils in blood of the patients increased risks of severe oral mucositis (12% to 32%) and *S. aureus* infection (33% to 57%) (Gonzalez-Barca *et al*., 2001).

1.3 Neutrophil cell death programmes

1.3.1 Apoptosis

Apoptosis, also known as 'programmed cell death', is a strictly regulated process (Kennedy and DeLeo, 2009). Neutrophils are exquisitely sensitive to apoptosis, hence their short half-life, and it plays a significant role in clearing effete neutrophils thus facilitating the

resolution of inflammation (Kennedy and DeLeo, 2009). Not only is apoptosis important for the balance between cell survival and cell death (homeostasis), but because it avoids loss of cell contents, it is also important for the prevention of neutrophil induced tissue damage (Luo and Loison, 2008, Iba *et al*., 2013).

A notable feature of neutrophil apoptosis is chromatin condensation, which changes the multi-lobed nucleus into a single structure consisting of short (180 bp) DNA strands (Kitazumi and Tsukahara, 2011). This then further leads to nuclear fragmentation and apoptotic body formation (Klionsky, 2004). Caspases are responsible for the cleavage of cellular proteins and structures, allowing cells to shrink and be cleared by tissue macrophages (Kitazumi and Tsukahara, 2011). Importantly, the plasma membrane is preserved during apoptosis, preventing the loss of histotoxic cell contents.

Initiation of apoptosis is via either intrinsic (e.g. ROS or mitochondria regulated) or extrinsic (by death receptor signalling e.g. FAS, TNFR) pathways (Kennedy and DeLeo, 2009). The intrinsic process, known also as the spontaneous pathway, refers to the apoptosis initiated by signals from within the cell. Many molecules are known to modulate spontaneous neutrophil apoptosis, and it is thought to be governed by a balance of pro- and anti-apoptotic proteins. For example, apoptosis can be initiated by the reduced expression of the anti-apoptotic protein Mcl-1, a key Bcl-2 family protein found in cytoplasm and nucleus (Moulding *et al*., 2001). Bcl-2-asscoiated X protein (BAX) is a pro-apoptotic member of the Bcl-2 family (Sawatzky *et al*., 2006). Upon cleavage, BAX translocates to the mitochondria, forming pores in the mitochondrial membrane and subsequent release of cytochrome C from mitochondria into the cytosol, which activates caspases and DNA cleavage (Maianski *et al*., 2004). Inhibition of BAX cleavage results in prolonged inflammation *in vivo* (Sawatzky *et al*., 2006), suggesting the importance of BAX for the resolution of acute inflammation.

The extrinsic pathway is activated by binding between exocellular ligands with specific receptors on the cell surface, from which a transmembrane signal is generated to activate caspase activity (Schulze-Osthoff *et al*., 1998). For instance, FAS-mediated apoptosis is stimulated by neutrophil produced FAS ligand (FASL), and can be suppressed by G-CSF, GM-CSF, and IFN (Liles *et al*., 1996). The FAS-FASL interaction results in clustering of FAS-associated death domain on the cytoplasmic side of plasma membrane and further promotes caspase activation and apoptosis (Kennedy and DeLeo, 2009).

1.3.2 NETosis

NETosis refers to cell death following the formation of NETs, and features a ruptured plasma membrane allowing collapse of the nuclear membrane and chromatin release as a DNA cloud (Fuchs *et al*., 2007, Yousefi and Simon, 2016). The objective of NETosis was believed to rescue and protect the local environment from the release of damage-associated molecular patterns (DAMPs) from this necrotic-like cell death, yet how the residues of neutrophils that underwent NETosis has cleared remains unknown (Yousefi and Simon, 2016). Recently NETosis was considered as a destructive process in publications, since it has been reported that NETosis could represent a necroptosis (Desai *et al*., 2016), and the persistence of neutrophil remnants could exacerbate inflammation and may induce autoimmune responses (Yousefi and Simon, 2016). The controversy as to whether NETosis is a beneficial or potentially harmful cell death format to the host remains until further explanation of the mechanism is offered.

1.3.3 Necrosis

Necrosis (including necroptosis) is a regulated neutrophil cell death characterised by the exhibition of cytoplasmic swelling, disorganised organelles, ruptured plasma membrane, loss of intracellular contents, and a lytic nucleus (Yang *et al*., 2015). Unlike apoptosis and NETosis, necrosis is an accidental and turbulent cell death format. The process is triggered

by bacteria and toxic molecules released from necrotic cells such as proteolytic enzymes (Iba *et al*., 2013). Inflammation can be induced by DAMPs released from necrotic cells (Yang *et al*., 2015), including uric acid, heat shock proteins and antimicrobial peptides. These molecules interact with pattern-recognising receptors which stimulate proinflammatory mediators (Iba *et al*., 2013). Inflammatory responses can also be triggered via the Nlrp3 inflammasome sensing of ATP released from necrotic cells (Iyer *et al*., 2009). Recently, a receptor interacting protein kinase-3 (RIPK3) and mixed lineage kinase domain-like (MLKL) dependent necroptosis pathway was described (Murphy and Vince, 2015). Necroptotic cell lysis and the secretion of pro-inflammatory molecules depends on RIPK3 phosphorylation of MLKL. Several signalling receptors are capable of activating RIPK3-MLKL necroptosis, such as TLRs, and IFN-regulatory factors (Murphy and Vince, 2015). Necrosis plays a pivotal role in host immune responses in microbial infections, as evidence was found that *S. aureus* is capable of inducing necrosis via LukGH secretion, and in turn promotes tissue damage and inflammation (Malachowa *et al*., 2012). Massive *S. aureus* replication was found within abscesses along with both viable and necrotic neutrophils (Kobayashi *et al*., 2015). Hence, *S. aureus* triggered necrosis induces inflammation and subverts host infection outcomes by eliminating immune cells and generating an ideal bacterial growth environment. Identification of necrosis-dependent mechanisms in *S. aureus*-neutrophil interaction may lead to novel specific therapeutic targets.

1.4 *S. aureus* evasion of neutrophil immunity

Neutrophil-modulated killing is the key defence against *S. aureus* in a healthy human immune system. Hence, it is not surprising that *S. aureus* has developed numerous evasion mechanisms to escape from this particular innate immune defence. This not only reveals the ongoing combat between host-pathogen interactions, but also reflects the importance of

each defence factor involved in the *S. aureus* infection (Rigby and DeLeo, 2012). The combat between neutrophils and *S. aureus* will be discussed step by step.

1.4.1 Inhibition of neutrophil recruitment

S. aureus impedes the process of neutrophil immunity at many steps, beginning with recruitment to the site of infection. The process of neutrophil rolling along the endothelial cell wall towards the site of *S. aureus* infection can be blocked by staphylococcal super antigen-like 5 (SSL5) which seizes the binding site of PSGL-1. Occupation of PSGL-1 results in the prevention of P-selectin ligand binding and consequently neutrophils are no longer able to migrate towards the infection site (Bestebroer *et al*., 2007) (Figure 1.3 A). In addition to PSGL-1, SSL5 also competitively interacts with glucosaminoglycan-binding sites of other glycoproteins to abrogate integrin activation for neutrophil attachment (Bestebroer *et al*., 2007). Furthermore, the firm adhesion step is modulated by *S. aureus* synthesized extracellular adherence protein (Eap), which inhibits ICAM-1 from interacting with neutrophilic β2 integrins by direct binding (Chavakis *et al*., 2002) (Figure 1.3 A).

1.4.2 Escape from neutrophil chemotaxis and activation

S. aureus also secretes several proteins to reduce neutrophil activation and therefore potentially depressing immune responsivity. Chemokine-dependent neutrophil activation can be inhibited by direct binding of SSL5 with chemokine receptors (Bestebroer *et al*., 2010b). SSL10 and SSL3 suppress chemokine CXCL12-mediated neutrophil response and TLR2-dependent neutrophil activation respectively (Bardoel *et al*., 2012, Walenkamp *et al*., 2009). Another protease synthesized by *S. aureus* known as staphopain A (ScpA) cleaves CXCR2 chemokines (Laarman *et al*., 2012) (Figure 1.3 B). Besides the chemokine pathway, CHIPS to impair neutrophil chemotaxis via inhibition of FPR 1 and C5aR. Further studies revealed FLIPr which is an FPR1 inhibitory protein generated by *S. aureus*, and CHIPS act

as FPR antagonists and prevent *S. aureus* from recognising formyl peptides and PSM (Kobayashi *et al*., 2010, Kretschmer *et al*., 2010) (Figure 1.3 B).

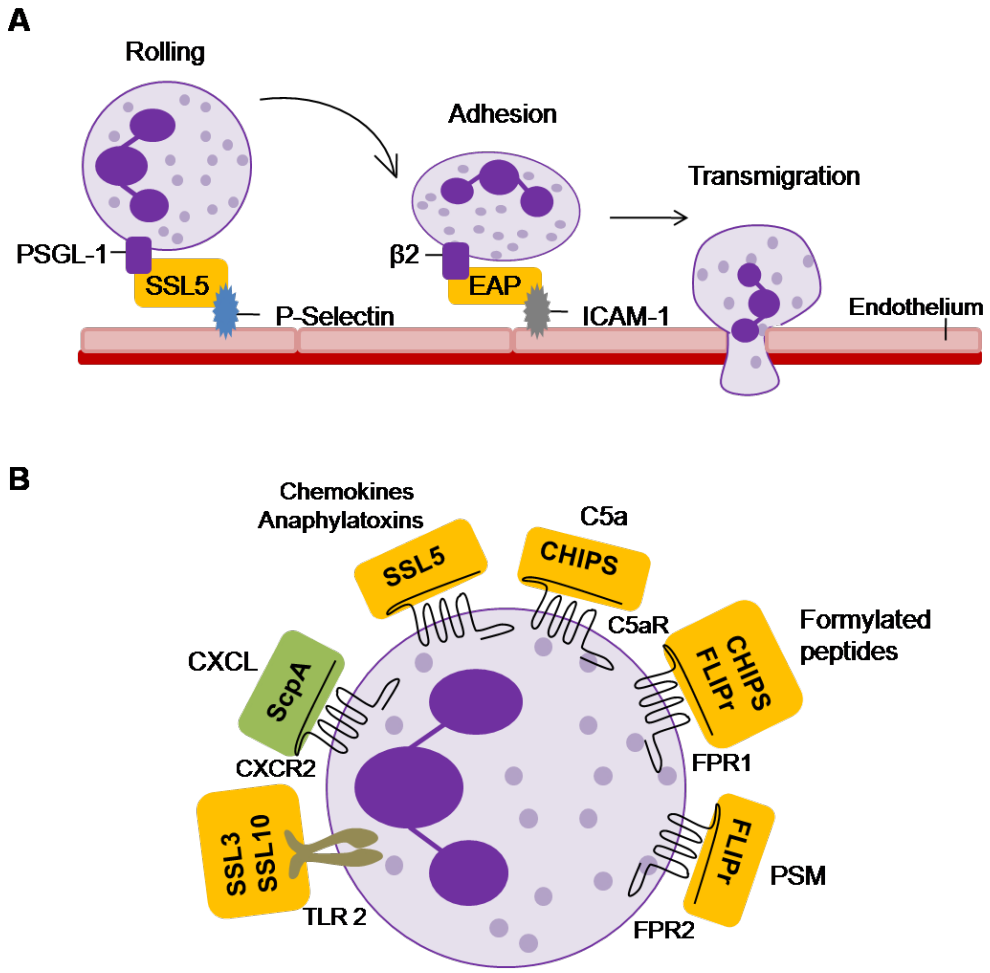

Figure 1.3 *S. aureus* evasion of (A) neutrophil recruitment and (B) neutrophil activation. CHIPS, chemotaxis inhibitory proteins; EAP, extracellular adherence protein; ICAM, intercellular adhesion molecule 1; FPR, formyl peptide receptor; PSGL, p-selectin glycoprotein ligand; PSM, phenol-soluble modulins. SSL, staphylococcal super antigen-like; TLR, toll-like receptor; ScpA, staphopain A.

1.4.3 Escape from opsonisation and phagocytosis

To overcome opsonisation-dependent phagocytosis, *S. aureus* produces the metalloprotease aureolysin to degrade C3 (Laarman *et al*., 2011). Together with staphylococcal complement inhibitor (SCIN) and staphylococcal binder of IgG (SBI), aureolysin blocks the neutrophil immune response by truncating C3 at the convertase site. An aureolysin knock-out study suggests the essential and sufficient role that aureolysin plays in C3 cleavage (Jongerius *et al*., 2010b, Rigby and DeLeo, 2012, Laarman *et al*., 2011). *S. aureus* extracellular complement-binding protein (ECB) and extracellular fibrinogen-binding protein (EFB) also bind with the C3 molecule and thereby prevent further phagocytosis (Jongerius *et al*., 2010a, Lee *et al*., 2004). Both ECB and EFB have been shown to enhance *S. aureus* survival and reduce neutrophil influx to the site of infection in a pneumonia model (Jongerius *et al*., 2012).In addition to interfering with the core function of C3, *S. aureus* also modulates C5, C1q, and Ig signalling. SSL7 binds to IgA and strongly suppresses C5 induced *S. aureus* phagocytosis (Bestebroer *et al*., 2010a). While two other anti-opsonic molecules namely SSL10 and staphylococcal protein A bind with IgG to prevent antibody recognition of *S. aureus* by neutrophils (Diekema *et al*., 2001, Itoh *et al*., 2010). As a result, those occupied antibodies leave *S. aureus* in a neutrophil compromised environment without being opsonized and phagocytosed (Langone, 1982).

1.4.4 Escape from neutrophil killing

To resist ROS-mediated killing, *S. aureus* shields itself with various antioxidants and enzymes which destroy or neutralise oxidant molecules (Spaan *et al*., 2013b). Staphyloxanthin, for example, is an antioxidant which consumes oxidants and prevents the bacteria from neutrophilic oxidative burst via an unidentified mechanism (Liu *et al*., 2005). Catalase is a cytoplasmic staphylococcal enzyme which reduces hydrogen peroxide (H_2O_2) to its inactive components H_2O and O_2 (Mandell, 1975). Superoxide dismutase also

eliminates harmful ROS following phagocytosis by converting superoxide anion to H_2O_2 (Deleo *et al*., 2009). Methionine sulfoxide reductase repairs oxidative damage and promotes *S. aureus* survival within neutrophils (Malachowa *et al*., 2011). A cell wall-anchored protein known as adenosine synthase can synthesise adenosine from adenosine monophosphate (Cronstein *et al*., 1990). The *S. aureus* adenosine can suppress neutrophil degranulation and superoxide burst, allowing *S. aureus* to escape from phagocytic clearance (Thammavongsa *et al*., 2009).

Neutrophils induce bacterial lysis through lysozyme degradation of the peptidoglycan matrix in the cell wall. Yet *S. aureus* utilizes autologous O-acetyltransferase A to modify the peptidoglycan and therefore protects itself against lysozymic lysis (Bera *et al*., 2005, Herbert *et al*., 2007). Furthermore, *S. aureus* either secretes staphylokinase to bind with host defensins, or alters the phosphatidylglycerol content of the cell membrane. Both mechanisms result in changes to the *S. aureus* cell surface leading to the cationic antimicrobial peptides (AMP) being repelled (Mishra *et al*., 2011, Peschel *et al*., 2001). In addition to mediating cell wall changes, *S. aureus* is also capable of cleaving AMPs by producing proteases such as aureolysin (Sieprawska-Lupa *et al*., 2004).

S. aureus also exploits an anti-NETs mechanism by staphylococcal nuclease degradation of NETs DNA and therefore escape from this environment (Berends *et al*., 2010). Extracellular nucleases have been also found in several pathogens including *S. aureus* (Thammavongsa *et al*., 2013), indicating *S. aureus* is capable of inducing both intracellular and extracellular neutrophil killing shut down.

The effectiveness of neutrophil evasion turns out to be key to the pathogenesis of *S. aureus*. It is exemplified by the increase in susceptibility and mortality to *S. aureus* infection among patients with deficient neutrophil functions, such as neutropenia, CGD, HIE, and LAD (Goldblatt and Thrasher, 2000, Rosenzweig and Holland, 2004, Edwards, 2005, Gonzalez-

Barca *et al*., 2001). It is evident that neutrophil immune activity is essential to eliminate *S. aureus*. However, research has found that bacterial survival inside neutrophils contributes to the pathogenesis of *S. aureus* infection and exacerbates diseases (Gresham *et al*., 2000). Moreover, this study also demonstrated enhanced host defence with neutrophil migration to the site of infection resulting in increasing pathogenic burden and host death (Gresham *et al*., 2000). The data may imply an underlying virulence mechanism where *S. aureus* use neutrophils as a niche for replication while inducing necrotic cell lysis and inflammatory responses. A conundrum is therefore raised as whether neutrophil activity contributes more for *S. aureus* survival or host immunity. Developing molecules that can control inflammatory responses while maintaining effective neutrophil antimicrobial activities is a key novel therapeutic strategy.

1.4.5 *S. aureus* induced neutrophil lysis

S. aureus has evolved additional mechanisms to escape from neutrophil defence, by generating a number of cytolytic toxins to kill neutrophils before, during and after phagocytosis, including PSMs, α-hemolysin, and leukotoxins (Teng *et al*., 2017). *S. aureus* synthesise three PSMs namely PSMα, PSMβ, and PSMγ (Surewaard *et al*., 2013). PSMα peptides possess the most pronounced neutrophil lysing ability by disruption of the cytoplasmic membrane from inside the phagosome, for which PSMα3 was identified with the strongest activity (Teng *et al*., 2017). PSMs lyse neutrophils in a receptor-independent manner, probably via membrane damaging activity bound with their strong amphipathy and α-helicity features of pore-forming peptides (Wang *et al*., 2007). PSMγ show moderate lytic activity and PSMβ peptides are non-cytolytic. The proinflammatory neutrophil responses such as chemoattraction, activation and CXCL8 release can be initiated by PSMα stimulation via FPR2 which senses the amphipatic α-helical structure of PSMs (Otto, 2014).

S. aureus β-Barrel pore-forming toxins including α-hemolysin induce leakage and ultimately lysis of leukocytes including neutrophils (Bhakdi and Tranum-Jensen, 1991, Valeva *et al*., 1997). As a water-soluble monomer, α-hemolysin oligomerises into a heptameric structure to assemble the lytic activity (Berube and Bubeck Wardenburg, 2013). In murine pneumonia studies, α-hemolysin is required to induce CXC chemokines which facilitates recruitment of neutrophils to the lung (Bartlett *et al*., 2008). Increased survival, decreased lung pathology, IL-1β secretion, and neutrophil recruitment to live bacteria was observed following α-hemolysin instillation in a pyrin domain containing protein (NLRP3) deficient model (Fink and Cookson, 2005), implicating the importance of NLRP3 in α-hemolysin regulated pathogenesis *in vivo*.

PVL is a bicomponent pore-forming exotoxin consisting of LukS-PV and LukF-PV subunits, and is an important virulence factor in necrotising diseases (Loffler *et al*., 2010). Interaction of LukS-PV with neutrophils triggers secondary binding of LukF-PV and subsequently initiates the pore-forming lytic activity. LukS-PV binds to human complement receptor C5aR as the target of PVL, which inhibits C5a mediated neutrophil activation (Spaan *et al*., 2013a). *S. aureus* produced leukocidins such as LukED and LukGH lyse neutrophil membranes after phagocytosis (Aslam *et al*., 2013, Ventura *et al*., 2010). LukGH triggers neutrophil death by targeting αM/β2 integrin (DuMont *et al*., 2013) and promotes post-phagocytosis *S. aureus* escape and subsequent bacterial outgrowth. Similarly, PSMs and α-hemolysin have also been suggested to directly damage phagosome and facilities escape and replication of *S. aureus* in the cytoplasm (Surewaard *et al*., 2013, DuMont *et al*., 2013, Grosz *et al*., 2014). The neutrophil lysis caused by PSMs is independent of receptor binding and may be due to the lytic nature of the proteins (Haas, 2007).

Previous related research from our group indicates that those and possibly other soluble *S. aureus* toxins subvert neutrophil apoptosis and switch cell death to necrosis, an undesirable

form of neutrophil cell death (Anwar thesis, 2014) (Figure 1.4). Resulting tissue damage is induced by potent proteases which are ordinarily bound within granules but released into the extracellular space (Anwar *et al*., 2009) (Hirsch *et al*., 1997). Evidently, *S. aureus* induced necrosis not only depletes valuable human immune cells, but also generates a proinflammatory environment and promotes their own survival within the host.

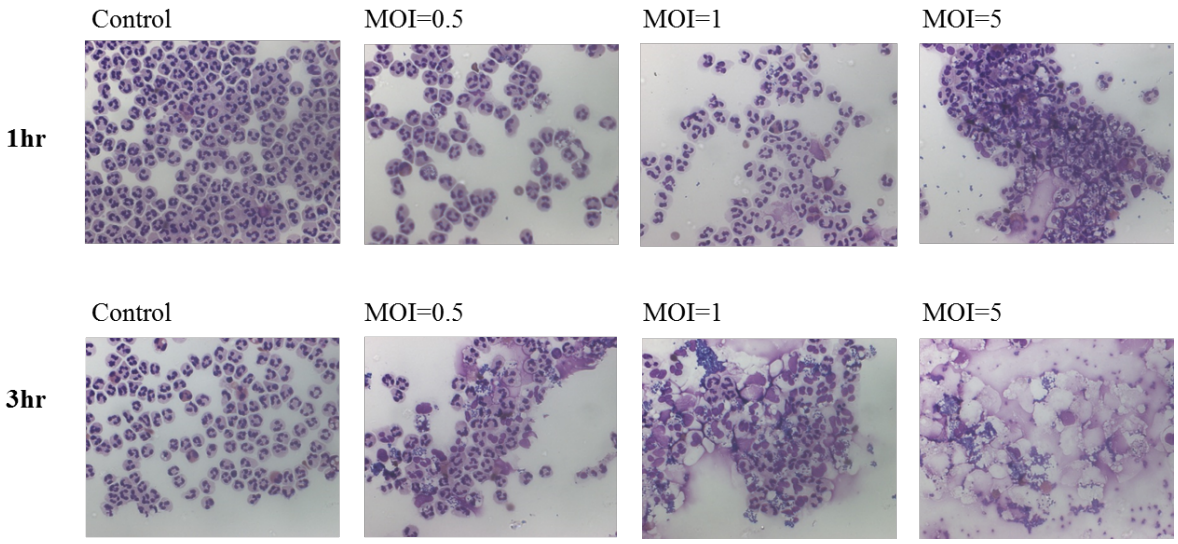

Figure 1.4. Neutrophil necrosis caused by exponential phase SH1000 at MOI of 0.5, 1, and 5 after 1 and 3 hours co-incubation (Anwar thesis, 2014). Neutrophil necrosis caused by *S. aureus* increased with both MOI and co-incubation time. Field width 200 µm.

1.5 Zebrafish embryos as a model of *S. aureus* infection

Over recent decades, huge progress has been made in the development of infection models for human-pathogen studies *in vivo*. The use of animal models, either murine or zebrafish, have contributed greatly to our knowledge on staphylococcal pathogenesis. The zebrafish embryo, which possesses both genetic manipulability and transparency allows visualisation of immune cells during infection and inflammation. This model has been initially used for developmental studies, and their potential importance as a novel model organism for host-pathogen interaction including for *Streptococcus pneumoniae* (Saralahti *et al*., 2014), *S. aureus* (Prajsnar *et al*., 2008), and mycobacteria (Swaim *et al*., 2006). Although *S. aureus* is not a natural fish pathogen, the zebrafish infection model has been established with clear acute infectious symptoms and host mortality, with both embryos (Prajsnar *et al*., 2008) and adults (Lin *et al*., 2007). Studies of zebrafish neutrophil biology advanced the understanding of neutrophil immune response and highlighted the importance of this model in human autoimmunity research (Henry *et al*., 2013, Shelef *et al*., 2013). The model has been widely used for identifying critical roles of phagocytes in immune response to *S. aureus* infection (Harvie and Huttenlocher, 2015, Torraca *et al*., 2014). Complete phagocytosis of *S. aureus* by zebrafish macrophages and neutrophils was shown by live imaging (Prajsnar *et al*., 2008). A subpopulation of zebrafish embryos showed phagocyte-dependent clearing of the infection, while remaining embryos displayed overwhelming outcomes, suggesting that *S. aureus* can subvert the phagocyte killing responses *in vivo* (Prajsnar *et al*., 2012). In light of this, the zebrafish embryo model was chosen in this thesis to study neutrophil-*S. aureus* interaction during infection.

The development of the zebrafish embryo is more rapid compared to mammalian species, achieving growth from one cell to a recognisable body shape within 24 hours post fertilisation (hpf) (Westerfield, 2000). The wildtype zebrafish embryos are almost fully

transparent from fertilisation to 3 days post fertilisation (dpf) (Isogai *et al*., 2001), allowing bacterial injection into an observable circulation valley by using light microscopy. Morpholino-modified antisense oligonucleotides have been developed to selectively knockdown transient gene expression, to allow the interrogation of candidate host genes in infection (Summerton and Weller, 1997). In light of this, macrophages and neutrophils can be depleted by pu.1 morpholinos for 48 and 36 hours post fertilisation (hpf) respectively, allowing the study of these cells in host-*S. aureus* interaction (Klemsz *et al*., 1990).

The zebrafish model shares many orthologs of phagocytes and signalling molecules with the human immune system (van der Vaart *et al*., 2012). Functional macrophages and primary neutrophils appear at 25 and 18 hpf respectively (Crowhurst *et al*., 2002), with the emergence of mature neutrophils at 2 days post fertilisation (Lieschke *et al*., 2001). In addition, the development of the adaptive immune system occurs 4-6 weeks after development of innate immune cells in zebrafish (Trede *et al*., 2001, Lam *et al*., 2004), which enables experiments focusing on *S. aureus*-phagocyte interaction at early embryo stages. There are three main limitations of using the zebrafish model. The necessity of maintenance at 28^{o}C might have an impact in some virulence factors of *S. aureus*, of which the optimal temperature is 37^{o}C. Human-specific immune evasion factors might not have same phenotypes in this model. Additionally, the divergence between zebrafish and humans occurred 450 million years ago. The genetic similarity is therefore less than other mammalian models such as mouse which diverged at 112 million years ago (Woods *et al*., 2000).

1.6 Hypothesis and aims

S. aureus is an extremely powerful human pathogen. It is rapidly evolving with antibiotic resistance mechanisms and a multitude of pathogenesis factors that overcome the neutrophil

immune response in many different ways. Clearly, it is necessary to look further into the relationship between neutrophils and *S. aureus* to understand how to promote killing of this microorganism which may lead to important novel therapeutics which would reduce morbidity and mortality of *S. aureus*-related infections.

We hypothesise that apart from known cytotoxin expression, *S. aureus* potentially induces neutrophil cell death via novel mechanisms. This PhD aims to identify immune modulating factors by screening *S. aureus* mutants of the NTML in flow cytometric neutrophil cell death assays. Strains attenuated in their ability to kill neutrophils will then be verified and subsequently, characterisation of the pathogenic mechanisms will take place, particularly focusing on neutrophil uptake of *S. aureus* and post-phagocytotic regulation of cell death. The overall aim is to identify viable targets for novel anti-MRSA therapy development to improve treatments for patients with severe and life-threatening *S. aureus* infections.

CHAPTER 2

Materials and methods

2.1 Media

All media in this study were made in distilled water (dH_2O) followed by autoclaving at 121^oC for 20 min, 103 kilopascals.

2.1.1 Brain heart infusion (BHI)

Brain heart infusion (Sigma)	37g/L

2.1.2 BHI agar

Brain heart infusion agar (Sigma)	52g/L

2.1.3 Lysogeny broth (LB)

Yeast extract (Oxoid)	10g/L
Tryptone (Oxoid)	5g/L
NaCl	5g/L

2.1.4 LB agar

Yeast extract (Oxoid)	10g/L
Tryptone (Oxoid)	5g/L
NaCl	5g/L
Agar (Oxoid)	1.5% (w/v)

2.1.5 LK

Yeast extract (Oxoid)	10g/L

Tryptone (Oxoid)	5g/L
KCl	7g/L

2.1.6 LK agar

Yeast extract (Oxoid)	10g/L
Tryptone (Oxoid)	5g/L
KCl	7g/L
Agar (Oxoid)	1.5% (w/v)

2.1.7 Baird-Parker agar

Baird-Parker agar base (Oxoid)	63g/L
Egg yolk tellurite emulsion (Oxoid)	5% (w/v)

2.1.8 RPMI-1640 media

Before use, 10% (v/v) heat inactivated foetal calf serum (Sigma-Aldrich) was added to RPMI-1640 media (Sigma-Aldrich and Thermo Fisher Scientific) and stored at 4^{o}C.

2.2 Antibiotics

Stock antibiotic solutions used were prepared and filter-sterilised (0.2 μm pore size) (Millex). Corresponding volume was added into agar media below 55^{o}C, or liquid media right before use to reach the working concentration. The antibiotics used in this project are listed in Table 2.1.

Antibiotics	**Stock concentration (mg/mL)**	**Working concentration (μg/mL)**	**Solvent**
Ampicillin (Amp)	100	100	dH_2O
Chloramphenicol (Cm)	30	30	95% (v/v) ethanol
Erythromycin (Ery)	5	2.5	95% (v/v) ethanol
Kanamycin (Kan)	50	25 or 50	dH_2O
Lincomycin (Lin)	25	12.5	50% (v/v) ethanol
Tetracycline (Tet)	5	2.5 or 5	50% (v/v) ethanol

Table 2.1 Concentrations of antibiotic solutions.

2.3 Bacterial strains and plasmids

2.3.1 Nebraska transposon mutagenesis library (NTML)

The Nebraska transposon mutant library derived from CA-MRSA USA300 was used for this project. The WT strain JE2, is identical to the *S. aureus* strain isolated from the Los Angeles County jail, except that it has been cured of plasmids (Fey *et al*., 2013). The Nebraska Transposon Mutant Library was constructed based on USA300 FPR3757 chromosomal genome sequence mapped transposition of *bursa aurealis* from the delivery plasmid pBursa into the nonessential protein coding sequences of JE2 genome (Fey *et al*., 2013).

The NTML was stored in twenty 96-well microtiter plates at -80ºC. Plates were thawed on ice before incubation of 50µL of stock culture in 150µL of varied media in each well for varied times at 37ºC, dependent on the experimental set up.

2.3.2 *Staphylococcus aureus* strains

S. aureus strains used in transformation and transductions are given in Table 2.2. Strains were obtained from -80ºC Microbank vial stocks (Pro-lab Diagnostics) and inoculated onto BHI agar with antibiotics where appropriate to select the resistant marker. The plates were kept at 4ºC for a week for short-term use. For long-term storage, a microbank bead stock was made from a single colony and stored at -80ºC.

For bacterial growth, a single colony was inoculated into 5 mL of BHI media, with or without antibiotics, in a 50 mL Falcon tube. The cultures were then incubated overnight at 37ºC with rotary shaking at 250 rpm. Subsequently, a sub-culture was made with 50 mL of BHI media in a sterile 250 mL conical flask to an OD_{600} of 0.05-0.1, and then grown to exponential phase at 37ºC on a rotary shaker at 250 rpm.

Strains	Relevant genotype/selection marker	Reference
SH1332	RN4220 pYL112 Δ19, a plasmid carrying the L45a integrase gene; Cm^R	(Lee *et al*., 1991)
SH4861	(USA300) Leukocidin family SAUSA300_1974 disrupted by Tn *bursa aurealis* Ery^R Lin^R	This study
SH4862	(USA300) Leukocidin family SAUSA300_1975 disrupted by::Tn *bursa aurealis* Ery^R Lin^R	This study
SH4854	(USA300) *lspA*::Tn *bursa aurealis* Ery^R Lin^R	This study
SH4851	(USA300) *saeS*::Tn *bursa aurealis* Ery^R Lin^R	This study
SH4860	(USA300) *purB*::Tn *bursa aurealis* Ery^R Lin^R	This study
SH4850	(USA300) *tatC*::Tn *bursa aurealis* Ery^R Lin^R	This study
SH4859	(USA300) *fumC*::Tn *bursa aurealis* Ery^R Lin^R	This study
SH4863	(USA300) *hlgA*::Tn *bursa aurealis* Ery^R Lin^R	This study
SH4858	(USA300) *udk*::Tn *bursa aurealis* Ery^R Lin^R	This study
SH4856	(USA300) pyruvate ferredoxin oxidoreductase, α subunit SAUSA300)1182 Tn *bursa aurealis* Ery^R Lin^R	This study
SH4852	(USA300) *clpP*::Tn *bursa aurealis* Ery^R Lin^R	This study
SH4857	(USA300) Hypothetical protein SAUSA300_1494 disrupted by Tn *bursa aurealis* Ery^R Lin^R	This study
SH4848	(USA300) Putative ribose operon repressor SAUSA300_0265 disrupted by Tn *bursa aurealis* Ery^R Lin^R	This study

SH4853	(USA300) Putative membrane protein SAUSA300_0917 disrupted by Tn *bursa aurealis* Ery^R Lin^R	This study
SH4847	(USA300) Putative membrane protein SAUSA300_0230 disrupted by Tn *bursa aurealis* Ery^R Lin^R	This study
SH4849	(USA300) Glycerol-3-phosphate transporter SAUSA300_0337 disrupted by Tn *bursa aurealis* Ery^R Lin^R	This study
SH4855	(USA300) Conserved hypothetical protein SAUSA300_1180 disrupted by Tn *bursa aurealis* Ery^R Lin^R	This study
SH4276	(USA300) JE2, USA300 LAC strain cured of plasmids p01 and p03	(Fey *et al*., 2013)
SH4868	(USA300) JE2 *geh:: ezrA*-eMos*;* Kan^R	This study
SH4866	(USA300) SJF4854 *geh:: ezrA*-eMos-*lspA;* Kan^R	This study
SH4867	(USA300) SJF4854 *geh:: ezrA*-eMos*;* Kan^R	This study
SH4864	(*S. aureus* 8325) *ΔclpP, clpP* depletion strain	(Michel *et al*., 2006)
SH4865	(*S. aureus* 8325) *ΔclpP,* containing pHPS9*clpP*	(Michel *et al*., 2006)

Table 2.2 *S. aureus* strains used in this project. Ery^R, erythromycin resistance; Lin^R, lincomycin resistance; Cm^R, chloramphenicol resistance; Kan^R, kanamycin resistance.

2.3.3 *Escherichia coli* strains

E. coli strains were grown and stored with same method as *S. aureus* strains, except using LB broth and agar instead of BHI. All *E. coli* strains used in this study are listed in Table 2.3.

2.3.4 Plasmids

Plasmids used in this study were purified by a GeneJET Plasmid *Miniprep* kit. Plasmids used in this study are given in Table 2.4.

2.3.5 Bacteriophage

For genetic transduction between strains, the bacteriophage Φ11 was used in this study (Mani *et al*., 1993) .

Strains	Relevant genotype/selection marker	Reference
Top 10	*F- mcrA Δ(mrr-hsdRMS-mcrBC) Φ80lacZΔM15 ΔlacX74 recA1 araD139 Δ(araleu)7697 galU galK rpsL (StrR) endA1 nupG*	Invitrogen
SJF4179	Top10 pGM074; Amp^R	Gareth Mc Vicker
SJF4045	Top 10 pKASBAR with Tet cassette replaced by Kan cassette that was amplified from pGL433b; Amp^R Kan^R	Amy Bottomley
SJF4056	Top 10 pGM073 is pKASBAR + *ezrA-psmOrange*; Amp^R	Gareth Mc Vicker

Table 2.3. *E. coli* strains used in this study. Kan^R, kanamycin resistance; Amp^R, ampicillin resistant.

Plasmids	Relevant genotype/selection marker	Reference
pKASBAR	Hybrid vector of pCL84 and pUC18 for integration into *S. aureus* lipase gene (geh) encoding the attP integration site of L54a phage; Amp^R (*E. coli*), Tet^R (*S. aureus*)	(Bottomley *et al*., 2014)
pKASBAR-Kan^R	Kanamycin resistant derivative of pKASBAR; Amp^R (*E. coli*), Kan^R (*S. aureus*)	(Bottomley *et al*., 2014)
pGM073	pKASBAR containing ezrA-psmorange under the putative *ezrA* promoter; Amp^R (*E. coli*), Tet^R (*S. aureus*)	Gareth McVicker
pGM074	pKASBAR containing ezrA-psmorange under the putative *ezrA* promoter; Amp^R (*E. coli*), Kan^R (*S. aureus*)	Gareth McVicker

Table 2.4. Plasmids used in this study.

2.4 Determination of bacterial cell density

2.4.1 Spectrophotometric measurement

Bacterial density was quantified by spectrophotometric reading at 600 nm (OD_{600}). A Biochrom WPA Biowave DNA spectrophotometer and a Jenway 6100 spectrophotometer were used to measure OD_{600} of individual bacterial cultures. Samples were diluted 1:10 in fresh media to achieve a measurable concentration when appropriate.

A Perkin VICTOR x3 2030 plate reader or a VARIOSKAN FLASH plate reader were used for OD_{600} measurement of NTML strains with orbital shaking at fast speed for 0.2 sec before reading.

2.4.2 Direct cell count

Colony forming unit (CFU) count results were obtained using the Miles and Misra method (Miles *et al*., 1938) as follows. The bacterial inoculum was serially diluted as 1x volume of suspension added to 9x volume of PBS buffer up to 10^8 fold, with a fresh pipette tip used for each dilution. Three 10µl drops of each dilution were applied onto the surface of BHI agar. The plates were kept on the bench (RT) to dry before overnight incubation at 37^{o}C. The dilution which yielded 15-50 full-size discrete colonies was noted and in which the colonies were counted. The CFU count per ml was calculated by using the following equation: CFU/mL = Average number of colonies for a given dilution x 100 x the dilution factor.

2.5 Buffers and solutions

All buffers and solutions were made with dH_2O, stored at RT, and sterilized by autoclaving when necessary, unless otherwise stated.

2.5.1 Phosphate buffered saline (PBS)

NaCl	8g/L
Na_2HPO_4	1.4g/L
KCl	0.2g/L
KH_2PO_4	0.2g/L

The pH of PBS buffer was adjusted to 7.4 with NaOH.

2.5.2 Phage buffer

$MgSO_4$	1mM
$CaCl_2$	4mM
NaCl	0.6%(w/v)
Tris-HCl pH 7.8	50mM
Gelatin	0.1% (w/v)

2.5.3 TAE (50x)

Tris	242g/L
Na_2EDTA pH 8.0	0.05M
Glacial acetic acid	5.7% (v/v)

TAE working solution was made by diluting 50x stock solution 1:50 with dH_2O.

2.5.4 DNA loading buffer (6x)

Bromophenol blue	0.25% (w/v)
Xylene cyanol FF	0.25% (w/v)
Glycerol	30% (v/v)

2.5.5 Chemicals and enzymes

All chemicals and enzymes used in this study were of analytical grade level. Chemicals were purchased from Sigma or Fisher Scientific. All restriction enzymes, polymerases, Gibson assembly mix kit, DNase and corresponding buffers were purchased from New England Biolabs or Fermentas. The stock solutions' concentrations and storage of chemicals used in this study is listed in Table 2.5.

Stock solution	Concentration	Solvent	Storage
Lysostaphin	5 mg/mL	20 mM sodium acetate pH 5.2	-20°C
Saponin	1% (w/v)		RT
Adenine	20 mg/ml	0.5 M HCl	-20°C
Inosine	50 mg/ml	dH_2O	-20°C

Table 2.5. Storage and concentration of stock solutions of chemicals used in this study.

2.6 DNA purification techniques

2.6.1 Genomic DNA purification

A QIAGEN DNeasy Blood & Tissue kit was used to extract and purify genomic DNA. *S. aureus* strains were incubated overnight, then 1 mL of the culture was centrifuged at 12,000 g for 3 min. The cell pellet was resuspended in 190 µL of dH_2O followed by addition of 10 µL of stock lysostaphin and incubation at 37°C for 2 hr. The genomic DNA isolation was conducted following the manufacture's protocol afterwards.

2.6.2 Plasmid DNA purification

A GeneJET Plasmid *Miniprep* kit was used to purify plasmids from *E. coli* based on the manufacturer's instructions.

2.6.3 PCR productions purification

A GeneJET PCR Purification kit was used to purify amplified DNA fragments from PCR reactions based on the manufacturer's instructions.

2.6.4 Gel extraction of DNA

The target band of DNA was excised from a 1% (w/v) TAE agarose gel strained with 0.5 µg/mL ethidium bromide using a UV transilluminator. A GeneJET Gel Extraction kit was used to purify DNA from the gel slice following manufacturer's protocol.

2.7 *In vitro* DNA manipulation techniques

2.7.1 Primer design

Primers used for PCR reactions in this study are listed in Table 2.6. They were oligonucleotides (usually 20-50 nucleotides) synthesised based on the DNA sequences of *S. aureus* USA300 FPR3757 strains and plamids pGM073 and pGM074. Restriction enzyme cut sites were introduced at the 5' end of primers when necessary for cloning. Primers used

to amplify DNA fragments used in transformation were ~20 nucleotides while the primers for Gibson assembly were ~50 base pairs long. Primers were designed with NCBI Primer-BLAST tool (http://www.ncbi.nlm.nih.gov/tools/primer-blast/) and further checked using OligoAnalyzer tool (eu.idtdna.com/calc/analyser) to rule out potential hairpin formation. The primers were synthesised by Eurofins MWG operon (http://www.eurofinsdna.com) and prepared in sdH_2O. The stock and working concentrations of primers were 100 µM and 10 µM separately. Primers were stored at -20^oC before use.

2.7.2 PCR amplification

2.7.2.1 Phusion polymerase

High Fidelity phusion polymerase (Thermo Scientific) has 3'-5' proofreading activity and therefore was used for PCR amplification in this study when the accuracy of product is required. The reaction mix was prepared as below:

Phusion High Fidelity Master Mix (2x)	25 µL
Template DNA	50-200 ng
Forward primer (10 µM)	1 µL
Reverse primer (10 µM)	1 µL
sdH_2O	To 50 µL

Primers	Sequence (5'-3')	Application
USA300_1974F	ACACGTACAGCTACAACAAGTG	Primers used to verify the existence of the transpon insertion in the strain corresponding to the USA300 strain number given in the primer name.
USA300_1974R	TCGCCCATAAATTTCCATTTCGT	
USA300_1975F	GCAGCAACGACTCAAGCAAA	
USA300_1975R	TGAATCGAATTTACCACCTGAGC	
USA300_0994F	AGGCCCATACGATGCGAAAG	
USA300_0994R	TGCTGCTGCAACTCTTCCAA	
USA300_1889F	CGCTATGAAGCATGGTTAGAAGT	
USA300_1889R	GCGTTGCAATGTTTGCGTTG	
USA300_2365F	AGCCCCTTTAGCCAATCCAT	
USA300_2365R	TGGACCAGTTGGGTCTTGTG	
USA300_0690F	GTCACGAAGTCCCTATGCGT	
USA300_0690R	TGTTGCGTAATTTCAGAAGCCA	
USA300_1801F	CAGCTATTGCTACGGTTGAAGC	
USA300_1801R	ACGTGCATAGCAGTTGGGAA	
USA300_0347F	CCGTGCCATCGGTTCTACTT	
USA300_0347R	GCAATGACAGGCGAAATGT	
USA300_0265F	TGTTGCTAGAGAAGCTGGTGT	
USA300_0265R	TAGCGAAGATTGCAGTGGCA	
USA300_0917F	CGCTGATACTCCAGAAGAAGCAA	
USA300_0917R	GCAATACCGAGCATCATAGCAC	
USA300_1089F	AATGGTGCTGCATGGGGAAT	
USA300_1089R	ACAACTGCAACATCGTCATCT	
USA300_1494F	GCGATGTACAAACTAGCACTCA	
USA300_1494R	ATTCGGATGCGATTCAGGCA	
USA300_1568F	GGCATAGCTGGTGGATCTGG	

USA300_1568R	TTGAACGCCCACGCTCTTTA	
USA300_1180F	TCTCATGTTTTGTTCATCCTCTCA	
USA300_1180R	TGTAACACATCTTCTCTTCTGCAA	
USA300_0337F	GCGGAAGTAAGACTGCCCTT	
USA300_0337R	TGCCCATACCCATTTATTGTTCA	
USA300_0752F	AGGAAAGAGAAAAGCTCAAACA	
USA300_0752R	CCATTGATGCAGCCATACCG	
USA300_1182F	AGGTGCTACTAGCGCATTGA	
USA300_1182R	TCCATAACTTCAGACGCAGGT	
USA300_1092F	AGGACTACCAATATCAGCAGCG	
USA300_1092R	ACAAGCAAGGTTATCATTGCAACA	
USA300_0230F	ACAAAGTGCCCAATCGAACA	
USA300_0230R	TGCTGGCGTAGTTTTAGCAGT	
lspA-F	GAATTCGTACGGGCCCGGGCTTACTTAA CCTCCTTCTCC	Amplification of each individual gene fragment with native promoter region from USA300 JE2 genome for Gibson assembly.
lspA-R	CCATGTAGGCCAAGTCAAATGAATAATT AAGTTCATATTTAATGTCAAAA	
purB-F	GTACGGGCCCGCGGCATCAGTATTAATC TGCCATAGATAATTG	
purB-R	ATCCGGCCATGTAGGCCAGATCTTATGCT AATCCAGCGCG	
pfo-F	TTCGTACGGGCCCGCGGCCTATACCATCT CCTTTATTTCAG	
pfo-R	CCATGTAGGCCAGATCAATTACGTAAGT AAACATTCGAATTG	
clpP-F 1	GTACGGGCCCGCGGCCTATATTTCCTCCT TGTAATAACTG	
clpP-R 1	ATCCGGCCATGTAGGCCAGATCTTATTTT GTTTCAGGTACCATC	

clpP-F 2	GTACGGGCCCGCGGCTATATTTCCTCCTTGTAATAACTGTTACTCATTATTTTACATATT	
clpP-R 2	CGGGATCCGGCCATGTAGGCCAGATCTTATTTTGTTTCAGGTACCATCACTTCATCAA	
lspA-F S	TTAACCTCCTTCTCCTTTTTATTGGAAG	Sequencing primers for confirmation of successful construction of integrated pGM073 plasmid
lspA-R S	GAGTTGTCTCATGGACGATTGATT	
purB-F S	ATCAGTATTAATCTGCCATAGATAA	
purB-R S	TTATGCTAATCCAGCGCGTTCGAA	
pfo-F S	CTATACCATCTCCTTTATTTCAGTAGC	
pfo-R S	CATTCGAATTGGACCCTATCGTC	
pGM074-F	GGTCATTCTCTAACGTACACGAGCGTC	Amplify from each side of the insertion site of pGM074 plasmid to verify successful complement plasmid construct.
pGM074-R	CTTTACACTTTATGCTTCCGGCTCGTA	

Table 2.6. Primers used in this study.

The Veriti Thermal Cycler (Applied Biosystems) was used to carry out PCR reactions. The lid was preheated to 105°C and the following thermal cycling setting was used:

Initial denaturation	1 cycle	98°C	30 s
Denaturation	30 cycles	98°C	15 s
Annealing		48-60°C	15 s
Extension		72°C	15-30 s/kb
Final extension	1 cycle	72°C	7 min

2.7.2.2 *E. coli* colony PCR

For rapid screening of gene insertions in *E. coli*, DreamTaq Green Master Mix (Thermo Scientific) was used for PCR amplification. The reaction mix is prepared as below. A single colony was inoculated onto an agar plate with a sterile toothpick, and then mixed into the reaction mix.

DreamTaq Green Master Mix (2x)	25 µL
Forward primer (10 µM)	1 µL
Reverse primer (10 µM)	1 µL
sdH_2O	23 µL

The reaction was conducted in Veriti Thermal Cycler with pre-heated lid at 105°C followed by the reaction program as below:

Initial denaturation	1 cycle	94°C	1 min

Denaturation	30 cycles	94°C	30 s
Annealing		48-60°C	30 s
Extension		72°C	2 min
Final extension	1 cycle	72°C	7 min

2.7.3 Restriction endonuclease digestion

Restriction enzymes used in this study were purchased from New England Biolabs or Promega. The digestion was carried out with supplied buffer according to the manufacturer's protocols. The reaction was performed at 37°C for 1-3 hr. Targeting DNA fragments were further purified (section 2.6.4) if needed for DNA cloning.

2.7.4 Gibson assembly

The DNA vector was restriction endonuclease digested (section 2.7.3) and purified (section 2.6.4). Gene inserts were PCR amplified (section 2.7.2.1) and purified (section 2.6.3 and 2.6.4). The Gibson assembly was completed in a final volume of 20 µL:

Vector DNA	50 ng
Gene insert	150-250 ng
Gibson Assembly Master mix (2x)	10 µL
sdH_2O	To 20 µL

The assembly mix was incubated at 50°C for 2 hr followed by transformation into competent *E. coli* cells.

2.7.5 Agarose gel electrophoresis

Separation of DNA samples were performed in 1% (w/v) agarose gels stained with 10-15 µL ethidium bromide (Fisher Scientific) in a horizontal electrophoresis gel tank (Life Technologies, Scie-Plas). In 1x TAE buffer, DNA samples were loaded after mixing with 5x DNA loading dye (Thermo Scientific). In a neighbouring well to the sample, 10 µL of Gene Ruler 1kb DNA ladder (Fermentas) was loaded for assessing DNA fragment sizes. The size of DNA ladder fragments are showed in Table 2.7. Gels were run at 120 V for 45-60 min at RT. Then the DNA was visualized at 260 nm and imaged using a UVi Tec Digital camera and UVi Doc Gel documentation system.

2.7.6 DNA sequencing

PCR amplified DNA products and plasmids were sequenced by GATC Biotech. Results were analysed by SnapGene v 3.0.3 or Geneious v 6.0.

2.7.7 DNA concentration measurement

A NanoDrop 3300 fluorospectrometer was used to detect DNA concentration with operating software v.2.8.0. A corresponding blank measurement of either 1 µL of sdH_2O or elution buffer was used to compare to 1 µL of each DNA sample loaded to determine concentration at 260 nm.

Marker	DNA fragment size (bp)
Fermentas Gene Ruler 1 kb DNA ladder	10000
	8000
	6000
	5000
	4000
	3500
	3000
	2500
	2000
	1500
	1000
	750
	500
	250

Table 2.7 DNA fragments of ladder used as size markers for gel electrophoresis in this study.

2.8 Transduction techniques

2.8.1 Phage lysate

A single colony of *S. aureus* donor strain was inoculated in 5 mL of BHI media overnight at 37°C followed by a sub-culture. Phage lysate was made by mixing 5 mL of phage buffer, 100 µL of Φ11 phage lysate and 50 µL of *S. aureus* culture. The lysate was incubated at 25°C stationary for 8-24 hr. Once it had become clear, 50 µL of *S. aureus* culture was added and the lysate was incubated again. This was repeated until saturated *S. aureus* culture has cleared, following which the lysate was filter sterilized (0.2 µm pore size) and stored at 4°C.

2.8.2 Phage transduction

A single colony of *S. aureus* recipient strain was inoculated in 50 mL of LK media in a sterile 250 mL flask overnight at 37°C with shaking at 250 rpm. The culture was then centrifuged at 5,000 g for 10 min to harvest the cells. The pellet was resuspended in 3 mL of LK media. The transduction mixture was prepared by adding 500 µL of recipient culture, 500 µL of phage lysate, 1 mL of fresh LK, and 10 µL of 1 M $CaCl_2$ in a 25 mL Universal tube. The samples were incubated at 37°C stationary for 30 min, and incubated for another 15 min with shaking at 250 rpm. 1 mL of pre-prepared ice cold 0.02 M sodium citrate was added to the samples immediately after the incubation. The mixture was incubated on ice for 5 min. Subsequently the cells were harvested at 5,000 g for 10 min in a centrifuge pre-cooled to 4°C. The pellet was resuspended in 1 mL of ice cold 0.02 M sodium citrate followed by incubation on ice for 45-60 min. Aliquots of 200-300 µL were spread onto LK agar plates with 0.05% (w/v) sodium citrate and selective antibiotics. The plates were incubated at 37°C for 24-96 h. Colonies were spread onto BHI agar with selective antibiotics to confirm the existence of the correct resistance profile.

2.9 Transformation techniques

2.9.1 Transformation of *E. coli*

2.9.1.1 Transformation of chemically competent *E. coli* cells

NEB5α chemically competent *E. coli* cells (New England Biolabs) were thawed on ice. For one 50 µL aliquot of competent cells, 4 µL of assembly reaction or 1 ng of plasmid DNA was added. The mixture was gently swirled and incubated on ice for 30 min. The cells were heat shocked at 42°C for 30-45 sec and removed to ice immediately for 2-5 min. 950 µL of pre-warmed SOC media (New England Biolabs) was added. The cells were incubated at 37°C with shaking at 250 rpm for 1 hr. 100 µL aliquots were spread on LB agar with selective antibiotics. The plates were incubated at 37°C for 12-24 hr.

2.9.1.2 Transformation of electrocompetent *E. coli* cells

E. coli electrocompetent cells (Invitrogen) were defrosted on ice. For a 50 µL aliquot, 1 ng of plasmid DNA or 4 µL of assembly reaction was added and tube was gently swirled. The cells were transferred into a 1 mm electroporation cuvette (Bio-Rad). Electroporation was conducted at 1.75 kV, 25 µF and 200 Ω with a Bio-Rad GenePulser Xcell Electroporation system. The bacteria were covered immediately with 800 µL of pre-warmed SOC media (New England Biolabs) and removed to be incubated at 37°C with shaking at 250 rpm for 1-2 hr. 100 µL aliquots were spread on LB agar with selective antibiotics. The plates were incubated at 37°C for 12-24 hr.

2.9.2 Transformation of *S. aureus*

2.9.2.1 Preparation of *S. aureus* electrocompetent cells

S. aureus RN4220 (SH1332) was streaked on BHI agar and incubated overnight at 37°C. A single colony was inoculated into 400 mL of fresh BHI media and incubated at 37°C with shaking at 250 rpm for 10-12 hr. The cells were sub-cultured in 400 mL of BHI media with 8 µg/mL of CM starting from OD_{600} of 0.1, incubated at 37°C with shaking at 250 rpm until they reach an OD_{600} of 0.4-0.6. The bacteria were harvested by centrifugation at 5,000 g for

10 min at room temperature (RT) in eight 50 mL aliquots. Cells were washed with 25 mL of sdH_2O for 3 times and merged into one tube. The pellet was then washed once with 20 ml of sterile 10% (v/v) glycerol and once, and resuspended in 10 mL of sterile 10% (v/v) glycerol. The bacteria were incubated at RT for 30 min before centrifugation at 5,000g for 10 min. The pellet was resuspended in 1 mL of sterile 10% (v/v) glycerol. Cells were split into 50 µL aliquots and snap-frozen in liquid nitrogen and stored at -80°C.

2.9.2.2 Transformation of electrocompetent *S. aureus* cells

A 25 µL aliquot of electrocompetent *S. aureus* RN4220 cells (section 2.9.2.1) were defrosted on ice. 1 µg of plasmid DNA was added and the tube was gently swirled. The mixture was transferred to a 1 mm electroporation cuvette (Bio-Rad) and electroporated at 2.3 kV, 25 µF and 100 Ω with a Bio-Rad GenePulser Xcell Electroporation system. 1 mL of pre-warmed SOC media (New England Biolabs) was added immediately to recover the cells. *S. aureus* were then transferred into a 15 mL centrifuge tube and incubated at 37°C with shaking at 250 rpm for 3 hr. 200-300 µL aliquots were spread on BHI agar with selective antibiotics. The plates were incubated at 37°C for 12-96 hr.

2.10 Neutrophil cell culture

2.10.1 Ethics

Primary neutrophils were isolated from healthy human peripheral venous blood by Percoll gradient centrifugation. The donors had consented in accordance with a protocol approved by South Sheffield Research Ethics Committee (study number STH13927).

2.10.2 Purification of neutrophils from peripheral blood

Neutrophil isolation was carried out *ex vivo* by following an established Percoll gradient protocol which minimizes activation of neutrophils (Sabroe *et al*., 2005). The experiment

was performed in a sterile class II microbiological safety cabinet (Walker). All the media and solutions used were pre-warmed to 37^{o}C.

Venous blood was drawn and aliquoted into 50 mL centrifuge tubes containing 3.8% v/v sodium citrate (1mL sodium citrate per 9mL blood) (Martindale). Following centrifugation at 1,200 rpm for 20 min at RT, the platelet-rich plasma (PRP) was removed and centrifuged at 2,000 rpm for 20 min to obtain platelet-poor plasma (PPP). Six mL of 6% w/v dextran (Sigma) was added to the remaining blood and topped-up with 0.9% w/v saline to 50mL. After gentle mixing by rolling the sealed tubes, excess blood was removed from the lids and the tubes were left for 30 min (RT) to sediment erythrocytes. Following sedimentation, the upper white cell rich layer was centrifuged at 1,000 rpm for 6 min (RT). A leukocyte-rich population was obtained as a cell pellet. The cells were resuspended with 2mL of PPP and overlayed on to Percoll (Amersham Pharmacia Biotech) gradients prepared in 15mL centrifuge tubes consisting of 2mL of the 51% v/v Percoll/PPP lower phase (1.02mL of Percoll with 0.98mL of PPP) overlayed by 2mL of the 42% v/v Percoll/PPP upper phase (0.84mL of Percoll with 1.16mL of PPP). The gradients were centrifuged at 1,100 rpm for 11 min without a deceleration brake. Three populations of cells were separated: above the upper Percoll layer was situated the PBMC layer, the neutrophils were located in between two Percoll layers (Figure 2.1), while the red cells were pelleted at the bottom of the tube. PBMC were firstly removed to 10mL of PPP. Neutrophils were aspirated from the intermediate phase to 10mL of PPP. Hank's Balanced Salt Solution (HBSS) was added to neutrophils to make up 35mL, and cell counts were counted out using a hemocytometer. Neutrophils were further centrifuged at 1,500 rpm for 6 min (RT) and were resuspended in RPMI (+10% v/v fetal bovine serum (FBS)) at final concentration of 5x10^{6}/mL.

2.10.3 Screening of NTML

2.10.3.1 Preparation of *S. aureus* and *S. aureus* supernatant

USA300 wild type JE2, *S. aureus* strains identified from the screen, and *S. aureus* transductants and complements were prepared from beads stock. The strains were streaked out on BHI agar plates and incubated overnight at 37°C. A single colony was used to inoculate into 5 mL of BHI media and incubated overnight at 37°C with shaking at 250 rpm. The bacterial samples were diluted to OD_{600} of 0.05 in 10mL of BHI the following morning and cultured at 37°C with shaking at 250 rpm for 3 hr. The OD_{600} was measured (section 2.4.1) and the CFU count was determined (section 2.4.2). The culture was split into 100 µL aliquots and stored at -20°C. Before use, the aliquots were thawed and centrifuged at 5,000 g for 3 min. After transferring the supernatant for use, the cell pellet was resuspended in a corresponding volume of RPMI (+10% v/v FBS).

For preparation of NTML bacteria, following Section 2.3.1, the NTML overnight culture was sub-cultured by adding 10 µL of library strains to 190 µL of fresh BHI media and incubated at 37°C for 3 hr before centrifugation at 5,000 g for 10 min to harvest the bacterial. The pellets were resuspended in 200 mL of RPMI (+10% v/v FBS) to maintain original density for use.

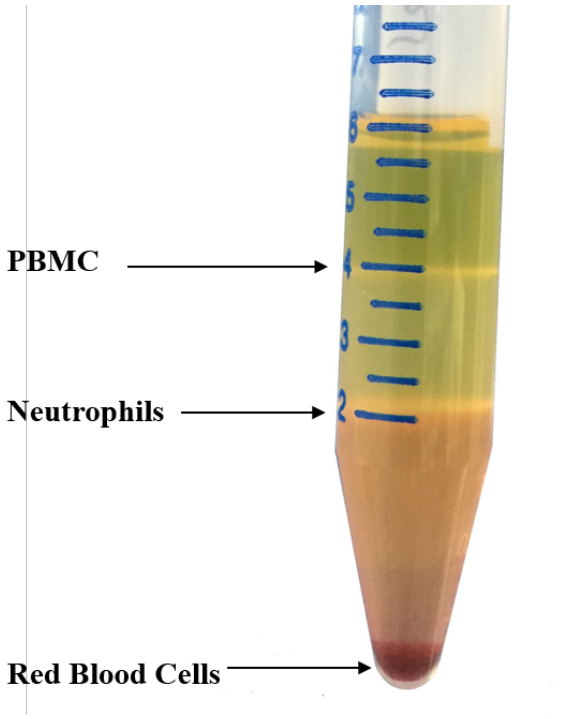

Figure 2.1 Isolation of primary human neutrophils using Percoll gradient centrifugation method.

2.10.3.2 Neutrophil culture/co-culture

Neutrophil cultures were performed in a 96 well plate format. The Nunc 96-well Microplates (Thermo Scientific) were used to meet the requirements of the flow cytometer. 50 µL of neutrophils at $5x10^6$/mL (section 2.10.2) were added to each well together with 45 µL of RPMI (+10% v/v FBS). Five µL of each *S. aureus* (section 2.10.3.1) strain was added to each well to achieve the desired multiplicity of infection (MOI). The plate was incubated in a tissue culture incubator (Sanyo) at 37°C with 5% v/v CO_2. Cells were cultured in duplicate and were taken forward at target time points for cytospin analysis. Apart from NTML plates, an additional plate was included with controls in each experiment. A mixture of 50 µL of neutrophils at $5x10^6$/mL and 50 µL of RPMI (+10% v/v FBS) was added to each of 3 wells as media controls. The 4th well consisted of 50 µL of neutrophils at $5x10^6$/mL, 45 µL of RPMI (+10% v/v FBS), and 5 µL of USA300 wild type JE2. The co-culture of neutrophils and *S. aureus* for the screen of NTML was performed at MOI of 10 and the plates were incubated for 3 hr (Figure 2.2).

2.10.3.3 ToPro-3 staining

ToPro-3 (Molecular Probes, Invitrogen) is a vital dye that only generates a fluorescent signal when entering cells lost membrane integrity, and intercalated with DNA. It is used for neutrophil cell lysis measurement. After 3 hr of neutrophil-NTML co-culture (section 2.10.3.2), 100 µL of sterile PBS was added to the 1st media control (unstained); the 2nd media control sample was frozen at -80°C for 5 min, thawed and vortexed at highest speed, and strained with 100 µL of ToPro-3 (1:10,000 in sterile PBS) (positive control). 100 µL of ToPro-3 (1:10,000) was added to the 3rd media control (media control for baseline) and every well of neutrophil-*S. aureus* co-culture to make final volume of 200 µL. The ToPro-3 staining was performed avoiding excessive exposure to light.

2.10.4 Assessment of neutrophil viability

2.10.4.1 Morphological assessment

A monolayer of neutrophil-*S. aureus* co-culture was generated by adding 100 µL cell suspension from each well and centrifuging onto glass slides at 300 rpm for 2 min in a neutrophil-monolayers-forming set chamber and a cytospin centrifuge (Sanyo). The cells were dried at RT and fixed by methanol. Red and blue Giemsa Wright dye (Diff Quick) was used to stain the bacteria and neutrophils. Subsequently a glass coverslip was fixed to the glass slide using DPX mount reagent (BDH) and dried overnight in a fume hood. The morphology of cells was assessed using light microscopy at 1,000x magnification under an oil immersion lens.

Neutrophil cell lysis was assessed based on morphological features including lack of chromatin bridges, cell shrinkage, cell swelling, and nuclear condensation (Hamasaki *et al*., 1998). In phagocytic index assays, duplicate slides of each sample were visually assessed, and the number of viable neutrophils with and without engulfed *S. aureus*, and engulfed *S. aureus* cells were counted from one slide. At least 300 neutrophils were counted per slide for phagocytic index quantification.

2.10.4.2 Flow cytometric detection

An Applied BioSystem Attune Acoustic Focusing Cytometer (Thermo Scientific) was used to assess neutrophil viability. The plates containing neutrophil media controls and co-culture samples were run through the Attune plate reader system at a speed of 500µL/min and stopped once 70µL of each sample has been aspirated. Neutrophils were recorded at a forward scatter (FSC) of 1600, side scatter (SSC) of 2700, and RL1 channel of 1250 for ToPro-3.

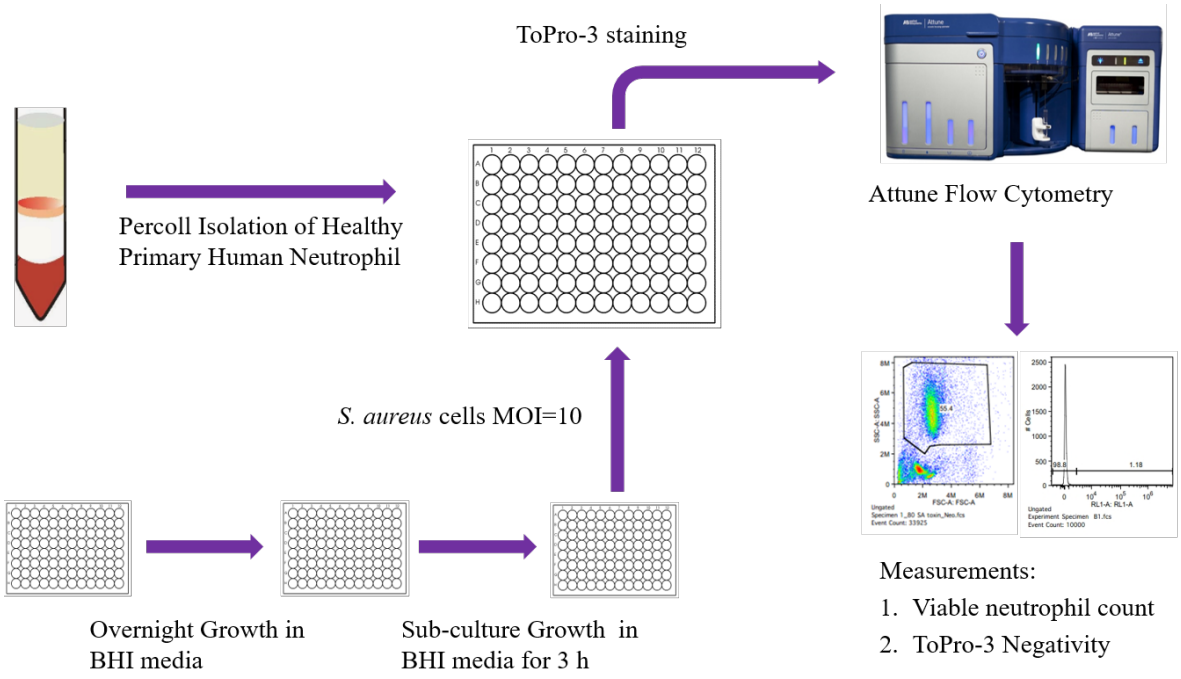

Figure 2.2. Working flow chart of the main procedures involved in the screen of NTML. Neutrophils isolated from healthy human blood by Percoll gradient centrifugation were incubated with each *S. aureus* mutant produced from an overnight culture and 3 hr sub-culture in BHI at MOI of 10, in a 96 well plate format. ToPro-3 (1:10,000) was used to stain the cells for cell death measurement. The assay result as identified by viable neutrophil cell count and ToPro-3 negativity was measured by Attune flow cytometry. The data was further analysed by FlowJo software.

2.10.4.3 Quantification of absolute viable neutrophil numbers and ToPro-3 intensity

The recorded flow cytometric data was analysed by FlowJo™ cytometry analysis software (TreeStar). The FSC/SSC dot plot of PBS stained media control was used to verify the viability of neutrophils in each experiment. The area where viable neutrophils locate was gated to generate an automatic viable neutrophil cell count. The gate was applied to the whole group to count absolute viable neutrophils of each sample.

The Cell count/RL1 histogram of PBS stained media control was used to set up the baseline of negative ToPro-3 intensity. The baseline was applied to all other samples and ToPro-3 staining was verified by the positive intensity produced by the Freeze/thaw (F/T) media controls (section 2.10.3.3). The exported absolute viable neutrophil counts and ToPro-3 intensity were further analysed using GraphPad Prism v. 6.0 (GraphPad).

2.10.5 Lysostaphin pulse chase neutrophilic bacterial killing assay

Lysostaphin pulse chase method was used in neutrophilic bacterial killing assay to quantify intracellular surviving bacterial without influences from extracellular activity. It relies on the principle that lysostaphin kills extracellular *S. aureus* rapidly, but not penetrating the neutrophils and therefore not affecting intracellular bacteria (Easmon *et al*., 1978). This assay was carried out to allow enumeration of surviving bacteria following an initial phagocytosis period.

Neutrophils were infected at an MOI of 5 as described at section 2.10.3.2. Triplicates of each treatment was prepared for determining bacterial number at different time points. The time course for co-incubation was initial infection of 90 min, followed by 30 min with lysostaphin (20 μg/mL) (Sigma). After 30 min of incubation, one sample of each treatment was centrifuged at 2,000 rpm for 2 min. The pellets were resuspended with 200 μL of 1% saponin (w/v in PBS) (Sigma) and incubated at RT with regular pipetting and vortexing for

10 min. Following this the intracellular *S. aureus* load was determined by Miles and Misra method described in section 2.4.2. The intracellular bacterial number of a second sample of each treatment was measured again after 90 min of co-incubation. Meanwhile, lysostaphin was added to the 3rd group of samples at 90 min and incubated further for 30 min to kill extracellular *S. aureus*. The post lysostaphin neutrophils were lysed by saponin and plated out with same method.

2.11 Fluorescent microscopy imaging

To explore if mutant strains display different phagosome interactions comparing to WT, *S. aureus* and neutrophils were labelled with fluorescent markers for the phagocytic index assay. The fluorescent staining and fixing of cells, and imaging was carried out at RT avoiding exposure to light. All buffers used for washing in staining procedures contain 1% BSA (w/v Sigma).

2.11.1 Alexa Fluor 647 and pHrodo staining of *S. aureus* and pKH67 staining of neutrophils

A total of $5x10^8$ *S. aureus* (Section 2.10.3.1) were aliquoted and centrifuged at 5,000 g for 3 min. The supernatant was removed and the pellet was resuspended in 200 µL of PBS (pH 9). Then 5 µL of Alexa Fluor 647 (10mg/mL) (Thermo Scientific) and 0.2 µL of pHrodo (10mM) (Thermo Scientific) was added and vortexed. The mixture was incubated avoiding light at 37°C with shaking at 200 rpm for 30 min. The stained bacteria were washed with 500 µL of PBS (pH 8) and centrifuged at 13,200 rpm for 3 min. The pellet was washed again with 500 µL of 25mM Tris (pH 8.5) and centrifuged at 13,200 rpm for 3 min. The sample was resuspended in PBS (pH 7.4) for use.

The co-culture of stained *S. aureus* with neutrophils was performed with the same method as section 2.10.3.2 at MOI of 5. After the co-incubation, the samples were centrifuged at

400 g for 5 min. Supernatant was removed carefully and the pellet resuspended in 250 µL of Diluent C from the pKH67 kit (Sigma-Aldrich). Protected from light, 1 µL of pKH67 (Signma-Aldrich), a green fluorescent dye used for neutrophil cell membrane labelling, was added and the mixture was incubated at RT for 5 min with regular mixing. 500 µL of heat inactivated FBS was added and incubated for 1 min at RT to stop the staining. The cells were harvested by centrifugation at 400 g for 10 min. The pellet was gently washed with 500 µL of PBS (pH 7.2) three times and resuspended with 100 µL of PBS for fixing.

2.11.2 Fixing and staining for fluorescence microscopy

The stained *S. aureus* infected neutrophils (section 2.11.1) were centrifuged onto round coverslips (which were temporarily placed onto microscope slides) at 300 rpm for 2 min in a cytospin centrifuge (Sanyo). The slides were air-dried at RT and incubated with 50 µL paraformaldehyde (4% w/v) for 15 min. The slides were washed three times with 50 µL PBS for 5 min. The fixed cells were stained with 50 µL DAPI (1:10,000 in PBS) and incubated for 15 min. The slides were again washed three times with 50 µL of PBS for 5 min. Fluoromount G-12 was used to fix the coverslip upside down onto a glass slide. The slides were dried in fume hood overnight and stored at -4^{o}C.

2.11.3 Olympus upright fluorescence microscope imaging

The cells (Section 2.11.2) were visualised using an Olympus upright fluorescence microscope and fluorescence images were acquired using the imaging software. The wavelengths of the fluorophores and corresponding filters used are listed in Table 2.8. The exposure time, contrast and brightness was adjusted using the software settings before taking photos.

Fluorophores	Excitation wavelength	Emission wavelength	Filter
Alexa Fluor 647	633	Far-red	Cy5
pKH67	490 nm	502 nm	FITC
DAPI	358 nm	461 nm	DAPI
pHrodo	532 nm	585 nm	TxRed

Table 2.8 The excitation and emission wavelength and corresponding filters of fluorophores used in this study.

2.11.4 ImageJ analysis

All fluorescent images (section 2.11.3) were analysed as type 8-bit using Fiji (ImageJ). Different channels were merged. Intact neutrophils were manually drawn around the cell area based on DAPI and pKH67 staining, and added to the software manager. A Bug-counter program was used to count *S. aureus* numbers in each neutrophil.

2.12 Zebrafish techniques

2.12.1 Zebrafish strains

London Wild Type (LWT) strains were used for all the fish experiments in this thesis.

2.12.2 Ethics

Zebrafish embryos under 120 hr post fertilization are not protected under the Animals (Scientific Procedures) Act 1986 and all experiments were carried out based on this premise.

2.12.3 Zebrafish E3 medium (x10)

The 10 x stock E3 is composed of chemicals below. A working stock (x1) was prepared by diluting in distilled water. A final concentration of $5x10^{-5}$% w/v methylene blue was added to prevent fungal growth (Nusslein-Volhard and Daham, 2002). Subsequently the 1 x E3 medium was autoclaved for 20 min at 121^{o}C and 15 psi.

$MgSO_4$	3.3 mM
$CaCl_2$	3.3 mM
KCl	1.7 mM
NaCl	50 mM

2.12.4 Zebrafish anaesthesia

Zebrafish embryos were anaesthetised in 0.02% (w/v) tricaine for 8 min prior to bacterial injection. The stock solution of 0.4% (w/v) 3-amino bezoic acid ester tricaine (Sigma) was made in 20 mM tris-HCl (pH=7). The stock and working solution was kept in -20^{o}C and -4^{o}C separately in dark.

2.12.5 Methylcellulose

Methylcellulose was prepared as 3.0% (w/v) in E3 medium. The solution was further aliquoted into 20mL syringes and kept in -20 ^{o}C. Each aliquot was thawed in 28.5 ^{o}C before use.

2.12.6 Zebrafish embryo preparation

LWT Zebrafish eggs were marbled from 4-5pm and collected at 10am the next day (Day 0). The eggs were transferred from the tank into a petri dish with aquarium water to prevent potential harm from chlorine. After visual examination using a dissecting microscope (Leica) to check the eggs had developed correctly (reaching the "High stage" in Figure 2.3), the eggs were selected and incubated in E3 medium at 28.5^{o}C in petri dishes.

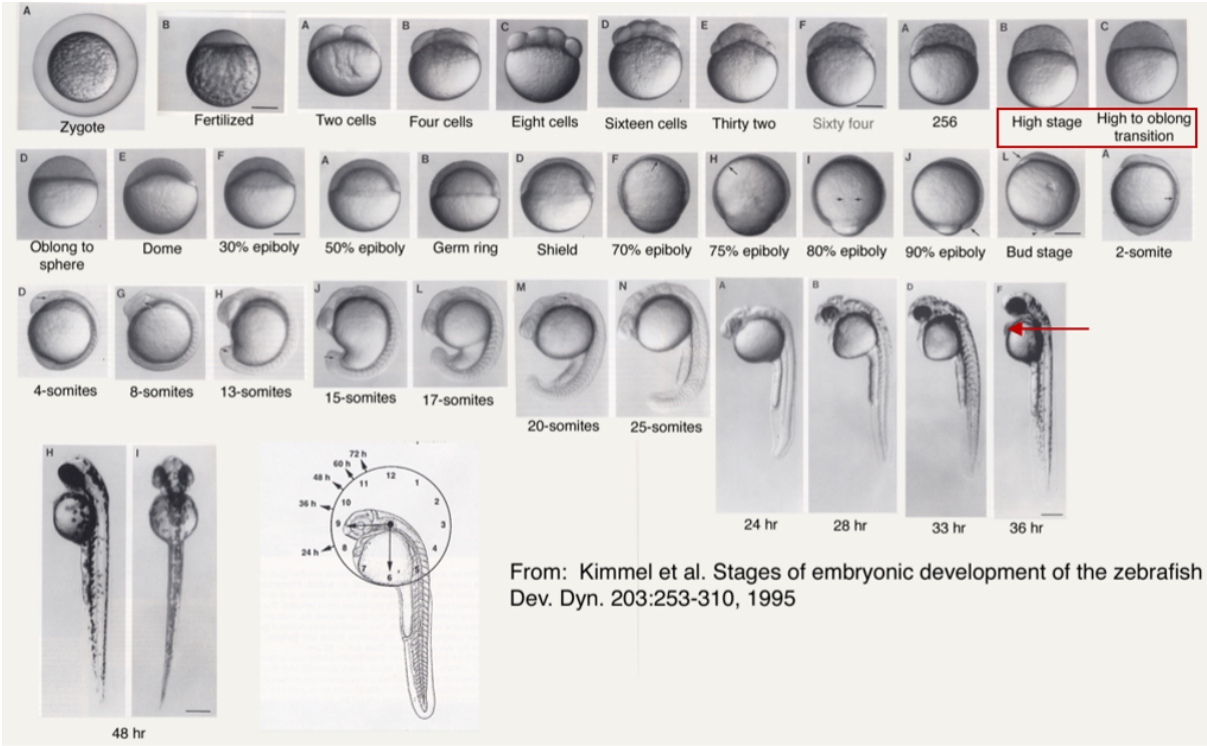

Figure 2.3. Zebrafish development and lifecycle. The embryos at high stage - high to oblong transition stage were picked on day 0 to obtain correct development for this study. The embryos were dechorionized before bacterial injection. Each treatment group contains 20-30 embryos and the injection was performed on day 1. The needle injecting point is at the circulation valley highlighted by the arrow.

Prior to bacterial injection on Day 1, the chorion were removed to leave the embryo free. For survival studies of which around 35 embryos were injected per group, the dechorionation was performed manually. For determination of bacterial growth studies and morpholino oligonucleotide injection studies, of which approximately 120 embryos were injected per group, pronase dechorionation was used for higher efficiency. All zebrafish eggs were covered with pronase solution at a final concentration of 2mg/mL pronase in E3 medium in a glass beaker for 20-25 min at RT. After visual confirmation of thinner chorion, the pronase solution was removed before washing off all the chorion with E3 medium.

2.12.7 *S. aureus* preparation for zebrafish embryos injection

All strains of *S. aureus* used for injecting into embryos were cultured overnight followed by a 3 hr sub-culture from OD_{600} of 0.05±0.01 in a 250mL flask of BHI medium. The bacterial culture was further aliquoted into 15mL centrifuge tubes and kept in -20^{o}C for long-term storage. Each aliquot was thawed, centrifuged, and resuspended in an adjusted volume of PBS for the required dose.

2.12.8 Microinjection of *S. aureus* in zebrafish embryos

Microinjection needles were made by heating and pulling non-filament glass capillary tubes (Kwik-Fil). Then the prepared bacterial suspension was vortexed and loaded to the needle by using the 10µl microcapillary pipette tips (Fisher Scientific Ltd). After mounting the needle to the rig which connected with a pneumatic micropump (WPI, PV820 Pneumatic Picopump), a micromanipulator (WPI, Marzhauser etslar MM33 Rechts) and a gas tank (Boc Linda), the injected volume was calibrated using a graticule slide to approximately 1nL.

Immediately before injections, zebrafish embryos were immersed in 0.02% (w/v) tricaine solution for 8 min and removed onto 3.0% (w/v) methylcellulose. Bacteria was then injected

in the circulation valley of the embryo sideways from the top of the yolk (Figure 2.3). Afterwards, embryos were removed from the methylcellulose into E3 medium in Petri dishes and incubated in 28.5^{o}C for 1 hr to dissolve the remaining methylcellulose. Following one wash with E3 medium, embryos were transferred to individual wells of 96 well plates with 100µL E3.

To verify the amount of injected bacteria, both pre-injection and post-injection doses were quantified by diluting 4 injections in 1mL sterile PBS. Five 10µl drops were spotted onto BHI agar. After overnight incubation at 37^{o}C, the number of CFU was calculated from the counts.

2.12.9 Post injection determination of zebrafish embryo mortality

Each *S. aureus* strain was injected into 20-30 embryos for survival studies. The mortality of zebrafish was carried out by visual assessment based on cessation of heartbeat and circulation. Standard time points are 20, 26, 44, 50, 68, 74, 92 hr after injection.

2.12.10 Bacterial growth determination of *S. aureus* in zebrafish

Five viable and all dead zebrafish embryos of each standard time point (showed in section 2.6.9) were transferred along with 100µl E3 medium to ceramic bead-containing 0.5mL microtubes (Alphalabs,). Embryos were homogenised for 30 seconds (Precellys 24) and serially diluted in sterile PBS followed by full plating of 100µl onto BHI agar. CFU were calculated accordingly based on colony counts obtained after overnight incubation at 37^{o}C.

2.12.11 Microinjection of pu.1 morpholino modified antisense oligonucleotides in zebrafish embryos

Pu.1 morpholino modified antisense oligonucleotides sequence is showed below (Gene Tools). The injection of morpholinos binds to complementary bases specifically and

prevents translation of the genes (Rhodes *et al*., 2005). The existence of morpholino oligonucleotides knocked down the translation start codon (ATG).

Morpholino target	Sequence 5'-3'
Pu. 1	GATATACTGATACTCCATTGGTGGT

2.12.12 Microinjection of pu.1 morpholino oligonucleotides into zebrafish eggs

A working solution at concentration of 1 mM of pu.1 morpholino was made from 2 mM stock solutions in distilled water. The oligonucleotides were injected into the yolk sac of embryos within 30 min after fertilisation (1 to 4 cells stage in Figure 2.3). The same method of microinjection was used as described in section 2.6.8.

2.13 Statistical analysis

All survival studies and pu.1 experiments were repeated for 3 times with around 30 injected zebrafish embryos per strain. The Kaplan-Meier method was applied for the survival curves. The log-rank (Mantel Cox) test was done to compare survival curves of different strains. Regarding the determination of bacterial growth in zebrafish experiments, 96 zebrafish embryos were injected per strain for N of 1. The replicates of data were not combined due to zebrafish batch variation.

All statistical analysis was completed by GraphPad Prism Version 6.0. Representative data are shown from repeating experiments. The significant difference was labelled as: * $p<0.05$, ** $p<0.01$, *** $p<0.001$, ns=non-significant.

Chapter 3

Optimisation for the NTML Screen

3.1 Introduction

S. aureus has long been recognised as a highly adaptive and dangerous human pathogen. It has rapidly evolved antibiotic resistance mechanisms and has a multitude of pathogenesis factors that subvert the host innate immune system. Neutrophils and macrophages are crucial elements of our defence against *S. aureus* yet *S. aureus* renders neutrophils ineffective on many levels. *S. aureus* produces several exotoxins, most notably PVL, to cause rapid and profound neutrophil cell lysis. In order to identify novel *S. aureus* factors involved in neutrophil cell death, a genome-wide *S. aureus* screen in a human neutrophil cell death assay was carried out.

The Nebraska Transposon Mutant Library (NTML) containing 1952 mutated *S. aureus* strains has been used in several studies of antimicrobial resistance and virulence gene function (Fey *et al*., 2013). The library was previously screened for increased susceptibility to antimicrobials including vancomycin, gentamicin, linezolid, ciprofloxacin, oxacillin, and daptomycin. Sixty-eight mutants were identified with roles in intrinsic antimicrobial resistance of *S. aureus* (Vestergaard *et al*., 2016, Johnston *et al*., 2016). In addition, the NTML was used to analyse the modulation of *sigS* expression (Burda *et al*., 2014). Finally, in a *S. aureus- P. aeruginosa* interaction study, the NTML revealed the importance of nine *S. aureus* genes in forming a thickened colony morphology at the cooperative *S. aureus- P. aeruginosa* interface (Frydenlund Michelsen *et al*., 2016).

These studies demonstrate that an unbiased screening methodology is a powerful strategy to identify genes involved in bacterial function. Yet none of the previous NTML screens

involved the study of human immune responses to *S. aureus.* I have set out to establish a novel NTML screen in a human neutrophil cell death assay in order to identify genetic mutants which fail to induce neutrophil death. The specific aim of this chapter is to establish and optimise the screening protocol.

The interaction of *S. aureus* and neutrophils can be assessed by flow cytometry, as a widely-used laser-based technology which can be applied to the detection and characterization of different cell types in a heterogeneous population (Anwar *et al.*, 2009). The analysis of individual cells is carried out simultaneously across multiple parameters. Measurements of cell size, granularity, and fluorescence intensity of ToPro-3 (for neutrophil cell death measurement) allow accurate assessment of neutrophil viability. The Attune flow cytometer comes with laser trimming technology which enables automatic counting of cells in each sample, thereby estimating cell loss. Another distinct advantage of the Attune for high-throughput studies is the plate reader component with automatic washing and re-sets, allowing sample acquisition from a 96 well plate. Therefore, the Attune flow cytometer was selected for the high-throughput screen of NTML.

Results

3.2 Growth curve and CFU assessment of JE2

The numbers of *S. aureus* required for the screen co-incubation was calculated based on three MOI (Table 3.1). The absolute neutrophil number per well was $2.5x10^5$ based on using 50µl of cell suspension at $5x10^6$/ml in a final volume of 100µl.

Neutrophils/well	**MOI**	***S. aureus* Volume (µl)**	***S. aureus* CFU/ml**
$5x10^6$/ml x 50µl $=2.5\ x10^5$	2	50	$1.0\ x10^7$
	5	50	$2.5\ x10^7$
	10	50	$5.0\ x10^7$

Table 3.1. Neutrophils vs *S. aureus* screen parameters. The bacterial density of *S. aureus* required was calculated under screen design as 50 µl neutrophils added with 50 µl bacterial suspension per well. Neutrophils were cultured at an optimal density ($5x10^6$/ml) prior to co-incubation. Therefore, the concentration of *S. aureus* required for screen at different MOI was calculated based on the equation below. MOI: multiplicity of infection; CFU: colony forming unit.

CFU of *S. aureus* = (No. of neutrophils/well) x MOI / *S. aureus* Volume

Since the screen would need to be carried out in RPMI (+10% v/v FBS), because the first optimization experiment was to verify the growth of WT *S. aureus* in RPMI (+10% v/v FBS). Sub-culturing *S. aureus* in RPMI before incubating with neutrophils in the screen will allow the bacteria to become acclimatised to a 'non-standard' growth medium. BHI was used as control since it is a rich media for *S. aureus* growth.

JE2 follows a typical growth curve and grows exponentially after 2 hrs in both BHI and RPMI (Figure 3.1). In RPMI, *S. aureus* enters stationary phase after 4 hr (Figure 3.1, B), compared with 6 hrs for BHI (Figure 3.1, A). The maximal density in RPMI (+10% v/v FBS) (OD_{600}=0.554±0.03) is ten-fold lower than in BHI cultures (OD_{600}=5.59±0.02). This therefore raised concerns that sub-culture in RPMI media prior to infection with neutrophils in the screen will not yield sufficient CFU/mL.

To assess if *S. aureus* can grow to an appropriate density in 96 well plates, taking into consideration the NTML screen format, JE2 was cultured in 96 well plates as per the planned screen design: 3 hr incubation of a single colony in BHI followed by 1:20 culture in BHI or RPMI (+10% v/v FBS) for overnight incubation, followed by a 2 or 3-hr sub-culture (1:20) in corresponding media (i.e. BHI to BHI & RPMI to RPMI).

The average OD_{600} value of BHI culture was higher than that of RPMI (+10% v/v FBS) cultures at both 2 and 3 hr (Table 3.2), which is consistent with the CFU counts (BHI: $5x10^8$/mL compared to $5x10^7$/mL for RPMI at 3hr). For infection of neutrophils at the highest MOI of 10, the CFU/mL required for original *S. aureus* inocula is 5.0 $x10^7$/ml (Table 3.1). which equals the CFU yield at 3 hr of RPMI sub-culture (Table 3.2). Therefore, sufficient wild type *S. aureus* cells were produced from both BHI and RPMI (+10% v/v FBS) after 3 hrs sub-culture.

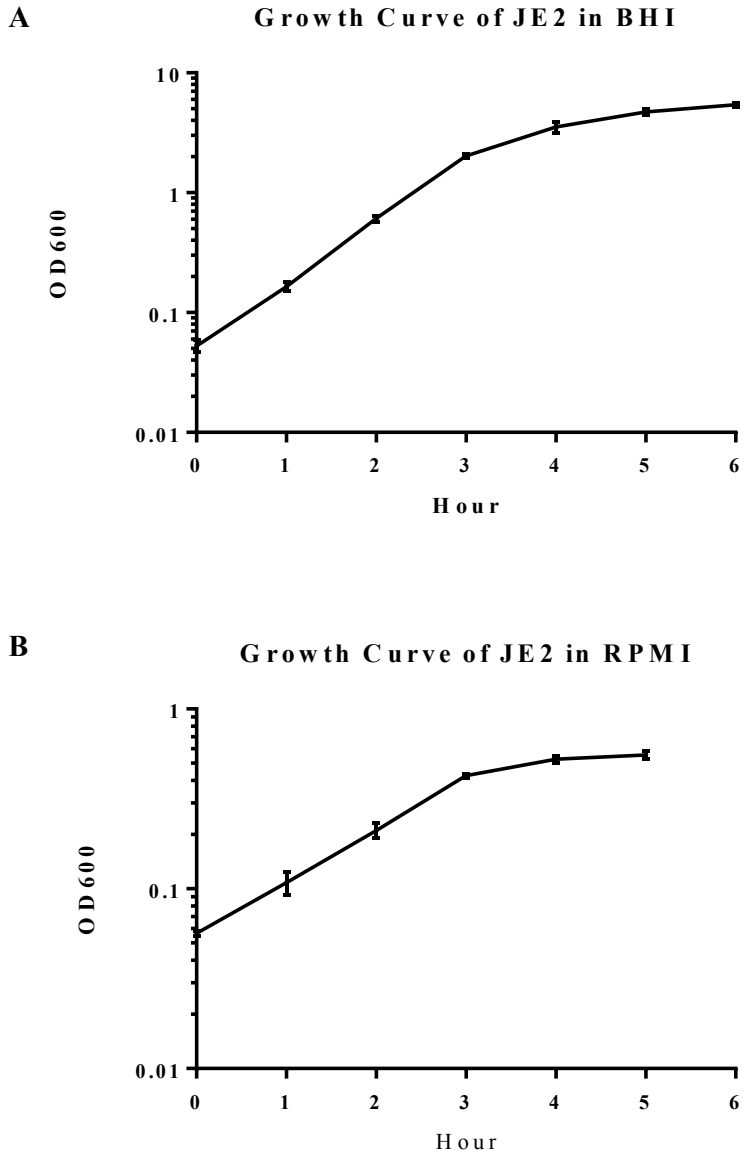

Figure 3.1 Growth curves of *S. aureus* JE2. Standard deviations are shown as error bars.

(A). JE2 was grown in BHI media after an inoculation to an OD_{600} of 0.05 at 37°C in a 5mL culture. N=3

(B). JE2 was grown in RPMI (10% v/v FBS) after an inoculation to an OD_{600} of 0.05 at 37°C in a 5mL culture. N=3

Notes: the standard deviation of some timepoints are too small to be visualized.

Media	Sub-culture	Average OD_{600}	CFU/ml±SD
BHI	2hr	0.334±0.028	(4.5±1.5) $x10^8$
	3hr	0.401±0.032	(5.0±1.9) $x10^8$
RPMI (+10% v/v FBS)	2hr	0.165±0.018	(7.0±3.0) $x10^6$
	3hr	0.241±0.011	(5.0±1.6) $x10^7$

Table 3.2. Growth and CFU of *S. aureus* JE2 in 96 well plate format.

JE2 was sub-cultured (1:20 v/v) in either BHI or RPMI (+10% v/v FBS) after an overnight culture in 96 well plate format at 37°C in 200µL media. N=3

SD: standard deviation

3.3 Growth curve of the NTML library

In order to further develop the screen protocol, the growth conditions for the NTML library required optimisation. After validation of wild type *S. aureus* growth, a single NTML plate (plate 1B, containing 96 mutants), chosen at random, was cultured in combinations of RPMI (+10% v/v FBS) and BHI to ascertain the growth rates of the mutants. Under the conditions of the screen, combinations of media were used in order that *S. aureus* could be sub-cultured in RPMI (+10% v/v FBS) immediately prior to the neutrophil screen. This is important to know, since culturing *S. aureus* entirely in BHI and then transferring to neutrophil cultures in RPMI (+10% v/v FBS) may mean the bacteria undergo a period of shock and therefore turn off important genes involved in pathogenesis.

Plate 1B was thawed on ice for 30min, sub-cultured to another plate and incubated overnight in either RPMI (+10% v/v FBS) or BHI and then sub-cultured for 1-5 hrs, in either RPMI (+10% v/v FBS) or BHI. Initial experiments showed a lack of growth in RPMI (+10% v/v FBS) under the conditions to be used for the screen (data not shown). For bacteria that were cultured overnight in BHI and sub-cultured in BHI, a consistent increase in OD_{600} was observed between 1 hr (0.075 ± 0.011) and 5 hr (0.461±0.050), which demonstrates regular *S. aureus* growth (Figure 3.2). Hence, to ensure productive growth of *S. aureus*, NTML strains will be incubated overnight in BHI media followed by a 3 hrs sub-culture in BHI for the screen. Although changing the culturing media from BHI to RPMI (+10% v/v FBS) is not the most ideal condition for NTML strains, sufficient bacterial growth was prioritised over *S. aureus* functionality.

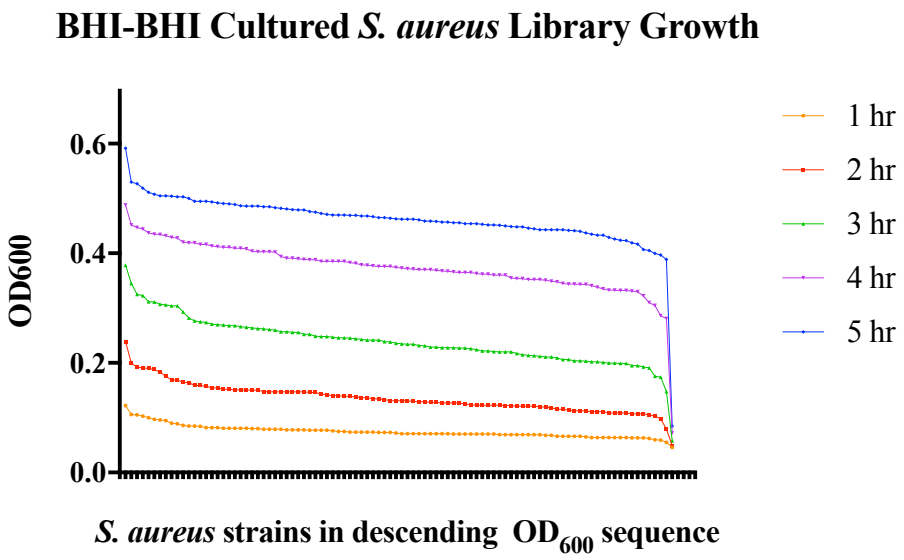

Figure 3.2. Representative bacterial yields during growth of 96 NTML strains in plate 1B. Cultures were obtained by adding 10µL library strain to 190 µL BHI media followed by overnight incubation at 37°C. The growth yields of different time points were generated from a sub-culture in BHI media. OD_{600} of the 96 *S. aureus* mutants are showed in descending sequence. N=2

3.4 Confirmation of neutrophil viability in bacterial growth media

During handling, it is possible that BHI media could be carried over from the *S. aureus* sub-culture. It was therefore important to determine if BHI had any effects on neutrophil cell loss which would make interpretation of the screen difficult. Neutrophils were incubated with addition of BHI at 5%, 10%, 20% and 50% v/v for 4 hrs, and subjected to Attune flow cytometry (Figure 3.3 A). The forward scatter (FSC) and side scatter (SSC) of the dot plot distinguishes a mixture of cells based on their size and granularity, respectively. The FSC and SSC parameters and gating strategies applied in this study are well established for identification of viable human neutrophils (Nagelkerke *et al*., 2014, Brittan *et al*., 2012). Attune flow cytometry automatically counts numbers of cells without the need for reagents such as CountBright beads. Therefore, absolute cell number within the gating area was estimated. In comparison with RPMI (+10% v/v FBS), the addition of BHI media results in a similar percentage of healthy neutrophils for all BHI conditions (Figure 3.3 B).

3.5 ToPro-3 staining of neutrophils

ToPro-3 is a fluorescent vital nuclear dye which cannot penetrate the cell membrane unless there is significant damage (Mioulane *et al*., 2012). Importantly ToPro-3 distinguishes between cells that have died by apoptosis and necrosis since apoptotic cells have an intact plasma membrane (Hart *et al*., 2000). The basic principle of these experiments is to validate ToPro-3 staining as a robust and sensitive high-throughput assay for neutrophil cell death caused by *S. aureus*.

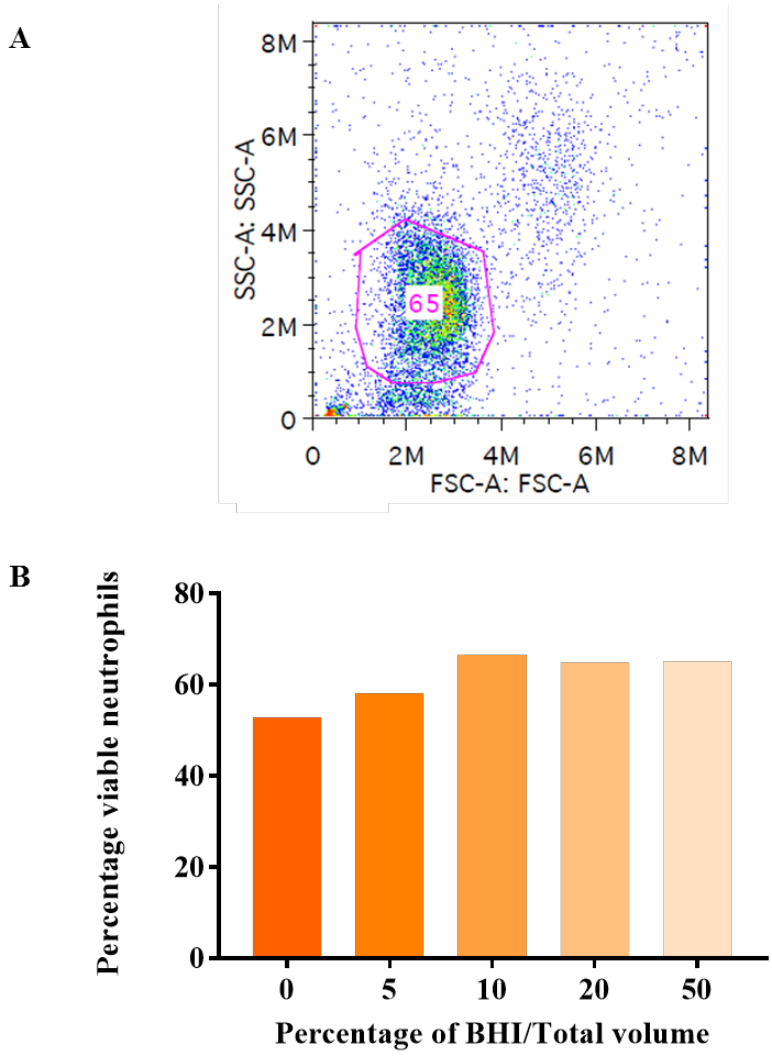

Figure 3.3. Effect of bacterial growth media on neutrophil cell loss.

(A) Representative flow cytometric dot plot of 10% v/v BHI media treated neutrophils showing a gated region around intact and viable neutrophils based on their forward scatter (FSC) and side scatter (SSC) profile.

(B) Neutrophils were incubated in RPMI (+10% v/v FBS) with 5%, 10%, 20%, and 50% v/v of BHI media in 96-well plates. Percentage of viable neutrophils over total cell population was determined by Attune flow cytometer detection and FlowJo data analysis. N=2

Unpublished work from a previous group member (Dr. Sadia Anwar) shows that JE2 supernatant has potent killing activity towards neutrophils. Therefore, JE2 culture supernatant was used to optimise neutrophil lysis and cell loss. To do this, a single colony of JE2 was inoculated overnight in BHI media. The bacterial suspension was centrifuged to remove cells and the supernatant was filter sterilised, diluted 1:1 with sterile media and incubated with neutrophils for 1 hr.

The Attune flow cytometer was used to detect neutrophil FSC and SSC profiles, cell number and ToPro-3 positivity. ToPro-3 is a fluorescent vital dye that enters cells that have undergone a necrotic/lytic cell death . Negative and positive internal staining controls were included: neutrophils without ToPro-3 in order to set the background threshold of fluorescent intensity (Figure 3.4 A) and as a positive staining control, neutrophils were frozen at -80^{o}C for 10 min and thawed (Figure 3.4 B). By so doing, the plasma membrane of the neutrophil is directly damaged, which allows ToPro-3 to penetrate and bind with nuclear DNA (McGann *et al*., 1988).

Neutrophils incubated with media (media control, Figure 3.4 C) along with the PBS control sample (Figure 3.4 A) generates FSC/SSC and ToPro-3 profiles depicting typically healthy cells. A damaged cell debris profile (low FSC/low SSC, 81.6% ToPro-3 positive) was generated following F/T treatment (Figure 3.4 B). JE2 supernatant treated samples produced a higher level of ToPro-3 positivity (42.1%) compared with the media control (1.04%), and the FSC/SSC profile displaying increased density of debris and fewer neutrophils in the viable FSC/SSC region, indicating cell lysis (Figure 3.4 D).

To further confirm the robustness of the Attune flow cytometry ToPro-3 assay, the same samples were run through both Attune and FACSCalibur flow cytometers. The FACSCalibur is one of the most well established and commonly used flow cytometers and

a good validation of the sensitivity of the Attune. The FSC/SSC profiles generated by the two flow cytometers displayed a very similar population for each sample (Figure 3.5). The healthy neutrophil population in the PBS staining control was detected by both FACSCalibur (Figure 3.5 A) and Attune (Figure 3.5 I). The F/T samples displayed dead cells in both flow cytometric FSC/SSC profiles (Figure 3.5 C&K). JE2 supernatant treated samples showed neutrophil activation (shift towards higher FSC) and loss of live cells (lower density of viable population) (Figure 3.5 E, G, M & O). The ToPro-3 fluorescence detected by both flow cytometers correlates with the FSC/SSC profiles in that the more cell loss showed in dot plots, the higher ToPro-3 signal was measured. The ToPro-3 positivity of the F/T and both JE2 supernatant treatments from FACSCalibur were 76.7%, 38.8% and 50.2% respectively (Figure 3.5 D, F & H) which was comparatively higher than the intensity detected by Attune (58.1%, 25.4% and 32.7%, Figure 3.5 L, N & P). The reason for this is likely to be because the FACSCalibur was set to a lower fluorescence threshold (FL4: 410) than the Attune (RL1: 1250), resulting in increased reading (2.33% of PBS control, Figure 3.5 B). Overall, a highly consistent pattern of the corresponding samples was found comparing the two flow profiles.

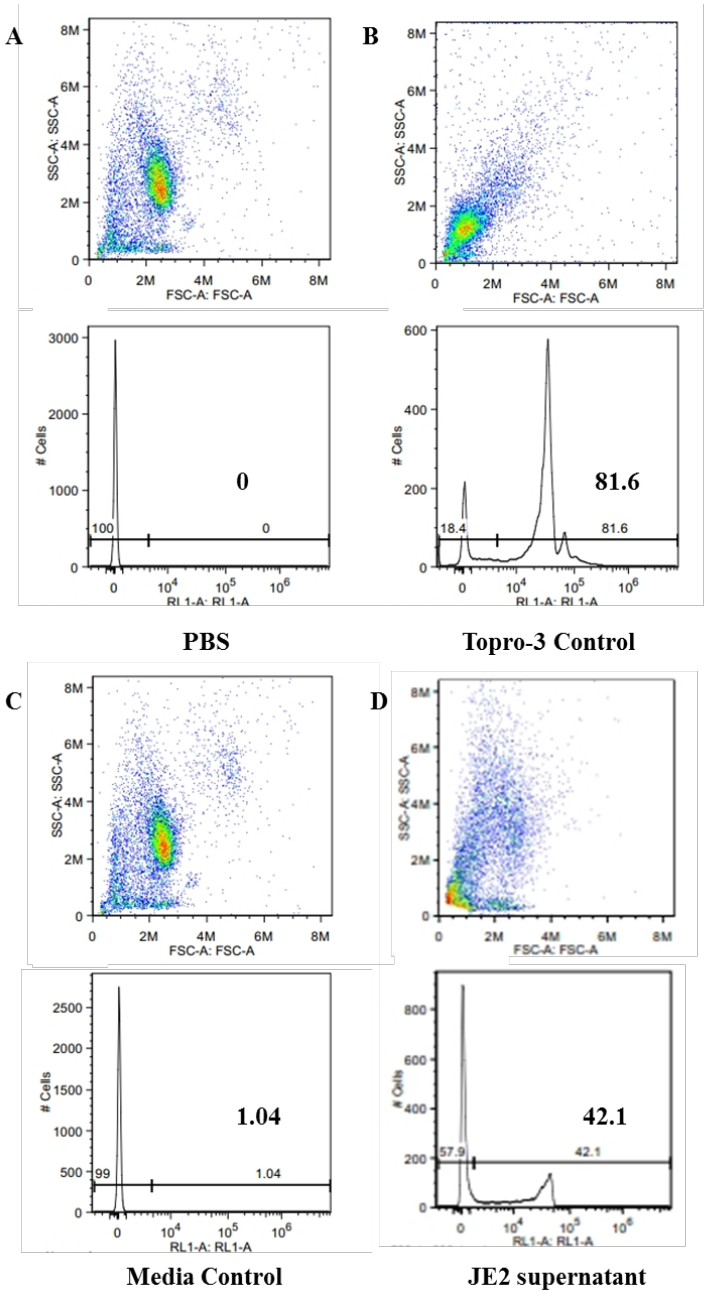

Figure 3.4. Validation of ToPro-3 staining for neutrophil cell death. Representative Attune flow cytometry profiles showing cell size and granularity (dot plots) and ToPro-3 fluorescent intensity (histograms) of (A) PBS stained neutrophil media control, (B) ToPro-3 (1:10,000 in PBS) stained neutrophils freeze-thaw (F/T) condition, and (C) ToPro-3 stained media control. (D) One hr of 50% v/v *S. aureus* supernatant treatment resulted in rapid and massive viable cell loss in FSC/SSC, and increased ToPro-3 positivity. Numbers in histograms refer to the percentage of ToPro-3 positive population.

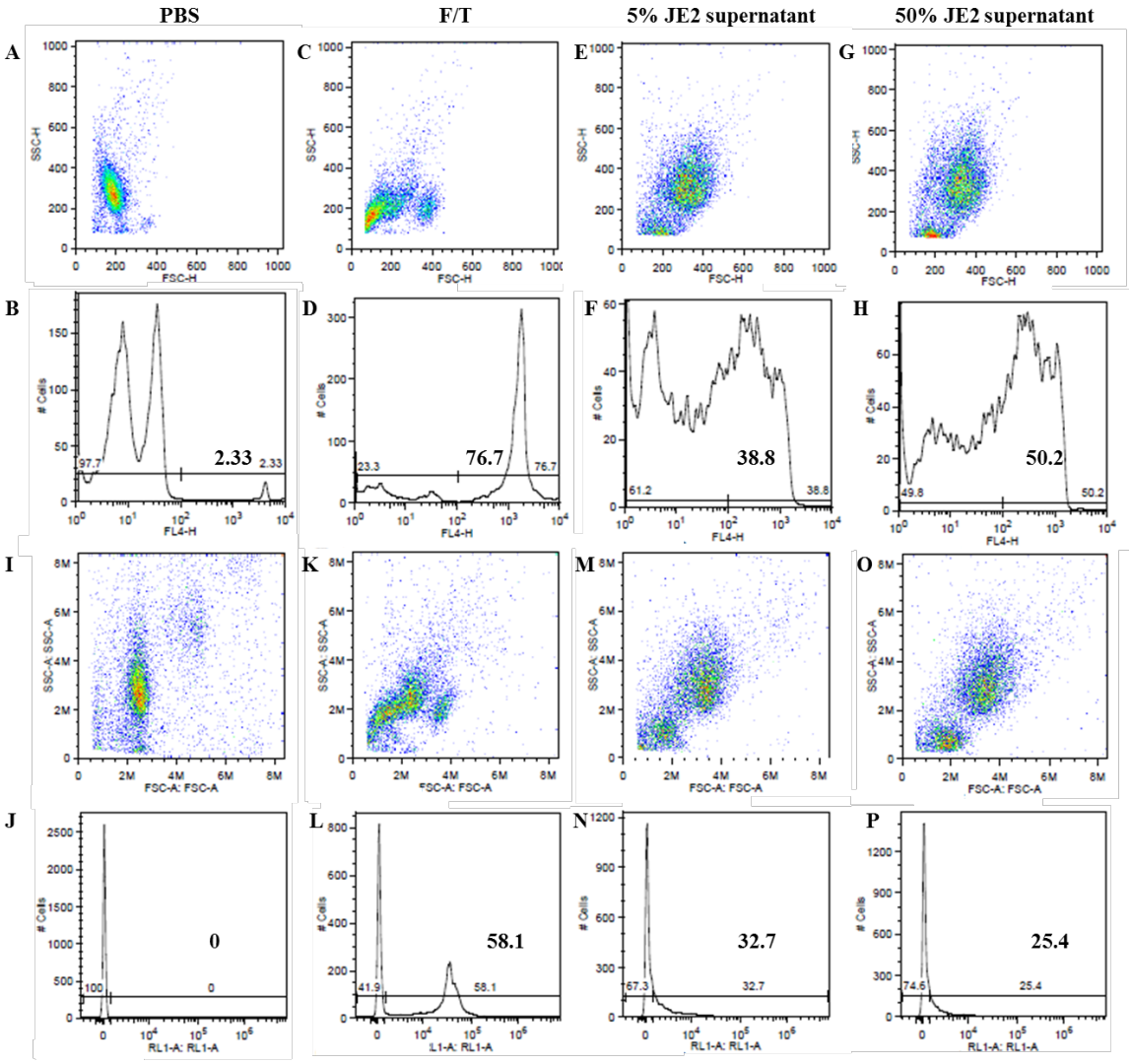

Figure 3.5. Validation of flow cytometric detection by Attune. Flow cytometry profiles generated by (A-H) FACSCalibur flow cytometer and (I-P) Attune flow cytometer. Numbers shown in histograms are percentage of ToPro-3 positive population. N=1

(A-B & I-J) PBS stained neutrophil media control. (C-D & K-L) ToPro-3 (1:10,000 in PBS) stained neutrophils that have been freeze-thawed (F/T). (E-F & M-N) Neutrophils incubated with 5% of JE2 supernatant for 1 hr. (G-H & O-P) Neutrophils incubated with 50% of JE2 supernatant for 1 hr.

3.6 Quantification of neutrophil cell death

S. aureus supernatant was used to quantify the absolute viable neutrophil cell count in the flow cytometrical assay. Neutrophils were treated with media or JE2 supernatant at 5% and 50% v/v for 3 hr after which they were stained with ToPro-3 for measurement of cell counts and fluorescence positivity by Attune flow cytometry (Figure 3.6). As expected, the ToPro-3 staining controls suggest robust staining results: 96.6% positivity for the F/T sample, and only 1.56% positivity for the media control. The dot plots of samples treated with 5% and 50% v/v *S. aureus* supernatant displayed obvious cell loss compared with the media control as illustrated by lack of viable neutrophil population (as shown by the gated region), while the histograms showed a higher level of ToPro-3 positivity generated by JE2 supernatant treatment (42.1% and 48.6%) compared to the media control (1.56%) (Figure 3.6A). The absolute viable neutrophil counts showed consistent results with the flow FSC/SSC profiles, neutrophil cell lysis caused by JE2 supernatant was revealed by determining cell counts (Figure 3.6 B). After a 3 hr incubation, the media control has approximately $10x10^4$ viable neutrophils. Treatment with 5% and 50% v/v staphylococcal supernatant reduced the number to $4x10^4$and $3.5x10^3$, respectively.

Hence, the broad parameters for neutrophil cell death assay was established for NTML screening. The virulence of *S. aureus* towards neutrophil cell lysis can be analysed by assessing viable cell counts and ToPro-3 positivity. Meanwhile, in order to rule out potential impact of *S. aureus* excreted toxins, as the screen is aimed for post phagocytosis death of neutrophils, the supernatant of NTML strains would be removed before infecting neutrophils.

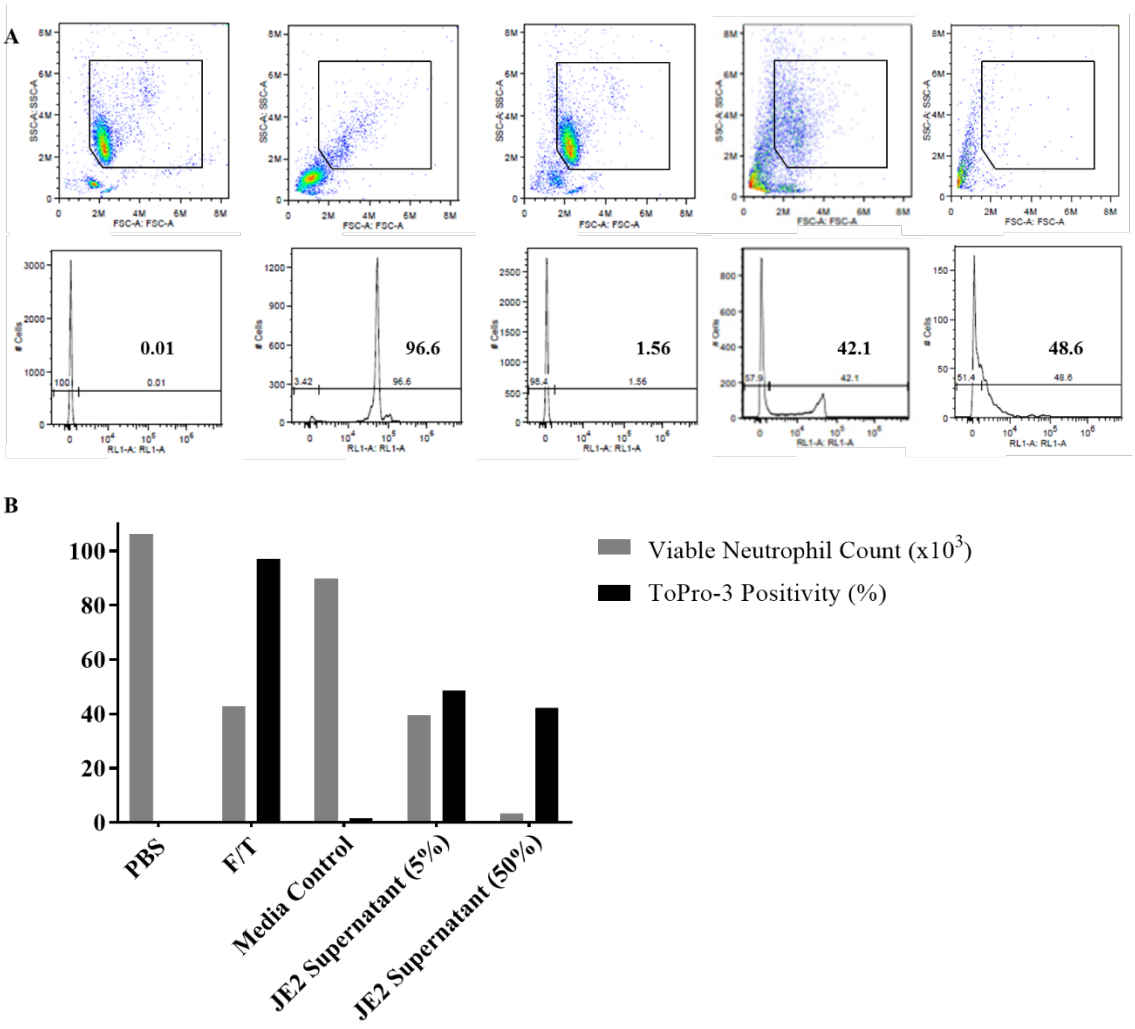

Figure 3.6. Quantification of neutrophil cell death assay by ToPro-3 staining and Attune flow cytometric detection. Representative result of neutrophils treated with JE2 supernatant at 5% and 50% v/v for 3 hr. Viable neutrophil numbers and ToPro-3 positive intensities were assessed using Attune flow cytometry. (A) Attune flow cytometric results of FSC/SSC files and ToPro-3 histograms (numbers refer to ToPro-3 positive percentage). (B) Quantification of neutrophil cell death assay established with healthy neutrophil cell counts and ToPro-3 intensity. Viable cell counts were generated by gating strategy shown in A.

3.7 Determination of effective MOI for NTML screen

It was necessary to optimise the *S. aureus* MOI to ensure sufficient neutrophil cell lysis caused by WT JE2, while allowing the opportunity to identify attenuated NTML strains. To find out the optimal MOI, co-culture with JE2 cells at an MOI of 1, 10 and 20 for 3 hrs was carried out. ToPro-3 staining was verified with positivity for PBS only (0%), F/T (33.2%) and media control (1.49%) (Figure 3.7A). Neutrophils treated at an MOI of 10 and 20 lost the majority of viable cells (Figure 3.7 B). The dot plots show a distinct healthy neutrophil population with JE2 at an MOI of 1. Consistently, in comparison with cells infected at MOI of 1 (2.14%), higher ToPro-3 positivity was associated with *S. aureus* treatment at MOI of 10 (11.1%). The infection at an MOI of 20 resulted in a similar FSC/SSC profile and lower ToPro-3 intensity (8.71%) compared to MOI of 10 (11.1%), suggesting saturated cell death with an MOI higher of 10. This experiment was repeated 3 times and results were highly consistent (Figure 3.7 C&D). The MOI of 10 was therefore selected for screen use.

Apart from revealing the optimal MOI, it was important to verify phagocytosis of the bacteria since the screen is designed to identify pathogenic factors mediating post-phagocytosis neutrophil death. Monolayer cytospins of neutrophils cultured with alive JE2 at MOI of 10 for 1 hr were prepared and *S. aureus* were clearly visible inside neutrophils, validating phagocytosis during the co-incubation (Figure 3.8). A population of neutrophils engulfed multiple *S. aureus* while the remaining did not ingest any. Infected neutrophils appeared vacuolated and bacteria were visible within these vacuoles. No morphological changes associated with cell death were observed, indicating longer time required for staphylococcal neutrophil cell lysis at an MOI of 10.

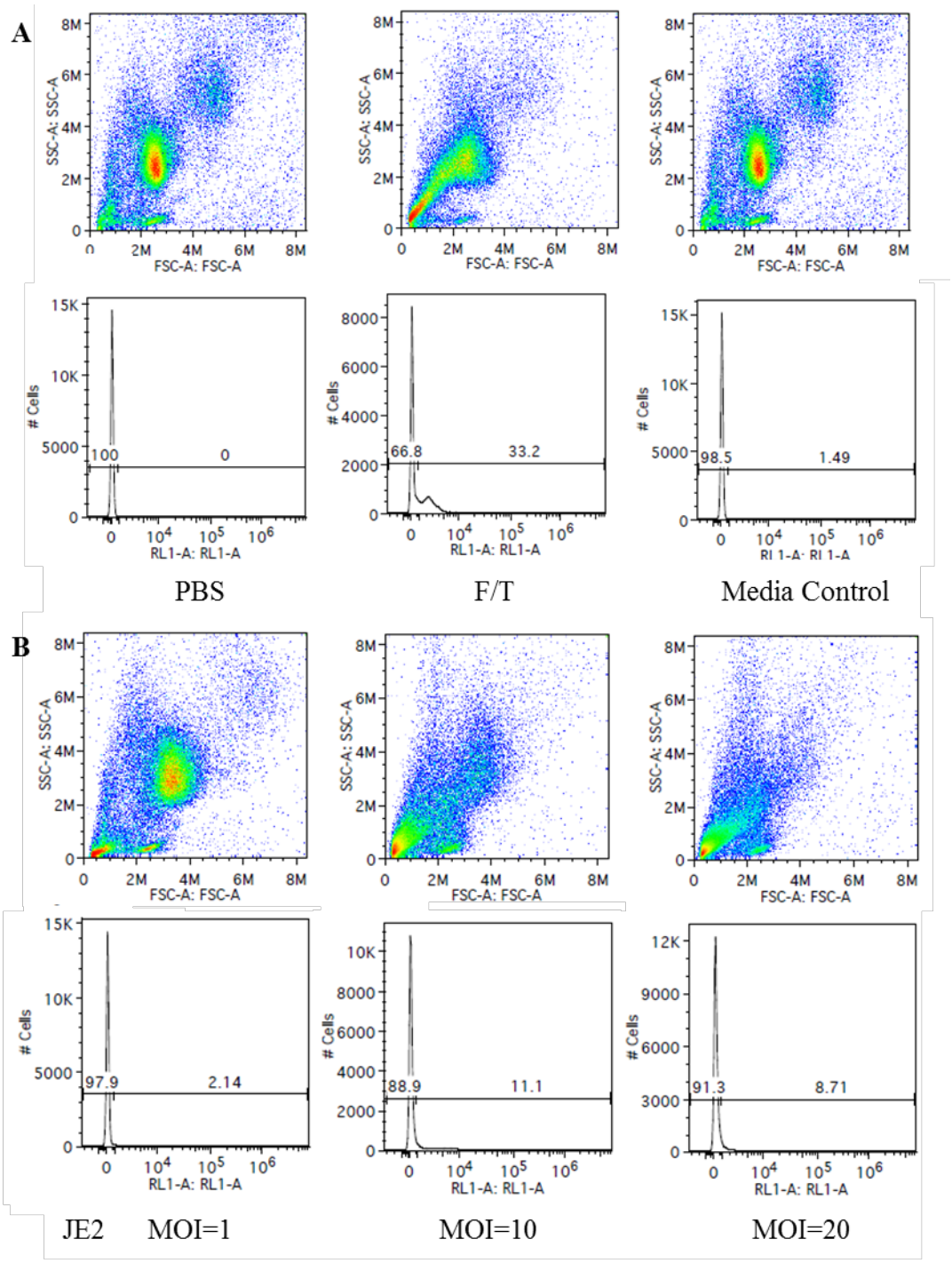
A
SSC-A: SSC-A
FSC-A: FSC-A
Cells
RL1-A: RL1-A
100
0
66.8
33.2
98.5
1.49
PBS
F/T
Media Control
B
97.9
2.14
88.9
11.1
91.3
8.71
JE2
MOI=1
MOI=10
MOI=20

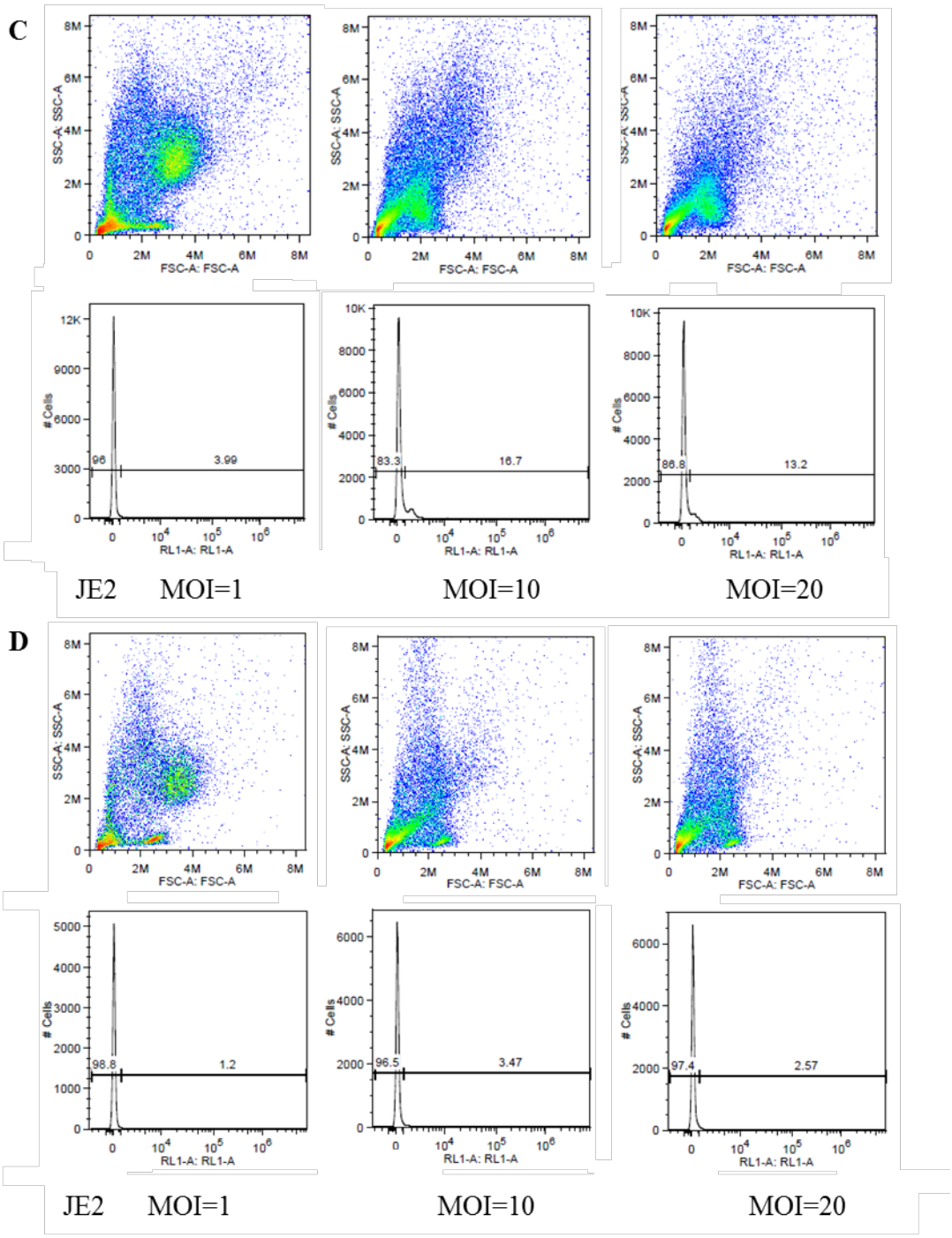

Figure 3.7 Determination of optimal MOI for the NTML screen. Attune Flow cytometry profiles of neutrophils treated with exponential growth phase JE2 at MOI of 1, 10, and 20 for 3 hr. Results from 3 independent experiments (1st:A-B, 2nd: C, 3rd: D) are shown. PBS: unstained neutrophil media control. F/T: ToPro-3 (1:10,000 in PBS) stained neutrophils after freeze-thawed (F/T) condition. Media control: ToPro-3 stained neutrophils in RPMI (+10% v/v) media.

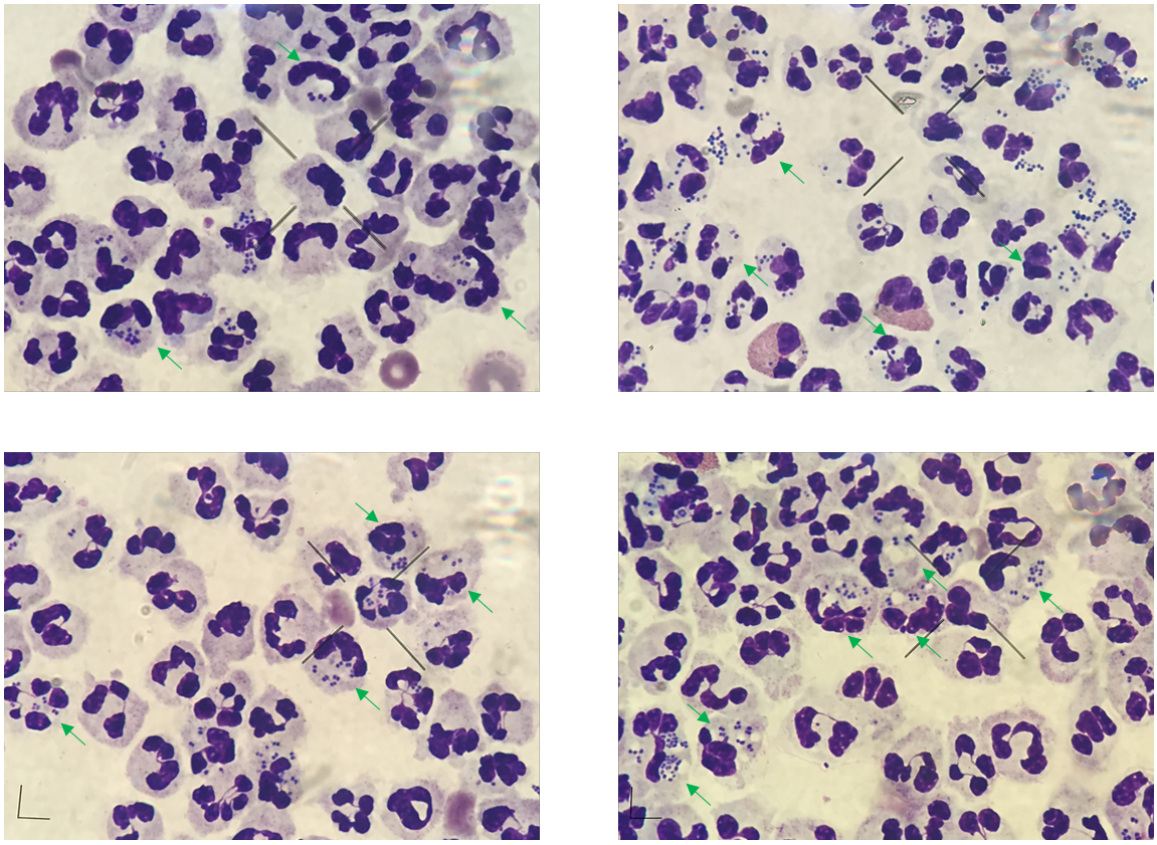

Figure 3.8 Visual validation of neutrophil uptake of *S. aureus*. Qualitative imaging showing neutrophils infected by JE2 at an MOI of 10 for 1 hr. The lines are intrinsic within the light microscopy setup. Samples were stained with red and blue Giemsa Wright dye (Diff Quik). Intracellular *S. aureus* were observed in a number of neutrophils, verifying the occurrence of phagocytosis during NTML screening. Four independent fields, each showing *S. aureus* as small purple dots within vacuolated neutrophils (green arrows).

3.8 Verification of *S. aureus*-neutrophil co-incubation time

To verify optimal *S. aureus*-neutrophil co-incubation time for the NTML screen, JE2 treatment at an MOI of 10 was carried out for 1, 1.5, 2, 2.5, and 3 hr. The assay was repeated twice with duplicates and representative profiles are showed in Figure 3.9.

After 1 hr of JE2 infection, 45.3% of events were healthy neutrophils. The percentage of viable neutrophils reduced with time to 35.3% and 36.6% at 1.5 and 2 hr respectively. Correspondingly, the increasing ToPro-3 positivity indicates more neutrophil cell death (5.85%, 10.4% and 11.4% at 1, 1.5 and 2 hr respectively). At 2.5 hrs of co-incubation, the viable neutrophil population can no longer be observed from the FSC/SSC profiles. With 17.6% viable cells and 14.8% of ToPro-3 positivity, it is demonstrated that JE2 requires at least 2.5 hr to cause massive neutrophil cell loss. After 3 hrs of co-incubation, only 15.8% of cells stayed viable. The slight reduction in the percentage of ToPro-3 positive events (13.8%) reflects cell lysis and loss of nuclear material. The results validated the optimal time length for *S. aureus*-neutrophils co-incubation as 3 hrs for thorough cell lysis caused by JE2.

3.9 Testing response of neutrophils from different donors

Considering the amount of time required to set-up and run each NTML plate, the screen was designed to assay 2 NTML plates per day over 5 days (not necessarily consecutive). This requires neutrophils from at least 10 donors to complete a total of 20 plates. It is therefore necessary to rule out potential variation in *S. aureus* mediated neutrophil cell death between individual donors.

An MOI response experiment was performed at MOI of 1, 10, 20, and 100 with cells from 2 different donors. As Figure 3.10 shows, neutrophils from both individuals responded to JE2 treatment in a similar way. Compared to infection at an MOI of 1, decreased viable

neutrophil cell density was shown in the FSC/SSC files at an MOI of 10 (Figure 3.10 A). Although the difference between absolute viable cell counts was less obvious (Figure 3.10 B), the infection at an MOI of 20 and 100 led to loss of live neutrophil population in FSC/SSC files (Figure 3.10 A). Consistently, the ToPro-3 positivity of samples at an MOI of 10 (11.1% and 16.7%) were higher than samples at an MOI of 1 (2.14% and 3.99%), suggesting increasing neutrophil cell death (Figure 3.10 A). The ToPro-3 positivity of samples at MOI of 20 (8.71-13.2%) or more (11-11.3%) were at similar level, illustrating saturation of infection at MOI higher than 20. Overall, the pattern of responses was highly similar between donors at different MOIs. The only variation revealed by this experiment that might have an effect on screen results analysis is the different starting cell counts. The media control of donor B (approx. $1.2x10^5$) had 32.6% fewer cells compared with donor A (approx. $1.6x10^5$) (Figure 3.10 B). This is probably due to the inevitable difference in the neutrophil isolation preparation rather than donor variation. Considering the ultimate control for screen is the neutrophil cell death caused by WT *S. aureus*, reliability of the screen would not be compromised by variation of neutrophil number within an acceptable range. To minimize the potential effect of this, the screen of NTML was to be conducted with ToPro-3 staining and JE2 control every day. Data of each plate would be analysed separately with corresponding controls.

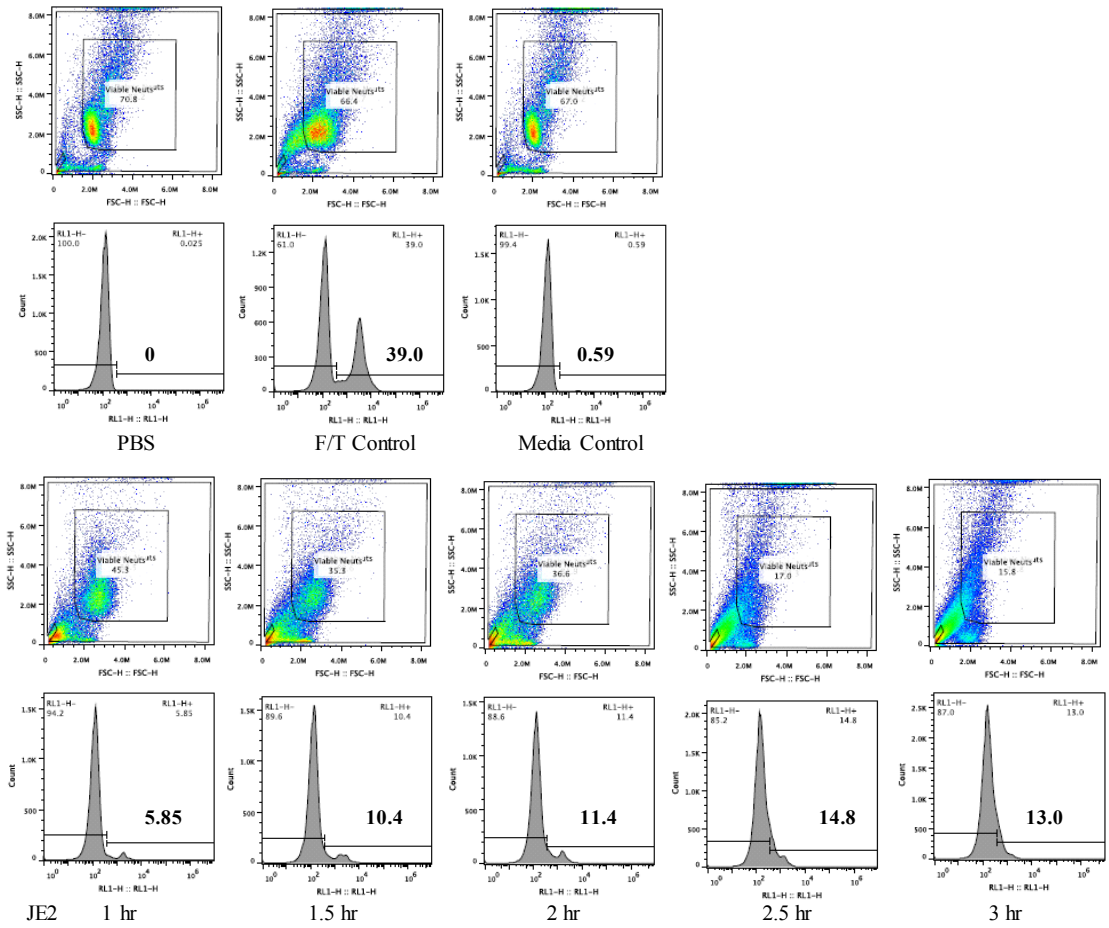

Figure 3.9. Determination of co-incubation time for the NTML screen. N=3

Representative flow cytometry profiles of neutrophils infected by exponential growth phase JE2 at an MOI of 10 for 1, 1.5, 2, 2.5, and 3 hr. The response towards *S. aureus* treatment started to display distinct changes in neutrophil population (FSC/SSC) by 2.5 hours co-incubation. The central gate in FSC/SSC files was used for quantification of viable neutrophils. The outer gate excluding cell debris and was applied for ToPro-3 measurement. PBS: unstained neutrophil media control. F/T: ToPro-3 (1:10,000 in PBS) stained neutrophils at frozen-thawed (F/T) condition. Media control: ToPro-3 stained neutrophils in RPMI (+10% FBS) media. Numbers in histograms are percentage of ToPro-3 positive population.

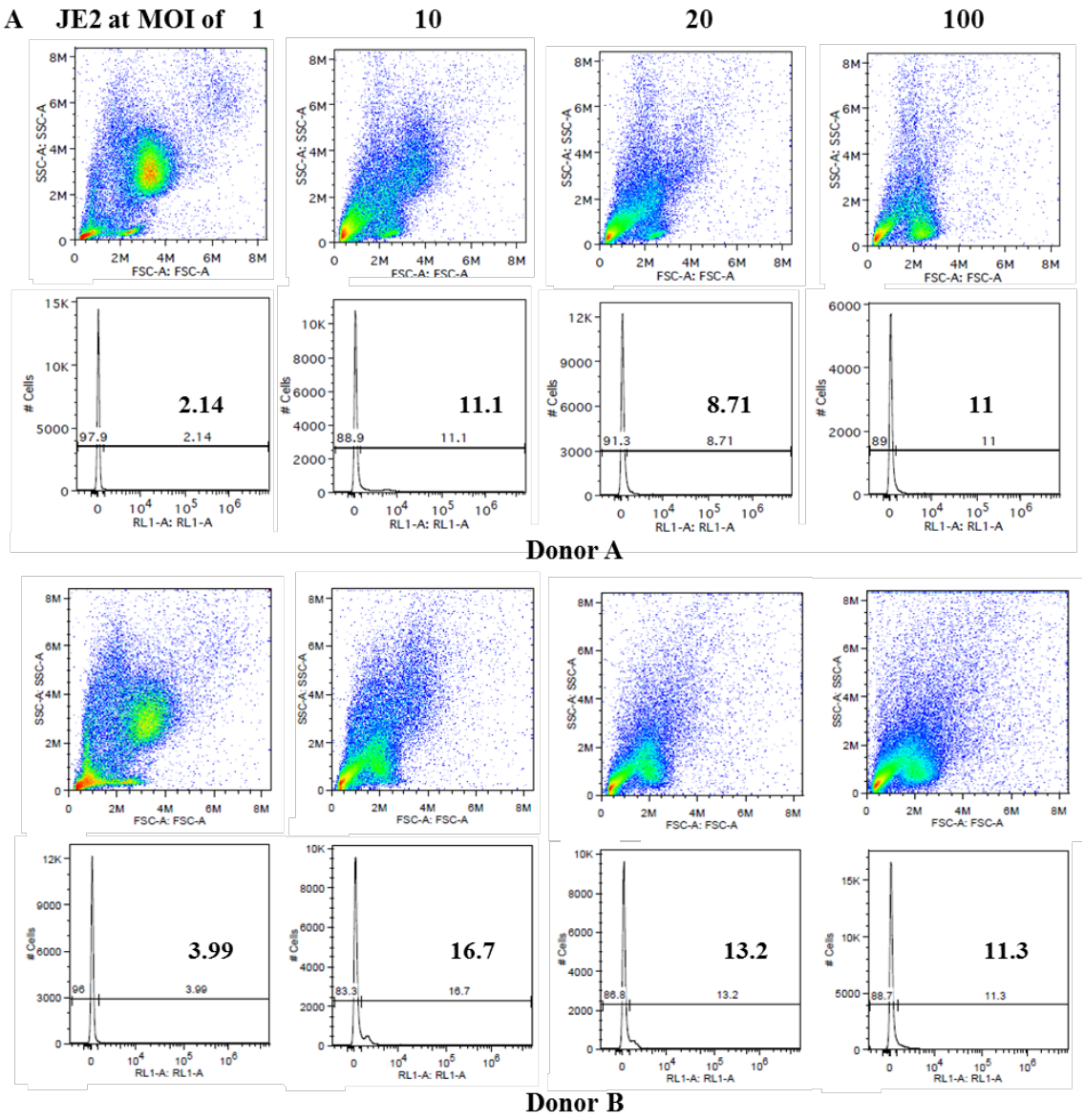
A JE2 at MOI of 1
10
20
100
SSC-A: SSC-A
FSC-A: FSC-A
Cells
RL1-A: RL1-A
2.14
11.1
8.71
11
97.9
88.9
91.3
89
Donor A
3.99
16.7
13.2
11.3
96
83.3
86.8
88.7
Donor B

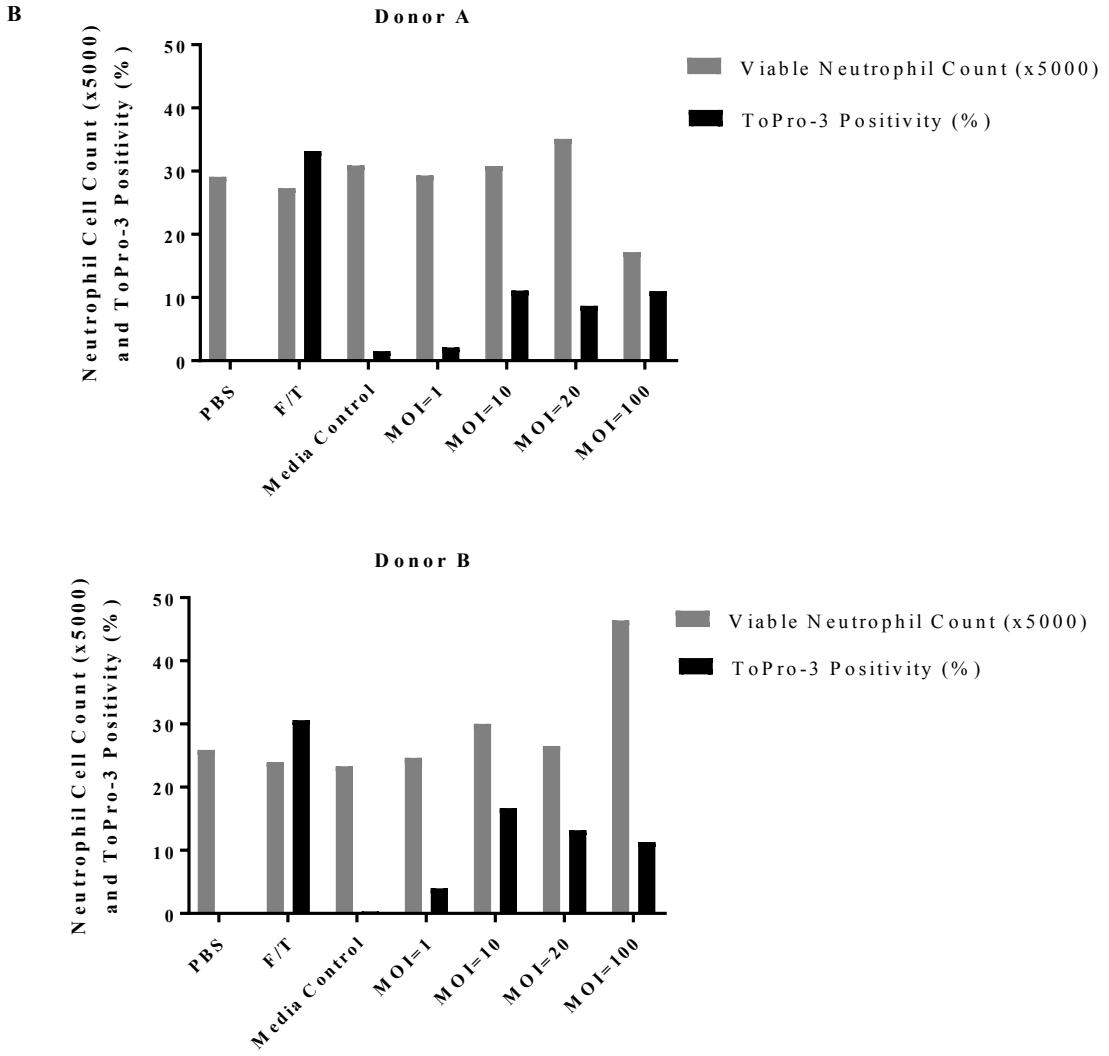

Figure 3.10 Verification of responses of neutrophils from different donors.

(A) Attune flow cytometry profiles of 3 hr co-incubation results generated by neutrophils from two donors at an MOI of 1, 10, 20 and 100. (B) The viable neutrophil counts and ToPro-3 positivity of each sample. N=1.

3.10 Discussion

The main aim of this chapter was to identify the optimal experimental conditions for a genome wide *S. aureus* screen in a flow cytometric neutrophil cell death assay. The research has shown that BHI is the preferred bacterial growth media, generating consistently high CFU/mL and ideal growth curve trends. It is also demonstrated that the WT strain, JE2 caused neutrophil cell death as determined by ToPro-3 positivity and cell counts. The optimal concentration and co-incubation time of *S. aureus* treatment on neutrophils was determined to be MOI of 10 and 3 hr. Any potential differences in neutrophil responses to *S. aureus* treatment appear independent of donor variation. The design of screen was now fully optimized and could be carried out.

3.10.1 Optimisation of *S. aureus* growth

In order to carry out the screen, it is important to standardize the conditions for the interaction. The expression of a number of *S. aureus* virulence factors are growth phase regulated (Casadevall and Pirofski, 1999). Virulence factors can be broadly categorized into those affecting attachment (exponential phase), immune evasion (both exponential and stationary phase), and tissue penetration (stationary phase) (Novick, 2003a, Novick, 2003b). Several studies revealed upregulated endotoxins and exotoxins expression at post-exponential phase of *S. aureus* growth (Cheung *et al*., 2004, Shaw *et al*., 2005). The actively expressed genes include *lukS/F*, *hlgA* and *psm*, which are well-established inducers of neutrophil lysis (Oogai *et al*., 2011). Nevertheless, prior to the secreted toxins having an effect, the virulence factors involving in regulation of *S. aureus*-neutrophil interactions greatly influence the outcomes for both bacteria and host cell (Greenlee-Wacker *et al*., 2015)

For instance, clumping factor A (ClfA) is a staphylococcal surface protein with fibrinogen-binding activity. The expression of its corresponding gene, *clfA*, is highly activated during exponential phase of growth (Novick, 2003b). ClfA is a virulence factor leading to sepsis

and arthritis (Josefsson *et al*., 2001). During the bacteremia phase of infection, ClfA enhances *S. aureus* virulence by coating the microbial with fibrinogen, and therefore shielding it from phagocytosis (Foster, 2005). This protective role of ClfA, was observed as inhibiting phagocytosis from both murine macrophages and human neutrophils (Josefsson *et al*., 2001). Another key virulence factor regulator of *S. aureus, sae*, is most active during the exponential phase of growth (Benson *et al*., 2012, Bronner *et al*., 2004). A key role for *saeR* in regulation of purine synthesis and amino acid metabolism in mid-log phase (Voyich *et al*., 2009). Mutation of the *saeRS* system attenuated *S. aureus* virulence in a murine sepsis infection study (Voyich *et al*., 2009). Hence, in order to maximise expression level of *S. aureus* virulence factors related to the modulation of immune responses, and to reduce effect of secreted toxins, the screen of NTML would be carried out with *S. aureus* in exponential phase of growth.

3.10.2 Optimisation for Attune flow cytometry detection method

For neutrophil assessment, ToPro-3 is a widely used vital dye (Mioulane *et al*., 2012) and I have shown it is suitable for use in this assay. It was important to evaluate the use of ToPro-3 using the 96 well plate format, since vital dyes such as this, can leach into intact cells over time. The staining method was validated by ToPro-3 staining controls so all screen experiments would be carried out with unstained (PBS), F/T, and media control samples (Figure 3.4). The accuracy of the Attune measurement of ToPro-3 positivity was further validated by using the FACSCalibur as a comparator.

The flow cytometry assay was based upon a previous study from our group (Anwar thesis, 2014). Quantitative data analysis revealed that *S. aureus* causes reduction of neutrophil cell counts together with increased ToPro-3 positivity (Figure 3.6), which is consistent with previous results obtained from *S. aureus* treatment of eosinophils (Prince *et al*., 2012). It is important to analyse the absolute neutrophil cell numbers and ToPro-3 positivity in parallel

since low viable cell numbers may falsely lead to low ToPro-3 positivity simply because there are few nucleated intact cells remaining. For example, each of the cell debris fragments is counted by Attune flow cytometer as one cell event, which leads to a high absolute cell count, even though cell death has occurred.

An MOI of 10 was found to be the most reliable MOI in terms of causing a consistent amount of neutrophil lysis. The highly similar response of neutrophils from different donors to JE2 treatment suggests there was no influential effect generated by donor variation. However, the variation of overall neutrophil cell counts indicate that the number of neutrophils obtained from prep each time was different. Consequently, an additional neutrophil sample incubated with JE2 should be added to each experiment for comparison.

To confirm the neutrophil death pattern, cytospins of 1 hr JE2 treated neutrophils at an MOI of 10 was prepared and shows significant phagocytosis of *S. aureus*. This is consistent to previous findings showing neutrophil necrosis following phagocytosis of *S. aureus* (Anwar, 2004, PhD thesis; (Flannagan *et al*., 2016). The phagocytosis of *S. aureus* confirms bacterial uptake by neutrophils, which generates confidence in conducting the screen to investigate pathogenic factors that may affect *S. aureus* virulence following phagocytosis.

Multiple methods were applied for flow cytometric data analysis during the optimisation. In early experiments the entire cell population of each sample was used for ToPro-3 measurement (e.g. Figure 3.4). Subsequently, the absolute viable neutrophil number was generated automatically from gating of the viable population (e.g. Figure 3.9). To further improve the accuracy of ToPro-3 staining specifically on neutrophil lysis, damaged cell debris (low FSC/low SSC) was removed from the data set for ToPro-3 histogram analysis (e.g. Figure 3.9). This duel gating strategy will be used throughout the NTML screening and validation experiments for maximal accuracy.

3.10.3 Novelty of NTML screen for neutrophil related virulence factors

Similar screening techniques have been widely used for identifying virulence factors of *S. aureus*. To discover essential genes for *S. aureus* survival in porcine blood, a transposon mutant library was made in ST398 background and screen *in vitro*. Twenty-four genes were identified (Christiansen *et al*., 2014). A selectively made sub-library of USA300 mutants containing 251 strains from NTML was screened for transcriptional regulators involved in staphylococcal leukocidin expression (Balasubramanian *et al*., 2016) Another staphylococcal toxin-focused study used CRISPR technology to perform a genome-wide loss-of-function screen. A number of myeloid cell membrane microdomains associated proteins were identified as necessary for *S. aureus* to attach and mediate α-hemolysin toxicity (Virreira Winter *et al*., 2016).

Screening has also been successful for the identification of *S. aureus* virulence factors *in vivo*. Das *et al* generated a transposon mutation library consists of 25,000 *S. aureus* (6850 background) mutants, which was screened in a mice infection model for underpinning genes involved in prolonged intracellular survival (Das *et al*., 2016). A gene encoding transcription factor repressor of surface protein named *rsp* was identified from the screen. Moreover, it exhibited a great positive influence on *S. aureus* survival in human neutrophils. Twenty-four genes have been identified with attenuated virulence in a murine model, by screening a collection of *S. aureus* insertion mutants (Benton *et al*., 2004). Including *saeS*, a histidine kinase sensor-response regulator gene, the identified mutants showed significantly less bacterial growth in the spleens and localised abscess infections than the WT.

Instead of looking into key genetic factors involved in secreted toxin production, the screen of *S. aureus* mutants in a neutrophil death assay allows identification of virulence factors

that are associated with post-phagocytosis cell death, and possible mechanisms involved in *S. aureus* escape from phagosomes. In this study, NTML will be screened with human innate immune cells for the first time. Recently, the quick-developed flow cytometry technique provided a novel output for high-throughput experiments. The Attune flow cytometer was applied to develop a novel model of genome-wide screen.

CHAPTER 4

Identification of *S. aureus* strains with altered neutrophil interaction

4.1 Introduction

Mutational analysis is a widely-applied method for exploring microbial components associated with environmental adaptation, including interactions with host cells. A common approach for generating mutations in genes of interest is through allelic replacement. By comparing to the wild type strain, phenotypic differences in the mutant correspond to roles of the gene product (Beasley *et al*., 2011, Bubeck Wardenburg *et al*., 2008, Palmqvist *et al*., 2002). However, this well-established methodology is only appropriate for the study of candidate genes, since it would be arduous and time consuming to cover genome-wide mutagenesis.

Transposon-mutagenesis strategies have been developed as a powerful tool for functional analysis of multiple essential and pathogenicity-related genes from a single screen. Transposons were first discovered by Barbara McCintock and refer to genetic elements that can change their location within a genome (McClintock, 1948). Among the two major classes of transposons, Class II including *mariner*, are DNA transposons. Their typical structures consist of terminal inverted repeats flanking a transposase encoding gene and functional genes such as antibiotic resistance. The insertion and excision of Class II transposons are highly regulated by interaction of transposase with the inverted repeats. The transposon inserts in random loci in host DNA can cause mutations and influence gene expression (Hamer *et al*., 2001, Hayes, 2003). Unlike recombination-associated chromosomal DNA manipulation, transposon integration can take place without

homologous gene fragments, and therefore can be used for creating a full gene complement of a species (Choi and Kim, 2009).

Transposon mutagenesis generally starts with its delivery into the background of interest via a plasmid. During bacterial growth, transposition events occur with mediation by transposase. Subsequently, the carriage plasmid is lost by growth on media without antibiotics at a temperature non-permissive for plasmid replication. Identification of insertion mutants with the phenotype of interests allows gene function to be acetated (Fey *et al*., 2013, Bae *et al*., 2008). By using transposon mutagenesis methodology, *S. aureus* genes involved in virulence factor regulation have been widely studied (Balasubramanian *et al*., 2016, Christiansen *et al*., 2014, Das *et al*., 2016, Shaw *et al*., 2005).

A genome-wide *S. aureus* mutant library has been created at the University of Nebraska. The background strain is the CA-MRSA strain USA300 (JE2 background), which is a clinically relevant strain isolated from a soft tissue infection in the Los Angeles County Jail LAC (Fey *et al*., 2013). It has been characterised as a valuable resource for host-*S. aureus* interaction study. A *Mariner* based *bursa aurealis* transposon was used to generate the NTML. Detailed procedures used to produce the library are showed in Figure 4.1. The NTML consists of 1,952 *S. aureus* mutants each with single transposon inserted in the coding sequence of a non-essential gene. Genomic DNA sequences of all mutants were aligned with *S. aureus* USA300 FPR3757 chromosomal DNA to identified transposon insertion sites. Upon the production of NTML, haemolysis, protease activity, and pigment formation were assessed and the library is available to all researchers for *S. aureus* studies (Fey *et al*., 2013). This chapter aimed to screen the NTML with primary human neutrophils *in vitro* to identify genes involved in *S. aureus* virulence. A neutrophil cell death model was applied for the screen.

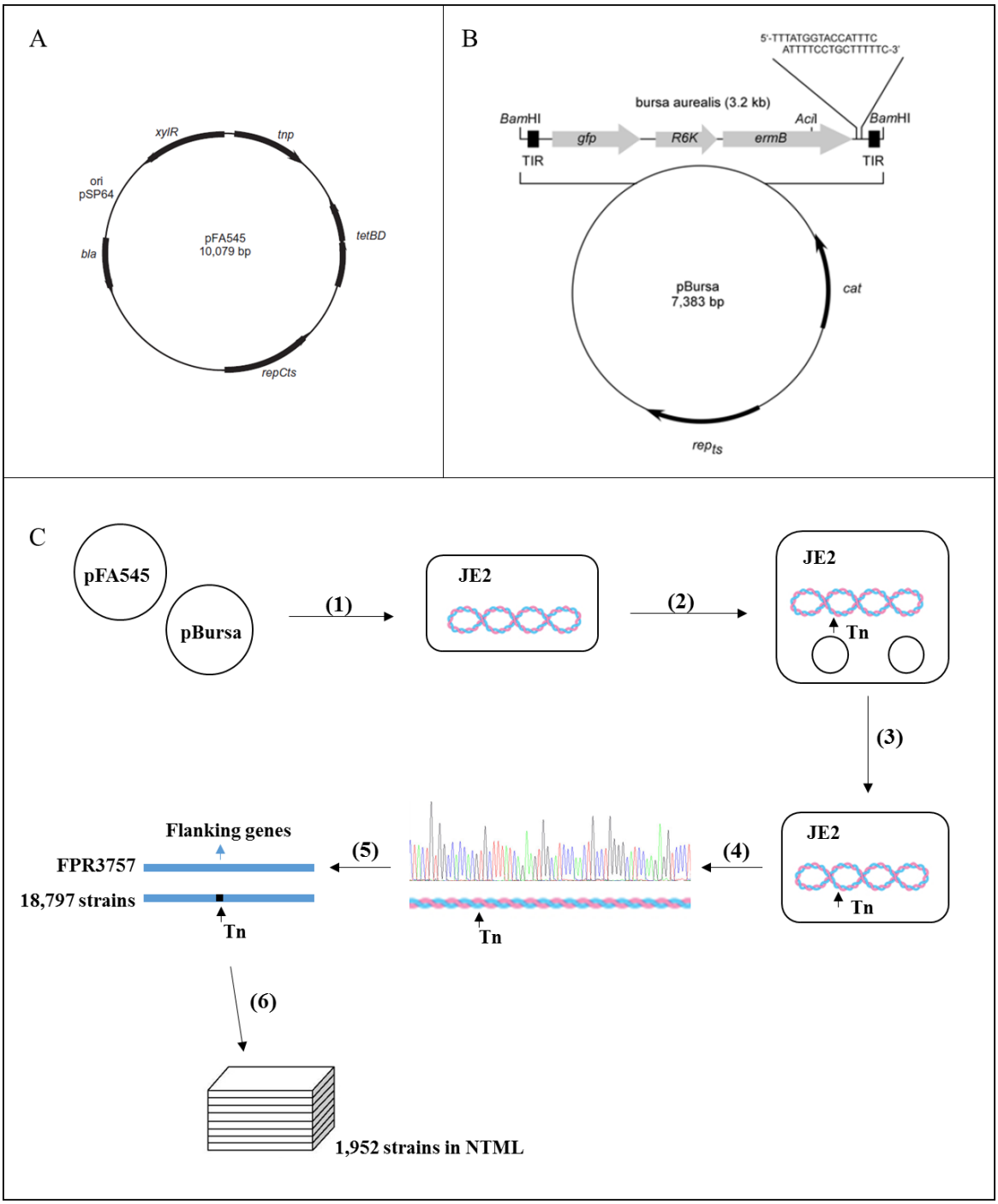

Figure 4.1. Plasmids and procedures applied for producing NTML.

(A) Map of transposase plasmid pFA545 with ampicillin resistance (*bla*) marker, tetracycline resistance cassettes (*tetBD*), mariner transposase (*tnp*), and temperature-sensitive plasmid replicon (*repCts*) (Bae *et al*., 2008).

(B) Map of plasmid pBursa containing a *mariner* transposon, *Bursa aurealis*. The transposable element consists of mariner terminal inverted repeats (TIR), green fluorescent protein gene (*gfp*), replication origin (R6K), and erythromycin resistance gene (*ermB*). The plasmid possesses a temperature-sensitive plasmid replicon (*repts*) and chloramphenicol resistance gene (*cat*) (Bae *et al*., 2008).

(C) Construction of the NTML. Tn: Transposon

(1). The pFA545 and pBursa plasmids were transduced into JE2.

(2). The transductants were incubated on solid media at 30^{o}C for 48 hr for transposition to take place.

(3). A single colony was suspended in 45^{o}C water to inhibit replication of plasmids. Antibiotics were used to select positive transposon inserts and incubate bacteria at the non-permissive temperature to remove plasmids. Bacteria that showed erythromycin resistance, but tetracycline and chloramphenicol susceptibility were selected.

(4). Transposon insertion sites of the 18,797 strains were sequenced to identify the transposon insertion sites.

(5). The sequences of transposon inserts were aligned with genomic DNA of USA300 FPR3757 to identify the DNA flanking the transposon position.

(6). By discarding strains with transposon inserted into intergenic fragments and last 10% of coding sequences, the remaining 1,952 strains were arrayed in 96 well plates as NTML.

4.2 First round of NTML screen

Following optimisation experiments to establish the screen conditions (Chapter 3), the 1st round of screening was carried out using exponential phase NTML *S. aureus* mutants at an MOI of 10 for 3 hr at 37ºC with 5% CO_2. This was followed by high-throughput flow cytometric detection of viable neutrophil count and ToPro-3 positivity. Neutrophils from 9 donors were used to complete the 1st round of screen (n=1).

4.2.1 Identification of *S. aureus* mutants with attenuated neutrophil lysis by viable neutrophil count and ToPro-3 negativity

The aim of the 1st round of screening was to identify mutants that were attenuated in their ability to cause neutrophil cell death. To do this, the viable neutrophil population was gated in dot plots based on FFC/SSC parameters as per Chapter 3. ToPro-3 positive and negative events were also counted. The absolute viable neutrophil number and percentage of ToPro-3 negative events of each sample were quantified by FlowJo™ analysis (section 2.10.4.3). Figure 4.2 presents data for every mutant strain collected across 9 independent neutrophil experiments. Each panel represents an individual 96 well plate (1A-5D). Two plates were screened on the same day (e.g. 1A & 1B, 1C&1D etc) except for plate 5C and 5D. For each treatment condition/mutant, the viable neutrophil count (left hand axis) and ToPro-3 negativity (right hand axis) was plotted as a single line together with media control, JE2 WT, and average of the plate (orange dotted line) (Figure 4.2). The average of each plate refers to the mean viable neutrophil cell number and mean ToPro-3 negative percentage of the 96 wells. The average value of the plate is considered as an important reference point since the majority of mutants will not be attenuated and therefore should theoretically be similar to WT.

1A

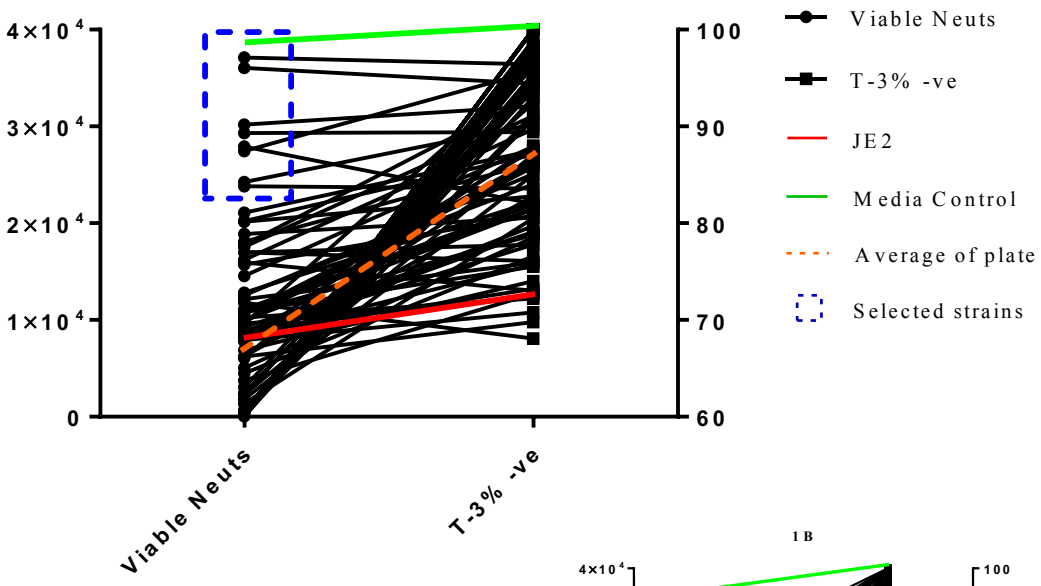
4×10 4
3×10 4
2×10 4
1×10 4
0
100
90
80
70
60
Viable Neuts
T-3% -ve
Viable Neuts
T-3% -ve
Media Control
Average of plate
Selected strains

1B

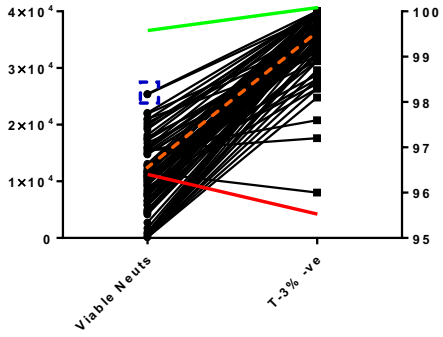
4×10 4
3×10 4
2×10 4
1×10 4
0
100
99
98
97
96
95
Viable Neuts
T-3% -ve

1C

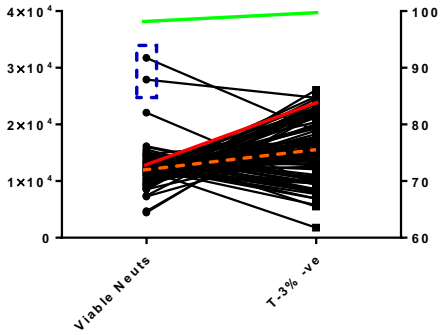
4×10 4
3×10 4
2×10 4
1×10 4
0
100
90
80
70
60
Viable Neuts
T-3% -ve

1D

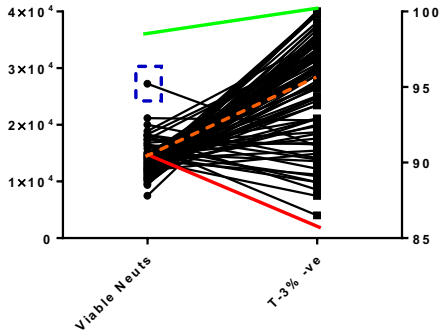
4×10 4
3×10 4
2×10 4
1×10 4
0
100
95
90
85
Viable Neuts
T-3% -ve

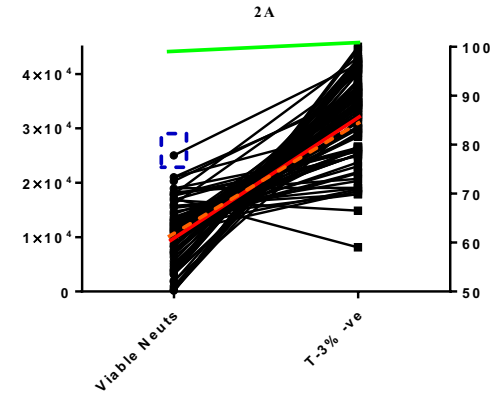
2 A
4x10 4
3x10 4
2x10 4
1x10 4
0
100
90
80
70
60
50
Viable Neuts
T-3% -ve

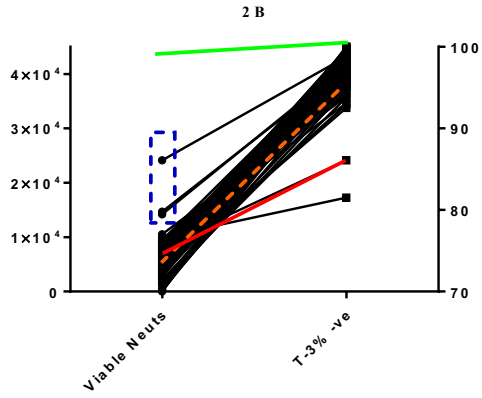
2 B
4x10 4
3x10 4
2x10 4
1x10 4
0
100
90
80
70
Viable Neuts
T-3% -ve

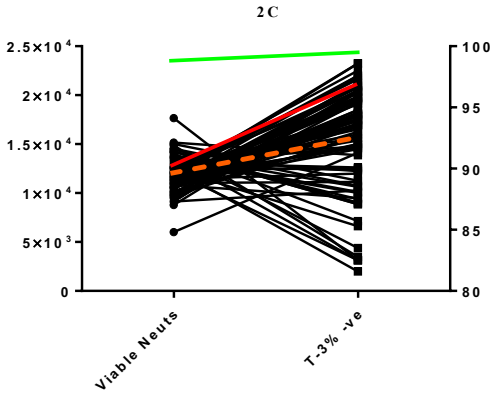
2 C
2.5x10 4
2x10 4
1.5x10 4
1x10 4
5x10 3
0
100
95
90
85
80
Viable Neuts
T-3% -ve

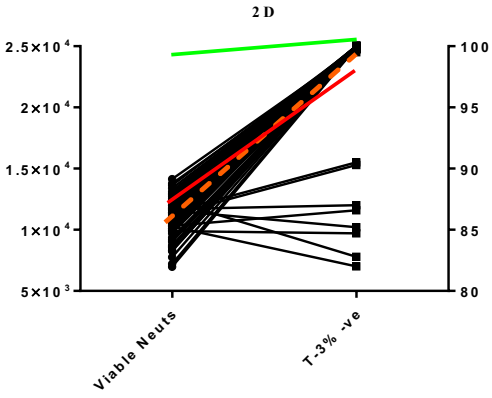
2 D
2.5x10 4
2x10 4
1.5x10 4
1x10 4
5x10 3
100
95
90
85
80
Viable Neuts
T-3% -ve

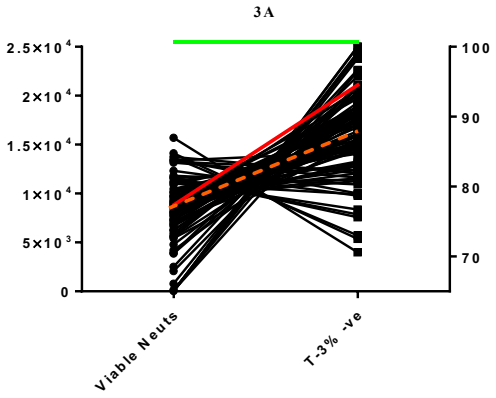
3 A
2.5x10 4
2x10 4
1.5x10 4
1x10 4
5x10 3
0
100
90
80
70
Viable Neuts
T-3% -ve

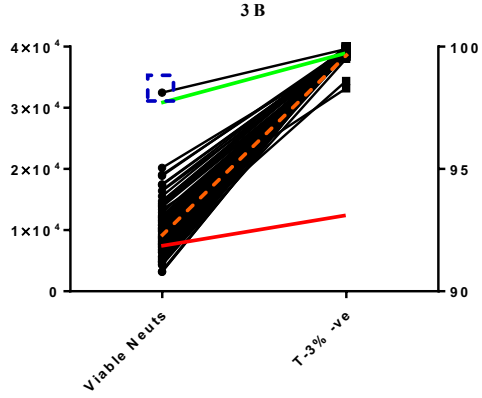
3 B
4x10 4
3x10 4
2x10 4
1x10 4
0
100
95
90
Viable Neuts
T-3% -ve

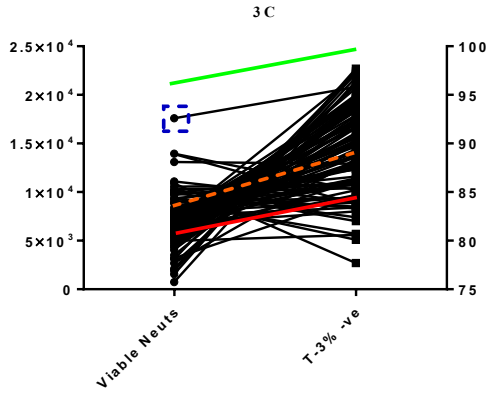
3 C
2.5×10 4
2×10 4
1.5×10 4
1×10 4
5×10 3
0
100
95
90
85
80
75
Viable Neuts
T-3% -ve

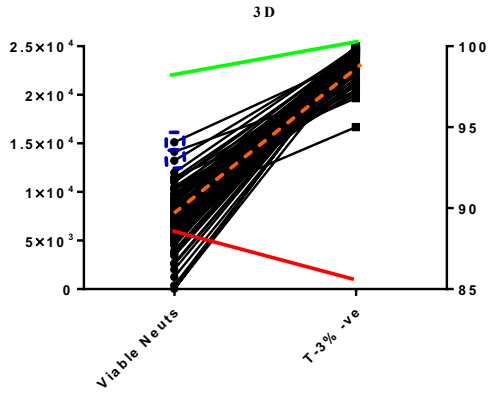
3 D
2.5×10 4
2×10 4
1.5×10 4
1×10 4
5×10 3
0
100
95
90
85
Viable Neuts
T-3% -ve

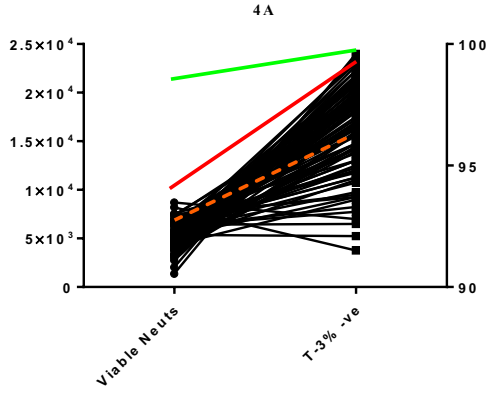
4 A
2.5×10 4
2×10 4
1.5×10 4
1×10 4
5×10 3
0
100
95
90
Viable Neuts
T-3% -ve

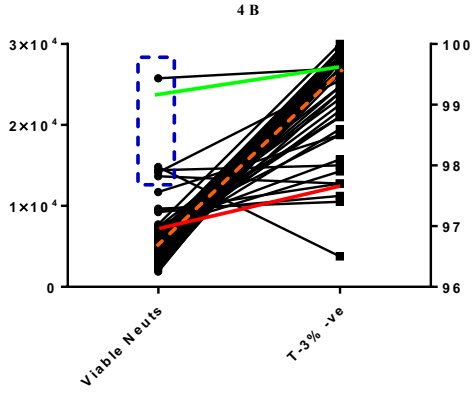
4 B
3×10 4
2×10 4
1×10 4
0
100
99
98
97
96
Viable Neuts
T-3% -ve

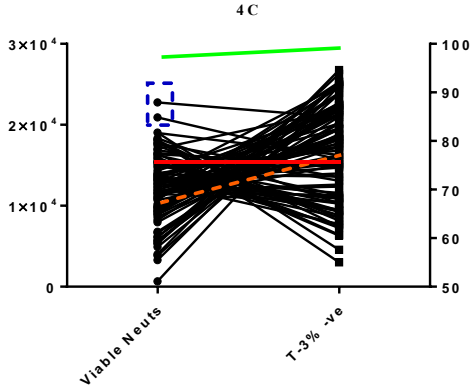
4 C
3×10 4
2×10 4
1×10 4
0
100
90
80
70
60
50
Viable Neuts
T-3% -ve

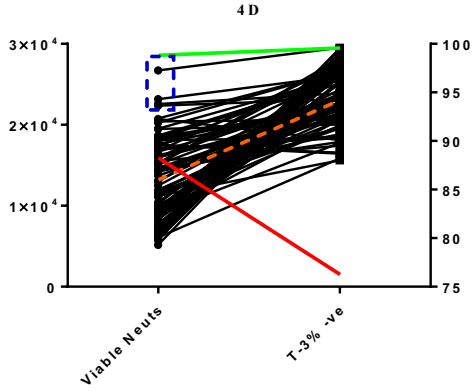
4 D
3×10 4
2×10 4
1×10 4
0
100
95
90
85
80
75
Viable Neuts
T-3% -ve

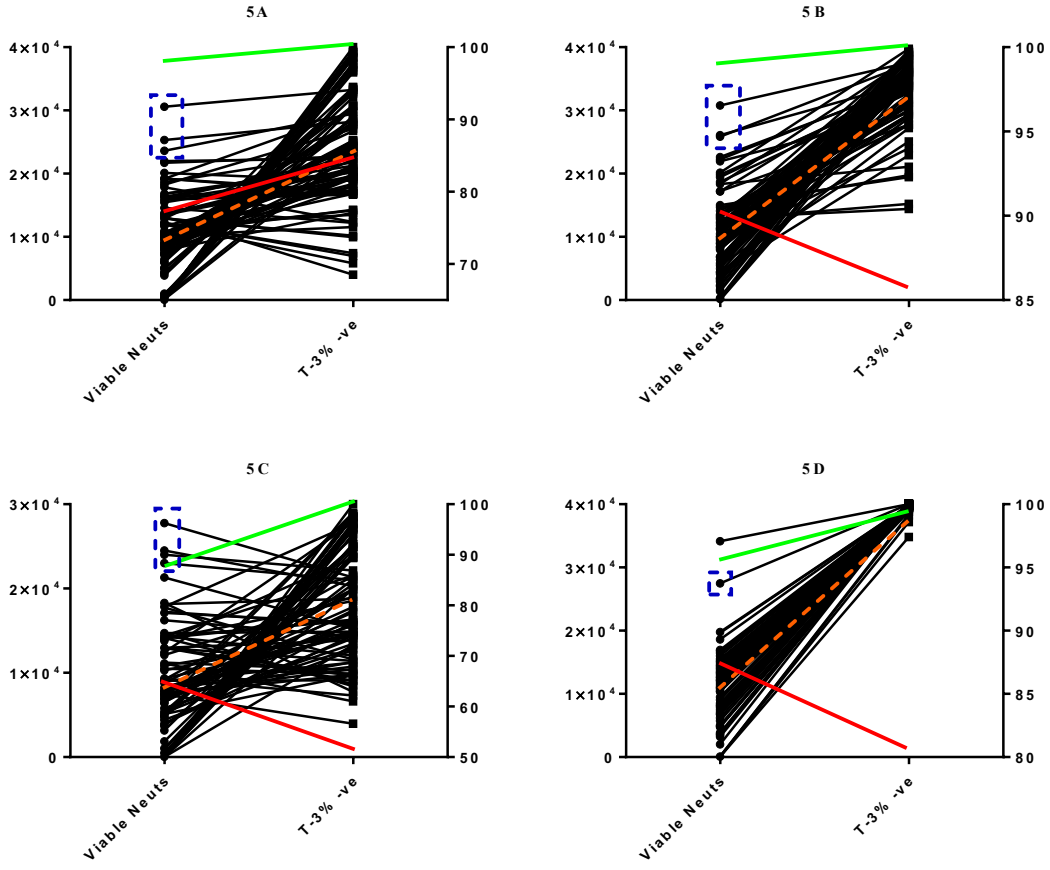

Figure 4.2 Selection of *S. aureus* mutants from the NTML showing attenuated neutrophil cell lysis based on absolute viable neutrophil count and ToPro-3 negativity (%) result in the 1st round of screen. Data shown in 20 96-well plates format with corresponding media control (green solid line), JE2 wild type treatment (red solid line) and mean value of each plate (orange dotted line). Each plate consists of 96 *S. aureus* mutants from the NTML. Neutrophils were incubated at 37ºC for 3 hr with individual NTML mutant at MOI of 10, followed by staining withToPro-3 (1:10,000) and Attune flow cytometry detection. Viable neutrophil counts were generated by healthy cell gating. The majority of *S. aureus* mutants resulted in massive neutrophil cell loss. To identify the attenuated mutants, mean value plus two times of standard deviation of viable cell count was applied to distinguish potential 'hits' from the rest of strains. Identified strains are highlighted in blue boxes.

Each plate was analysed individually. Initial identification of attenuated mutants (ie. those that were less effective at inducing neutrophil lysis) was done by identifying mutants that resulted in a high number of viable neutrophils and a high percentage ToPro-3 positivity. These strains are highlighted by blue dotted boxes. This was initially done visually and later verified by showing the viable neutrophil count of each attenuated strain was >2 standard deviations from JE2. For instance, in plate 1C, the media control (green solid line) suggests the co-incubation started with approximately 38,000 viable neutrophils in each well. After 3 hr incubation with JE2 WT, more than 25,000 neutrophils were lysed and ToPro-3 negative population decreased to 85% (red solid line). The majority of *S. aureus* mutants resulted in less than 18,000 viable cells and 95% ToPro-3 negativity, indicating massive neutrophil cell loss. To identify the attenuated mutants, mean value (12,323) plus two times standard deviation (7,038) of viable cell count of plate 1C were applied (19,361) to distinguish potential 'hits' from the rest of the strains. Then the mutants with ToPro-3 negativity that was lower than JE2 mean value was further ruled out, leaving 2 identified strains from this plate (Figure 4.2, 1C).

Throughout the screen of 20 NTML plates, neutrophil media control showed viable cell counts of 30637±7183 and high ToPro-3 negativity (99.73%±0.17%). JE2 treatment consistently led to massive neutrophil cell loss (19778±7168) and low ToPro-3 negativity (84.45%±11.45%) (Figure 4.2), suggesting a robust screen model for neutrophil cell death in the assay. The average of 9 NTML plates displayed similar killing efficiency compared to JE2, and highly representative neutrophil cell death result of major mutants (1C, 2A, 2B, 2D, 3B, 3D, 4B, 5B, 5D plates). Six plates showed comparatively more variation of viable cell count and ToPro-3 intensity among the 96 strains (1A, 3A, 4C, 5A, 5C plates). Typically, 1-6 attenuated mutants were identified from each plate with the exception of 2C, 2D, 3A, and 4A plates which yielded none (Figure 4.2). In total, 42 *S. aureus* mutants were selected

as having an attenuated ability to lyse neutrophil *in vitro* based on viable neutrophil count and ToPro-3 negativity results.

4.2.2 Identification of *S. aureus* mutants with attenuated neutrophil lysis by FSC/SSC profiling

In addition to performing data analysis based on viable neutrophils and ToPro-3 negativity, flow cytometric dot plots were also used to identify attenuated *S. aureus* mutants. This is important, as it is a more discriminatory strategy since it allows to observe changes in the cellular shape and size as a result of cell lysis, which is not possible just by counting viable neutrophils. This extra level of analysis allows us to identify as many potential candidates as possible. Flow cytometric FSC/SSC profiling (dot plot) of all 1,920 NTML mutants were therefore visually assessed and arbitrarily ranked to select attenuated strains.

The data file of NTML screen dot plots exceeded the space restriction of this thesis (Google Drive). As a representative of strains from plate 1A, the media control displays 81.4% of viable neutrophils, which appear within the viable neutrophil gate as a compact population, with a smaller sub-population with increased FSC and SSC (Figure 4.3 A). The JE2 treated sample is visibly different, with the cell dense area appearing outside the viable gate, in the lower left corner where the debris is typically found (Figure 4.3 B). A mutant in well E7 resulted in 53.3% of viable neutrophils (Figure 4.3 C), which is much higher than JE2 (12.6%). This strain was selected based on viable neutrophil and ToPro-3 analysis (Figure 4.2), but also is clearly attenuated by looking at the FSC/SSC distribution. A mutant in well C6 led to similar cell loss (17.8%) compared to JE2, indicating full staphylococcal virulence of this strain (Figure 4.2 F). Strains in well A1(36.8%) and D7 (27.8%) showed a clear viable population suggesting attenuated immune cell lysis (Figure 4.3 D & E), yet were not

identified in Figure 4.2. Consequently, the *S. aureus* mutants corresponding to A1 and D7 were added as attenuated candidates from the screen.

The flow cytometric cell scatter plots of all NTML strains were assessed in this way and compared to JE2. A total of 113 *S. aureus* mutants with a clearly different FSC/SSC profile were selected. The mutants identified from both methods described above are listed in the following table, labelled by their corresponding well in NTML (Table 4.1). Among the 118 strains, 37 were identified by both methods (common). Of the remaining 80, mutants were picked from either flow cytometric cell scatter assessment (76) or viable neutrophil and ToPro-3 data analysis (4). All 118 strains were listed in Table 4.2 and taken forward into the 2nd round of screening.

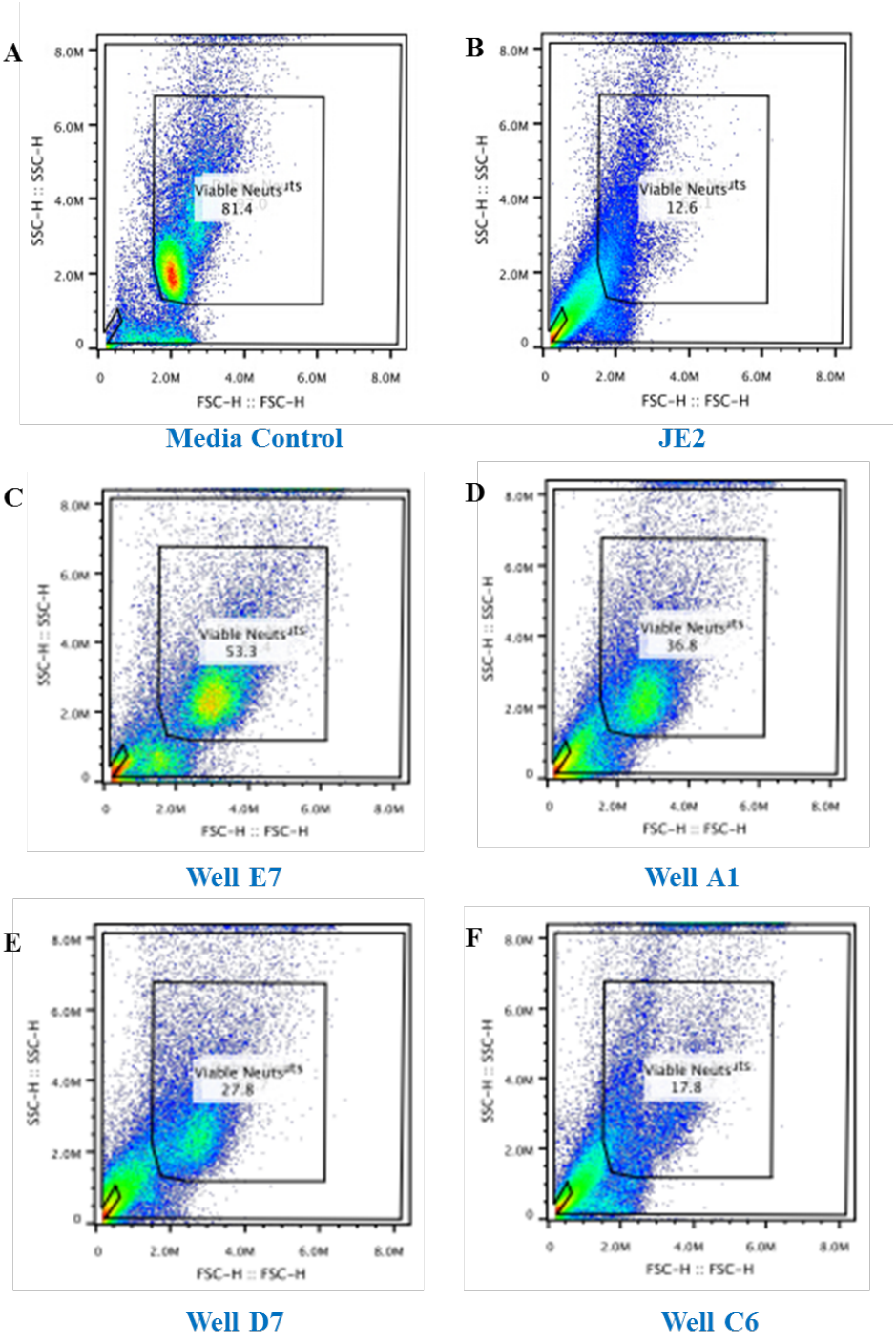

Figure 4.3 Flow cytometric cell scatter plots (FSC/SSC) of the media control (A), JE2 treated neutrophils (B), and co-incubation results of 4 wells in plate 1A (C-F) from the 1st round of screen. Neutrophils were co-incubated with *S. aureus* strains for 3 hr at MOI of 10. The FSC and SSC indicates size and granularity of cells. Gated area refers to the viable neutrophil population (%).

Plate	Viable Neutrophils and ToPro-3	FSC/SSC Profiling	Common
1A	E7 G11	A1 B2 D7 D11 E1 E10	F10 F11 D12 H1 F12 F7
1B		B12 F10 F11 G11	B11
1C			G5 H5
1D			E11
2A		B6 D4 D5 D6 D7 G6	E6
2B			E1 D6
2C	None		
2D			
3A			
3B		B9 D6 E6	D12
3C		B12	H4
3D	H5		F9
4A	None		
4B			H2 D12 F7 G2
4C		B4 C2 C11 D1 D8 D9 D10 E1 E2 E7 E9 E10 F2 F7 F8 F9 G4 G8	E8 D4
4D		A5 B8 B9 C7 C8 D5 D7 D8 D9 E7 F7 F9 G7 G8 H8	H7 H6 G9 C9 B7
5A		B4 C10 D1 D6 D9 F2	E8 E9 G2
5B		B10 G5 G7	E10 F10 F11
5C	C4	B5 C5 F7 A3 A4 A5 B1 B10 C1 C7 D1 E5 H12	D5 C6 E12
5D			F8

Table 4.1. Combination of identified wells of each plate with *S. aureus* mutants generating attenuated neutrophil cell lysis result from the 1st round of screen. The strains are referred to their well and plate numbers in NTML library. The mutants selected by both methods are only listed under 'common' column.

Plate	Well	Strains	Gene Description
1A	A1	USA300_1327	cell surface protein
	B2	AUSA300_2406	putative transporter
	D11	USA300_1393	phiSLT ORF2067-like protein, phage tail tape measure protein
	D12	USA300_0210	maltose ABC transporter, permease protein
	D7	USA300_2242	urease accessory protein UreF
	E1	USA300_0217	DNA-binding response regulator, AraC family
	E10	USA300_2551	anaerobic ribonucleotide reductase, large subunit
	E7	USA300_0319	putative membrane protein
	F10	USA300_0648	ABC transporter, permease protein
	F11	USA300_0640	putative membrane protein
	F12	USA300_2504	acyltransferase
	F7	USA300_2573	immunodominant antigen B
	G11	USA300_1980	acetyltransferase, GNAT family
	H1	USA300_2149	6-phospho-beta-galactosidase
1B	B11	USA300_0181	non-ribosomal peptide synthetase
	B12	USA300_0341	putative membrane protein
	F10	USA300_0230	putative membrane protein
	F11	USA300_1939	phi77 ORF015-like protein, putative protease / phage portal protein
	G11	USA300_2360	multidrug resistance protein
1C	G5	USA300_0720	putative iron compound ABC transporter, ATP-binding protein
	H5	USA300_2452	transcriptional regulator, MarR family
1D	E11	USA300_0662	acetyltransferase, GNAT family
2A	B6	USA300_1140	cell wall hydrolase
	D4	USA300_2089	pyrimidine nucleoside phosphorylase
	D5	USA300_0265	putative ribose operon repressor
	D6	USA300_0347	Sec-independent protein translocase TatC
	D7	USA300_1801	fumarate hydratase, class II
	E6	USA300_0161	capsular polysaccharide biosynthesis protein Cap5J
	G6	USA300_0917	putative membrane protein
2B	D6	USA300_1889	adenylosuccinate lyase
	E1	USA300_0017	adenylosuccinate synthetase
3B	B9	USA300_1182	pyruvate ferredoxin oxidoreductase, alpha subunit
	D6	USA300_1732	putative transposase
	D12	USA300_0752	ATP-dependent Clp protease proteolytic subunit
	E6	USA300_1938	phi77 ORF006-like protein capsid protein
3C	B12	USA300_0667	hypothetical protein
	H4	USA300_1092	uracil permease
3D	F9	USA300_0064	arginine/oirnithine antiporter
3D	H5	USA300_1536	hypothetical protein
4B	D12	USA300_0690	sensor histidine kinase SaeS
4B	F7	USA300_0899	adaptor protein

4B	G2	USA300_2042	hypothetical protein
4B	H2	USA300_1494	hypothetical protein
4C	B4	USA300_1255	oxacillin resistance-related FmtC protein
	C2	USA300_0728	conserved hypothetical protein
	C11	USA300_1596	S-adenosylmethionine:tRNA ribosyltransferase-isomerase
	D1	USA300_2541	malate:quinone-oxidoreductase
	D4	USA300_0957	hypothetical protein
	D8	USA300_0337	glycerol-3-phosphate transporter
	D9	USA300_1225	aspartate kinase
	D10	USA300_0709	5'(3')-deoxyribonucleotidase
	E1	USA300_2490	TetR family regulatory protein
	E2	USA300_0213	Gfo/Idh/MocA family oxidoreductase
	E7	USA300_2365	gamma-hemolysin component A
	E8	USA300_2389	putative drug transporter
	E9	USA300_1853	conserved hypothetical protein
	E10	USA300_0590	hypothetical protein
	F2	USA300_0409	conserved hypothetical protein
	F7	USA300_1244	large conductance mechanosensitive channel protein
	F8	USA300_0683	transcriptional regulator, DeoR family
	F9	USA300_1180	conserved hypothetical protein
	G4	USA300_1003	conserved hypothetical protein
	G8	USA300_2069	conserved hypothetical protein
4D	A5	USA300_1797	conserved hypothetical protein
	B6	USA300_1283	phosphate ABC transporter, phosphate-binding protein PstS
	B8	USA300_1843	D-isomer specific 2-hydroxyacid dehydrogenase family protein
	B9	USA300_0385	conserved hypothetical protein
	C7	USA300_2300	transcriptional regulator, TetR family
	C8	USA300_2023	anti-sigma-B factor, serine-protein kinase
	C9	USA300_2048	hydroxyethylthiazole kinase
	D5	USA300_1687	FtsK/SpoIIIE family protein
	D7	USA300_1934	phi77 ORF020-like protein, phage major tail protein
	D8	USA300_1718	aresenical pump membrane protein
	D9	USA300_2083	acetyltransferase
	E7	USA300_2055	UDP-N-acetylglucosamine 1-carboxyvinyltransferase
	F7	USA300_1519	hypothetical protein
	F9	USA300_0630	ABC transporter ATP-binding protein
	G7	USA300_1563	acetyl-CoA carboxylase, biotin carboxylase
	G8	USA300_2030	hypothetical protein
	G9	USA300_2620	hypothetical protein
	H6	USA300_1368	L-asparaginase
	H7	USA300_0505	glutamine amidotransferase subunit PdxT
	H8	USA300_1992	accessory gene regulator protein A
5A	B4	USA300_0706	putative osmoprotectant ABC transporter ATP-binding protein

	C10	USA300_0431	hypothetical protein
	D1	USA300_0141	phosphopentomutase
	D6	USA300_0945	isochorismate synthase family protein
	D9	USA300_2350	hypothetical protein
	E8	USA300_2359	amino acid ABC transporter amino acid-binding protein
	E9	USA300_2482	hypothetical protein
	F2	USA300_2040	hypothetical protein
	G2	USA300_0996	dihydrolipoamide dehydrogenase
5B	B10	USA300_0657	hypothetical protein
	E10	USA300_2548	hypothetical protein
	F10	USA300_0244	zinc-binding dehydrogenase family oxidoreductase
	F11	USA300_0471	hypothetical protein
	G5	USA300_0566	amino acid permease
	G7	USA300_1051	hypothetical protein
5C	A3	USA300_2456	hypothetical protein
	A4	USA300_1274	peptide ABC transporter ATP-binding protein
	A5	USA300_0827	hypothetical protein
	B1	USA300_1356	3-dehydroquinate synthase
	B5	USA300_1926	phi77 ORF044-like protein
	B10	USA300_2043	hypothetical protein
	C1	USA300_0936	ABC transporter ATP-binding protein
	C4	USA300_0646	sensor histidine kinase
	C5	USA300_1089	lipoprotein signal peptidase
	C6	USA300_0994	pyruvate dehydrogenase E1 component, beta subunit
	C7	USA300_1097	orotidine 5'-phosphate decarboxylase
	D1	USA300_1187	hypothetical protein
	D5	USA300_0857	hypothetical protein
	D6	USA300_1139	succinyl-CoA synthetase subunit alpha
	E5	USA300_0334	MarR family transcriptional regulator
	E12	USA300_0982	hypothetical protein
	F7	USA300_0839	hypothetical protein
	H12	USA300_0035	hypothetical protein
5D	F8	USA300_1171	hypothetical protein

Table 4.2. The 118 *S. aureus* mutants identified from the 1st round of screen of NTML. They were all taken forward for further study. The genetic background of the mutants was not decoded until completion of the 2nd round of screen, but is included here for reference.

4.2.4 Identification of internal control *S. aureus* mutants

Until this point, the screen was performed blindly, which is to say that the genetic background of each strain was not revealed and each mutant was only identifiable by a well coordinate. It is highly important to do so, in order to completely exclude potential influence of researcher's subjective consciousness of the screen, and therefore ascertain every strain in NTML is treated equally. Since there are already neutrophil lytic factors described for *S. aureus*, these represented an in-built positive control for this assay. In this instance, strains mutated in genes: *agrA* refers to accessory gene regulator A. It plays an essential role in high-level expression of secreted proteins such as PSM and highly likely involved in abscess formation in *S. aureus* induced infections (Voyich *et al*., 2009, Thoendel *et al*., 2011, Boles and Horswill, 2008). Gene *saeS* is involved in membrane-associated protein kinase function which is essential for immune evasion mechanism of *S. aureus* (Benson *et al*., 2012, Bronner *et al*., 2004). Both genes are well known in producing factors that lyse neutrophils and therefore being selected as internal controls.

Experiments which included the *saeS* and *agrA* mutants were identified in order to determine whether they failed to induce neutrophil lysis as hypothesised. Screening of NTML plates containing *saeS* mutant started with 14,745 healthy neutrophils and 99.4% ToPro-3 negativity (Figure 4.4). The treatment of JE2 leads to decreased viable neutrophils (8,703) and reduced ToPro-3 negativity (97.9%) and the mean viable neutrophil number for all strains was 5,209. The *saeS* mutant resulted in 14,149 viable cells and 99.4% ToPro-3 negativity, suggesting attenuation of the neutrophil cell lysis. The media control from the screening *agrA* experiment contained 28,502 viable neutrophils and 99.7% ToPro-3 negative population. JE2 resulted in 15,263 viable neutrophils and 76.5% ToPro-3 negativity and the mean value of all mutants was 12,877 neutrophils. The *agrA* mutant resulted in 20,797 viable neutrophils and high ToPro-3 negativity (97.2%), also resulted in

a visible healthy neutrophil population in the dot plot, validating the observational method (Figure 4.4). Both *agrA* and *saeS* mutants result in greater number of viable neutrophils, and ToPro-3 negativity compared to the corresponding JE2 treated sample and mean of mutant values. These internal controls are a good validation and proof of principle for the screen and give confidence in the chances of identifying novel genes involved in neutrophil lysis.

4.3 A second, focused round of NTML screening

Of the 1,920 strains screened, 118 were identified as attenuated and to validate this further, each of the 118 strains was taken forward from the preliminary screen and rescreened a 2nd time. The *S. aureus* mutants identified from the 1st round of screen were sub-cultured (10 μL culture in 190 μL of fresh BHI per well) to two new 96 well plates for the following focused 2nd round of screen. The 2nd round of screen was performed with same method as the 1st round of screen, but was repeated 3 times with 3 independent neutrophil donors.

4.3.1 Identification of *S. aureus* mutants with attenuated neutrophil lysis by viable neutrophil count and ToPro-3 negativity

Each experiment of the 2nd round of screening consists of two plates: plate A with 96 *S. aureus* mutants and plate B containing 22 strains. The absolute viable neutrophil number and ToPro-3 negative percentage of each *S. aureus* mutant infected neutrophil sample was quantified by the same method as described above (section 4.2.1), and plotted by a single line together with media control, JE2 WT, and average of each plate (Figure 4.5).

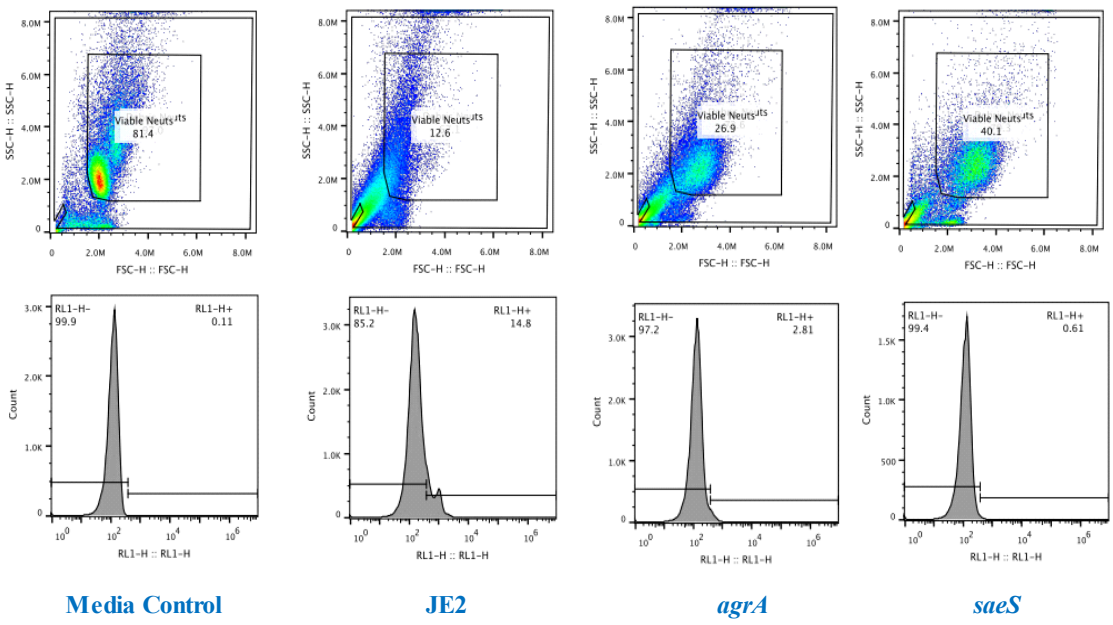

	Media Control	JE2	Mean of Mutants	*agrA*	*saeS*
Viable Neutrophils	14745	8703	5209		14149
Negative T-3%	99.4	97.9	99.5		99.4
Viable Neutrophils	28502	15263	12877	20797	
Negative T-3%	99.7	76.5	94.8	97.2	

Figure 4.4 Illustrative FSC/SSC dot plots and ToPro-3 histograms of media and JE2 controls, and internal positive controls of the NTML screen namely *agrA* and *saeS*. Neutrophils were co-incubated with *S. aureus* strains for 3 hr at MOI of 10, followed by staining of ToPro-3 (1:10,000) and Attune flow cytometry detection. The viable neutrophil count and ToPro-3 negativity (%) of the strains are listed in the table below together with corresponding controls. T-3: ToPro3.

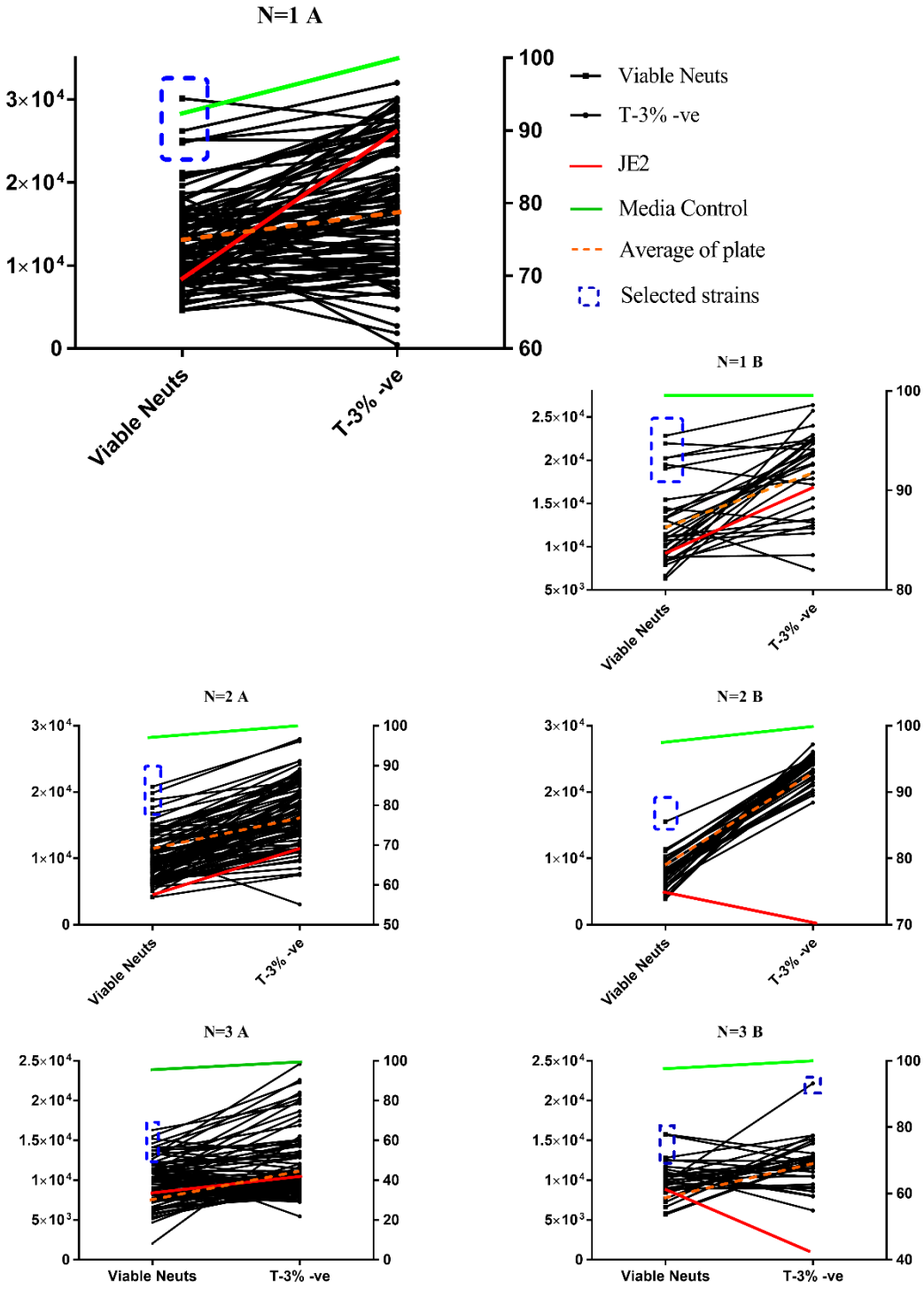
N=1 A
Viable Neuts
T-3% -ve
JE2
Media Control
Average of plate
Selected strains
N=1 B
N=2 A
N=2 B
N=3 A
N=3 B

Figure 4.5 Selection of attenuated *S. aureus* mutants based on the absolute viable neutrophil count and ToPro-3 negativity (%) result generated by each strain in the 2nd round of screening. Data shown in 96-well plate format with corresponding media control (green solid line), JE2 wild type treatment (red solid line) and mean value of each plate (orange dotted line). Plate A consists of 96 *S. aureus* mutants and plate B contains the remaining 22 strains identified from the 1st round of screen. Neutrophils were incubated at 37°C for 3 hr with individual NTML mutant at MOI of 10, followed by staining with ToPro-3 (1:10,000) and Attune flow cytometry detection. Mean value plus two times of standard deviation of viable cell count was applied to identified attenuated strains highlighted in blue box.

The co-incubation started with 24,000-28,000 healthy neutrophils (100% ToPro-3 negative) per well. After 3 hr of JE2 treatment, less than 10,000 neutrophils remained viable and the ToPro-3 negative population decreased (66.7% ± 20.5%). Most *S. aureus* mutants resulted in less than 15,000 viable neutrophils and were therefore not considered to be attenuated (Figure 4.5). It is worthy of note that unlike data from the 1st round of screening, the average neutrophil cell death result of mutants in 2nd round of screen (orange dash line) display higher viable neutrophil amount than JE2 (red line), indicating comparatively attenuated virulence than WT which would be expected. The strains with viable neutrophil count or ToPro-3 negativity two times of standard deviation higher than the mean value were selected as candidate strains (highlighted in blue box) (Figure 4.5). From the 3 repeating experiments, 10, 7, and 17 attenuated mutants were selected. The corresponding well and plate number of identified strains are listed in Table 4.3.

4.3.2 Identification of *S. aureus* mutants with attenuated neutrophil lysis by flow cytometric cell scatter

In addition to performing data analysis based on viable neutrophils and ToPro-3 negativity, flow cytometric FSC/SSC profiles were also used to identify attenuated *S. aureus* mutants from the 2nd round of screening.

As a representative figure, the flow cytometric dot plots of media control, JE2 and two mutant strains are shown in Figure 4.6 A. The media control displays 80.6% of viable neutrophil population among all detected events. Infection of JE2 resulted in visible cell loss in the viable gating area (14.9%). The *S. aureus* mutant in well B4 led to 61.4% of healthy neutrophils after 3 hr of co-incubation. This strain has been selected from the viable neutrophils and ToPro-3 comparison analysis (highlighted in blue dashed box) (Figure 4.2, B). The screening of the mutant in well A2 produced result with a comparatively smaller

yet distinguishable cell population in viable gating area (36.8%). This strain was therefore added to the list of identified candidates. As the mean value showed in Figure 4.2 B, the majority of strains resulted in comparatively higher viable cell count and ToPro-3 negativity than JE2. The overall attenuated neutrophil cell death is the reason of not selecting well A2 from the analysis.

The flow cytometric cell scatter plots of all rescreened strains were assessed in this way and compared to JE2. In the three experiments, 40, 39, and 35 mutants with an obviously different dot plot profile which were selected from the three repeating experiments respectively. Among them, 10, 7, and 17 strains were identified by both methods. In total 71 *S. aureus* strains have been picked up at least once from the analysis. Their corresponding well and plate numbers are listed in Table 4.3.

N	Plate	Viable Neutrophils and ToPro-3	FSC/SSC Profiling	Common
1	A		A8 A12 B5 B6 B7 B8 B9 C2 C6 C8 D3 D4 D6 D8 D9 D10 D11 E2 E6 E12 F6 F7 G7 G9 G12 H11	A9 A10 A11 D2 E7
	B		A2 A9 A7 B10	B1 B2 B3 B4 B9 B12
2	A		B2 B3 B4 B11 C3 C6 C11 D2 D6 D10 D11 D12 E2 E3 E5 E8 E12 F1 F6 F9 G3 G6 G7 H4 H8 H11 G1 G2	A10 A11 D3 D4 D7 E7
	B		A3 A4 A5 B12	B4
3	A		A8 B5 B6 B11 C5 C11 D1 D5 D3 D4 D9 D11 E1 E6 F2 H2	A9 A10 A11 C6 D2 D7 D6 E2 E7 F1 F6 G1 G2
	B	A2 C6	A12 B4	B12 C1 C7

Table 4.3. Combination of identified wells of each plate with *S. aureus* mutants generating attenuated neutrophil cell lysis result from the 2nd round of screen. The strains are referred to their well and plate numbers in a new sub-library I made that consists of two 96 well plates (A and B). The mutants selected by both methods are only listed under 'common' column.

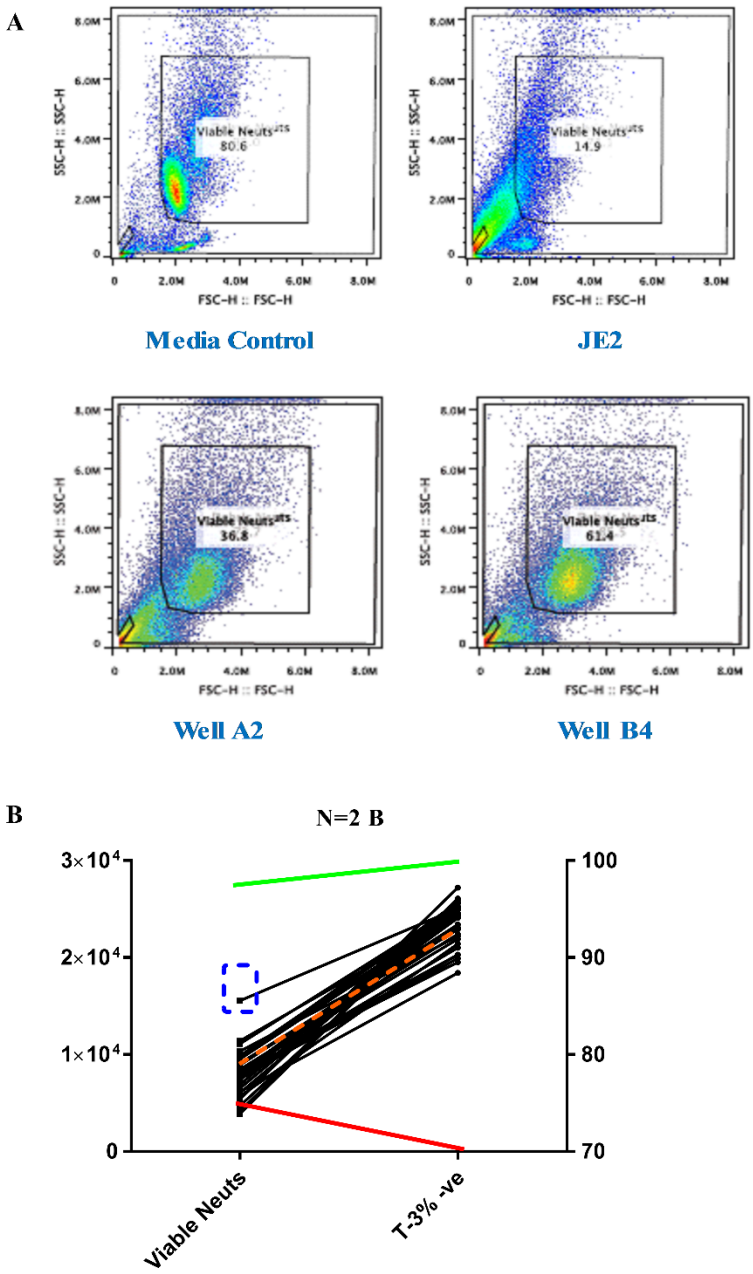

Figure 4.6 (A) Flow cytometric FSC/SSC profiling of media and JE2 controls, and Well A2 and B4 co-culture results of plate B in the 2nd repeating experiment of 2nd round of NTML screen. (B) The viable neutrophil number and ToPro-3 negativity (%) of the 22 *S. aureus* mutants were displayed together with media control (green), JE2 (red), and mean value of the plate (orange). The sample highlighted in blue box is Well B4.

T-3: ToPro-3; -ive: negativity

4.3.3 Arbitrary ranking system of *S. aureus* strains

The *S. aureus* mutants identified from each experiment of the 2nd round of screening were combined and listed in Table 4.3. Among the 118 strains, some *S. aureus* mutants were consistently attenuated in their ability to induce neutrophil cell death, such as well B4 in plate B. It was selected from either flow cytometric cell scatter and viable neutrophils or ToPro-3 comparison in all three repeating experiments. Strains such as well A11 of plate A was identified by both methods in 2 experiments and by FSC/SSC profiling in the 3rd experiment. Well A8 of plate A, consistently displayed healthy neutrophil population in flow cytometric dot plots, but the number of viable neutrophils were not high enough to be selected by this method.

To determine which of the *S. aureus* mutants identified from 2nd round of screen resulted in the most robust attenuated neutrophil cell lysis, an arbitrary ranking system was introduced to comprehensively compare the attenuation among the 118 strains. If a *S. aureus* mutant appeared once from either FSC/SSC profiling, or from viable neutrophils and ToPro-3 counts, 1 point was scored. For instance, well A8 of plate A scored 3 points for being identified three times by FSC/SSC profiling only. *S. aureus* strains that were commonly selected by both methods scored 2.5 points. For example, well B4 of plate B scored 7.5 points in this ranking system. Well A11 of plate A therefore scored 6 points.

Based on the points by the ranking system, 74 *S. aureus* mutants were recorded with either 0 or 1 point, while the remaining 34 strains scored greater than 2 points (Figure 4.7). The mutants were ranked and the top scoring 34 strains were selected from the 2nd round of screen as *S. aureus* showing robust attenuation in neutrophil cell lysis. The identified 34 strains are listed in Table 4.4.

Rank/34	Points	Gene ID	Gene description	Name
1	7.5	USA300_1974	Leukocidin/Hemolysin toxin family protein	
1	7.5	USA300_1975	Aerolysin/leukocidin family protein	
1	7.5	USA300_1494	hypothetical protein	
4	6	USA300_0265	putative ribose operon repressor	
4	6	USA300_1089	lipoprotein signal peptidase	*lspA*
4	6	USA300_0994	pyruvate dehydrogenase E1 component, beta subunit	*pdhB*
7	5	USA300_0690	sensor histidine kinase SaeS	***saeS***
7	5	USA300_1889	adenylosuccinate lyase	*purB*
7	5	USA300_0347	Sec-independent protein translocase TatC	*tatC*
7	5	USA300_1801	fumarate hydratase, class II	*fumC*
7	5	USA300_0917	putative membrane protein	
7	5	USA300_2365	gamma-hemolysin component A	*hlgA*
13	4.5	USA300_0230	putative membrane protein	
13	4.5	USA300_1092	uracil permease	*pyrP*
15	3.5	USA300_1992	accessory gene regulator protein A	***agrA***
15	3.5	USA300_1182	pyruvate ferredoxin oxidoreductase, alpha subunit	
15	3.5	USA300_0752	ATP-dependent Clp protease proteolytic subunit	*clpP*
18	3	USA300_0337	glycerol-3-phosphate transporter	
18	3	USA300_1180	conserved hypothetical protein	
18	3	USA300_1568	uridine kinase	*udk*
21	2.5	USA300_0566	amino acid permease	
21	2.5	USA300_1051	hypothetical protein	
21	2.5	USA300_2088	S-ribosylhomocysteinase	*luxS*
21	2.5	USA300_1356	3-dehydroquinate synthase	*aroB*
25	2	USA300_1393	phiSLT ORF2067-like protein, phage tail tape measure protein	
25	2	USA300_0210	maltose ABC transporter, permease protein	
25	2	USA300_0648	ABC transporter, permease protein	
25	2	USA300_0662	acetyltransferase, GNAT family	
25	2	USA300_1732	putative transposase	
25	2	USA300_2042	hypothetical protein	
25	2	USA300_0957	hypothetical protein	
25	2	USA300_1843	D-isomer specific 2-hydroxyacid dehydrogenase family protein	
25	2	USA300_0505	glutamine amidotransferase subunit PdxT	
25	2	USA300_0141	phosphopentomutase	*deoB*

Table 4.4. The 34 *S. aureus* mutants identified from the screen of NTML in human neutrophil cell death assay.

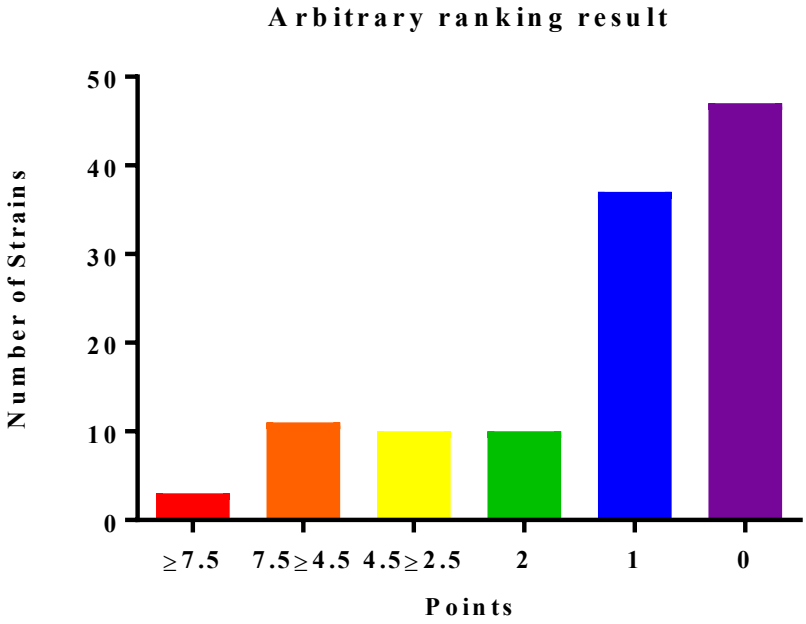

Figure 4.7 Distribution of the number of *S. aureus* mutants with different scores based on the selection of attenuated neutrophil cell lysis result during 2nd round NTML screen. If a *S. aureus* mutant appeared once from either FSC/SSC profiling, or from viable neutrophils and ToPro-3 counts, 1 point was scored. *S. aureus* strains that were commonly selected by both methods scored 2.5 points. This figure displays the points added from 3 independent experiments. The 34 *S. aureus* scored higher than 2 points were identified as strains with robust attenuated NTML mutants.

4.3.4 Verification of NTML mutant growth in 2nd round of screen

Although the bacterial culture preparation has been optimized and the screen was carried out aiming at MOI of 10, it is not feasible to standardise the actual number of *S. aureus* and neutrophils from one prep to another. To determine if potential mutants showing attenuated neutrophil lysis was because of a growth defect, bacterial growth of the 118 strains was measured during the 2nd round of screen to quantify the variation. A Perkin VICTOR x3 2030 plate reader was used to detect the OD_{600} of the strains.

The OD_{600} of *S. aureus* mutants were measured following 3 hr of sub-culture, immediately before the neutrophil co-culture. In each repeated experiment, the OD_{600} of the *S. aureus* strains was plotted with a corresponding viable neutrophil number after 3 hr of treatment, together with JE2 marked in red and media control in green (Figure 4.8). There was no correlation between OD_{600} and neutrophil number (R square values for the three experiments are 0.0225, 0.0695, and 0.0050), suggesting that the attenuation of neutrophil cell lysis was not because of differences in bacterial cell number.

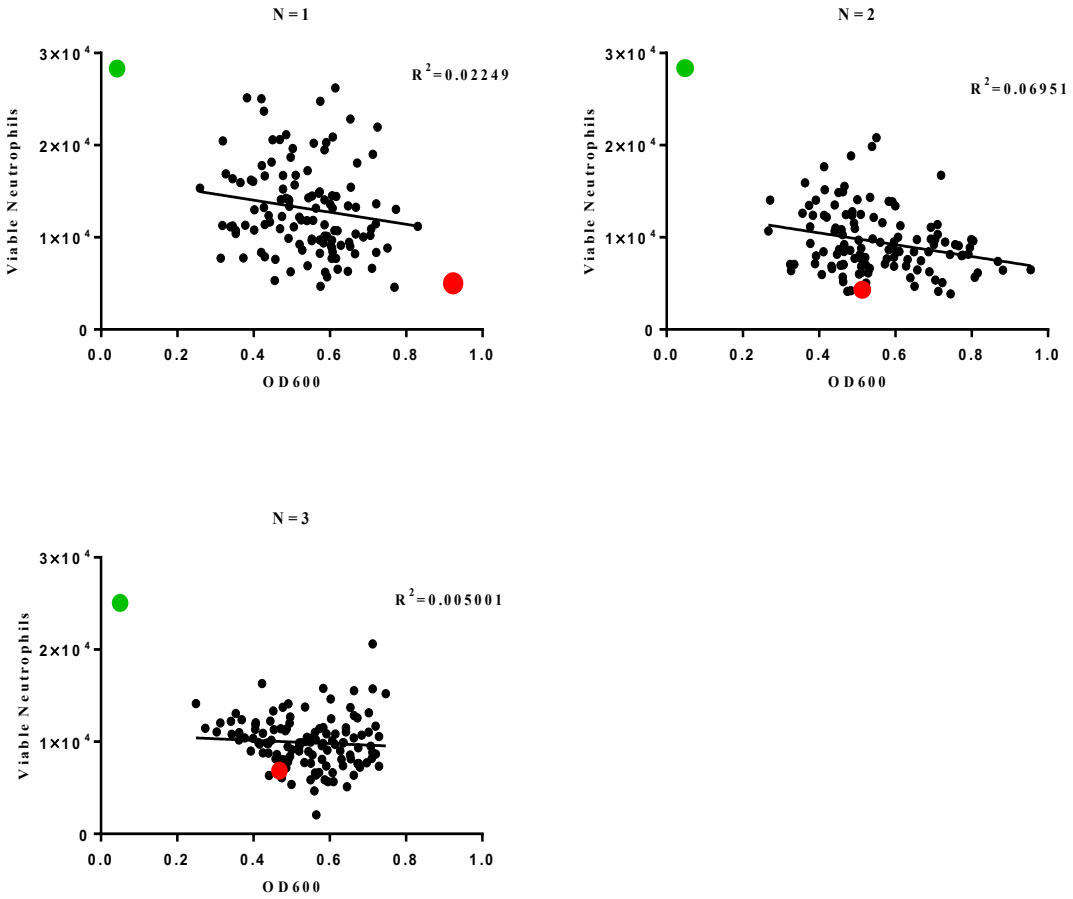

Figure 4.8 The OD_{600} of the 118 *S. aureus* mutants in the 2nd round of screen with corresponding viable neutrophil count after 3 hr of treatments. The bacterial density was measured after 3 hr of sub-culture in fresh BHI media. The viable neutrophil counts were generated by gating of the healthy neutrophil population from the flow cytometry data. The green and red dots indicate data of media control and JE2 treated sample. Linear regression analysis was carried out and the R square value of the 3 repeating experiments are 2.25%, 6.95% and 0.50% separately.

4.4 Transduction of selected mutations into a wildtype USA300 background

4.4.1 Transduction of transposon insertion into JE2

The aim of the transduction experiment is to verify that the mutant phenotype of attenuated neutrophil cell lysis was directly associated with the transposon insertion, and not the result of non-related genome mutation. The process of transduction involves the transfer of DNA flanking transposon insertion site from the *S. aureus* mutant to JE2 by a bacteriophage. Due to time limitation, transduction of only the top ranked 20 ranked mutants (Table 4.4) with the exception of *agr*A (since its role in neutrophil cell death has been well-studied) was performed into the USA300 background. Although repeated attempts were made, two transposon inserts failed to be transduced into JE2 (USA300_0994 and USA300_1092). The methods used for transduction are described in section 2.8.2.

4.4.2 Confirmation of successful transduction

The precise transposon insertion site of each *S. aureus* mutant was provided from the NTML database. Based on the *S. aureus* USA300 FPR3757 genomic DNA, primers were designed 400 bp upstream and 400 bp downstream of the insertion sites. The primer sequences are listed in section 2.7.1. The transductant colonies with correct inserts would generate PCR products of the full transposon of approximately 4,000 bp (Figure 4.9). The colonies without transposon inserts would amplify a small fragment about 700 bp. The PCR amplification products from 3 colonies of each strain were examined by gel electrophoresis (Section 2.7.5) and the genomic DNA extracted from JE2 was used as negative control. The results showed that 17 of the 19 *S. aureus* strains that produced colonies after transduction were successful transductants (Figure 4.9). The verified colonies were stored as beads stock at -80^{o}C for further study.

4.4.3 Identification of transductants showing robust attenuated neutrophil cell lysis

The neutrophil cell death assay was carried out with the transductants in two batches with the same method as the screen. Apart from the neutrophils and JE2 controls, 5 internal positive and 8 internal negative control strains were added for validation of the phenotype assay (Table 4.5). The internal positive controls consist of NTML mutants that showed consistent of attenuated virulence against neutrophils from the 2nd screen of NTML. The internal negative controls were randomly chosen from the NTML strains that were not attenuated. Three colonies of each strain's transductants were used in this study apart from SAUSA300_1089 (2), SAUSA300_1494 (1) and SAUSA300_2365 (1) due to limited number of given colonies. Both batches of transductants were assessed in 3 independent neutrophil cell death assays.

Neutrophil controls	PBS	**1st Batch Transductants**	SAUSA300_0265
	ToPro-3		SAUSA300_0347
	Media control		SAUSA300_0690
***S. aureus* control**	JE2		SAUSA300_0917
Internal positive controls	USA300_1974		SAUSA300_1801
	USA300_1975		SAUSA300_1889
	*agr*A		SAUSA300_1974
	*sae*S		SAUSA300_1975
	*lux*S		SAUSA300_2365
Internal negative controls	USA300_0872		SAUSA300_1494
	USA300_1056		SAUSA300_1089
	USA300_0116	**2nd Batch Transductants**	SAUSA300_0230
	USA300_2468		SAUSA300_0337
	USA300_2549		SAUSA300_1180
	USA300_0099		SAUSA300_1182
	USA300_0629		SAUSA300_1598
	USA300_0915		SAUSA300_1752

Table 4.5. Controls and two batches of *S. aureus* transductants studied in the neutrophil cell death assay.

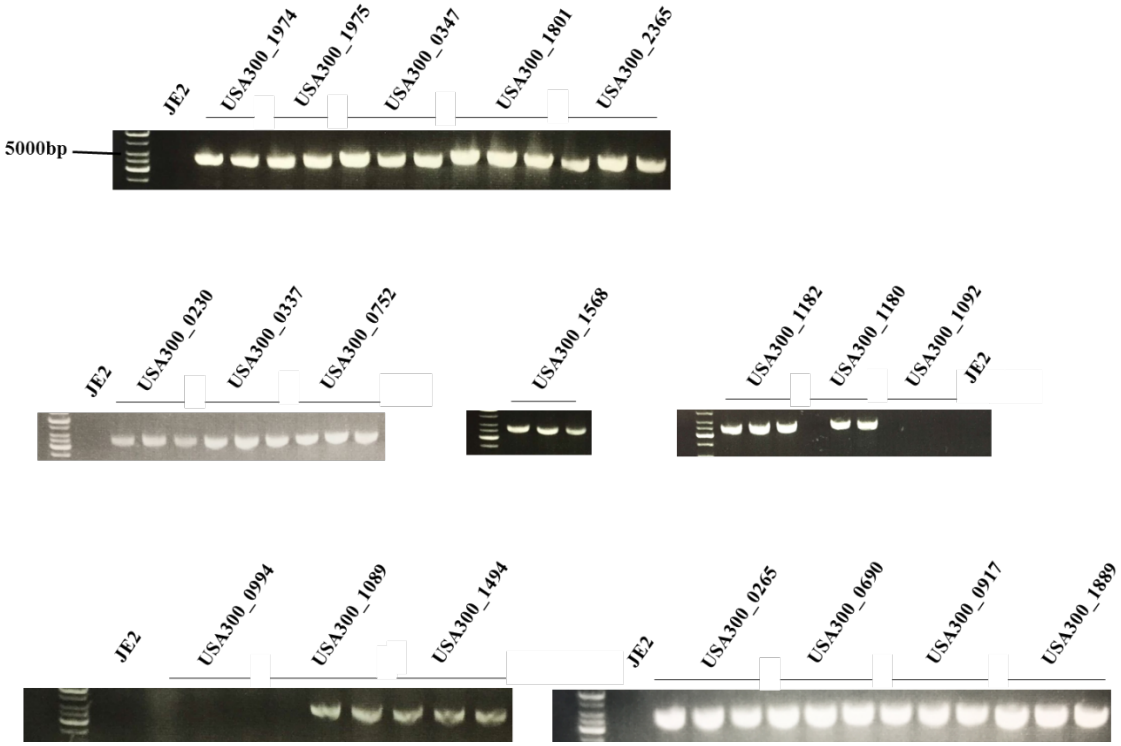

Figure 4.9 Confirmation of genetic transduction result for the 19 *S. aureus* mutant's genes identified from the 2nd round of screen. PCR products of 400 bp upstream and 400 bp downstream of transposon insertion site of each gene were assessed by 1% (w/v) agarose gel electrophoresis. Positively transduced strains would give full transposon product at approximately 4,000 bp. In exception of USA300_1092 and USA300_0994, the rest 17 genes were successfully transduced into USA300 background.

4.4.4 Evaluation of *S. aureus* transductants by the neutrophil cell death assay

The absolute viable neutrophil number and ToPro-3 negativity of each *S. aureus* transductant infected neutrophil sample was compared with the media control (green line), JE2 (red line), and internal controls (purple symbol for attenuated and olive symbol for non-attenuated) (Figure 4.10). The media control consistently displayed high viable neutrophil number (33,000±5527) and ToPro-3 negativity (>99%). JE2 treatment resulted in 25,000±6183 cell loss and reduced ToPro-3 negative intensity (60.3%±5.4%). The internal non-attenuated controls shown similar viable cell count and ToPro-3 profiling compared to JE2. Majority of internal confirmed controls caused less neutrophil death (15,833±4488) and higher ToPro-3 negativity (76.5%±9.3%) compared to JE2. Transductants showing higher viable cell number and ToPro-3 negativity than JE2 and internal negative controls were selected (blue box) (Figure 4.10).

Take the 2nd repeating experiment result of 1st batch as an example, the media control consists of approximately 39,000 viable neutrophils. After 3 hr infection of JE2, less than 10,000 neutrophils remained alive and ToPro-3 negativity decreased to 60%. The treatment of internal non-attenuated controls resulted in less than 10,000 viable neutrophils and low ToPro-3 negativity (44%-64%). The internal attenuated controls displayed much higher viable neutrophils (19,000-30,000) and ToPro-3 negativity (72%-97%), suggesting robust attenuated neutrophil cell death. Eleven sets of transductants showing attenuated neutrophil cell lysis were selected from this experiment (blue box).

As per the data analysis of the NTML screen results, the FSC/SSC profiling with viable neutrophil populations were determined. The profiling of 1st repeat of 2nd batch of transductants is shown as a representative (Figure 4.11). JE2 treatment leaded to massive viable neutrophil cell loss compared to media control. The internal positive controls displayed a clear population in the viable neutrophil gating area. Internal negative controls

generated highly similar cell loss to JE2 WT, indicating profound neutrophil cell lysis. The FSC/SSC profiles of three biological repeats of SAUSA300_1182 and SAUSA300_1889 treated samples also shown visibly clear viable neutrophil populations. Thus, FSC/SSC profiles of all transductants were assessed to select strains resulted in visibly clear healthy neutrophil population.

Out of the 11 strains transduced from 1st batch, 4 strains were selected by both methods and one extra strain was added from FSC/SSC profiling assessment. From the 2nd batch of transduced strains, 2/6 strains were identified. The transductants selected from two methods were highly consistent (Table 4.6). A total 7 identified NTML transposon inserted genes are listed in Table 4.7. Among these 7 transduced genes, there are *saeS* and leukocidin genes, which are known to induce neutrophil lysis and which gives confidence in both the screen and molecular engineering processes.

Batch	N	Viable Neutrophils and ToPro-3	FSC/SSC Profiling	Common
1	1		C3 C6 C12 D1 D2	B7 B8 B9 C1 C2 C4 C5 C10 C11
	2		C6 D1 D2	B7 B8 B9 C1 C2 C3 C4 C5 C10 C11 C12
	3		C1 C3 C4 C5 C6 D1 D2	B7 B8 B9 C2
2	1		B9 C3	C1 C2 B7 B8
	2		C1 C2 C3	B7 B8 B9
	3			B7 B8 B9

Batch	Well	Strain
1	B7 B8 B9	SAUSA300_ 0690
	C1 C2 C3	SAUSA300_ 1974
	C4 C5 C6	SAUSA300_ 1975
	C10 C11 C12	SAUSA300_ 1889
	D1 D2	SAUSA300_ 1089
2	B7 B8 B9	SAUSA300_ 1752
	C1 C2 C3	SAUSA300_1182

Table 4.6 Combination of identified wells of each plate with transductants generating attenuated neutrophil cell lysis results. The strains are referred to by their well numbers in a sub-library I made in a 96 well plate containing each batch of transductants. The strains selected by both methods are only listed under 'common' column. The corresponding transductant strains of identified wells are listed below.

Gene Locus	Gene Description	Gene Name
USA300_1889	Adenylosuccinate lyase	*pur*B
USA300_0752	ATP-dependent Clp protease proteolytic subunit	*clp*P
USA300_1182	Pyruvate ferredoxin oxidoreductase, alpha subunit	*pfo*
USA300_1089	Lipoprotein signal peptidase	*lsp*A
USA300_1974	Leukocidin/Hemolysin toxin family protein	*luk*G
USA300_1975	Aerolysin/leukocidin family protein	*luk*H
USA300_0690	Sensor histidine kinase SaeS	*sae*S

Table 4.7 Description of the 7 identified NTML transposon inserted genes.

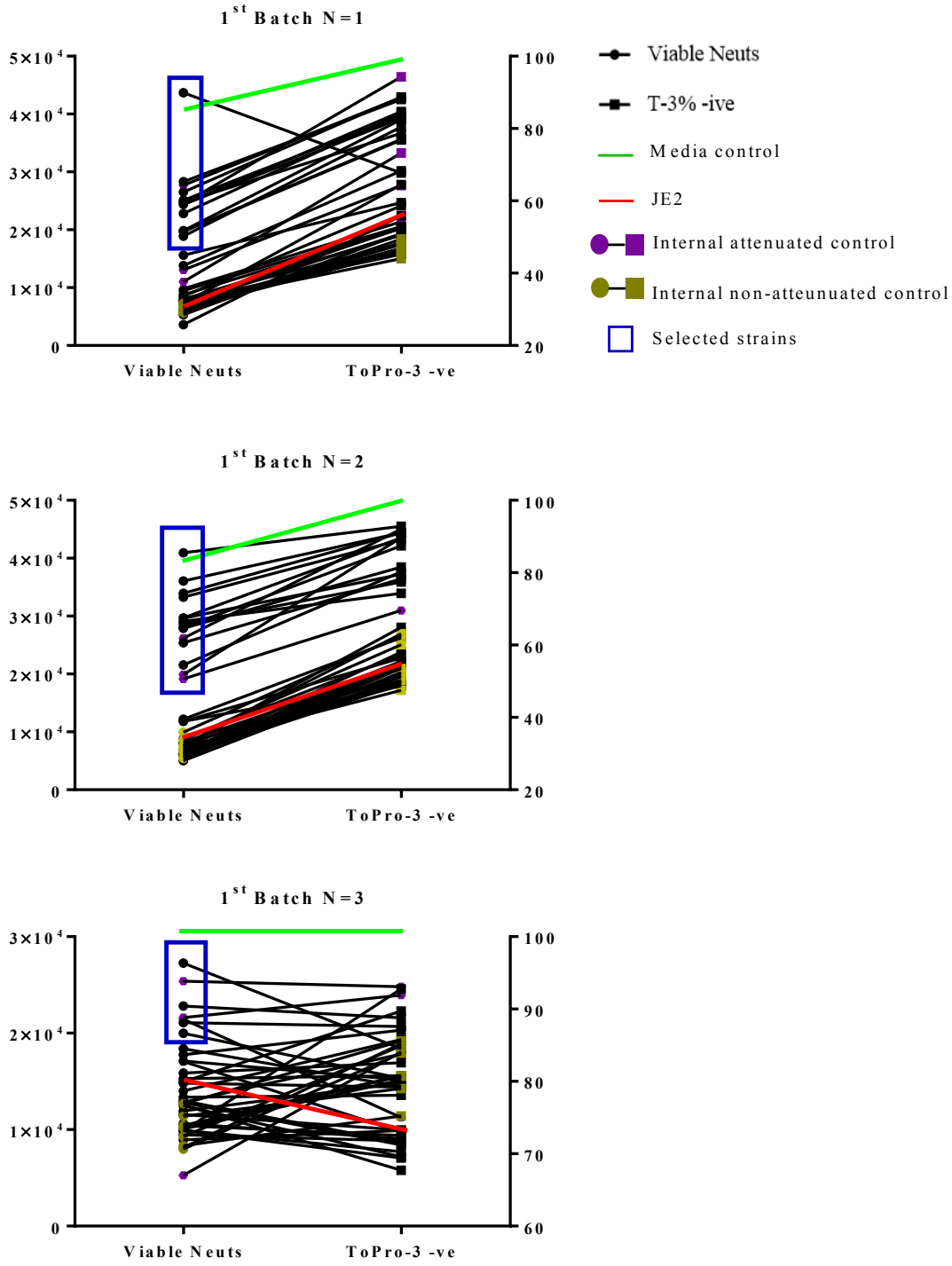
1st Batch N=1
5×10^4
4×10^4
3×10^4
2×10^4
1×10^4
0
100
80
60
40
20
Viable Neuts
ToPro-3 -ve
Viable Neuts
T-3% -ive
Media control
JE2
Internal attenuated control
Internal non-atteunuated control
Selected strains
1st Batch N=2
5×10^4
4×10^4
3×10^4
2×10^4
1×10^4
0
100
80
60
40
20
Viable Neuts
ToPro-3 -ve
1st Batch N=3
3×10^4
2×10^4
1×10^4
0
100
90
80
70
60
Viable Neuts
ToPro-3 -ve

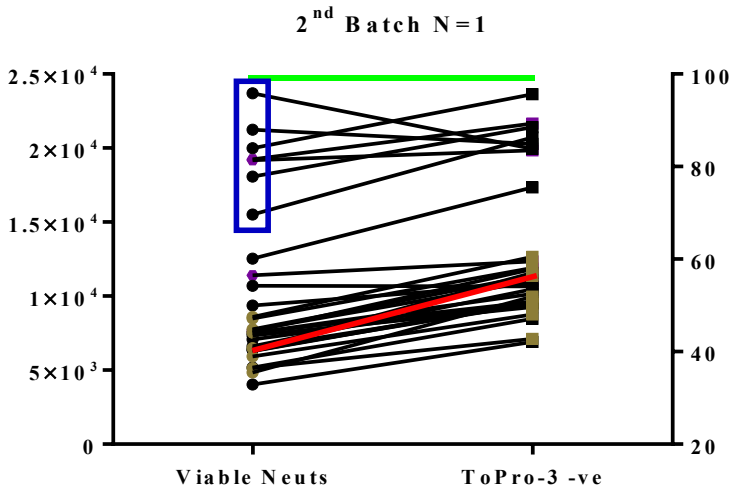
2nd Batch N=1
2.5×10 4
2×10 4
1.5×10 4
1×10 4
5×10 3
0
100
80
60
40
20
Viable Neuts
ToPro-3 -ve

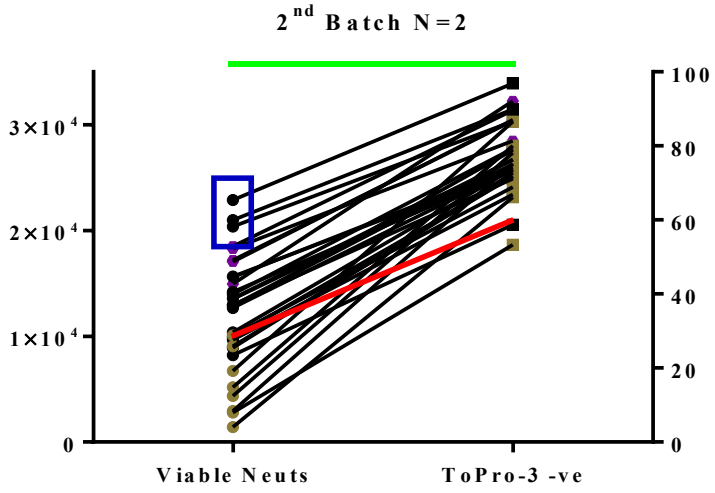
2nd Batch N=2
3×10 4
2×10 4
1×10 4
0
100
80
60
40
20
0
Viable Neuts
ToPro-3 -ve

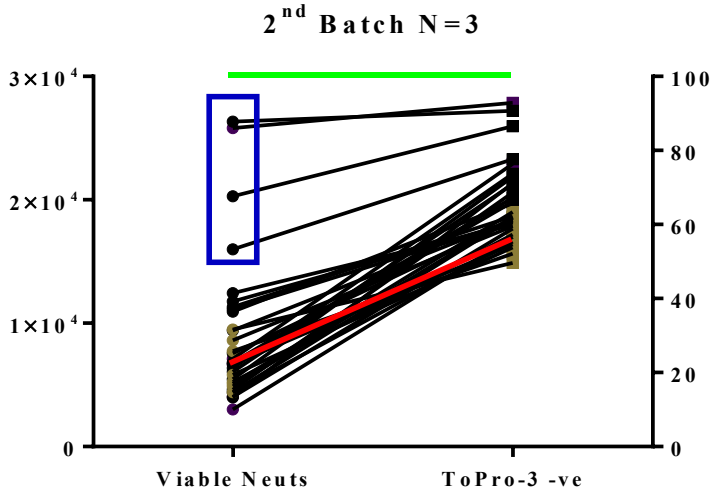
2nd Batch N=3
3×10 4
2×10 4
1×10 4
0
100
80
60
40
20
0
Viable Neuts
ToPro-3 -ve

Figure 4.10 Selection of attenuated transduced strains based on the absolute viable cell count and ToPro-3 negativity (%) result generated by the neutrophil cell death assay. Data is shown in two batches with corresponding result of media control (green), JE2 (red), internal attenuated controls (purple) and internal non-attenuated controls (olive). The 1st batch includes transductants corresponding to 11 *S. aureus* genes and the 2nd batch contains the remaining 6 gene transductants. Neutrophils were incubated at 37°C for 3 hr with individual transductants at an MOI of 10, followed by staining of ToPro-3 (1:10,000) and Attune flow cytometry detection. Transductants showing higher viable cell number and ToPro-3 negativity than JE2 and internal negative controls were selected (blue box).

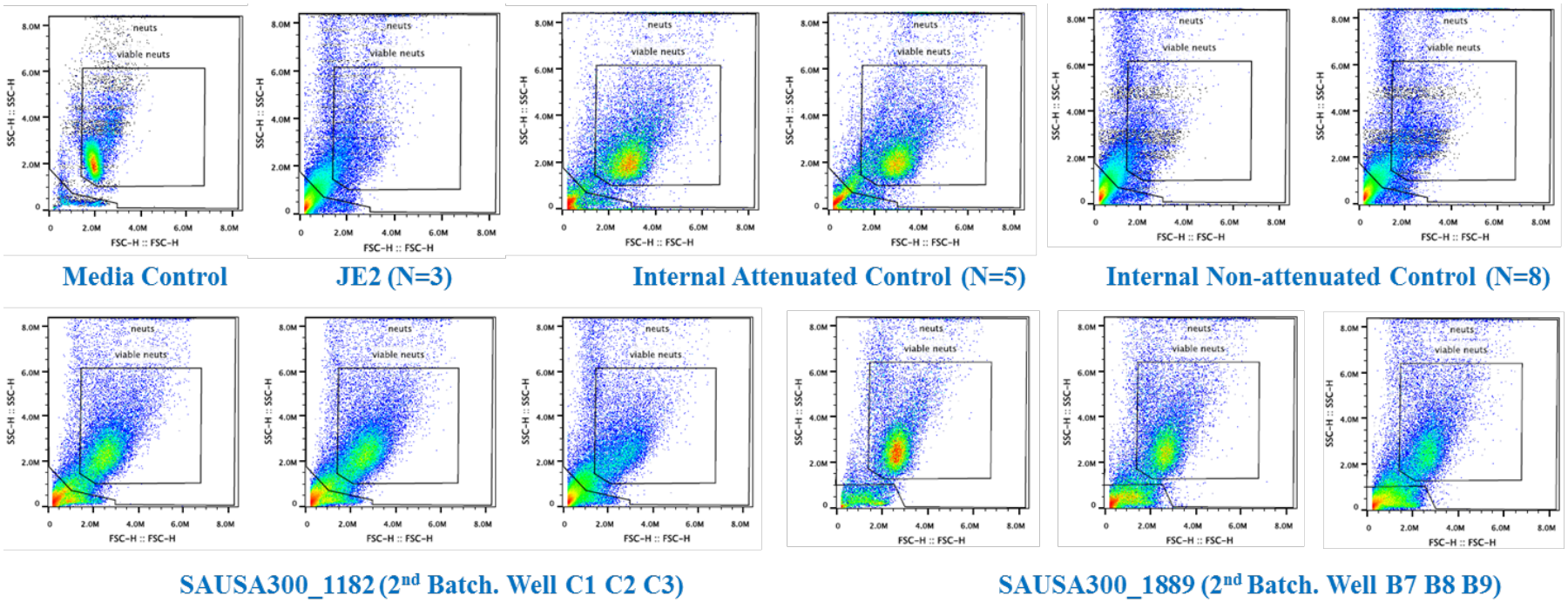

Figure 4.11 Representative flow cytometric FSC/SSC profiling of neutrophil cell death assay results of the 2nd batch transductants. The experiment was carried out with a media and JE2 control, 5 internal attenuated and 8 non-attenuated controls selected from NTML. Neutrophils were incubated at 37°C for 3 hr with individual transductants at MOI of 10, followed by staining of ToPro-3 (1:10,000) and Attune flow cytometry detection. Transductants with visibly different FSC/SSC profiles compared to JE2, namely SAUSA300_1182 and SAUSA300_1889 were identified as attenuated strains and are displayed as representatives

4.4.5 Growth curve of *purB, lspA. clpP* and *pfo*

Among the 7 transduced strains identified from the screen, leucocidin family genes (USA300_1974 and USA300_1975) and *sae*S are well studied key virulence genes of *S. aureus*. The remaining genes namely *purB, lspA, clpP, and pfo* have not previously been associated with neutrophil cell death or functions. Therefore, these four genes were selected for further study of potential pathogenicity involved in *S. aureus*-neutrophils interaction. The transductants of these gene mutant strains are named as *purB, lspA. clpP and pfo* in this thesis.

Growth curves of the four transduced strains were established in order to ensure no growth defects may be responsible for the attenuation observed (as per section 2.4.1). The JE2 growth curve demonstrated exponential growth after 2 hr of sub-culture in fresh BHI (Figure 4.12). After 7 hr of incubation, the OD_{600} reached 6.1. Both *lspA* and *pfo* produced a similar growth pattern and resulted in a comparable bacterial density (OD_{600} of 6.4-6.8 at 7 hr). *purB* grew exponentially from 2nd hr of culture and entered stationary phase after the 6th hr. *clpP* started exponential growth from 4th hr and resulted in similar bacterial mass (OD_{600} of 5.1) with *purB* (OD_{600} of 4.5) (Figure 4.12). Although one way ANOVA analysis of individual time points indicated significantly different growth pattern from1st to 4th hr (p^1=0.014, p^2=0.0058, p^3=0.0008, p^4=0.0014), the statistics of complete data set showed no significant difference between any of the transductants and JE2 (one way ANOVA, p=0.8873).

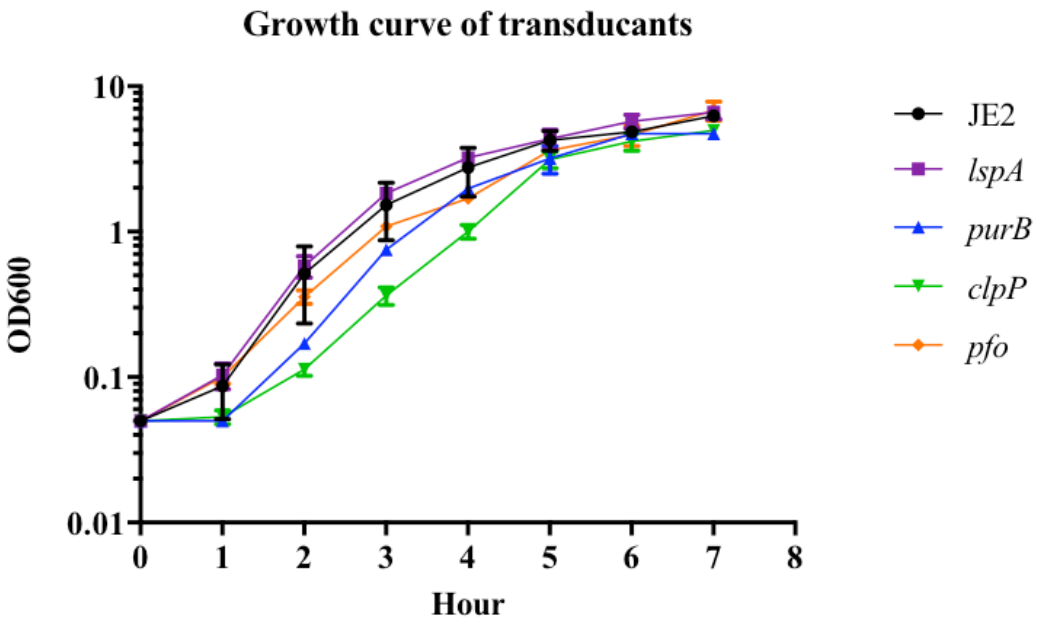

Figure 4.12. Role of *lspA*, *purB*, *clpP* and *pfo* in *S. aureus* growth *in vitro*. OD_{600} measured hourly shows comparable growth between the transductants with JE2. The growth was established in BHI media at 37°C with shaking at 250 rpm. Mean value and standard deviation of measurements from 3 independent experiments are shown. No significant difference was found among the strains (p=0.9567).

4.4.6 Bioinformatic analysis of the 4 strains of interest

Since none of the 4 mutants have been previously associated with neutrophil functions, it is important to obtain known information for these genes based on the gene IDs. The sequence features such as length of gene and protein, protein description and function were searched from NCBI protein databases. Known pathways that each gene has a role in were confirmed from Biocyc (https://biocyc.org/) and Kegg PATHWAY databases (http://www.genome.jp/kegg/pathway.html). The key information of each strain is listed in Table 4.8. PurB catalyses purine biosynthesis pathway. Pfo refers to pyruvate ferredoxin oxidoreductase α submit which has a role in pyruvate oxidation via the tricarboxylic acid cycle (TCA). *ClpP* produces caseinolytic protease which forms clp protease complex with *clpQ*. The clp protease complex hydrolyses proteins into small peptides with an ATP-dependent mechanism. *lspA* produced lipoprotein signal peptidase function as signal peptide cleavage for maturing membrane proteins of *S. aureus*.

The transposon insertion site was identified from the NARSA website. The position and flanking genes for each of the 4 genes of interest was obtained from Biocyc website and diagrammatically displayed in Figure 4.13. Flanking genes analysis was carried out using Biocyc website and the results indicated that *lspA* and *pfo* genes might be part of operons.

Gene Name	Gene Length	Protein Length	Function	Pathway
purB	1296 bp	431 aa	Catalyses 2 steps in purine synthesis	Purine biosynthesis
clpP	588 bp	195 aa	ATP-dependent protein hydrolysation	N/A
pfo	1761 bp	586 aa	Catalyses pyruvate oxidation	Tricarboxylic acid cycle
lspA	492 bp	163 aa	Catalyses the removal of signal peptides from prolipoproteins	Lipoprotein biosynthesis

Table 4.8 Information of sequence features, function, and pathway for the four NTML transposon inserted genes.

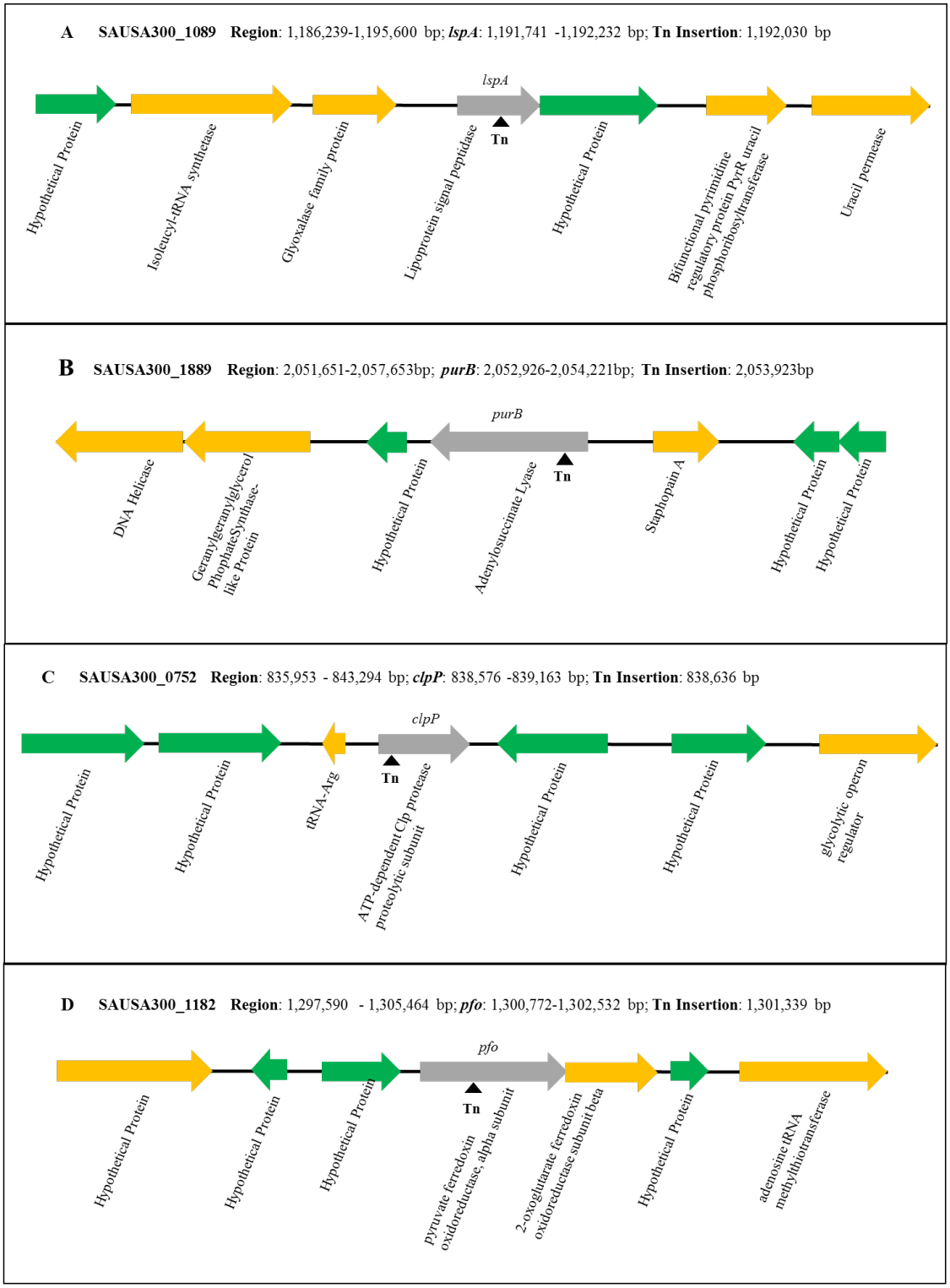

Figure 4.13 Transposon insertion position and surrounding genes for each of the 4 genes of interest. The *lsp*A (A) and *pfo* gene (D) are likely in operons with the downstream genes.

4.5 Complementation of verified transductants

4.5.1 Complementation of the 4 genes of interest with pGM073 derivative plasmid

To determine if the gene mutants of *lspA, purB, clpP*, and *pfo* were the reason for the phenotype of attenuated neutrophil cell lysis, attempts were made to genetically complement the four transductants of interest. The four mutations were genetically complemented with derivatives of the pGM073 plasmid expressing the corresponding genes to demonstrate their role in neutrophil cell lysis (Figure 4.14). The pGM073 plasmid is a pKasbar (pKB) derivative with *ezr*A and *PSmOrange* fragments (Bottomley *et al*., 2014). The *ezr*A and *PSmOrange* region was replaced by promoter and gene of interest to construct the complementation plasmid which was further amplified in *E. coli*. *S. aureus* RN4220 CYL316 strain possessing an integrase expressing plasmid was used as an intermediate strain, to allow site specific incorporation of the plasmid through recombination between an *attP* site encoded in pGM073 and *attB* site located at glycerol ester hydrolase (*geh*) gene of *S. aureus* after electroporation. The integration of plasmid DNA results in the loss of lipase activity (Lee & Iandolo, 1986). Although one study reported that isogenic mutants of the lipase genes reduces biofilm and abscess formation, and bacterial replication in the spleen, liver, and kidneys in an infected mice model, the experiments were conducted by chemically mutagenised *S. aureus* RN4220 (Hu *et al.,* 2012). More recent studies using USA300 Δ*geh* suggested that the most convincing role of lipase production was to enhance *S. aureus* colonisation and persistence on human skin (Cadieux *et al.,* 2014).

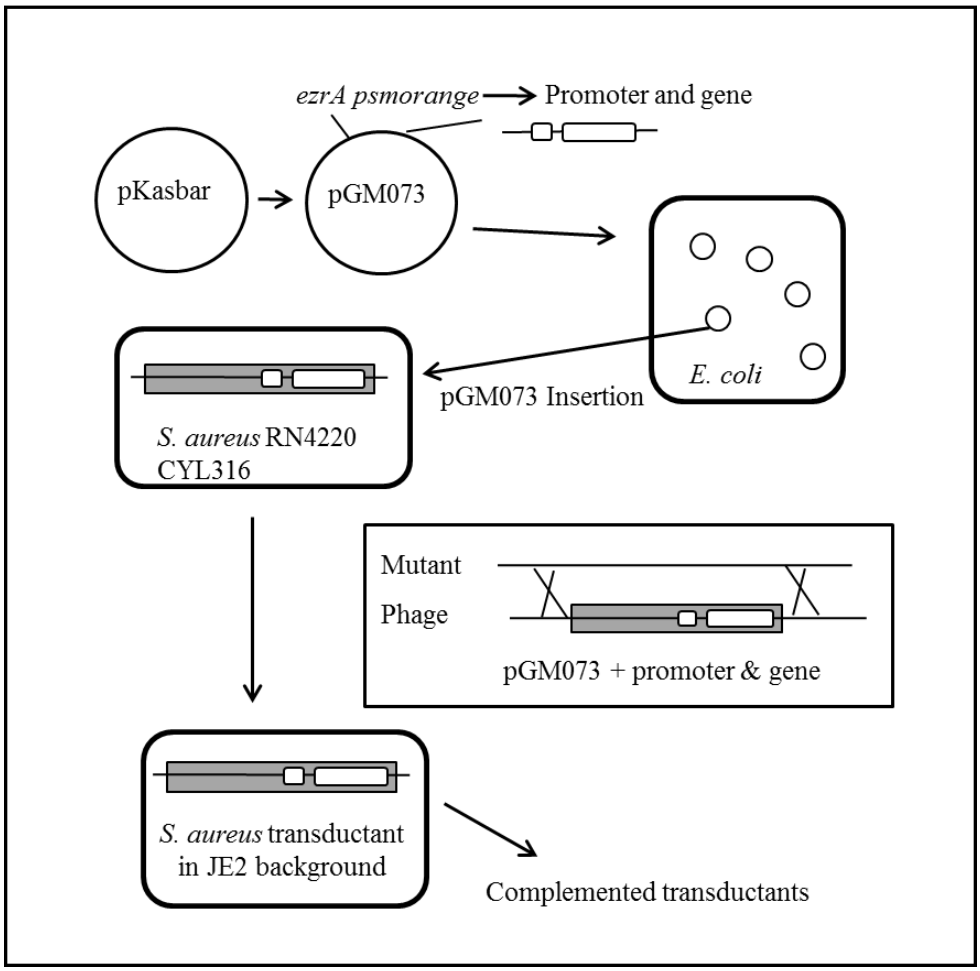

Figure 4.14 Diagram of the methods employed to genetically complement *S. aureus* transductants with the pGM073 system.

(1). The pGM073 plasmid is derived from pKasbar-Tet^R with *ezr*A and *PSmOrange* fragments. The *ezr*A and *PSmOrange* region was replaced by promoter and gene insert of interests to construct the complementation plasmid.

(2) The constructed plasmid was further amplified in *E. coli*.

(3) *S. aureus* RN4220 CYL316 possessing an integrase expressing plasmid was used as an intermediate strain, to have site specific incorporation of the plasmid into the *geh* of the corresponding transductant by electroporation. The complemented sector consists of promoter and gene of interest.

4.5.1.1 Construction of complementation plasmids

The native promoter and gene sequences of *lspA, purB, clpP* and *pfo* were PCR amplified from genomic DNA of JE2 WT by primers *lspA*-F-R, *purB*-F-R, *clpP*-F-R, and *pfo*-F-R. pGM073 derivatives were digested with BglII and NotI to remove the *ezr*A and *PSmOrange* region and ligated with gene inserts by Gibson assembly. All DNA fragments were verified by 1% w/v gel electrophoresis and the construction of the pKB-*lspA*-tet^R is shown diagrammatically as an example (Figure 4.15). Several attempts were made to amplify *clpP* promoter and gene sequence with additional *clpP*-F-R 1 and *clpP*-F-R 2 primers, yet no PCR product was synthesised. The pKB-*lspA*-tet^R and pKB-*pfo*-tet^R plasmids were constructed (Figure 4.16) and sequenced by GATC Biotech to confirm the correct gene inserts with primers *lspA*-F-R S, and *pfo*-F-R S. Although multiple attempts were made to isolate and send high concentration of pKB-*purB*-tet^R DNA inserts (418-440 µg/µl) to GATC Biotech, the sequencing consistently failed to produce any signal.

4.5.1.2 Integration of complementation plasmids into *S. aureus* RN4220

Electro transformation was carried out to integrate the verified pKB-*lspA*-tet^R and pKB-*pfo*-tet^R plasmids into competent RN4220 CYL316 cells. No colonies of *S. aureus* RN4220 grew on the plates. Attempts were made with optimizations of the protocol including increasing DNA concentration (80-250 µg/µl with 260/280 < 2); multiple pulses; using different batches of freshly made competent cells; reducing tetracycline concentration in the selective BHI agar; and elongating the incubation time of agar plates. Unfortunately, after several attempts this was proved unsuccessful.

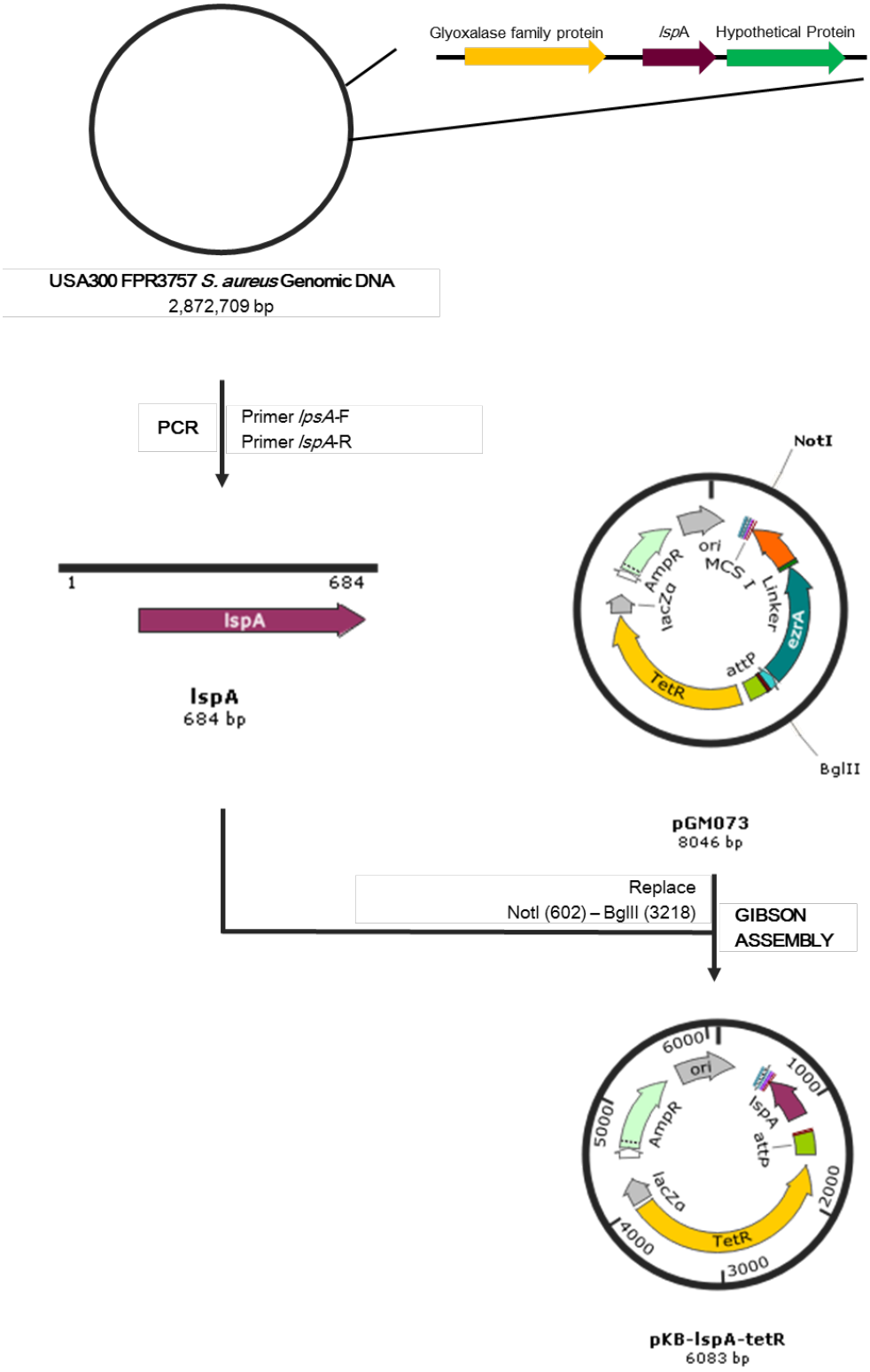

Figure 4.15 Construction of the pKB-*lspA*-tet^R complementation plasmid.

The *lspA* promoter and gene was PCR amplified from FPR3757 WT *S. aureus* genomic DNA and Gibson assembled into NotI and BglII cut pGM073, resulting in pKB-*lspA*-tet^R.

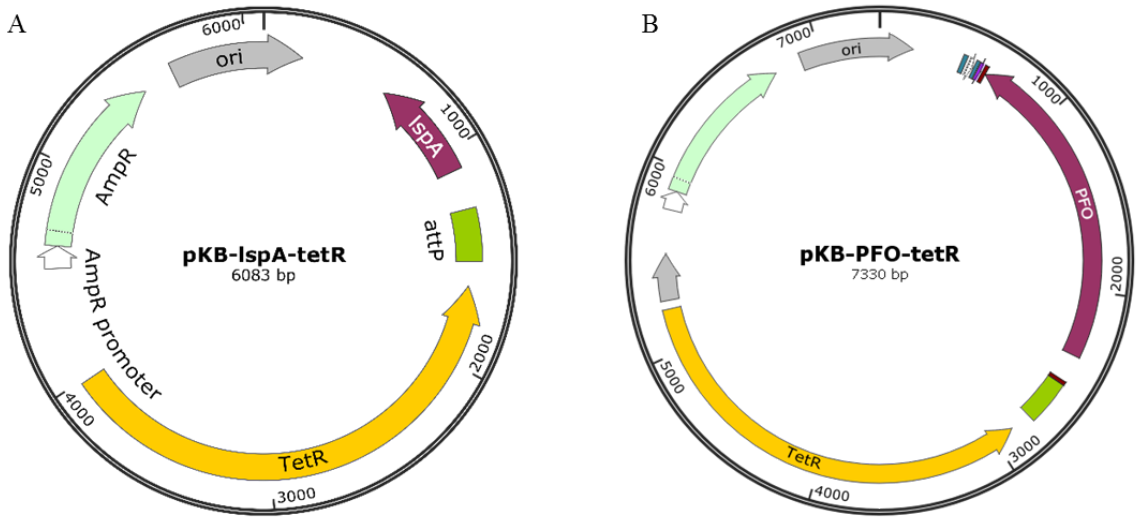

Figure 4.16 Physical map of the promoter and gene inserts in the complementation plasmids of the *lspA* and *pfo*.

A. pKB-*lspA*-tet^R

B. pKB-*pfo*-tet^R

4.5.2 Complementation of *lspA* with pGM074 derivative plasmid

The pGM074 plasmid shares same backbone as pGM073 but the resistance marker was replaced by a Kan^R cassette. Due to time limitation of this project, *lspA* was chosen for continuation of genetic complementation.

A constructed *clpP* transductant strain and φ85 phage complemented $clpP^+$ strain (Ery^R CM^R) in the *S. aureus* 8325 background were obtained from Knut Ohlsen's group (Michel *et al*., 2006).

4.5.2.1 Construction of a pKB-*lsp*A-kan^R complementation plasmid

Map of construction procedures involved in pKB-*lspA*-kan^R complementation plasmid is shown in Figure 4.17. The native promoter and gene sequence of *lspA* was PCR amplified from genomic DNA of JE2 by primers *lspA*-F-R and verified by 1% w/v gel electrophoresis (Figure 4.18 C). pGM074 derivative was cut by BglII and Not 1 to remove the *ezr*A and *PSmOrange* region and the plasmid backbone was purified after 1% w/v gel electrophoresis validation (Figure 4.18 B). After Gibson assembly of the digested plasmid with *lspA* sequence, the ligation was assessed by HindIII restriction enzyme digestion. With one HindIII cut site in the plasmid backbone and another one in *lspA* fragment (Figure 4.18 A), only successful constructed pKB-*lspA*-kan^R plasmid would generate 2 bands of expected sizes (1349 and 3686 bp) (Figure 4.18 D). The pKB-*lspA*-kan^R plasmid DNA was then verified by sequencing (GATC Biotech) using primers pGM074-F-R.

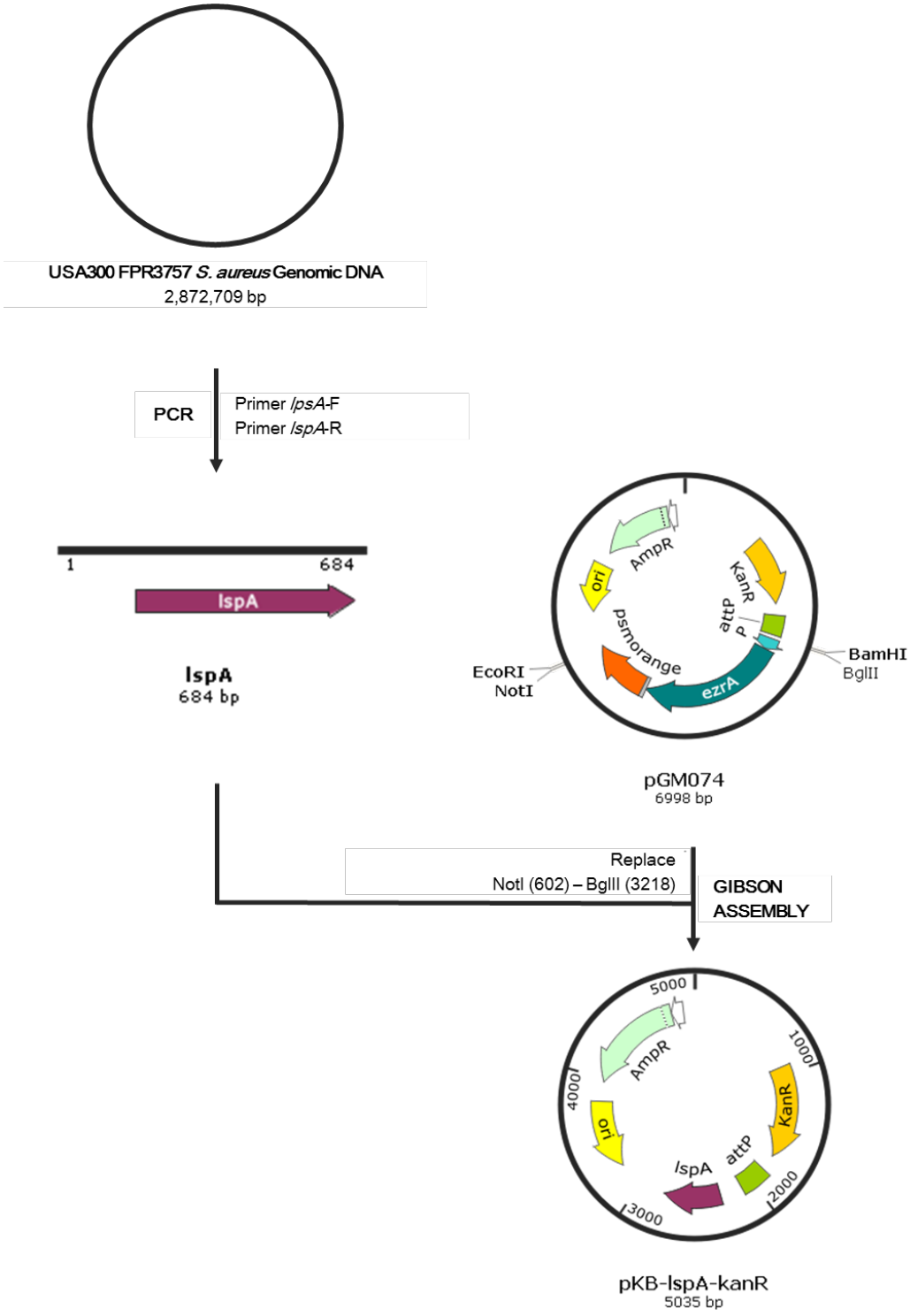

Figure 4.17 Construction of pKB-*lspA*-kan^R complementation plasmid.

The *lspA* promoter and gene was PCR amplified from FPR3757 WT *S. aureus* genomic DNA and Gibson assembled into NotI and BglII cut pGM074 derivative plasmid, resulting in pKB-*lspA*-kan^R.

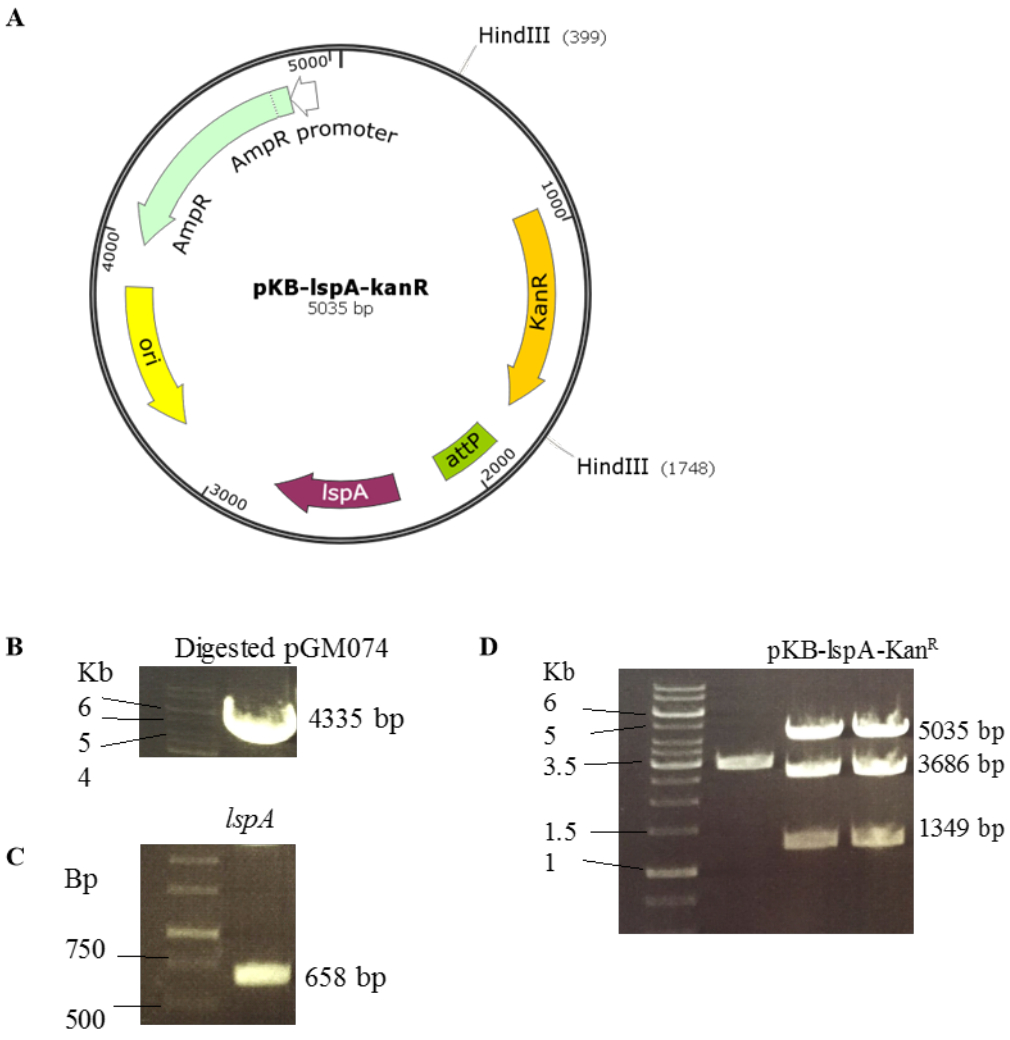

Figure 4.18 Verification of pKB-*lspA*-kan^R. Standard 1 kb DNA ladder was used for all gel eletrophoresis.

A. Map of pKB-*lspA*-kan^R construction with HindIII cutting sites.

B. NotI and BglII digested pGM074 derivative by gel electrophoresis for Gibson assembly.

C. PCR amplification of *lspA* promoter and gene fragments.

D. HindIII digestion of pKB-*lspA*-kan^R (triplicates) and gel electrophoresis.

4.5.2.2 Integration of pKB-*lspA*-kan^R plasmid into *S. aureus*

The pKB-*lspA*-kan^R plasmid was transformed into the RN4220 CYL316 strain, which contains the pYL112SA19 plasmid and therefore expresses the integrase enzyme required for site specific integration into the *geh* gene. Integration of the pKB-*lsp*A-kan^R plasmid into RN4220 is illustrated in Figure 4.19 A. Successful integration into RN4220 strain results in loss of lipase activity due to interruption of the *geh* gene. Baird-Parker plates were used to examine the colonies. Potassium tellurite in Baird-Parker results in black colonies. RN4220 CYL316 strain was used as the positive control and generated a precipitation zone around colonies, indicating hydrolysis of lipids in the agar. The transformants displayed loss of lipase function proving correct integration of pKB-*lspA*-kan^R plasmid into the chromosomal *geh* gene of RN4220 (Figure 4.19 B).

Subsequently the pKB-*lspA*-kan^R plasmid with gene insert was transferred from the RN4220 genome to *lspA* by bacteriophage transduction (method disclosed in Section 2.8.2), allowing homologous recombination of the gene into the genomic DNA. The resulting colonies were also verified on Baird-Parker plates with JE2 strain as positive control (Figure 4.19 C).

4.5.2.3 Complementation of *lsp*A control strains

Control strains for phenotype study of *lspA*$^+$ in neutrophil cell death assay were also constructed. The empty pKasbar plasmid was isolated from SH4045 *E. coli* strain and transformed into RN4220 CYL316. The DNA fragment containing integrated plasmid was moved into both JE2 and *lspA* by phage transduction, to generate JE2-pKB and *lspA*-pKB controls. The successful integration was confirmed by bacterial growth on Baird-Parker plates (Figure 4.19 D).

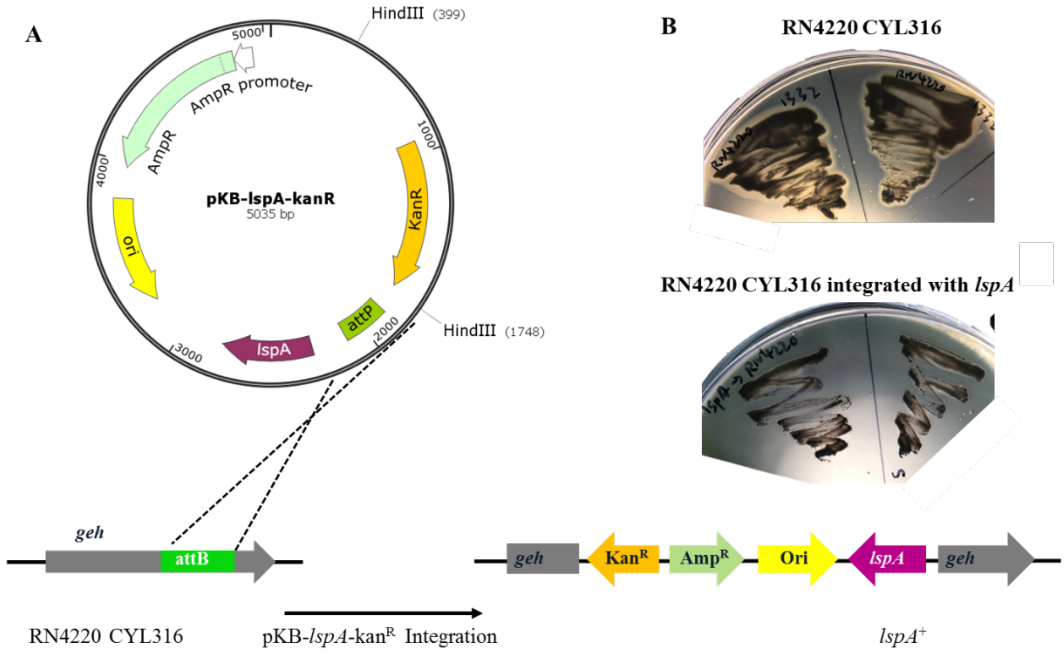
A
HindIII (399)
5000
AmpR promoter
AmpR
1000
4000
pKB-lspA-kanR
5035 bp
KanR
Ori
attP
lspA
2000
3000
HindIII (1748)
geh
attB
RN4220 CYL316
pKB-lspA-kanR Integration
B
RN4220 CYL316
RN4220 CYL316 integrated with lspA
geh
KanR
AmpR
Ori
lspA
geh
lspA+

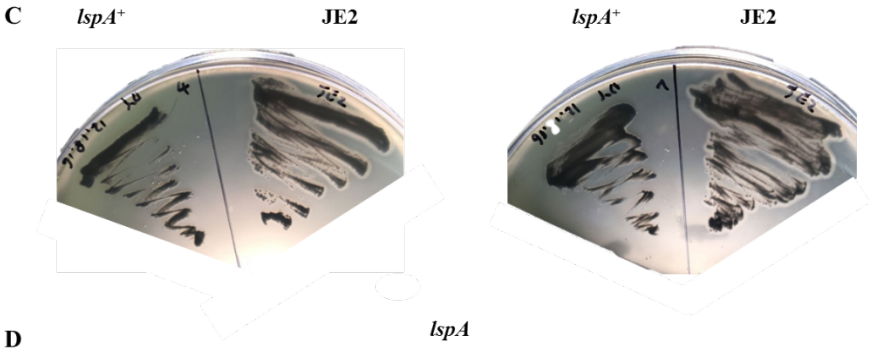
C
lspA+
JE2
lspA+
JE2

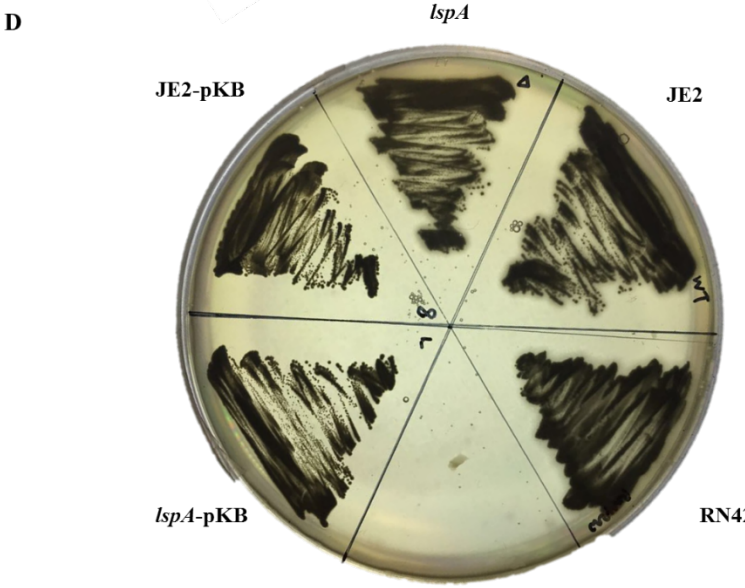
D
lspA
JE2-pKB
JE2
lspA-pKB
RN4220 CYL316

Figure 4.19 Site specific integration of the pKB-*lspA*-kan^{R} complementation plasmid into *S. aureus* RN4220 through homologous recombination between the *attP* site in pKasbar with *attB* site in the *geh* gene (A). Confirmation of successful integration of *lspA* promoter and gene insert into RN4220 CYL316 (B) and *lspA* (C) on Baird-Parker agar plates. Empty pKB integrated JE2 and *lspA* strains were also verified for use as control in further neutrophil cell death assay (D). *S. aureus* RN4220 CYL316, *lsp*A or JE2 strains were used as positive controls generating a zone of precipitation around the colonies, indicating intact lipase function.

4.5.2.4 Growth curve of complemented strains

Growth curves of the complemented strains were established from OD_{600} of 0.1 (method disclosed in section 2.4.1). JE2 generated standard growth curve and grew exponentially after 1 hr of sub-culture in fresh BHI. After 4 hr of incubation, the growth entered stationary phase and OD_{600} reached 4.1 at 5 hr. JE2-pKB strain showed highly similar growth pattern with JE2. Both *lspA*-pKB and *lspA*$^+$ strains displayed standard growth curve with exponential growth phase during 1st to 4th hr of incubation. Although the bacterial intensity of earlier time points was comparatively lower than JE2, the final OD_{600} at 5 hr (3.9 and 4.0 respectively) were not vastly different from the WT (Figure 4.20). ANOVA test showed no significant difference among the growth strains (p=0.9957).

The *clpP*$^+$ strain in *S. aureus* 8325 background produced a comparable growth curve to JE2 and reached stationary phase after 4 hr of incubation with OD_{600} of 3.9. Meanwhile the *clpP* did not enter exponential growth until 4 hr. At 6 hr *clpP* displayed similar OD_{600} (3.7) with JE2 at 5th hr (3.9) (Figure 4.20).

4.5.2.5 Neutrophil cell death assay of complemented strains

The neutrophil cell death assay was performed with the *lspA* and *clpP* complemented and control strains (Table 4.9) with same method as the screen. The neutrophil cell death assay was repeated 3 times.

The results of three repeating experiments were highly consistent, the media control displayed approximately 30,000-50,000 viable cells (Figure 4.21). Infection of JE2 leads to decreased viable neutrophils (<20,000). The *clpP* resulted in 30,000-60,000 viable cells, suggesting attenuation in cell lysis. The *clpP*$^+$ infected samples contained approximately 15,000 less viable neutrophils than corresponding *clpP*, indicating the concept of complemented virulence is achieved. Comparing to *lspA* which resulted in 30,000-40,000

viable cells, *lspA*$^{+}$ treatment reduced the viable count to 15,000-28,000. The co-incubation of JE2 complemented with empty pKB produced similar viable cell number (approx. 20,000) compared to JE2. The insertion of empty pKB in *lspA* leads to comparable healthy cell count (30,000-40,000) to media control. Therefore, the integration of empty pKB had no effect on bacterial virulence, indicating the genetic complementation of *lspA* enhanced the neutrophil cell lysis ability of the *lspA* mutant.

The flow cytometric FSC/SSC profiling and ToPro-3 histograms of a single experiment is shown as representative data (Figure 4.22). The F/T sample displayed 61.6% positive ToPro-3 intensity confirming successful ToPro-3 staining. Media control displayed a dense viable neutrophil population in the gated area, and 99.8% of ToPro-3 negativity. JE2 and JE2-pKB treatment lead to absence of viable neutrophil population in FSC/SSC plots together with reducing ToPro-3 negativity (79% and 86.7%), indicating profound cell lysis. Both *lspA* and *lspA*-pKB strains produced a high ToPro-3 negative count (96.6% and 97.3%) and a clear healthy neutrophil population, proving the integration of an empty pKB plasmid does not alter the virulence of *S. aureus*. Full neutrophil cell lysis was induced by the *lspA*$^{+}$ (loss of viable cells and 73.2% ToPro-3 negativity) suggesting fully restored virulence of the complement strain. The *clpP* mutant showed similar attenuation in neutrophil cell death with media control, with 76.7% of cells remaining viable and 98.2% of negative ToPro-3. On the contrary, *clpP*$^{+}$ generated massive killing of neutrophils (reduced population in gating area and 22.2% of positive ToPro-3), confirming the augmentation of bacterial virulence by genetic complementation.

Neutrophil controls	PBS
	ToPro-3
	Media control
***S. aureus* controls**	JE2
	JE2-pKB
***lspA* transductant**	*lspA*
***lspA* control**	*lspA*-pKB
***lspA* complement**	$lspA^{+}$
***clpP* transductant**	*clpP*
***clpP* complement**	$clpP^{+}$

Table 4.9. Controls and complement strains of *lspA* and *clpP* studied in the neutrophil cell death assay.

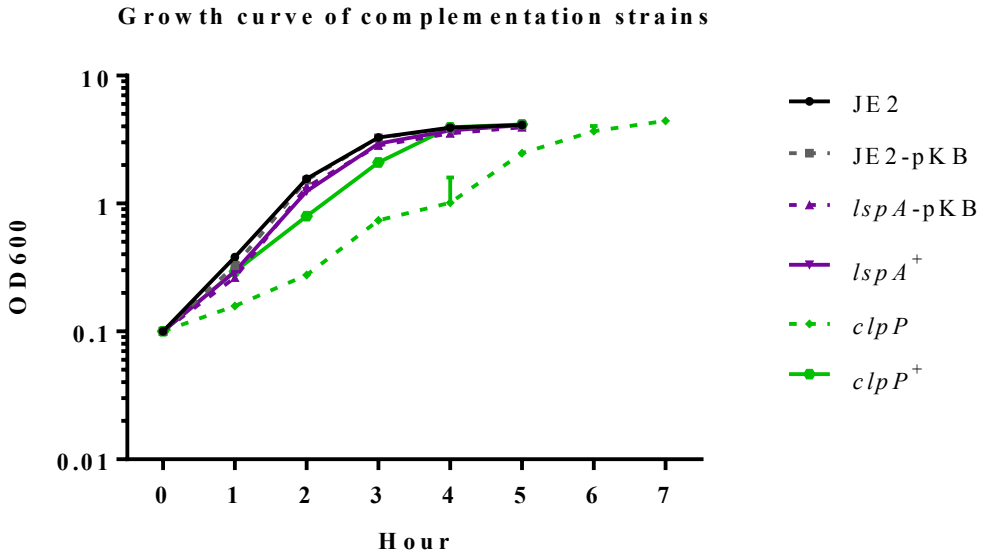

Figure 4.20 Growth curve of *lspA* and *clpP* complementation and control strains. OD_{600} measured hourly show comparable growth between the *lspA, lspA*$^{+}$, *lspA*-pKB, *clpP*$^{+}$ with JE2 and JE2-pKB. The *clpP* strain showed delayed growth pattern comparing to the remaining strains. The growth was established in BHI media at 37^{o}C with shaking at 250 rpm. Mean value and error bars (standard deviation) of measurements from 3 independent experiments are shown.

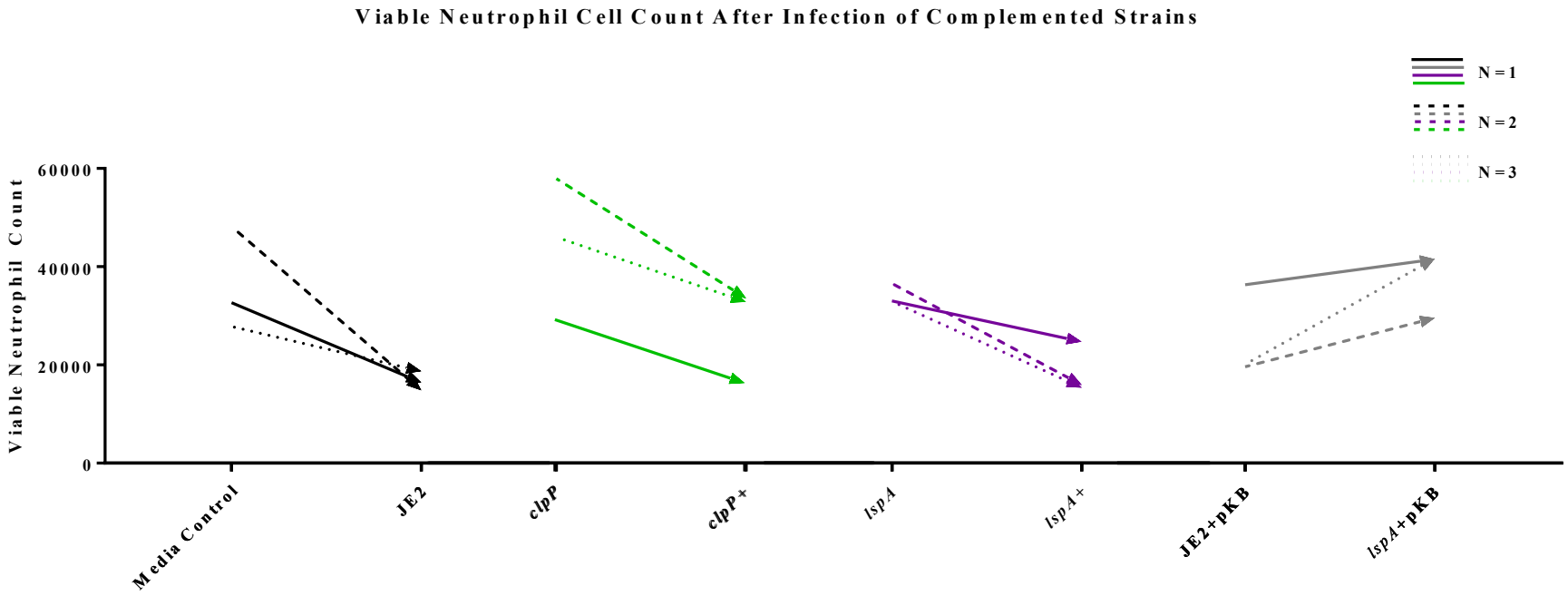

Figure 4.21 Viable neutrophil counts of after infection with complemented *lspA* and *clpP* strains. Primary human neutrophils were incubated with complemented and control strains at MOI of 10 for 3 hr. Viable cell counts were generated from flow cytometric data analysis. The quantification results from 3 independent experiments are shown in comparison between *clpP* and *clpP*$^{+}$*; lspA* and *lspA*$^{+}$; JE2+pKB and *lspA*+pKB, and media control with JE2 WT.

JE2+pKB: JE2 complemented with empty pKasbar backbone; *lspA*+pKB: *lspA* complemented with empty pKasbar backbone.

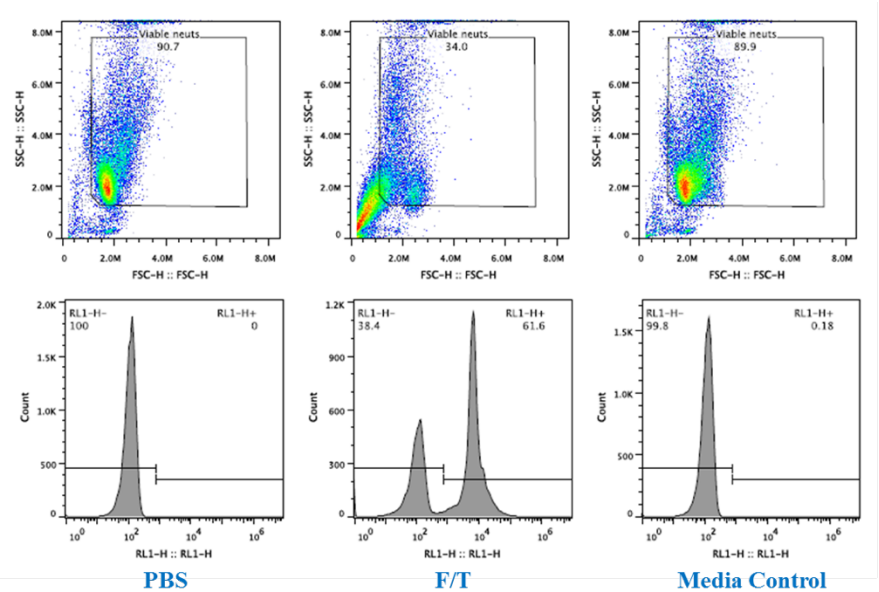
Viable neuts
90.7
Viable neuts
34.0
Viable neuts
89.9
SSC-H :: SSC-H
FSC-H :: FSC-H
RL1-H-
100
RL1-H+
0
RL1-H-
38.4
RL1-H+
61.6
RL1-H-
99.8
RL1-H+
0.18
Count
RL1-H :: RL1-H
PBS
F/T
Media Control

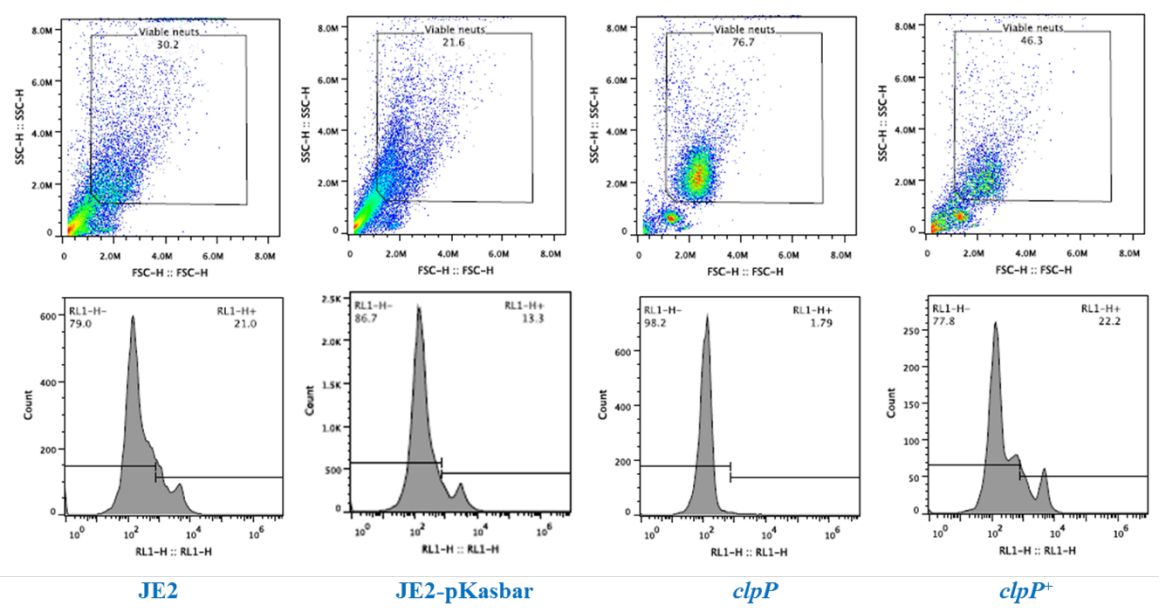
Viable neuts
30.2
Viable neuts
21.6
Viable neuts
76.7
Viable neuts
46.3
SSC-H :: SSC-H
FSC-H :: FSC-H
RL1-H-
79.0
RL1-H+
21.0
RL1-H-
86.7
RL1-H+
13.3
RL1-H-
98.2
RL1-H+
1.79
RL1-H-
77.8
RL1-H+
22.2
Count
RL1-H :: RL1-H
JE2
JE2-pKasbar
clpP
clpP+

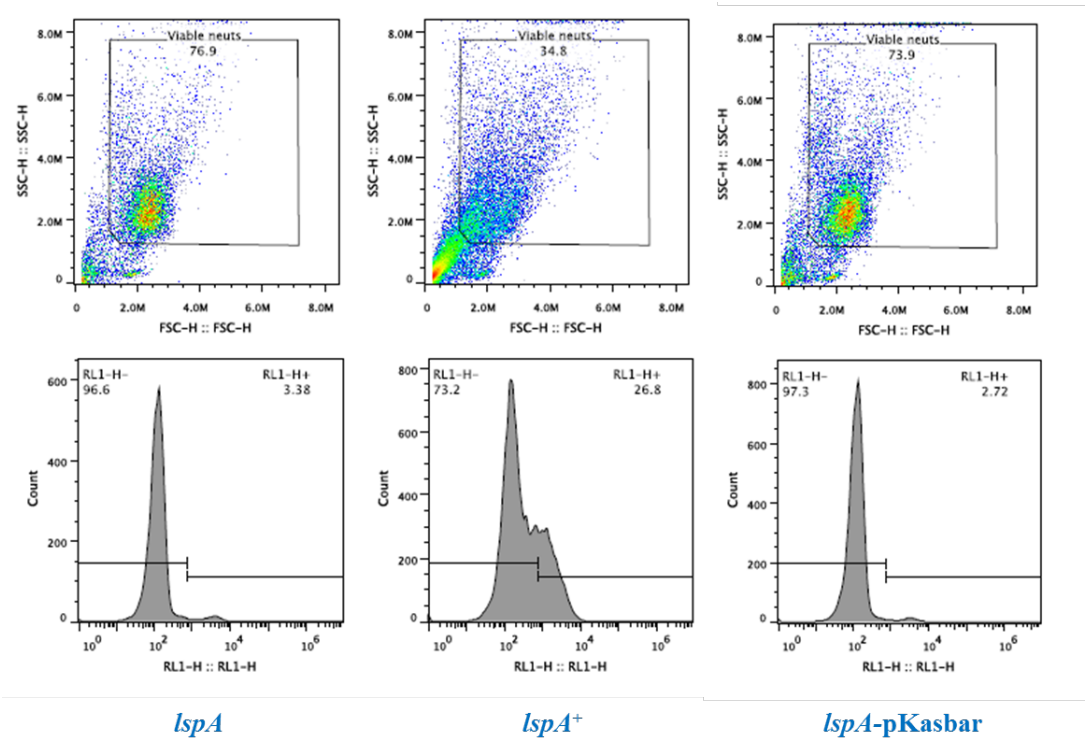

Figure 4.22 Representative flow cytometry results show genetically complemented *lspA* and *clpP* strains restored bacterial virulence in the neutrophil cell death assay. Neutrophils were co-incubated with *S. aureus* at MOI of 10 for 3 h at 37°C, followed by ToPro-3 (1:10,000) staining and Attune flow cytometric detection. F/T: Freeze/Thaw.

4.6 Discussion

The NTML consists of 1,920 transposon insertion *S. aureus* strains in a clinically relevant CA-MRSA background. It is a valuable resource for research on *S. aureus*, and it has allowed this project to identify genes that are important for the modulation of immune cell strategies, in an unbiased and high-throughput experimental model.

Screening of the NTML revealed mutations in 34 genes that resulted in attenuated neutrophil lysis. The 34 mutations included 5 genes categorised as transporters and 12 genes involved in biosynthetic pathways. Fourteen of the 34 genes have known functions, whereas 20 genes were hypothetical. Transposons from the most attenuated strains were transduced into a WT JE2 background and among them, 7 were attenuated in neutrophil lysis assays. Ten transductants failed to show attenuated neutrophil cell death which suggests that the original phenotype was perhaps the result of a mutation in other genomic DNA regions, rather than loss of the targeted gene function.

After identifying the function of each of the 7 attenuated transductants, 4 genes that were not previously associated with *S. aureus* virulence were focussed on: lipoprotein signal peptidase (*lspA*), adenylosuccinate lyase (*purB*), ATP-dependent *clp* protease proteolytic subunit (*clpP*) and alpha subunit of pyruvate ferredoxin oxidoreductase (*pfo*). The *clpP* complement strain in 8325 background was later obtained from a collaborrator. Complementation of *lspA* using a pGM074 derivative generated a successful genetic complement. The fully restored bacterial virulence (with respect to neutrophil lysis) of $lspA^{+}$ and $clpP^{+}$ confirmed linkage between the phenotype and the mutant genes.

4.6.1 Analysis of possible roles of identified genes in *S. aureus*-dependent neutrophil cell lysis

The attenuated neutrophil lysis phenotype was successfully repeated by genetic transduction of *pur*B mutant, proving disruption of this gene is sufficient to reduce bacterial virulence in modulating immune cell response. *Pur*B produces adenylosuccinate lyase which is known for catalysing two steps in purine biosynthesis in *S. aureus*. Even though the mutant did not exhibit a significant growth defect in rich nutrient media (BHI), whether SA*pur*B replicate or express full virulence as per the WT in RPMI (+10% FBS) remains unclear. Hence, it is important to identify whether the phenotype of the *pur*B mutant was caused by lack of nutrients or interaction with neutrophil immune strategies. Chemical complementation of *pur*B mutant will be conducted in future work.

pfo encodes pyruvate ferredoxin oxidoreductase α subunit, which catalyses pyruvate oxidation reaction in TCA cycle. Lack of function of this gene resulted in robust attenuation in bacterial virulence in this study. A possible reason could be that the pyruvate ferredoxin oxidoreductase plays an essential role in central metabolism of *S. aureus*. Continuous study will aim at identifying potential alternation of neutrophil cell responses caused by lack of Pfo, such as phagocytosis.

The requirement for *lsp*A and *clp*P in order to cause full neutrophil lysis was verified by genetic transduction and complementation. The lipoprotein signal peptidase expressed by *lsp*A functions to remove signal peptides from prolipoproteins and further produce mature lipoproteins. Lipoprotein is anchored on the outer membrane of *S. aureus* (Nakayama *et al*., 2012). It plays essential roles in host-pathogen interactions. It functions as pathogen-associated molecule patterns and mediates inflammation through activating TLR2 signalling cascades (Bubeck Wardenburg *et al*., 2006, Schmaler *et al*., 2010, Kim *et al*., 2015). Therefore, a question is raised by the significance of *lsp*A in lipoprotein biosynthesis: is lipoprotein responsible for mediating staphylococcal induced infection of immune cells, and how lack of this membrane protein may affect the interaction with human neutrophil?

Although this is speculative, I propose that the absence of mature lipoprotein downregulated neutrophilic uptake of the bacteria, and therefore prevent post-phagocytotic *S. aureus*-induced immune cell lysis. To address this hypothesis, experiments including phagocytic index assay would be helpful to underpin potential role of *lsp*A mediation in neutrophil responses in future work.

Caseinolytic protease proteolytic subunit, the product of *clp*P gene, is involved in ATP-dependent protein hydrolysation process (Truscott *et al.*, 2011). Much of what is known about removal of misfolded and aggregated proteins is that the protein hydrolysation process is crucial for *S. aureus* growth and functionality when they are exposed to a range of considerable environmental changes during infection. Presumably, the expression level of metabolism or other key virulence genes might also be determined by *clp*P-dependent control of gene regulator quantity. Consequently, lack of *clp*P could lead to irregulated protein homeostasis and compromised bacterial functionality, which failed to cause neutrophil lysis in the cell death assay. The potentially universal impact of protein degradation process indicates possibility of *clp*P to be involved in multiple mechanisms of *S. aureus*-neutrophil interaction. It is worthy of investigating potential attenuation of SA*clp*P in neutrophilic phagocytosis, bacterial growth during infection, and the pathogenesis in neutrophil-dependent manner.

Attempts to characterise the pathogenic mechanism of the 4 genes of interest in *S. aureus*-neutrophil interaction are the primary objectives of the next chapter.

4.6.2 How representative are the genes identified in the NTML screen for *S. aureus* virulence?

The two hypothetical leukocidin family genes (USA300_1974 and USA300_1975) resulted in attenuated bacterial virulence against human neutrophils. The outcome validated the

method established for the NTML screen since leukocidin is known to synergize with other virulent factors such as PVL to enhance the bacterial pathogenesis via induction of neutrophil lysis (Ventura *et al*., 2010). Similarly, *agr*A and *sae*S genes selection from the screen is in agreement with two other screening results (Benson *et al*., 2012, Boles and Horswill, 2008), proving the importance of accessory gene regulator A and membrane-associated protein kinase function for *S. aureus* virulence in modulating immune cells responses, and leading to neutrophil cell death.

Two genes identified from the screen that are involved in nucleotide and amino acid metabolism (*pyr*P and *aro*B) were proved as highly important for adaptation of oxidative stress and pH shock in a screen of essential genes in ST398 *S. aureus* background (Christiansen *et al*., 2014). The *hlg* family gene (*hlg*A) identified from NTML consistently illustrated the role of γ-hemolysin in *S. aureus* virulence (Gordon and Lowy, 2008). The expression product of *pdh*B is a subunit of pyruvate dehydrogenase multienzyme complex, which exists in the membrane fractions of *S. aureus* and regulates adaptation of osmotic stress (Vilhelmsson and Miller, 2002). *tat*C synthesis higly conserved *sec*-independent protein translocase and function as protein translocation system with *tat*A in *S. aureus* (Goosens *et al*., 2014). Unlike the most well-studied *sec* pathway as a general transport system, *tat* pathway was found with contribution of transporting virulence factors (Sibbald *et al*., 2006). A study performed in a mouse kidney abscess model showed significant lower virulence of *S. aureus* SA*tat*AC mutant than the wild type (Biswas *et al*., 2009). The *lux*S gene synthesis autoinducer producer protein which involves in 'quorum sensing', an essential mechanism for cell-cell signalling and therefore plays a key role in the formation of biofilms (Xu *et al*., 2006). According to Cluzel (Cluzel *et al*., 2010), *lux*S is involved in regulation of sporulation. Moreover, a novel metabolism role of *S. aureus lux*S has been found as monocistronic transcriptional subunit. The gene was transcribed throughout

intracellular growth in MAC-T cells (Doherty *et al*., 2006). The inactivation of *lux*S in several other pathogens leads to compromised virulence such as reduced expression of toxins (Vendeville *et al*., 2005). *Streptococcus pneumoniae lux*S mutant also resulted in attenuated infection in mice model (Stroeher *et al*., 2003), indicating a potentially important gene for *S. aureus* survival and bacterial virulence.

The importance of the majority of functional genes identified in our NTML screening has been supported by other researchers. Several other screens of *S. aureus* gene library generated different results. A recent study for *S. aureus* (JLA531) genes involved in AMP resistance revealed a range of genes including stress response and cell wall stimulation gene *yjb*H and *sgt*B (Johnston *et al*., 2016).

4.6.3 Limitation of NTML screen

The main limitation of this neutrophil cell death assay is that the primary screen was only performed once. This may have led to false negatives. False positives were also encountered but the 2nd round of screening refined these. Limitations of the screen method include the time frame only allowing assessing of maximum two NTML plates per day, because of which, variation of donor cell activity and neutrophil number per aliquot is bound to occur throughout the screen. This further makes it impossible to combine data from different days, and therefore limits the viability of comparing the 1,920 strains together. Additionally, although the bacterial intensity of NTML mutants has been verified within an acceptable range before co-incubation with neutrophils, the MOI of individual samples might not consistently be 10. Even though the methodology has limitations as described above, the solid neutrophil cell death assay model of the NTML screening provides robust targets for more in-depth studies of genetic mutants and functional assays.

CHAPTER 5

Role of identified *S. aureus* genes in virulence

5.1 Introduction

The NTML screen in Chapter 4 revealed a potential role for four *S. aureus* genes that were not previously associated with neutrophil cell death, namely *lspA, clpP, purB*, and *pfo*. The neutrophil killing of *lspA* and *clpP* mutants was fully restored by genetic complementation, further validating their role in neutrophil interaction.

The *purB* gene encodes adenylosuccinate lyase, which catalyses two reactions in the purine biosynthesis pathway: conversion of SAICAR (5'-phosphoribosyl-4-(N-succinocarboxamide)-5-aminoimidazole) to AICAR (5-amino-1-(5-phospho-D-ribosyl) imidazole-4-carboxamide), and adenylosuccinate to AMP (adenosine-monophosphate); with fumarate as by product of both reactions (Fyfe *et al*., 2010). IMP (inosine monophosphate, Adenylo-succ, N6-(1,2-dicarboxyethyl)-AMP), an intermediate product in this pathway, is a branch point for further ATP and GTP synthesis (Figure 5.1 A). PurB has a role before and a role after pathway branching, suggesting it is highly likely essential for both ATP and GTP synthesis.

Pfo is pyruvate ferredoxin oxidoreductase (PFOR) α subunit. It mediates the oxidative decarboxylation of pyruvate to acetyl-CoA and CO_2 (Figure 5.1 B). PFOR functions as both pyruvate synthase and pyruvate oxidase in *Clostridium thermoaceticum* (Furdui and Ragsdale, 2000). The dual roles of the enzyme links the Wood-Ljungdahl pathway of autotropic CO_2 fixation with incomplete reductive TCA (tricarboxylic acid) cycle in anaerobic organisms (Furdui and Ragsdale, 2000). Another study carried out in *Trichomonas vaginalis* revealed

PFOR, which normally located on the membranes of hydrogensosomes, is a surface-associated cell adhesion protein involved in host cell-binding activity (Meza-Cervantez *et al*., 2011).

Analogues of nitazoxanide, an inhibitor of PFOR in anaerobic bacteria, have been tested in a minimum inhibitory concentration assay with a range of species including *S. aureus* (Warren *et al*., 2012). Out of 9 tested analogues, *S. aureus* was susceptible to 3 and resistant to the rest. However, the group claimed *S. aureus* do not express PFOR (without providing solid reference), concluding that the inhibitory effects displayed by the positive analogues were due to their broad-spectrum antimicrobial activity against non-PFOR targets.

The lipoprotein signal peptidase encoded by *lspA* is a cytoplasmic membrane localized enzyme required for biogenesis of bacterial lipoproteins (Shahmirzadi *et al*., 2016). The peptidase functions through recognition of a diacylglycerol modification and cleaves between the modified cysteine residue and amino acid at position-1 (Hussain *et al*., 1982), which further generates mature lipoprotein (Figure 5.1 C). Lipoproteins are a distinctive class of membrane-anchored proteins commonly found in Gram-negative and Gram-positive bacteria. In Gram-positive microorganisms, lipoproteins are localized in the outer leaflet of the cytoplasmic membrane (Mazmanian *et al*., 2001). Known functions of lipoproteins include uptake of nutrients, protein secretion, antibiotic resistance, spore germination, etc (Sutcliffe and Russell, 1995).

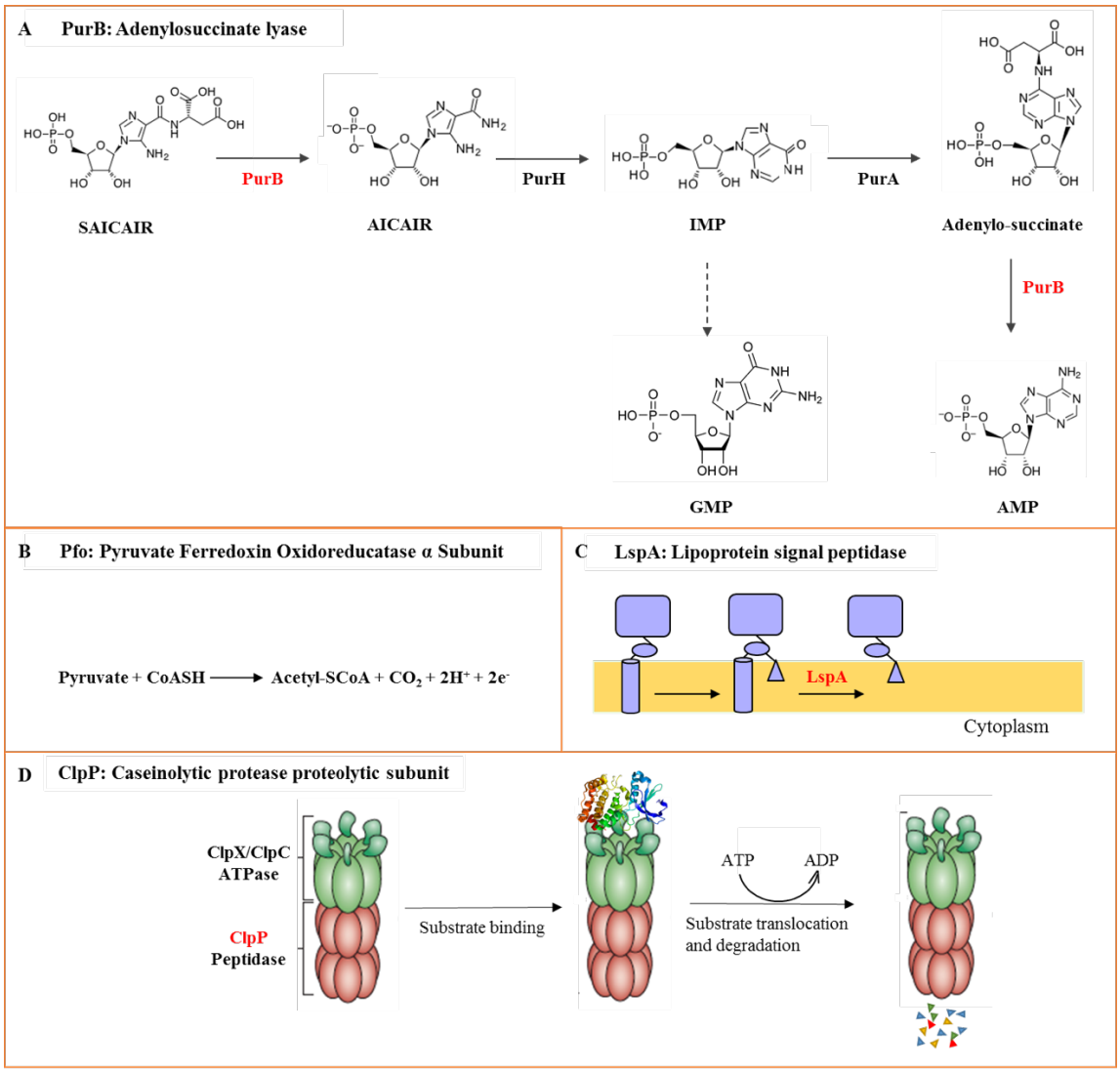

Figure 5.1 Diagrammatic illustration of roles of PurB, LspA, Pfo, and ClpP in *S. aureus*.

A. Purine *de novo* biosynthesis pathway.

B. Reaction of pyruvate oxidation in the TCA cycle.

C. Maturation of lipoproteins on the outer layer of cytoplamic membrane.

D. Mechanism of protein degradation regulated by the Clp protease.

Abbreviations: SAICAIR, 5'-phosphoribosyl-4-(N-succinocarboxamide)-5-aminoimidazole; AICAIR, 5-amino-1-(5-phospho-D-ribosyl)imidazole-4-carboxamide; GMP, guanosine monophosphate; IMP, inosine monophosphate, Adenyl succinate, N6-(1,2-dicarboxyethyl)-AMP; AMP, adenosine-monophosphate. Pathway information was acquired from the Kegg and Biocyc websites, and molecule images were obtained from WormFluxx.

ClpP is a caseinolytic protease proteolytic subunit, which forms part of the Clp chaperone protease complex with an ATPase specificity factor (ClpX and ClpC in *S. aureus*) (Frees *et al*., 2004). Clp proteases play a crucial role in misfolded or aggregated protein degradation and are therefore highly important for protein homeostasis (Kirstein *et al*., 2009). Substrates are recognized and bound by an ATPase such as ClpX. Subsequently the protein is unfolded and transferred into ClpP chamber, followed by proteolysis to complete degradation (Figure 5.1 D). Apart from protein turnover, studies have revealed potential roles for ClpP involved in stress adaptation and bacterial virulence. A β-lactone inhibition study of ClpP in *S. aureus* attenuated the production of extracellular virulence factors such as hemolysins and lipases (Bottcher and Sieber, 2008). Loss of ClpP in *S. aureus* resulted in derepression of genes involved in heat shock regulation (*hrcA* and *ctsR*), oxidative stress response, SOS DNA repair, and metal homeostasis (Michel *et al*., 2006).

All the genes identified in the NMTL screen have biochemical functions attributed to them. However, their link to neutrophil lysis is unknown. Hence, the primary objectives of the following chapter are to probe their importance to broader pathogenicity, and in particular *S. aureus*-neutrophil interactions.

The zebrafish embryo model of *S. aureus* pathogenesis has been previously established (Henry *et al*., 2013, Ellett *et al*., 2015). This host has many orthologs of the human innate immune system including neutrophils and cytokines (van der Vaart *et al*., 2012). Zebrafish neutrophils share highly similar morphological, biochemical, and functional features with human neutrophil (Lieschke *et al*., 2001), which readily permits understanding of neutrophil immunity against bacteria including *S. aureus* (Henry *et al*., 2013). *S. aureus* can be rapidly phagocytosed by neutrophils in the zebrafish embryo model. Yet the engulfed bacteria are not always eliminated subsequently (Prajsnar *et al*., 2008).

Results

5.2 *In vitro purB* chemical complementation

5.2.1 Adenine and inosine complementation assay for purine biosynthesis

As the purine *de novo* biosynthesis pathway shows, PurB is necessary for the conversion of SAICAIR to AICAIR which further converts to IMP (Figure 5.1 A). Hence, the absence of PurB leads to absence of IMP, resulting in lack of GTP or ATP synthesis.

Therefore, I hypothesised that lack of purines in the *S. aureus*-neutrophil coincubation leads to a defect in GTP/ATP synthesis which may inhibit the production of virulence factors that result in cell lysis. To determine whether neutrophil killing could be restored by chemical complementation, adenine and inosine (AI) were first added to solid BHI agar at a final concentration of 0.02 mg/mL for *purB* mutant growth. The chemicals were also added to RPMI media at the same concentration during the 3 hr co-incubation at MOI of 10. Neutrophils were stained with ToPro-3 and cell viability was assessed by Attune flow cytometry.

5.2.2 Bacterial neutrophil killing is restored in the chemical complemented *purB* strain

The viable neutrophil cell count and ToPro-3 negativity of each sample from a representative experiment is shown in Figure 5.2 A. A media control with and without AI complementation resulted in high viable neutrophil count (22,000-28,000) and high ToPro-3 negativity (>99%). AI positive and negative JE2 treatment lead to rapid neutrophil lysis, with approximately 10,000 viable count and 85% of ToPro-3 negativity. The *purB* incubation without AI in RPMI regardless if the strain was grown on BHI agar with or without AI, resulted in attenuated neutrophil cell death (15,000-21,000 viable counts) compared to JE2. However, the presence of AI in RPMI caused a profound *purB* induced neutrophil lysis regardless if BHI was complemented with AI, where the viable cell counts (7,000-12,000) and ToPro-3 negativity (87-91%) are highly similar to JE2.

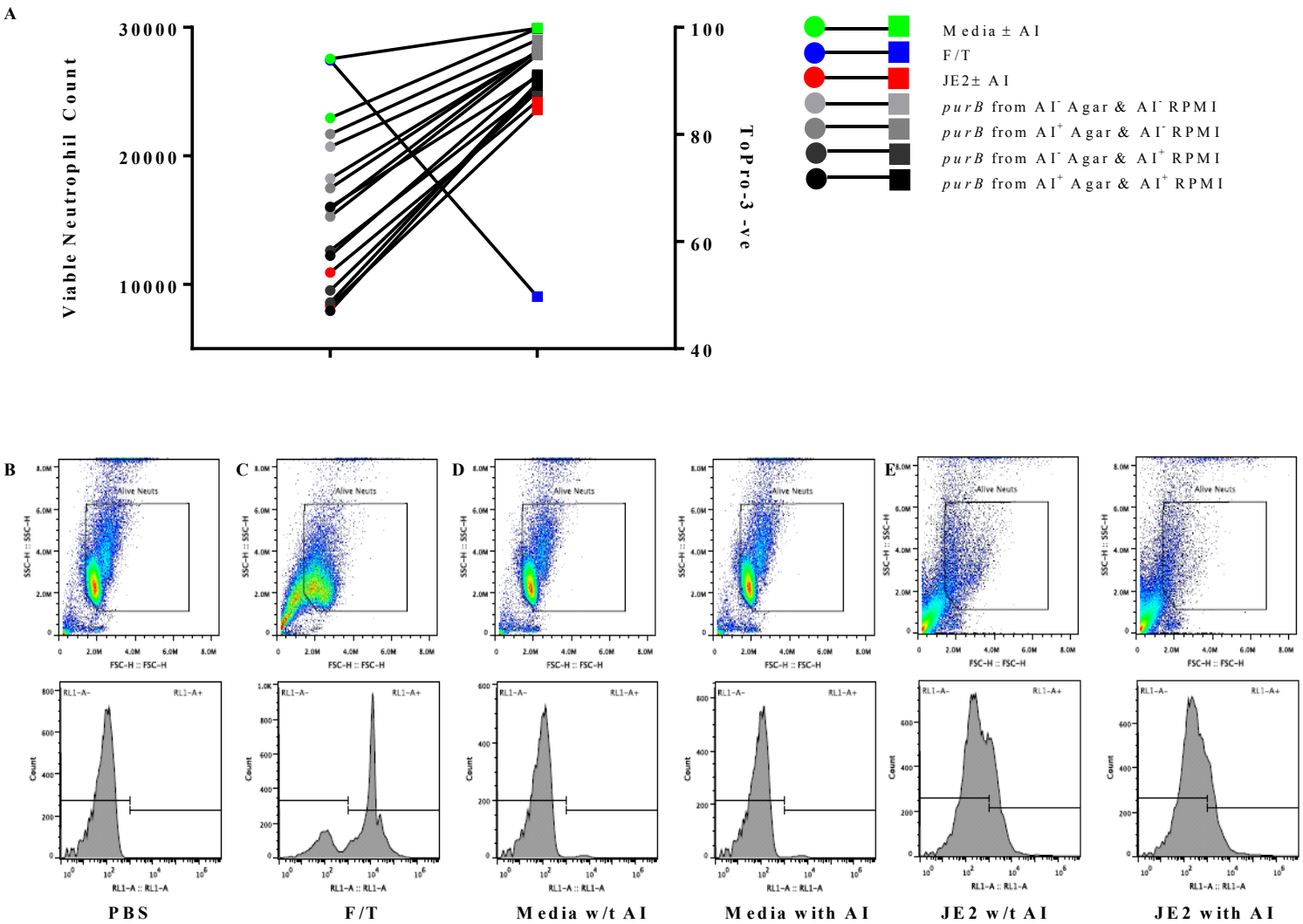
A
Viable Neutrophil Count
30000
20000
10000
100
80
60
40
ToPro-3 -ve
Media ± AI
F/T
JE2± AI
purB from AI- Agar & AI- RPMI
purB from AI+ Agar & AI- RPMI
purB from AI- Agar & AI+ RPMI
purB from AI+ Agar & AI+ RPMI
B
C
D
E
Alive Neuts
SSC-H :: SSC-H
FSC-H :: FSC-H
RL1-A-
RL1-A+
Count
RL1-A :: RL1-A
PBS
F/T
Media w/t AI
Media with AI
JE2 w/t AI
JE2 with AI

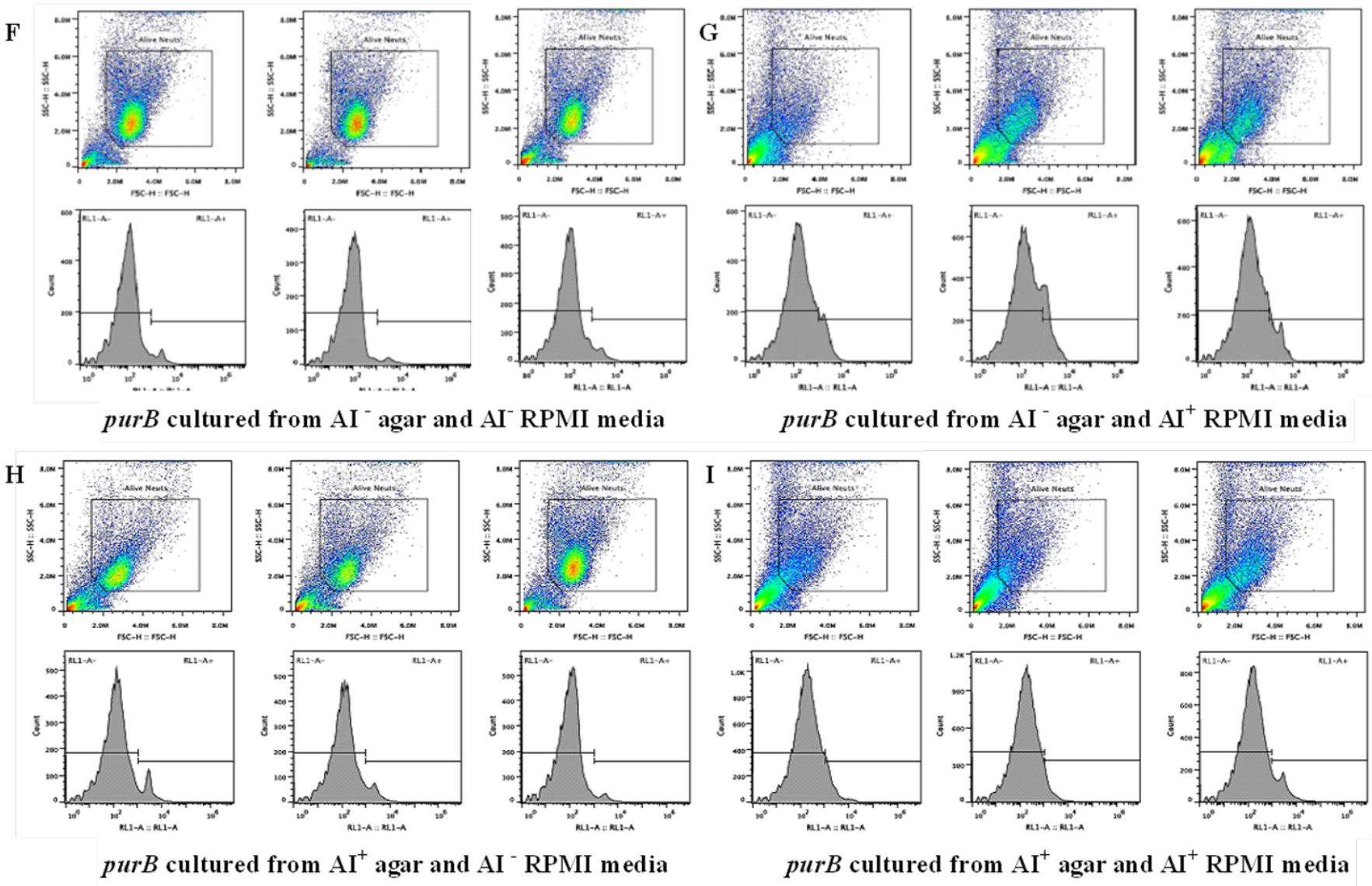
F
G
H
I
Alive Neuts
FSC-H :: FSC-H
SSC-H :: SSC-H
RL1-A-
RL1-A+
Count
RL1-A :: RL1-A
purB cultured from AI - agar and AI- RPMI media
purB cultured from AI - agar and AI+ RPMI media
purB cultured from AI+ agar and AI - RPMI media
purB cultured from AI+ agar and AI+ RPMI media

Figure 5.2. Chemical complementation of *purB* was performed with addition of adenine and inosine (AI) to solid BHI agar at a final concentration of 0.02 mg/mL, and RPMI media at same concentration during the 3 hr co-incubation at MOI of 10. The samples were stained with ToPro-3 and assessed by Attune flow cytometry. The assay was carried out 3 times in triplicates. Representative profiling from one independent experiment is shown.

A. Viable neutrophil count and ToPro-3 negativity of each sample. Flow cytometry profiling of B-C, ToPro-3 staining controls; D, media controls; E, JE2 controls; F, treatment of *purB* growth from BHI and RPMI without AI; G, treatment of *purB* inoculated in plain BHI and AI complemented RPMI media; H, treatment of *purB* cultured from AI positive BHI and negative RPMI; I, treatment of *purB* from AI complemented BHI and RPMI.

To verify the results by flow cytometric profiling analysis, the F/T sample displayed high ToPro-3 positivity in the histogram compared to PBS control, suggesting successful ToPro-3 staining (Figure 5.2 B-C). Both media control with and without adenine and inosine (AI) complementation showed a compact healthy population in the gated viable neutrophil area and very low ToPro-3 positivity, indicating the addition of AI does not cause neutrophil cell death (Figure 5.2 D). JE2 infected neutrophils with and without AI leads to profound cell lysis (leaving only a very small population in the viable neutrophils gate) and increased ToPro-3 positivity (Figure 5.2 E), suggesting AI complementation does not prevent neutrophils from being lysed by *S. aureus*. Hence, the controls proved that the chemical complementation of AI in RPMI media has no direct effect on neutrophil viability or affect the ability of WT JE2 to lyse neutrophils. The *purB* cultured from BHI agar and RPMI media without AI were attenuated in their ability to lyse neutrophils (Figure 5.2 F). The triplicate samples all displayed a compact viable neutrophil population with low ToPro-3 positivity, which is consistent with the level of attenuation in the screen. The *purB* grown on BHI agar containing AI but incubated with neutrophils without AI, left predominantly viable neutrophils (Figure 5.2 H). On the contrary, the addition of AI to RPMI media fully restored the neutrophil lysis ability of *purB*, as demonstrated by massive viable cell loss, increased density of debris, and increased ToPro-3 positivity (Figure 5.2 G&I). Clearly, chemical complementation was not required for *purB* to grow on BHI as this rich media is likely to contain sufficient purines, but was necessary during infection for *purB* to lyse neutrophils. Hence, lack of purine biosynthesis is a likely reason that *purB* fails to induce neutrophil cell lysis *in vitro.*

5.3 *In vitro* bacterial killing assay

The *lspA*, *purB* and *pfo* mutants showed robust attenuated neutrophil cell lysis compared to WT *S. aureus*. The attenuated cell lysis phenotype may be caused by a defect in either neutrophil phagocytosis or by enhanced killing of internalised bacteria. The bacterial killing

assay was therefore carried out with the 3 mutants to determine whether there are any differences in neutrophil uptake or neutrophil-mediated killing of the bacteria.

The *S. aureus* strains were co-incubated with neutrophils at MOI 5 to prevent technical difficulties caused by massive cell lysis. The number of intracellular bacteria was determined after 30 and 90 min of co-culture. Lysostaphin was added to the culture at 90 min incubated for a further 30 min to eliminate all extracellular *S. aureus*. The intracellular bacterial load was measured at 120 min. The experiment was repeated 3 times. The mean values and data from three experiments are shown in Figure 5.3.

Taking one independent assay as an example, the assay started with approximately $2.5x10^6$ *S. aureus*. After 30 min, 4.1% of JE2, 7.9% of *lspA*, 4.2% of *pfo*, and 8.9% of *purB* were internalized by neutrophils. At 90 min, the intracellular bacterial percentage was reduced to 2.1% of JE2, 2.2% of *lspA*, 5.0% of *pfo*, and 2.0% of *purB*, reflecting bacterial killing over this time period. The overall pattern of neutrophil uptake of the different *S. aureus* strains during the first hr of co-incubation is highly similar. Between the 90 and 120 mins, the absence of extracellular *S. aureus* provides an environment for neutrophil killing without further phagocytosis of bacteria. By comparing the internal bacterial number at 120 min with 90 min, 91.2% of JE2, 94.1% of *lspA*, 92.0% of *pfo*, and 94.0% of *purB* were eliminated by neutrophils. The combined data shows no obvious deficiency in internalisation or bacterial killing for any mutants, or any significant differences among the mean values (Figure 5.3), suggesting the attenuation of neutrophil cell lysis was not likely to be caused by lack of neutrophil engulfment or increased killing activity against the mutants.

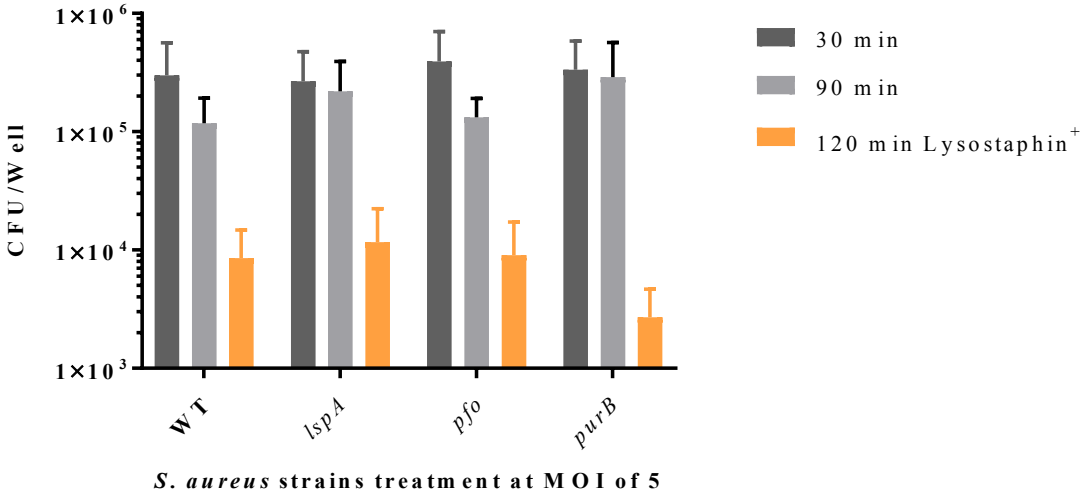

Figure 5.3 Neutrophils were co-cultured with *S. aureus* at MOI of 5. Phagocytosed bacterial numbers were quantified after 30 and 90 min by CFU plating. Lysostaphin was added to the culture (20µg/ml) at 90 min and incubated for a further 30 min to eliminate all extracellular *S. aureus.* The intracellular bacterial load was measured at 120 min. Mean values and standard deviations from 3 repeating experiments are shown.

5.4 *In vitro* phagocytic index assay

In the bacterial killing assay, even though the same MOI of bacteria were used for all experiments, there is variation in bacterial number engulfed by individual neutrophils at the initial stage, which likely can generate different infection outcomes. Although the bacterial killing assay showed a similar pattern of bacterial uptake and killing when comparing mutant strains and the WT, a potential difference of neutrophil phagocytic activity amongst mutants remains unclear. Therefore, it is important to measure rates of internalisation using a phagocytic index assay which reflects not only the proportion of neutrophils that have taken up bacteria, but also how many bacteria each neutrophil contains.

5.4.1 Quick-Diff staining images of *S. aureus*-neutrophils co-incubation

Phagocytic indices were assessed morphologically by light microscopy (Chapter 2.10.4.1). Representative figures of three independent experiments are shown in Figure 5.4 and indicating the presence of *S. aureus* as small purple inclusions inside the neutrophil. Images of *clpP* treatment were failed to be captured due to technical errors.

After 2 hr of co-incubation at MOI of 5, JE2 resulted in lysed neutrophils, some containing a high number of *S. aureus* (Figure 5.4). Treatment of *lspA*, *purB*, and *pfo* showed comparatively more viable neutrophils with small numbers of engulfed *S. aureus* (yellow arrows) than JE2, and fewer lysed neutrophils (red arrows). The results are in agreements with attenuated neutrophil cell death phenotypes shown in the NTML screen.

Considering the potential confounding influence due to neutrophil cell death and *S. aureus* amplification by JE2 after 2 hr, phagocytic index assay was carried out after 1 hr co-incubation.

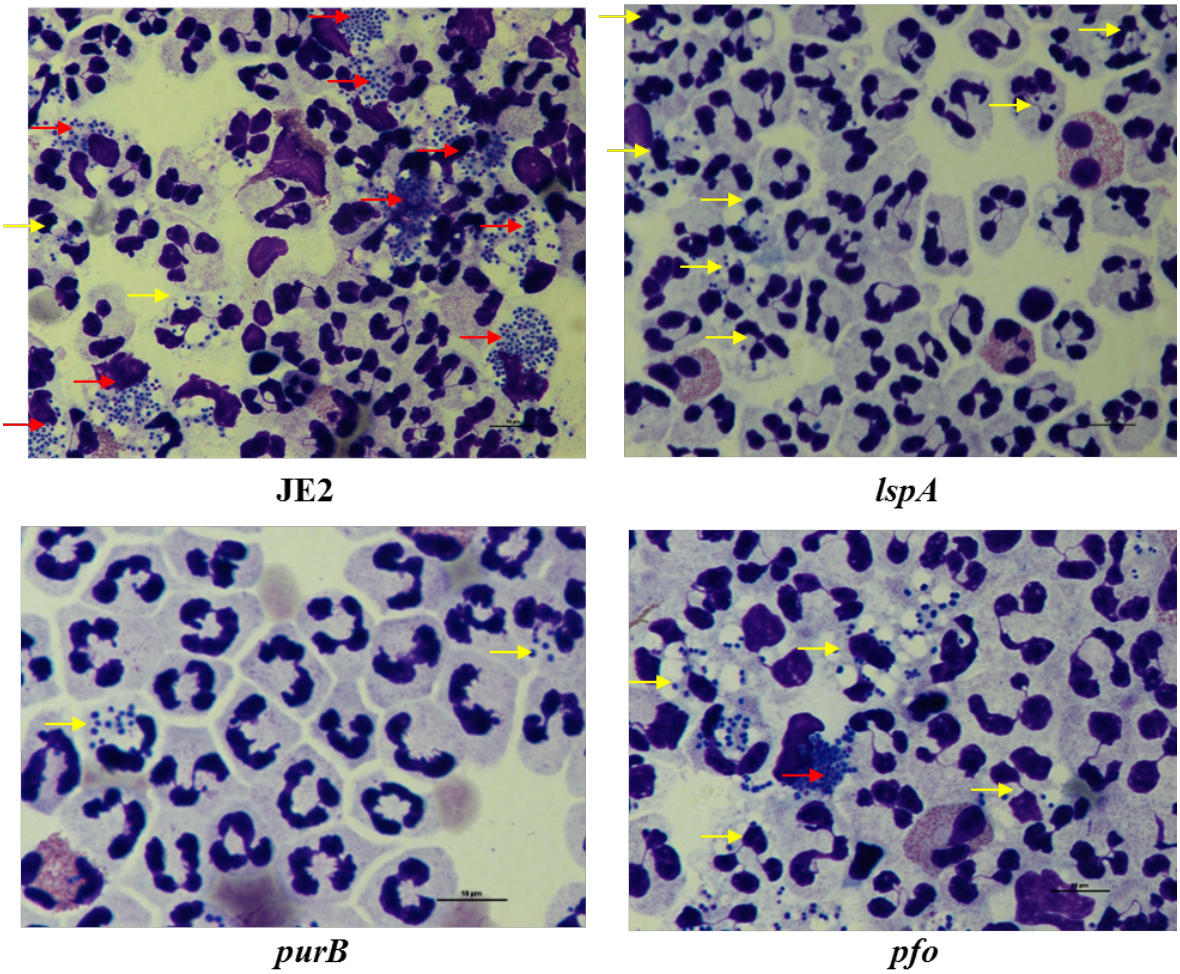

Figure 5.4. Diff-Quik staining images of *S. aureus*-neutrophil co-incubation. After 2 hr co-incubation of neutrophils with *S. aureus* at MOI of 5, the WT leads to a combination of a neutrophil population including live cells with (yellow arrows) and without phagocytised bacteria (purple dots), and lysed cells with massively replicated bacteria (red arrows). The three *S. aureus* mutants all resulted in a similar phagocytosis pattern but with less neutrophil death.

5.4.2 Phagocytic index calculation by Diff Quik staining

Neutrophils were incubated with *S. aureus* at an MOI of 10 for 1 hr. Cytospins were prepared for each group and 300 neutrophils were counted per slide. The number of engulfed bacteria and the number of neutrophils with and without engulfed bacteria were counted by light microscopy. To determine the variation in engulfment by neutrophils of the mutants comparing to the WT, the phagocytic index was calculated based on the formula below:

Phagocytic index = (Total number of engulfed *S. aureus*/Total number of neutrophils) x (Total number of neutrophils containing engulfed *S. aureus*/Total number of neutrophils) x 100

No significant difference in neutrophil phagocytic activity was observed between *purB* or *pfo* with JE2 (p>0.05). Both *clpP* (p=0.0002) and *lspA* (p=0.0018) showed significantly reduced neutrophil phagocytic activity in comparison to WT (Figure 5.5). Hence, defective neutrophil engulfment of *clpP* and *lspA* is a possible reason why these two mutants displayed attenuated neutrophil cell lysis.

5.4.3 Alexa Fluor 647 and pHrodo staining of *S. aureus*

The Diff Quik dyes allow effective staining of *S. aureus* but it is not possible to know the exact location of *S. aureus,* particularly whether the bacteria are in an intracellular compartment and within phagosomes. To address this, *S. aureus* were stained with pHrodo (Life Technologies) which is a pH sensitive red fluorescent cell wall dye that generates a fluorescent signal below pH 5, i.e. within the acidified phagosome (Zhu *et al*., 2015). This was used in combination with Alexa Fluor 647, which is a pH-insensitive, bright, far-red fluorescent dye. *S. aureus* strains were stained with pHrodo and Alexa Fluor 647 as described in section 2.11.1, followed by incubation with neutrophils for 1 hr at a MOI of 10 (and 50 due to dilution error). DAPI was used to stain the nucleus of neutrophils. The cells were imaged with an Olympus upright fluorescence microscopy system.

A representative figure of JE2 infected neutrophils at MOI of 50 showed *S. aureus* with red (pHrodo) and green (Alexa Fluor 647) fluorescence in neutrophils (Figure 5.6). Theoretically, Alex Fluor 647 shows all *S. aureus* (Figure 5.6 D) in the co-culture while pHrodo indicates bacteria within acidified phagosomes (Figure 5.6 C). However, quantification of fluorescent positive bacteria revealed that from all individual samples, the number of pHrodo positive *S. aureus* was consistently higher than the number of Alexa Fluor 647 positive bacteria, possibly caused by overall acidic environment. Attempts were made to further optimize the staining protocol and microscopy system. However imaging the of far-red channel failed to produce an adequate capture of the complete *S. aureus* population, suggesting low efficiency of Alexa staining. Additionally, the widespread pHrodo positive *S. aureus* covered most neutrophil intracellular compartments instead of only phagosomes as expected (Figure 5.6 A).

The phagocytic index assay was carried out at an MOI for 1 hr. treatment of pKH67 (Sigma), a green fluorescent cell membrane labelling dye, was performed to stain neutrophil membranes, which provides distinct boundary for quantification per cell. The Alexa Fluor 647 dye was not used in this assay due to it poor staining efficiency in previous experiments. Images from 3 independent experiments were taken using the same microscopy setting, a representative figure is shown in Figure 5.7 A. Among the thirty neutrophils, 16 cells remained intact in the absence of engulfed bacteria, 10 viable cells had phagocytosed *S. aureus*. The remaining 4 dead cells showed a large number of expelled pHrodo positive *pfo*, suggesting potential post-phagocytotic *S. aureus* survival and replication. The fluorescent stained cells displayed consistent results compared to neutrophil cell lysis result showed in section 5.4.1.

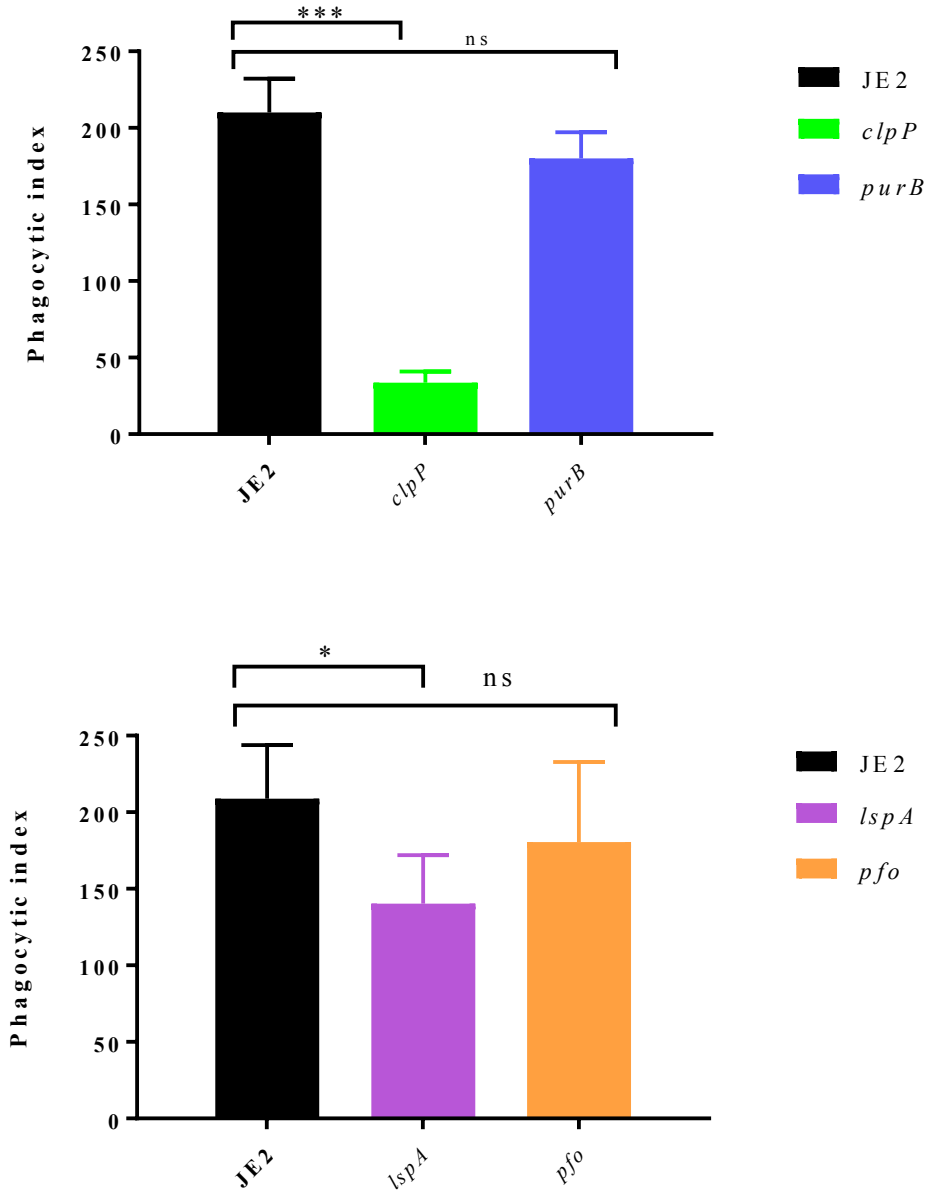

Figure 5.5 Phagocytic index assay of *clpP, purB, lspA* and *pfo* mutants in comparison to JE2. Healthy primary neutrophils were co-incubated with each strain at MOI of 10 for 1 hr followed by cytospin preparation with Quick-Diff staining. This assay was repeated 6 times, the mean values and standard deviations are shown. Both *clpP* (p=0.0002) and *lspA* (p=0.0018) showed significantly reduced neutrophil phagocytic activity in comparison to WT.

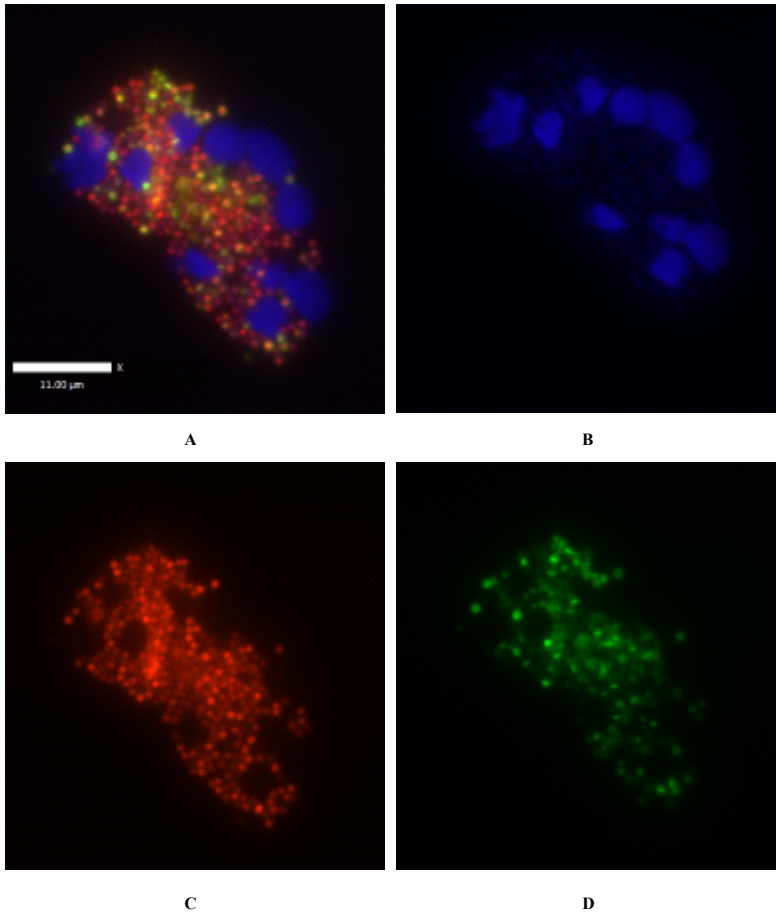

Figure 5.6 Representative images of a fluorescent stained neutrophil-*S. aureus* co-incubation. *S. aureus* was stained with pHrodo and Alexa Fluor 647 before co-incubation with neutrophils. Neutrophils were stained by DAPI and pKH67 after bacterial treatment. Fitters used for microscopy imaging were listed in Table 2.8. Co-culture of neutrophils and JE2 at MOI of 50 for 1 hr.

A. Overlay channel image

B. DAPI channel for DAPI detection

C. TxRed channel for pHrodo detection

D. Cy5 channel for Alexa Fluor 647 detection

5.4.4 Phagocytic index calculation by fluorescent staining

The number of pHrodo stained *lspA, clpP, pfo* and *purB* were counted automatically by ImageJ and the phagocytic index was determined accordingly, and shown in comparison with JE2 in Figure 5.7 B. JE2 displayed a phagocytic index of 3,701 on average, which is similar to *pfo* (3,470). *lspA* displayed comparatively higher phagocytic index (4,685), while *purB* (2,912) and *clpP* (1,955) showed lower phagocytic index. No significant difference was found in this assay, presumably because of the large variation of data. During the analysis of images, it was noticed that phagocytic index counts from one experiment was overall two-fold higher than the remaining two repeats, which compromised the combination of data and led to the large deviation. A few individual samples failed to produce sufficient countable cells due to technical errors. In addition, the range of phagocytic indices from the fluorescent staining is approximately 1000 to 8000 (Figure 5.7), which exceeds dramatically the normal range (50-300) (Figure 5.5). The data suggests that *S. aureus* were probably exposed in an acidic environment during pHrodo staining.

5.5 Analysis of *S. aureus* strains *in vivo*

5.5.1 Zebrafish embryo model of infection

The zebrafish embryo model of infectious disease has been developed for studying host pathogen interactions. It allows rapid, real-time *in vivo* pathogenesis studies of many microbes including *S. aureus* (Prajsnar *et al*., 2008). In order to explore the role of *lspA, purB, clpP*, and *pfo* in pathogenicity, the corresponding mutants were assessed using the zebrafish embryo model. A minimum of thirty LWT zebrafish embryos at 1 day old were injected with a dose of approximately 1500 CFU *S. aureus* strains. The bacteria were injected into the circulation valley of embryos (Figure 5.8) as described in section 2.12, a well-established route of infection. *S. aureus* infected embryos could be visually distinguished from un-infected embryos, based on the cloudy bacteria injected into the circulation valley (Figure 5.8). The

embryos were monitored twice a day till 92 hrs after injection and mortality was detected by cessation of heartbeat or destruction of tissue. All *in vivo* experiments in this study were conducted with a PBS injection control group. The survival rates in the PBS group were > 90% confirming health of the embryos and good zebrafish injection skills. All statistical analysis was completed by GraphPad Prism Version 6.0. Representative data are shown from independent experiments, but not combined due to zebrafish batch variation.

The survival curves of *S. aureus* infection demonstrated that mortality of zebrafish embryos is dependent on the infecting strain. As expected, embryos injected with WT mostly died (81.25%) within 92 hr (Figure 5.9 A). The *lspA* resulted in very similar survival curve to WT with a final death rate of 95.71% at 92 hr. In contrast, *purB* strain was not able to kill zebrafish embryos and resulted in only 10.55% of death. In separate experiment, WT consistently caused rapid embryo death, with a final survival rate of 3.85% (Figure 5.9 B). Although a delay of mortality pattern was observed, *pfo* produced similar survival rate to WT with 12.00% of viable embryos after 92 hr. Like *purB*, the *clpP* strain displayed attenuated embryo killing with 86.96% viability at 92 hr.

Many virulence factors of *S. aureus* are human specific or have host-dependent effects (Spaan *et al*., 2013b). Hence, the potential significance of *lspA* and *pfo* in humans cannot be ruled out due to lack of attenuation result in the zebrafish model. On the other hand, the significantly reduced pathogenicity of *purB* and *clpP* mutants *in vivo* suggests an importance of these two genes in host-pathogen interactions. The following experiments were aimed at investigating why *clpP* and *purB* failed to cause high level of killing. It was hypothesised that the absence of ClpP and PurB affects *S. aureus* survival or bacterial growth *in vivo*. Thus, the growth of *S. aureus* mutants was determined in *vivo*.

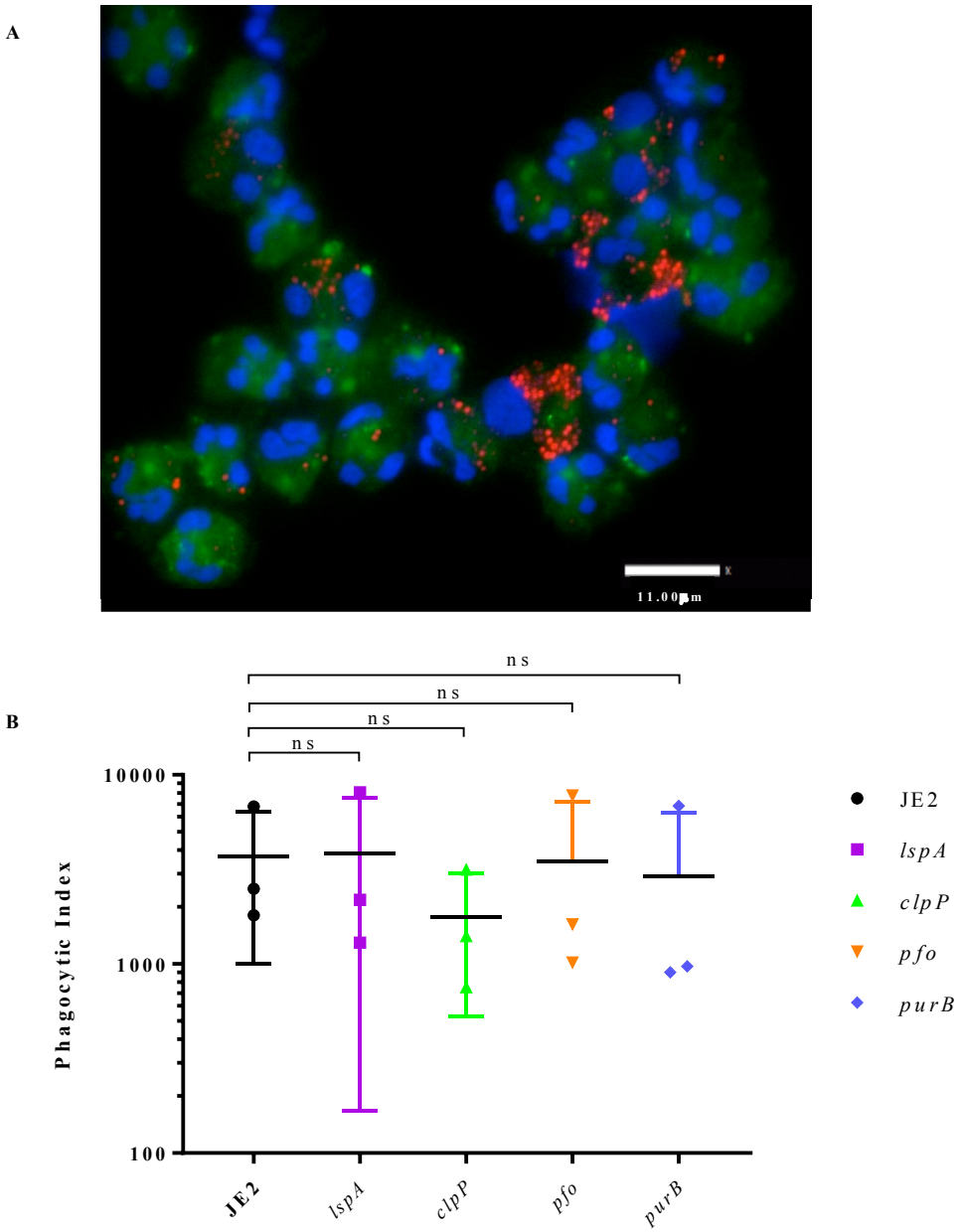

Figure 5.7 Phagocytic index assay with fluorescent staining.

A. Neutrophils treated with *pfo* at MOI of 10 for 1 hr. Overlay channels of DAPI (blue), pKH67 (green) and pHrodo (red) are shown in the image.

B. Phagocytic index count of *clpP, purB, lspA* and *pfo* mutants from pHrodo staining. The assay was carried out at MOI of 10 and incubated for 1 hr. The experiment was repeated 3 times, and a minimal total number of 300 neutrophils were counted from each strain. The mean value of calculated phagocytic index was used for comparison with the WT.

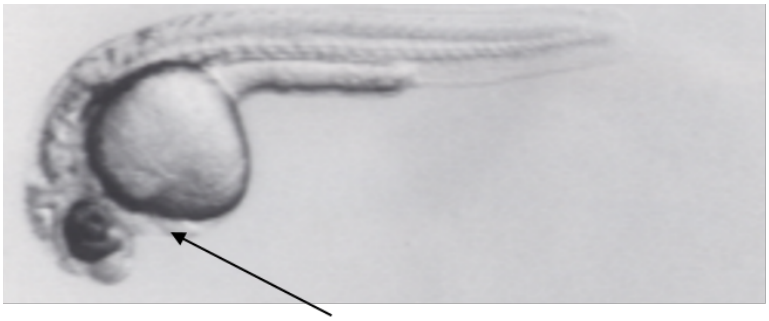

Circulation valley injection

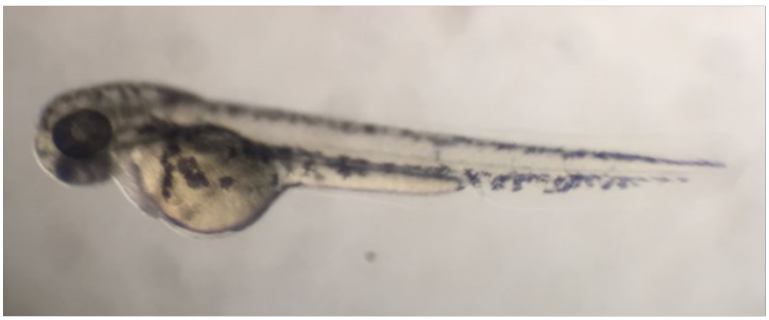

PBS injected embryo

***S. aureus* infected embryo**

Figure 5.8 Representative images to show zebrafish embryo injection point, morphology of healthy and *S. aureus* infected embryos. Bacterial strains were injected into the circulation valley of the embryo at 1 dpf. PBS injection was conducted within every independent experiment as a control. The cloudy bacteria shown in *S. aureus* infected embryo is visually clear during the maintenance of zebrafish. The embryos were monitored twice a day until 92 hr after injection and mortality was detected by cessation of heartbeat or destruction of tissue. The image showing circulation valley displays an embryo 24 hpf. The PBS and *S. aureus* injected embryos were imaged 48 hpf.

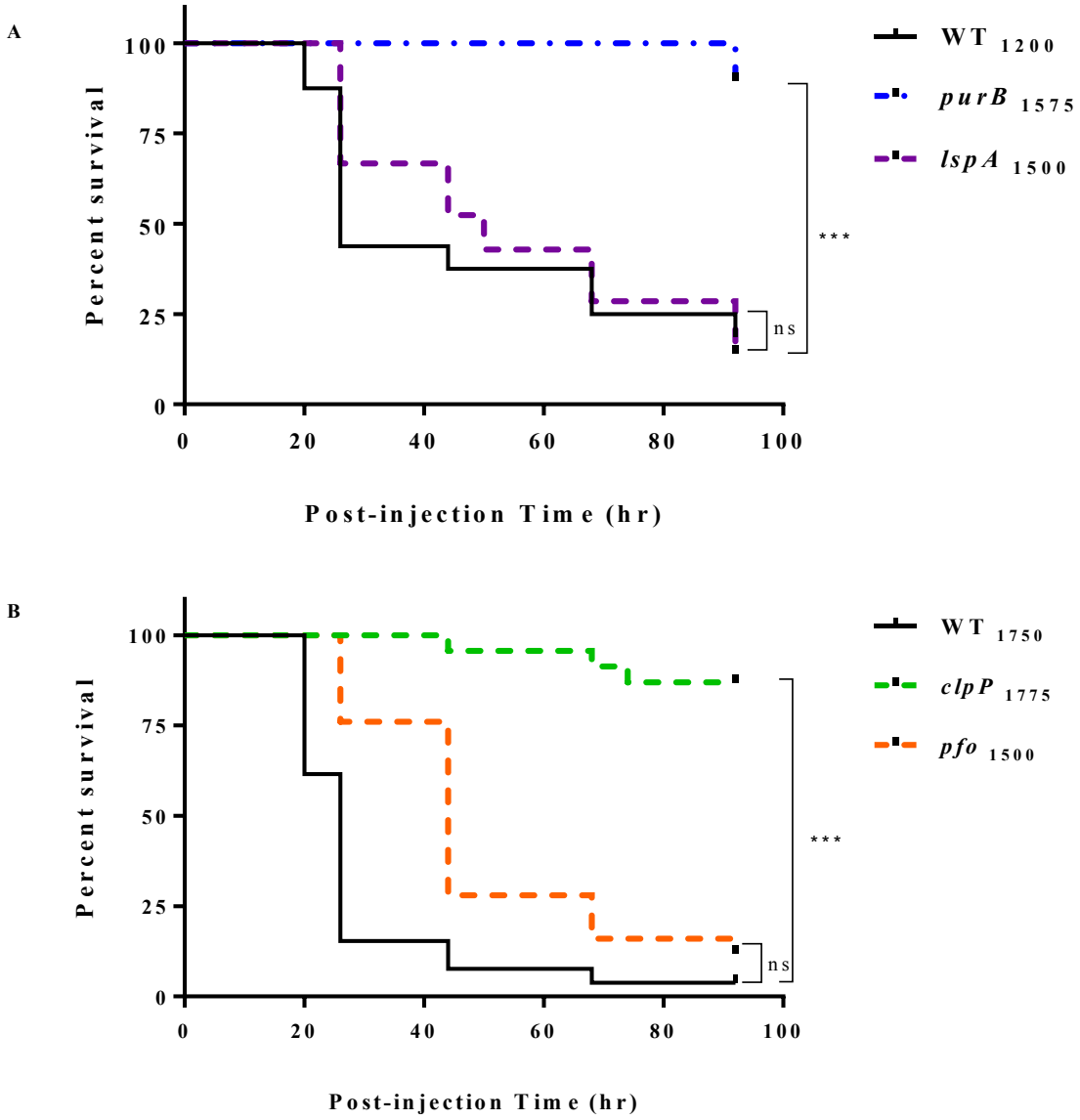

Figure 5.9 Virulence study of *clpP, purB, lspA*, and *pfo* in the zebrafish embryo model of infection. Survival of LWT zebrafish embryos was assessed upon injection of 1500 CFU JE2 or mutants. *** $p<0.0001$

5.5.2 Growth of *S. aureus* mutants *in vivo*

The survival study results raised a question as to whether the causality of attenuated zebrafish embryo killing involves deficiency of *purB* and *clpP* growth *in vivo*. To determine the bacterial growth in embryos, between 800-1000 CFU of *S. aureus* were injected in each zebrafish embryo at one dpf. From each experimental group, five live embryos and all dead embryos were collected, homogenised and plated out to measure bacterial CFU at each timepoint (Figure 5.10). The WT was able to kill a large number of zebrafish (53.6%) within 92 hr (Figure 5.10 E), and these dead fish contained over a thousand-fold more bacteria (>10^6 CFU) than the starting number (Figure 5.10 A), suggesting that WT has the ability to replicate *in vivo* and overcome the host. The embryos with less than 10^5 CFU (WT) remained viable. Similarly, *pfo* mutant was also able to replicate *in vivo* and kill zebrafish (53.6%) resulting in >10^6 CFU in dead embryos (Figure 5.10 B). Typically, the number of WT and *pfo* in infected live zebrafish gradually decreased following the injection, indicating clearing of *S. aureus in vivo*. Consistent with the *in vitro* neutrophil pathogenicity study (section 5.5.1). Both *purB* and *clpP* demonstrated defective virulence, with 96.87% and 87.5 % of survival at 92 hr respectively (Figure 5.10 F). All live infected embryos contain no more than 10^6 CFU of bacteria (Figure 5.10 C-D), indicating *purB* and *clpP* mutants failed to kill zebrafish due to either growth deficiency, or enhanced killing by immune cells *in vivo*.

5.5.3 Virulence phenotype in zebrafish embryo with compromised innate immunity

Following the growth assay, low bacterial numbers of *purB* and *clpP* has been identified as presumably the causality of attenuated zebrafish killing. Whether this was due to deficient replication, or better immune control by phagocytes was unknown. Even though *lspA* and *pfo* showed similar virulence as WT and led to zebrafish death, the importance of these two genes in staphylococcal modulation of human neutrophil was shown in NTML screen. Hence, it was important to determine pathogenesis in a phagocyte depleted model. Virulence of *S. aureus*

mutants was identified in zebrafish without neutrophil and macrophages. Morpholino oligonucleotides were used to induce a transient knock down of expression of myeloid cells. Morpholino refers to modified polynucleotides that are effectively able to block translation of a gene of interest. Its distinct structure consists of altered ribose or deoxyribose rings and phosphodiester bonds preventing hydrolysis upon injection (Bill *et al*., 2009). The morpholino used in this study is complementary to the translational start site of transcriptional factor, pu. 1, and aligning over the AUG start codon of target mRNA. After transportation into the cytoplasm, this double stranded RNA fragment cannot be recognized by ribosomes and subsequently is degraded (Bill *et al*., 2009). Consequently, the appearance of neutrophils is delayed until 36 hpf and macrophages until 48 hpf (McKercher *et al*., 1996, Rhodes *et al*., 2005, Klemsz *et al*., 1990). The pu.1 morpholino was injected into the yolk of embryos at the 1-4 cell stage. Following this, approximately 1000 CFU of *S. aureus* were injected 30 hr post fertilisation.

In the absence of neutrophils and macrophages, WT (JE2) leads to rapid zebrafish death at 22 hr after injection, with only 6.7% survival (Figure 5.11), demonstrating the importance of these cells in host response to *S. aureus*. *lspA* and *pfo* were attenuated, resulting in 0% and 12.9% survival by 44 hr post infection. Interestingly, the *clpP* mutant resulted in rapid killing with 16.85% alive zebrafish by 44 hr and 3.5% by 92 hr of infection, suggesting the pathogenicity was fully complemented by pu.1 morpholino treatment. However, the depletion of myeloid cells had no effect on virulence of *purB*, where 75% of embryos survived after 92 hr of infection.

A

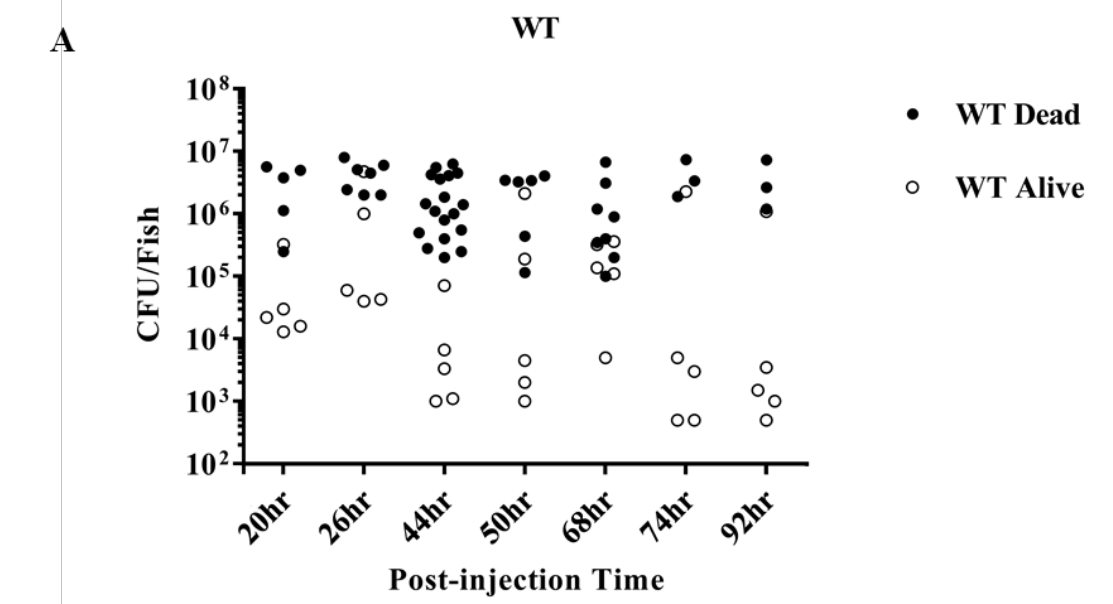
WT
CFU/Fish
10^8
10^7
10^6
10^5
10^4
10^3
10^2
20hr
26hr
44hr
50hr
68hr
74hr
92hr
Post-injection Time
WT Dead
WT Alive

B

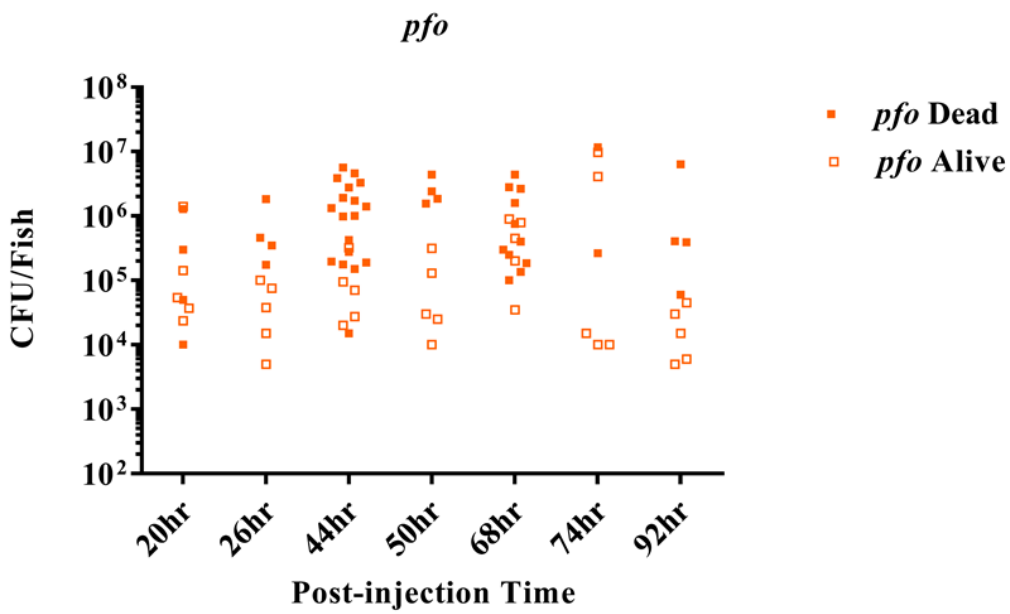
pfo
CFU/Fish
10^8
10^7
10^6
10^5
10^4
10^3
10^2
20hr
26hr
44hr
50hr
68hr
74hr
92hr
Post-injection Time
pfo Dead
pfo Alive

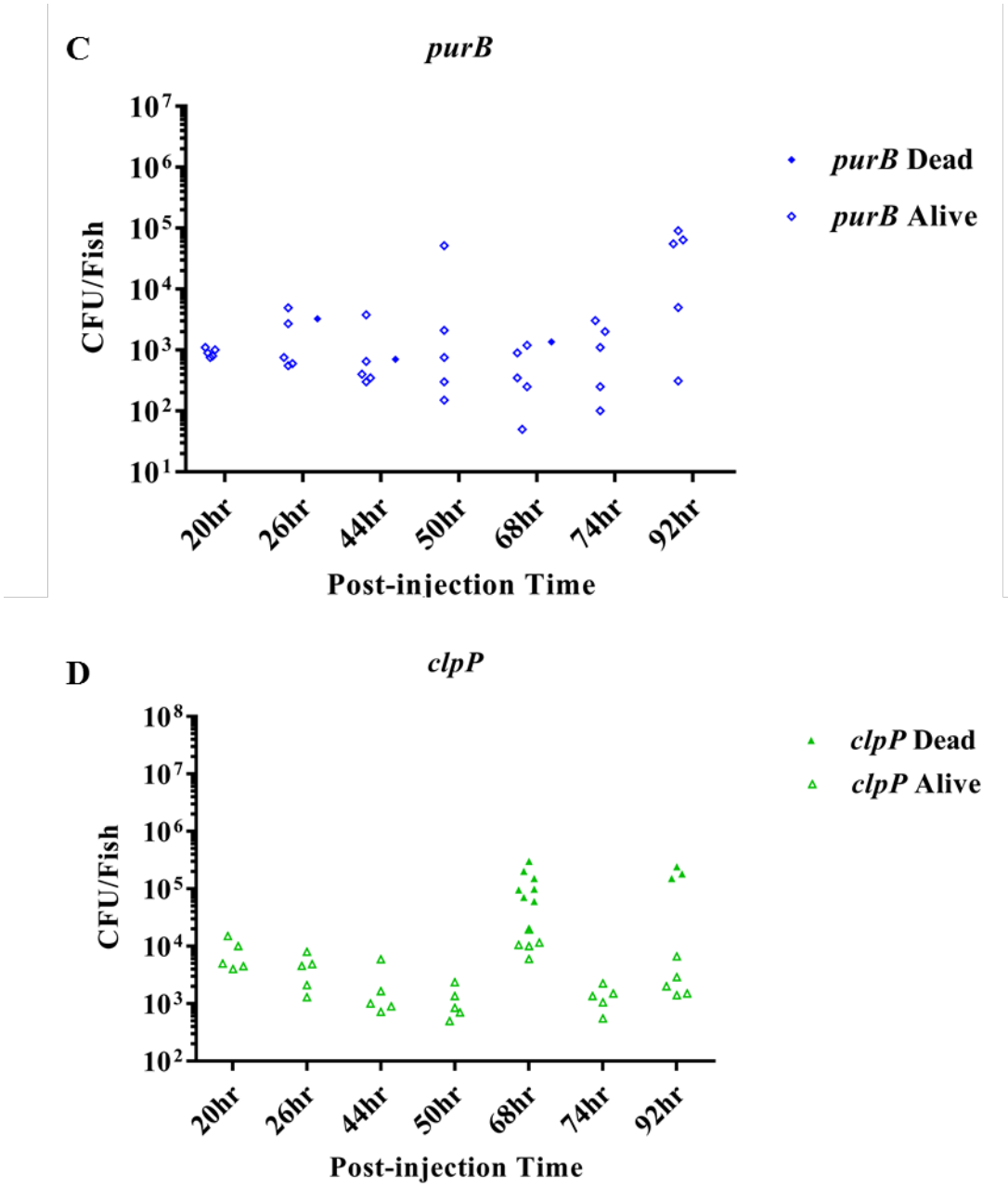
C
purB
CFU/Fish
10^7
10^6
10^5
10^4
10^3
10^2
10^1
20hr
26hr
44hr
50hr
68hr
74hr
92hr
Post-injection Time
purB Dead
purB Alive
D
clpP
CFU/Fish
10^8
10^7
10^6
10^5
10^4
10^3
10^2
20hr
26hr
44hr
50hr
68hr
74hr
92hr
Post-injection Time
clpP Dead
clpP Alive

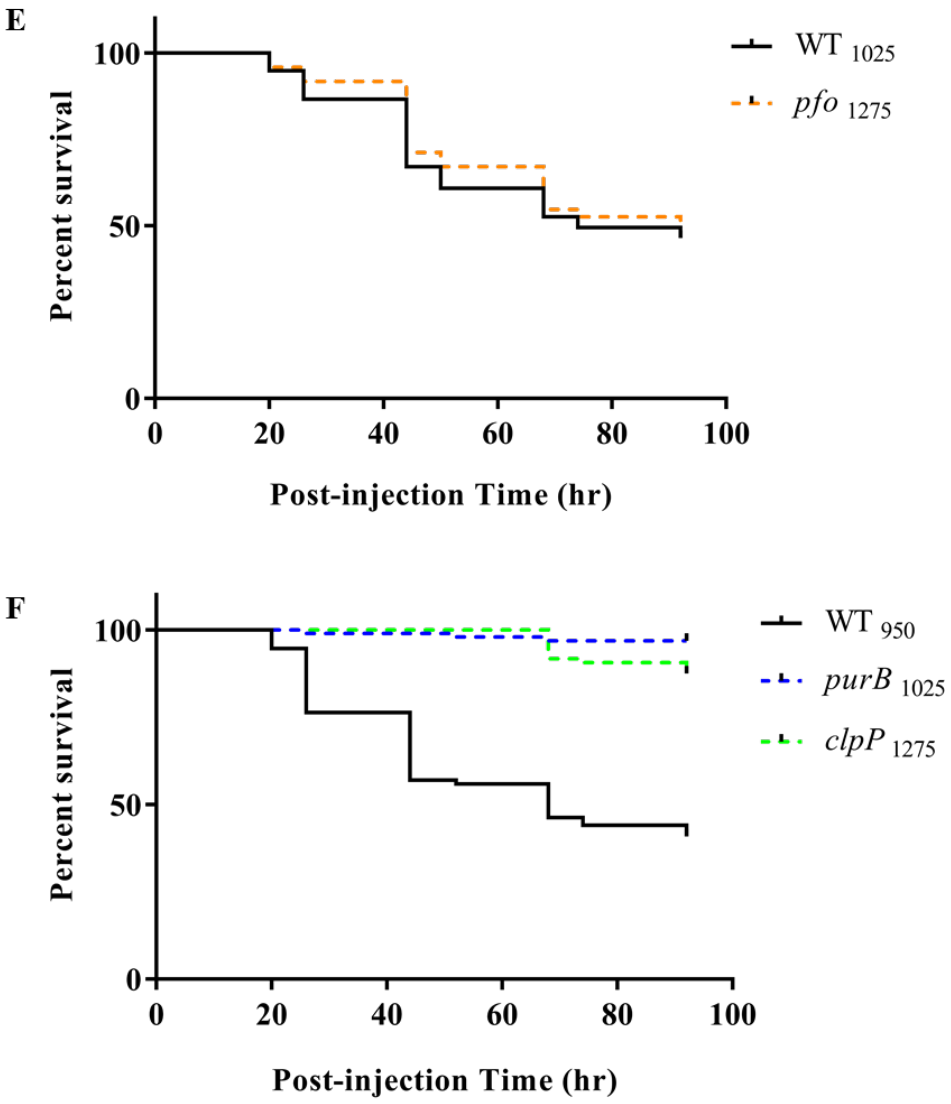

Figure 5.10 Survival curves and growth of *clpP, purB, pfo*, and WT in LWT zebrafish embryos. LWT zebrafish embryos were injected with 1000 CFU JE2 or mutants.

A-D). Growth of each bacterial population within zebrafish embryos.

E-F). Survival curves of *pfo, clpP,* and *purB* injection.

o = live embryos, • =dead embryos. At each timepoint 5 live embryos and any dead embryos were homogenized for CFU counts. N=1

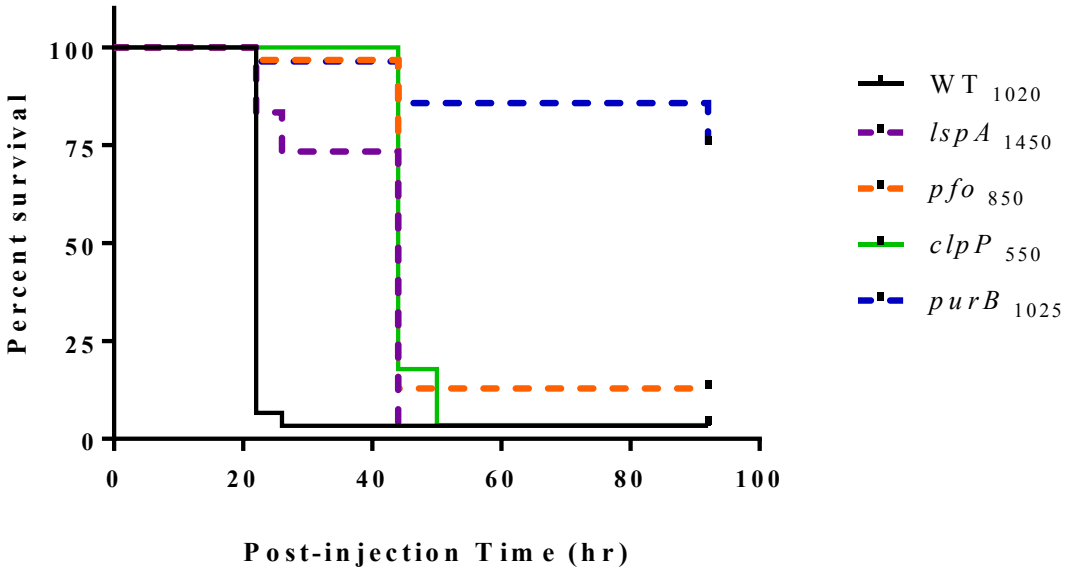

Figure 5.11 Representative survival curves of *clpP, purB, lspA*, and *pfo* together with WT in pu.1 morpholino injected LWT zebrafish embryos. Survival of LWT zebrafish embryos was assessed upon injection of 1000 CFU JE2 or mutants. N=2

5.6 Discussion

This chapter aimed to identify mechanisms responsible for the attenuation of neutrophil cell death, and to also characterise pathogenicity *in vivo*. Four genes not previously associated with *S. aureus* virulence against neutrophil responses namely *purB, lspA, pfo* and *clpP* were identified as being defective in lysing neutrophils (see Chapter 4). The virulence of the *purB* mutant was fully restored by chemical complementation of purines in co-culture media. Significantly reduced phagocytic index of *clpP* and *lspA* were observed in comparison to the WT *in vitro*. A *S. aureus*-zebrafish embryo model was performed to determine whether pathogenicity was affected *in vivo*. Out of the four strains, infection with *clpP* and *purB* were significantly less likely to result in death of zebrafish. Measurement of bacterial growth in zebrafish embryos revealed direct linkage of bacterial replication with host mortality. Low bacterial number compromised pathogenicity of *clpP* and *purB* in the zebrafish model. A transient gene knockdown using pu.1 morpholino resulted in loss of neutrophils and macrophages until 36-48 hpf respectively. Compared to the survival study in WT (phagocytes sufficient) zebrafish, WT, *lspA* and *pfo* infection resulted in enhanced embryo killing after a few hrs, suggesting the importance of phagocytes in host defence against *S. aureus* infection. Virulence of *clpP* was fully restored compared to JE2 in the absence of phagocytes demonstrating the importance of the *clpP* in phagocytic interactions. No change host survival was found with *purB* infection in the pu.1 knockdown likely indicating the attenuated phenotype resulted from *de novo* purine biosynthesis deficiency rather than regulation of phagocytes response.

5.6.1 Analysis of *purB*

Analysis of the *purB* mutant was carried out following the scheme shown in Figure 5.12. Adenylosuccinate lyase, the product of the *purB* gene, is a member of the aspartase-fumarase

superfamily of enzymes. The crystal structure of this protein has been determined from several organisms including *Homo sapiens, E. coli,* and *S. aureus* (Vedadi *et al*., 2007, Tsai *et al*., 2007, Fyfe *et al*., 2010). The dual substrate specificity of adenylosuccinate lyase in *S. aureus* was demonstrated as metabolism of SAICAR and adenylosuccinate (Figure 5.1). Hence, it controls the levels of ATP and GTP synthesis via the purine biosynthesis pathway. Previous studies based on metabolic reconstructions and bioinformatic comparisons predicted the *pur*B synthesized enzyme plays an essential role in *S. aureus* metabolism (Heinemann *et al*., 2005).

The importance of purine biosynthesis in the *S. aureus*-mediated infection process is poorly characterised. Recently, purine antagonists were developed for potential anti-bacterial therapy, due to the essential metabolism involvement (Gottlieb and Shaw, 2013). From a *S. aureus* abscess study in a murine model, *purA* was found to be attenuated (Lan *et al*., 2010).

Previous laboratory work (Dr. John Connolly) showed that *purB* is a purine auxotroph (data not published), which is consistent with a role of *purB* gene in *S. aureus* metabolism (Baxter-Gabbard and Pattee, 1970). Attempts were also made by Connolly to chemically complement the *purB* strain in the zebrafish embryo model with adenine and inosine, yet the bacterial virulence was failed to be restored. Since it was not possible to verify uptake of adenine and inosine by zebrafish, the requirement of purines for host mortality remains unclear. The experiment suggested low availability of purines in zebrafish embryos, which is in agreement with the attenuation of *purB* mutant in our survival study; and explains the lack of bacterial replication *in vivo*. The attenuated host killing phenotype in this study suggests the *de novo* purine biosynthesis is the limiting factor for *purB* mutant growth and pathogenesis in the zebrafish model, not phagocytes interactions.

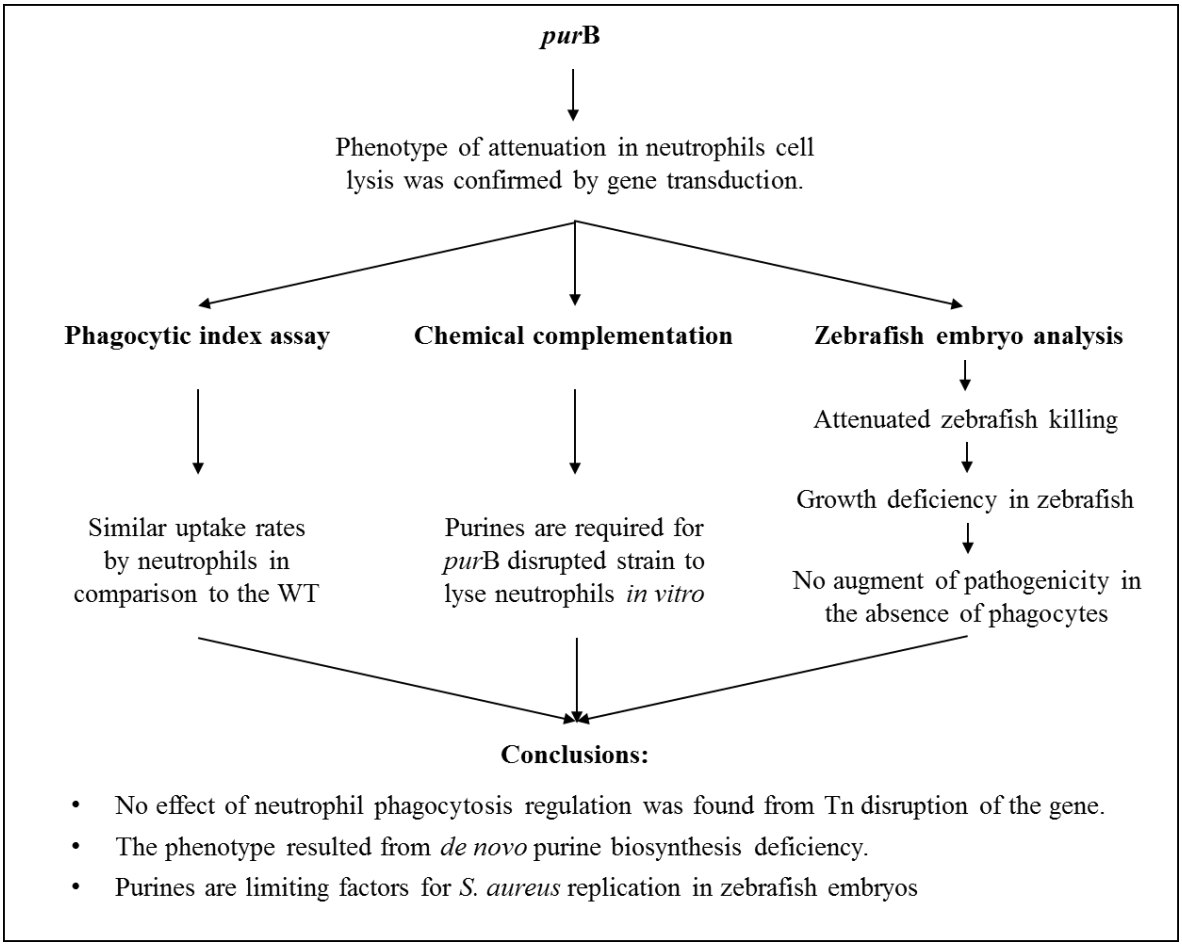

Figure 5.12 Diagram of the analysis of the *purB* gene.

Based on the assessment of phagocytic index (Figure 5.5), no deficiency in neutrophil uptake of *purB* mutant was found compared to WT, suggesting *purB* gene is not involved in modulation of phagocytosis. It was verified that BHI media is sufficient for normal growth of the *purB* mutant (Figure 4.12), while lack of chemical complementation in RPMI media lead to attenuated neutrophil lysis (Figure 5.2). Evidently, loss of purine biosynthesis is the limiting factor for post-phagocytosed *S. aureus* to lyse neutrophils, which implies the potential necessity of bacterial replication inside neutrophils for inducing immune cell death.

5.6.2 Analysis of *lspA*

Analysis of the *lspA* mutant was carried out following the scheme of the summarized data shown in Figure 5.13. The lipoprotein signal peptidase expressed by *lspA* is a cytoplasmic membrane localized enzyme required for biogenesis of bacterial lipoproteins (Shahmirzadi *et al*., 2016). LspA is anchored on the periplasmic leaflet of the membrane via a conserved lipid-modified cysteine residue at the N-terminus (Nakayama *et al*., 2012). The maturation of lipoproteins includes two or three modification steps. First, a diacylglyceryl group is transferred onto a lipobox cysteine by phosphatidyl glycerol diacelyglyceryl transferase (Lgt). Next LspA recognizes and cleaves the signal peptide at the +1 *S*-diacylglyceryl cysteine of the prolipoproteins (Nakayama *et al*., 2012). Structurally there are two types of lipoprotein: diacylated, and triacylated. Both forms of lipoproteins have been reported in *S. aureus* (Kurokawa *et al*., 2009). Moreover, variation between diacylated and triacylated lipoprotein structure in *S. aureus* has been found to be environment-dependent, particularly pH -mediated (Kurokawa *et al*., 2012).

Lipoproteins play essential roles in host-pathogen interactions. They function as pathogen-associated molecule patterns and mediate inflammation through activating TLR2 signalling cascades (Bubeck Wardenburg *et al*., 2006, Schmaler *et al*., 2010, Kim *et al*., 2015). A few studies strongly suggest that *S. aureus* lipoproteins induce production inflammatory cytokines

including TNF-α and IL-6 (Kurokawa *et al*., 2009, Bubeck Wardenburg *et al*., 2006). In a murine infection model, *lspA* mutant in the *S. aureus* Newman background failed to replicate in liver or to develop acute, lethal disease. Another gene required for lipoprotein maturation: *lgt*, is required for lipoprotein acylation. The *lgt* mutant induces less TNF-α and IL-6 production, proliferates to higher numbers compared to WT, and results in rapid and profound mortality of infected mice (Bubeck Wardenburg *et al*., 2006). In comparison to WT, infection of murine macrophages by lipoprotein deficient *S. aureus* results in lack of nitric oxide production, decreased expression of inducible nitric oxide synthase, and absence of TLR2 activation (Kim *et al*., 2015). Hence, mature lipoprotein is essential for initiating and sustaining effective activation of host immunity. In agreement with the significance of lipoproteins in immune cell recognition, the significantly reduced phagocytic index result of the *lspA* mutant in our study suggests that lack of lipoproteins prevents efficient neutrophil uptake of *S. aureus*. As well as activation and recruitment, the TLR2 signalling pathway has been found to inhibit neutrophil apoptosis (Sabroe *et al*., 2005). Thus, lipoprotein induced TLR2 activation is relevant to neutrophil cell death and impaired host defences against bacterial infection (Roger and Calandra, 2009), which also implies that TLR2 activation of neutrophils may be necessary for *S. aureus* to cause immune cell lysis, and the attenuated phenotype caused by *lspA* in our study is due to lack of TLR2 activator: lipoprotein. To address this hypothesis, TLR2 blocking antibodies could be used to identify neutrophil-*S. aureus* interaction in future work. The importance of *lspA* in *S. aureus* pathogenicity was also reported with the attenuated virulence of *lspA* mutant in *S. aureus* RN6390 background, where this mutant failed to be recovered from spleens and blood of mice after co-infection with a mixture of 96 *S. aureus* strains, suggesting LspA is essential for bacterial replication *in vivo* (Mei *et al*., 1997).

5.6.3 Analysis of *pfo*

Pfo encodes pyruvate ferredoxin oxidoreductase α subunit, which is involved in the oxidative decarboxylation of pyruvate to acetyl-CoA and CO_2 (Figure 5.1 B). Pyruvate ferredoxin oxidoreductase is an essential enzyme of central metabolism (Ballard *et al*., 2010, Dubreuil *et al*., 1996, Finegold *et al*., 2009, Hoffman *et al*., 2007, Horner *et al*., 1999). To date, a *pfo* phenotype has not been described in *S. aureus*-neutrophil interaction and the role of pyruvate ferredoxin oxidoreductase in staphylococcal pathogenicity is poorly investigated. In a mouse infection model, inhibition of pyruvate ferredoxin oxidoreductase was found to be efficacious against *Clostridium difficile* infection (Warren *et al*., 2012). Warren *et al* suggests the pyruvate ferredoxin oxidoreductase is important for bacterial virulence, which is consistent with the robust attenuated neutrophil lysis demonstrated by *pfo* (Figure 5.14). A study carried out in *T. vaginalis* reveals the pyruvate ferredoxin oxidoreductase is a surface-associated cell adhesion protein involved in host cell-binding activity (Meza-Cervantez *et al*., 2011). Inhibition of pyruvate ferredoxin oxidoreductase in *T. vaginalis* led to decreased parasite proliferation and adhesion to vaginal epithelial cells, and smaller tissue abscess formation in mice (Song, 2016). However, interruption of the staphylococcal *pfo* gene gave no alteration of neutrophil phagocytosis or bacterial replication in zebrafish (Figure 5.14). Thus, the cell binding function and role in bacterial growth is less likely to be applicable to *S. aureus pfo*. In support, the augmentation of *pfo* virulence in phagocyte depleted zebrafish indicates the gene function is involved in modulation of host innate immune defences. It may be that lack of oxidative decarboxylation of pyruvate reduced metabolic activity, which further negatively regulated post phagocytosed *S. aureus* survival. Further research to identify the link between deficiency of *pfo* and neutrophil cell lysis is required. Fluorescent labelling and time lapse microscopy can be combined to visualise the progress of host-pathogen interaction.

5.6.4 Analysis of *clpP*

Analysis of the *clpP* mutant was carried out following the scheme of the summarized data shown in Figure 5.15. Caseinolytic protease proteolytic subunit, the product of *clpP* gene, forms the Clp chaperone protease complex with an ATPase specificity factor. The main function of Clp proteases is protein degradation and the proteases are well conserved in most bacterial species (Savijoki *et al*., 2006, Frees *et al*., 2007). The chamber of Clp proteases consists of a barrel shaped structure that is formed by two heptameric ClpP rings (Figure 5.1). To be degraded, protein substrates are unfolded and translocated to the ClpP proteolytic chamber through Clp ATPase activity (Frees *et al*., 2007). In *S. aureus*, two ATPases namely ClpC and ClpX are found with this function (Figure 5.1 D). Additionally, two ATPases namely ClpL and ClpB act as chaperones without interaction with Clp peptidase (Martin *et al*., 2008).

During infection, microorganisms are exposed to a range of environmental changes which can affect viability. This exposure to stresses such as changes in oxidative potential, temperature, pH and antimicrobial peptides may result in protein misfolding. Consequently, the removal of misfolded and aggregated non-native proteins is crucial for bacterial growth and functionality (Truscott *et al*., 2011). The ClpB and ClpL chaperones contribute to stress tolerance through preventing unfolding or facilitating protein disaggregation (Glover and Lindquist, 1998). ClpCP is believed to degrade non-native proteins in *S. aureus* mediated by a teicoplanin resistance factor A (TrfA) (Feng *et al*., 2013). Inhibition of ClpP, ClpB and ClpC in *S. aureus* leads to reduced bacterial growth at high temperature (Frees *et al*., 2003, Frees *et al*., 2004, Frees *et al*., 2012). A threefold transcription of *S. aureus clp*P was observed at 30^{o}C, the expression at 20^{o}C was fourfold than normal level (37^{o}C), suggesting ClpP functionality plays an essential role in staphylococcal survival at low temperature (Michel *et al.* 2006). A global stress regulator known as Spx which positively modulated the disulphide-stress response, has been identified in the ClpP proteolytic chamber (Feng *et al*., 2013). The cellular homeostasis

under non-stress conditions are regulated by ClpXP degradation to achieve a low Spx concentration. Under disulphide stress, several oxidative stress tolerance genes are transcriptionally activated by stable Spx (Garg *et al*., 2009, Larsson *et al*., 2007, Nakano *et al*., 2003, Engman *et al*., 2012). Clp proteases also target DNA damage repair proteins. The transcriptional repressor LexA is degraded by ClpXP and ClpCP in *S. aureus* (Butala *et al*., 2009, Cohn *et al*., 2011).

Apart from stress tolerance, a large number of proteins involved in *S. aureus* metabolism and cell division, such as cell division protein family Fts and the pentaglycine cross bridge formation family Fem, have been found among the ClpP substrates (Frees *et al*., 2012). Another category of roles of the Clp complex have been identified in antibiotic resistance. Mutation of the *trf*A gene increased susceptibility of glycopeptide intermediate sensitive *S. aureus* strains to vancomycin and teicoplanin, possibly due to antibiotic stress response in conjunction with ClpCP proteolysis (Renzoni *et al*., 2009). Inhibition of ClpXP led to increased USA300 β-lactam resistance via changes in cell wall metabolism (Baek *et al*., 2014). Evidence was found that *clp*P mutants in Newman, USA300, and ST59 backgrounds lead to increased expression of fibronectin- and fibrinogen-binding proteins, and thickened biofilm formation, which was caused by the decreased *agr* activity (Liu *et al*., 2017). Unlike the polysaccharide intercellular adhesion-dependent biofilm, the constituents of biofilm formed by strains lacking ClpP only contains proteins and extracellular DNA, due to enhanced activity of peptidoglycan hydrolase Sle1. Nonetheless, the virulence of *clp*P mutant was not compensated by the increased cell surface proteins and biofilm formation in a murine infection model (Liu *et al*., 2017).

Without doubt the ClpP complex is essential for *S. aureus* protein maintenance and therefore closely involved in a range of key regulations of bacterial survival under stress and during antibiotic resistance. Moreover, significant phenotypes of *clpP* mutants were found in multiple

studies due to its role in regulating expression of virulence genes (Frees *et al*., 2003, Frees *et al*., 2005a, Frees *et al*., 2005b, Michel *et al*., 2006, Feng *et al*., 2013, Farrand *et al*., 2013). An approximately 100-fold decreased transcription of genes encoding extracellular protease including SspA, Aur, and Spl was found with deletion of *clpP*. Another example is 10-fold reduced transcription of α-hemolysin gene *hla* in *S. aureus* (Feng *et al*., 2013, Frees *et al*., 2003). In addition, inactivation of *clpP* affected expression of virulence factors such as *ssp*A and *spa* in a global transcriptomic and proteomic analysis in *S. aureus* (Frees *et al*., 2012).

Although the stability of transcriptional virulence regulators in *S. aureus* is highly likely dependent on ClpXP, none of the regulators were identified as substrates of ClpP (Michalik *et al*., 2012, Feng *et al*., 2013). The possibility of direct ClpP proteolytic influence on these regulators cannot be ruled out due to regulatory proteins are small, highly basic, and at low amount, which increases the experimental challenge of molecule detection through MS or gel electrophoresis. Alternatively, an indirect link between the virulence gene regulation and ClpXP was proposed based on the theory that *clpP* deletion induced stress might result in metabolic signals that further modify cellular virulence control. Moreover, the change of cell wall structure may have a negative impact on signal transfer and therefore reducing expression of virulence genes in *clpP* mutants (Frees *et al*., 2014). Whatever is the mechanism, the involvement of ClpP in *S. aureus* virulence gene regulation and pathogenesis has been well established.

The essential role of ClpP and ClpX in *S. aureus* virulence was found in a mouse model where inactivation of the proteases leads to absence of α-hemolysin expression and complete elimination of abscess formation (Mei *et al*., 1997, Frees *et al*., 2003). Abolished intracellular replication of *clpP* mutant was observed in bovine mammary cells (Frees *et al*., 2004). A recent study of *clpP* deficient *Legionella pneumophila* revealed lack of bacterial amplification and poor escape from endosome-lysosomal pathway in mammalian cells (Zhao *et al*., 2016).

In another species, *Lesteria monocytogenes, clpP* is also required for bacterial survival in murine macrophages (Gaillot *et al*., 2000). Cao *et al* (2013) uses ClpP as an antigen for mucosal immunization use against *Streptococcus pneumoniae*. This induced systemic and mucosal antibodies, reduced lung colonization and mice deaths in an intraperitoneal-sepsis model. The existence of anti-ClpP antibody complemented polymorphonuclear leukocyte killing of *S. pneumoniae in vitro* (Cao *et al*., 2013). In dendritic cells, *clpP* expression upregulated *S. pneumoniae* uptake and phagocytosis, and apoptosis rate of the infected immune cells (Cao *et al*., 2013).

Consistent with the evidence of universal significance of *clpP* in bacterial survival and virulence above, Tn disrupted *clpP* mutant showed decreased neutrophils uptake comparing to WT. The robust attenuated phenotype in neutrophil cell death assay indicated an essential role of *clpP* in *S. aureus* virulence against human neutrophils. It is highly likely that lack of ClpP function compromised stress resistance against the intra-phagosomal environment, leaving the bacteria static or killed by neutrophils, instead of lysing the immune cells. To test this, time lapse microscopy aimed at tracking post-phagosomal *clpP* could be conducted in further work. The other two genes encoding the Clp protease complex subunits in NTML namely *clpB* and *clpC* failed to show attenuated phenotype in the 1st round of screen. The *clpC* mutant lysed similar number of neutrophils comparing to JE2 (approx. 50%) st 3 hrs. The role of ClpB or ClpC may not be essential for *S. aureus* interaction with neutrophils in the sense that the intact ClpXP can maintain major functionality of the Clp protease complex; while the activity of *clpB* could be complemented by *clpL*. Results found upregulated gene expression of *clpB* and *clpC* following neutrophil phagocytosis of *S. aureus,* suggesting the ClpB chaperone and ClpC ATPase are likely to be actively involved in post-phagosomal survival and regulation of virulence factors (Voyich *et al*., 2005). I, however, did not identify *clpB* or *clpC* from the NTML, possibly due to false negativity bound by the nature of screen.

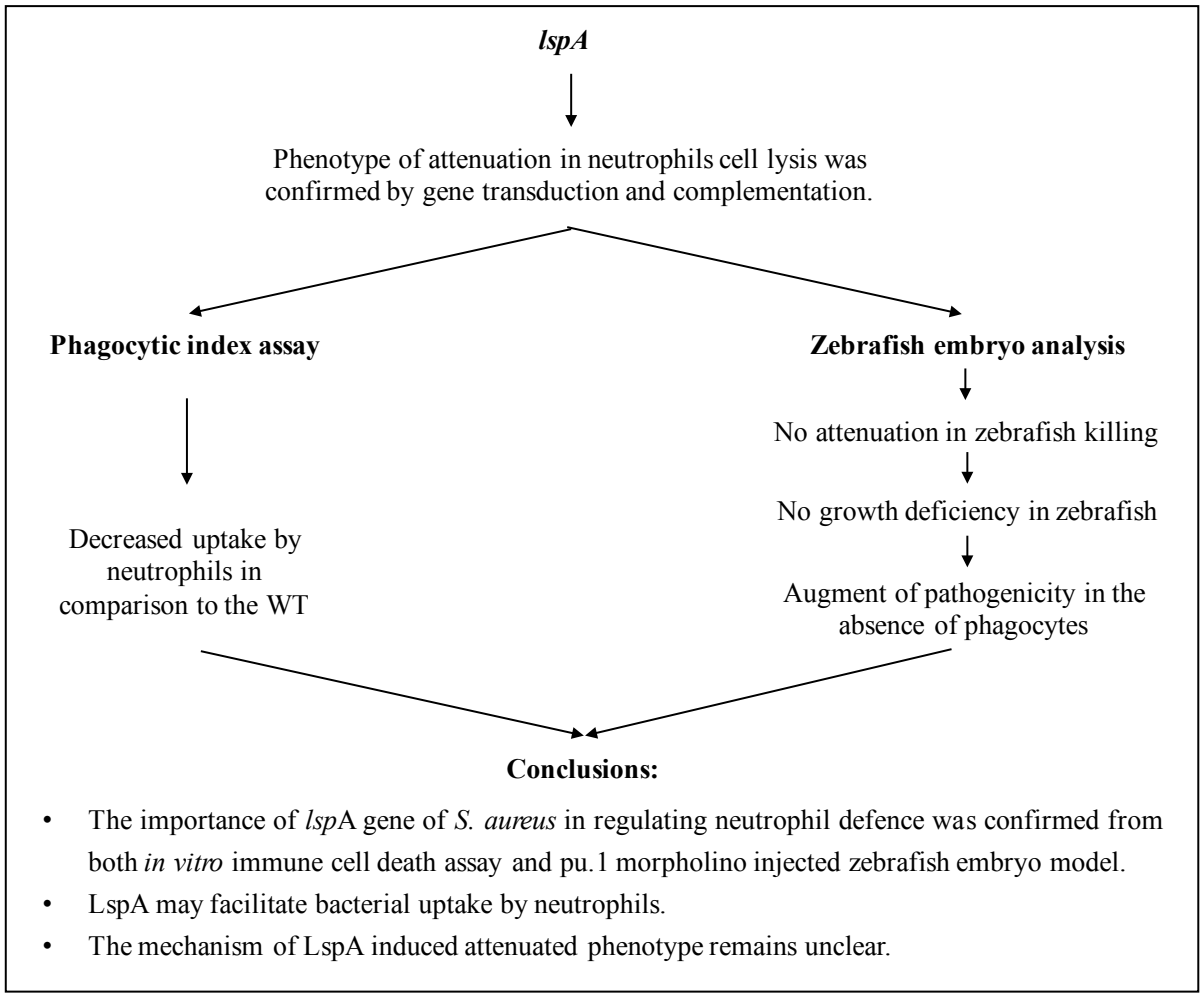

Figure 5.13 Diagram of *lspA* gene analysis summary.

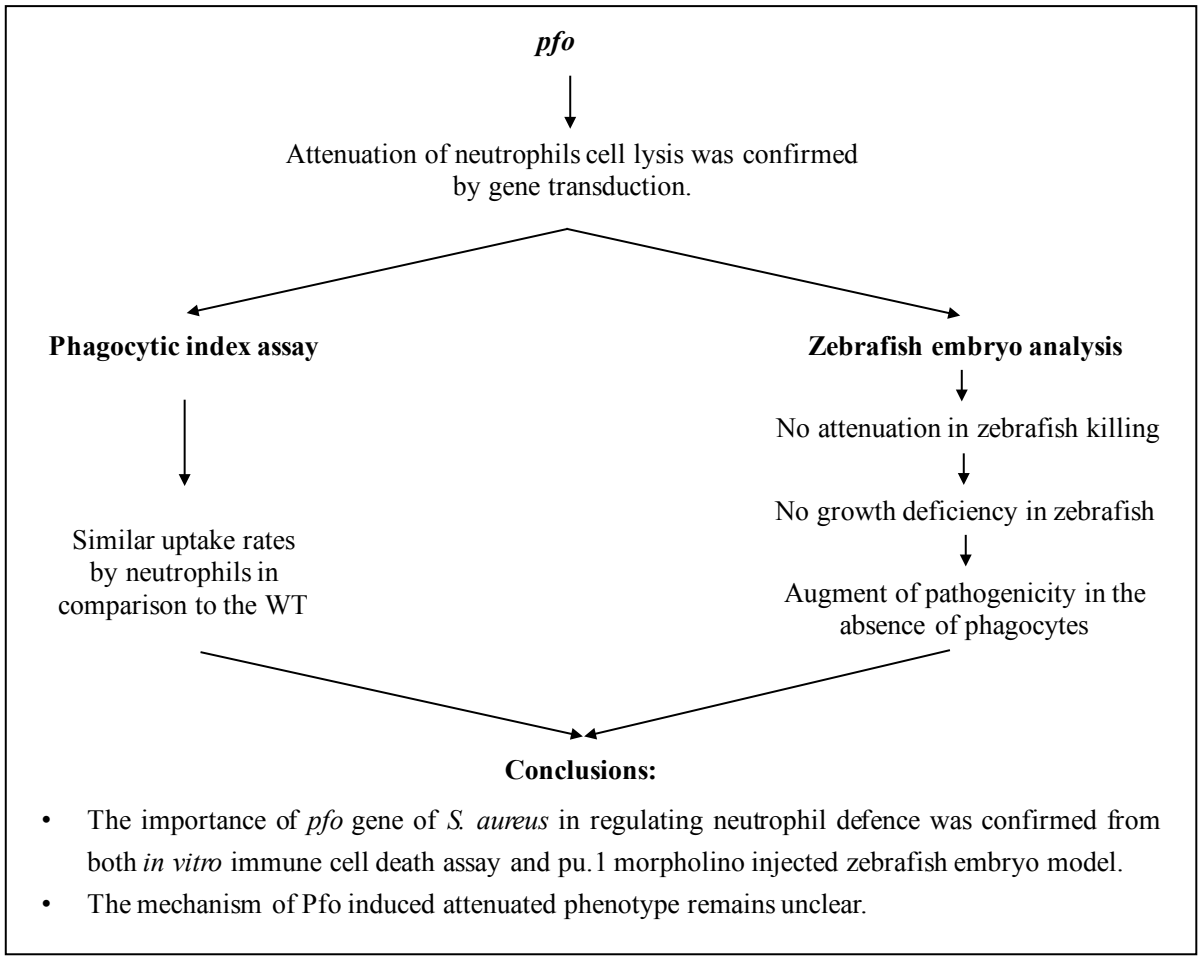

Figure 5.14 Diagram of the analysis of the *pfo* gene.

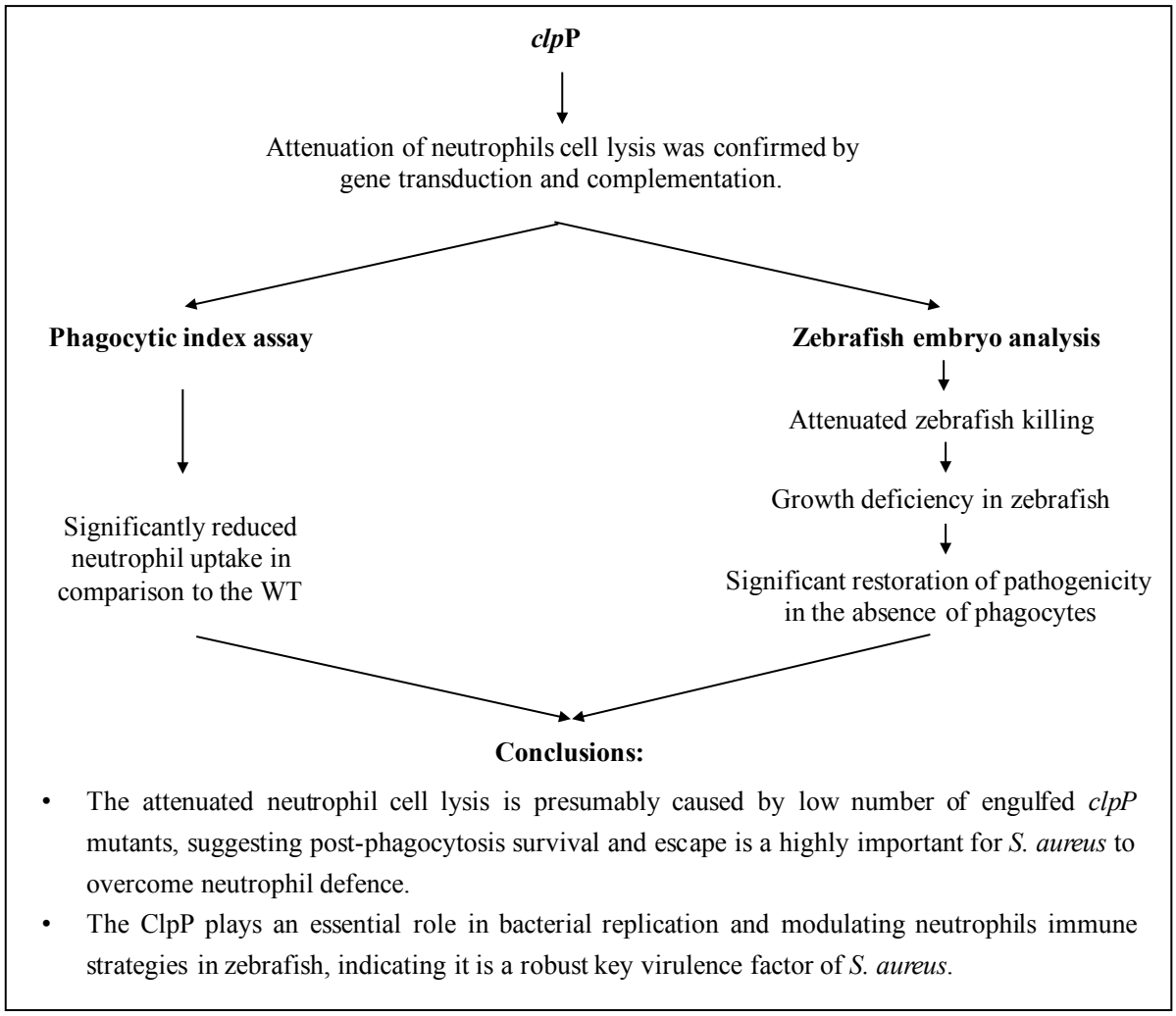

Figure 5.15 Diagram of the analysis of the *clpP* gene.

CHAPTER 6

Discussion

6.1 Summary of the findings of this thesis

I have identified four *S. aureus* genes, namely *purB*, *lspA*, *clpP*, and *pfo,* as having a role in the induction of human neutrophil cell death. These findings were generated by a genome-wide genetic screen of 1,920 *S. aureus* mutants in a flow cytometric assay of neutrophil lysis. The blinded nature of this assay and the identification of genes known to be critical in neutrophil cell death (*agrA* and *saeS*) validated the design of the model, which to our knowledge, has not been done before. These findings were confirmed in transductions and complementation of mutations, verifying that the phenotype is as a result of a lesion in the target gene. An *in vivo* zebrafish infection model showed that the *clpP*, but not *pfo* or *lspA* mutants were attenuated in their ability to kill zebrafish and concomitant with this, demonstrated a profound growth defect *in vivo*. Infection of pu.1 phagocyte deficient zebrafish displayed a significant augmention of pathogenicity of the *clpP*, but not the *purB* mutant, suggesting staphylococcal ClpP is involved in neutrophil responses.

For the *purB* mutant, a deficiency in purine biosynthesis and therefore a failure to properly replicate in a nutrient poor environment (i.e. the intra-neutrophil compartment) is likely to explain the reduction in neutrophil lysis. This was confirmed by the addition of adenine and inosine in chemical complementation experiments. In terms of *pfo*, pyruvate synthesis and oxidation reactions regulated by Pfo comprise a number of intermediate compounds in the TCA cycle, and lack of this metabolic modulator may be a limiting factor for *S. aureus* pathogenesis globally, although further experiments are required to elucidate the mechanism. A defect in phagocytosis of the *lspA* mutant suggests a potential role for lipoproteins in

neutrophil recognition and phagocytosis. Significantly reduced engulfment of the *clpP* mutant indicates that ClpP is required for neutrophil phagocytosis. Necessity of *clpP* for bacterial growth *in vivo* and killing of phagocyte competent zebrafish suggests the importance of *clpP* in bacterial survival and pathogenesis. This is possibly via Clp ATPase regulated post-phagocytosed stress tolerance but perhaps more likely, *clpP* modulated expression of secreted toxins such as α-hemolysin (Feng *et al*., 2013).

6.2 How the findings advance the understanding of neutrophil defence against *S. aureus*

This is the first description for a role for *lspA, clpP, purB* and *pfo* in *S. aureus* induced neutrophil cell lysis. The fully restored virulence of the *purB* mutant by chemical complementation suggests that the attenuated phenotype was due to lack of *de novo* purine synthesis. The *in vivo* infection on the phagocyte depleted zebrafish embryo model displayed similar host survival compared to the phagocyte competent model, which further validated a phagocyte-independent role of PurB.

Pyruvate metabolism has not been previously characterised as a limiting factor for the virulence of any aerobic bacteria. Previous studies revealed that *pfo* is required for parasite proliferation and anaerobic bacterial virulence (Warren *et al*., 2012, Song, 2016). The *pfo* mutant showed robust attenuated neutrophil lysis and enhanced host killing in phagocyte depleted zebrafish embryos. It is possible that the lack of downstream production of the pyruvate pathway inhibits ATP synthesis and therefore limits bacterial survival in the phagosome, due to lack of energy required for stress resistance and neutrophil cell lysis inducer production. In future experiments, time-lapse microscopy could be used to track and characterise neutrophil responses regulated by the *pfo* mutant in future work. Proliferation of

pfo mutants in *S. aureus*-neutrophil co-incubation can also be determined by a DNA staining assay.

Although the importance of staphylococcal lipoproteins in human-pathogen interaction has been reported previously including recognition and activation of neutrophil inflammatory response through TLR2 activation (Kurokawa *et al*., 2009, Bubeck Wardenburg *et al*., 2006), the mechanisms involved in modulation of immune cell lysis is unknown. In this study, the *lspA* mutant led to attenuation of neutrophil cell lysis, and significantly lower phagocytic index compared to JE2 (WT), suggesting lytic factors might be expressed after bacterial phagocytosis. Taken together, my results may promote a hypothetical mechanism of staphylococcal regulated neutrophil responses, where mature lipoprotein induced signals are essential to cause host cell lysis. It could be speculated that this neutrophil response is triggered by membrane receptors including TLR2, which are expressed on the neutrophil surface. Although apoptosis is the most commonly characterised cell death mediated by TLRs (Kaczmarek *et al*., 2013), necroptosis, a form of necrosis, can be induced through TLR3 and TLR4 stimulation in murine macrophages (He *et al*., 2011). Potential TLR2 dependent lipoprotein induced neutrophil cell death can be tested using TLR2 inhibitors with *lspA* and *lgt* mutants.

The pleotropic role of ClpP in protein homeostasis, stress adaption, and virulence factor expression (Truscott *et al*., 2011) means it is challenging to pinpoint exactly which process is key to the induction of neutrophil lysis. Nonetheless, this thesis presents a role for *clpP* in human neutrophil cell lysis for the first time. Based on the findings of this thesis, a three-step process is proposed here as the mechanism of *clpP* modulated neutrophil response. Firstly, *clpP* may be involved in neutrophil uptake of *S. aureus*. Following bacterial uptake, ClpP may be required to facilitate the stress adaption in the phagosomal environment, allowing bacterial survival. Thirdly, *clpP* promotes production of lytic factors which causes neutrophil cell death.

6.3 Implications of these findings for the development of novel therapeutic strategies

The evolution of prevalent and multiple antibiotic resistance genes has significantly limited the effectiveness of antibiotic strategies (Brumfitt and Hamilton-Miller, 1989, Charles *et al*., 2004). In light of this, novel antibacterial or immune activating drugs are urgently needed. The aim of this thesis was to identify mechanisms in which *S. aureus* disables neutrophils in order to develop preventative therapeutic strategies that would repair human immune responses. The results of the screen have likely identified global regulators of *S. aureus* biology and may induce neutrophil cell lysis in indirect ways.

This thesis demonstrated a role for ClpP in both enhancing bacterial virulence in immune cell lysis *in vitro*, and promoting staphylococcal pathogenesis and interaction with neutrophils *in vivo*, making it the target with more therapeutic potential than the other genes. Inhibitors of ClpP could be a promising drug for clinical application to prevent *S. aureus*-induced neutrophil lysis and enhance bacterial elimination. Recently, the natural products acyldepsipeptides (ADEPs) were studied as potent modulators for ClpP protease activity (Brotz-Oesterhelt *et al*., 2005, Socha *et al*., 2010, Ye *et al*., 2016). The interaction of ADEPs with staphylococcal ClpP and ATPase leads to overactivation of ClpP and potent inhibition of bacterial activity (Ye *et al*., 2016). The bactericidal effect of ADEP4 against *S. aureus* has been demonstrated in a mouse model of chronic infection (Conlon *et al*., 2013), indicating a realistic step forward for *in vivo* application.

6.4 Limitations of the approaches in this thesis

Limitations of the NTML screen include a single 1st round of screening, which may have resulted in false negatives and missed 'hits'. False positive strains were eliminated by a more focused and repeated 2nd round of screening. Multiple data analysis methods including viable

cell counts, ToPro-3 fluorescent intensity, and FSC/SSC flow cytometric profiling were combined to thoroughly quantify neutrophil cell death. Key virulence genes of *S. aureus* such *saeS* and *agrA* were identified among the 34 genes identified from NTML, demonstrating that the blindly conducted screen model successfully generated robust results. Also, I did not have the capacity to follow up on all 34 mutants with genetic transduction and complementation verification, prioritising mutants with the greatest and most reliable effects on neutrophil lysis, which may have also result in lost hits.

Another limitation of the zebrafish model is the necessity of culture temperature at 28ºC, at which, the expression of virulence factors might be compromised. Additionally, there are greater genetic variations between zebrafish and humans, which diverged 450 million years ago, compared to murine model at 112 million years ago (Woods *et al*., 2000). However, compared to murine models, it is less expensive and time consuming to maintain zebrafish embryos. Advantages of this models include the fact that the innate immune system of zebrafish embryo is highly similar to the human and the model also allows genetic manipulation of phagocyte development.

Another general limitation is that many *S. aureus* virulence factors are human specific or have host-dependent effects (Spaan *et al*., 2013b), which might explain the lack of attenuated host killing caused by *lspA* and *pfo*. As *S. aureus* is not a natural pathogen of fish (Prajsnar *et al*., 2008) and the virulence factors *S. aureus* use to evade the human immune system may not be relevant in the same way in zebrafish.

6.5 Future work

The robust attenuated neutrophil cell lysis, and significantly reduced phagocytic index result generated by the *lspA* mutant in this thesis suggests it is possible that lipoprotein signalling in neutrophils is necessary for *S. aureus* to induce necrosis. It is therefore important to identify

relevant neutrophil receptors involved in *S. aureus* lipoprotein interactions. Future work will involve investigating potential attenuation in neutrophil cell lysis caused by *S. aureus* with treatment of receptor blocking antibodies. Inhibition of candidate receptors including TLR2 and TLR4 is expected to show reduced bacterial uptake and attenuated JE2 induced neutrophil cell lysis, and therefore validating the necessity of lipoprotein-TLR interaction in phagocytosis and *S. aureus* induced cell lysis.

Apart from its significance in *S. aureus* growth and functionality, it was also reported that *clpP* has an impact in modulating expression of other bacterial virulence factors such as *agrA* and *saeS* which are known to be required for the expression of neutrophil lytic genes (Frees *et al*., 2003, Frees *et al*., 2005a, Frees *et al*., 2005b, Michel *et al*., 2006, Feng *et al*., 2013, Farrand *et al*., 2013). Thus, *clpP* may modulate *S. aureus*-neutrophil interaction through phenotypic functions and possibly via multiple gene products. To further underpin the mechanism of *clpP* induced neutrophil cell lysis, qPCR can be used to interrogate the expression of major virulence genes including PVL and leukocidin. If the level of lytic gene expression is lower in *clpP* mutants compared to WT, indirectly *clpP* regulated neutrophil cell lysis can be characterised. Alternatively, the attenuated phenotype caused by the *clpP* mutant in our study may be due to lack of stress adaptation in the phagosomal environment. To address this hypothesis, fluorescent labelling and time lapse microscopy can be combined to visualise the interaction between *S. aureus* and neutrophils, both *in vitro* and *in vivo*. *S. aureus* stained with pHrodo and Alexa Fluor 647 can be used to infect neutrophils from either human or zebrafish embryos (Ellett *et al*., 2015, Starnes and Huttenlocher, 2012). The *clpP* mutant is expected to be phagocytosed by neutrophils but unable to proliferate or escape due to compromised stress responses.

During data analysis for the phagocytic index assay in chapter 5, it was noticed that the majority of neutrophils that began to display a clear necrotic morphology containing high

numbers of *S. aureus* per cell, indicating large numbers of engulfed bacteria might generate high local concentrations of lytic factors. This suggested that the outcome of infections might depend on the initial contact between the pathogen and neutrophils. Hence, for additional understanding of the pathophysiology *S. aureus* induced neutrophil cell death, it is important to study what is the minimal number of the bacteria needed to lyse the immune cells. A JE2 strain expressing enhanced GFP can be generated by transformation (Ellett *et al*., 2015) and applied to *in vitro* infection of human neutrophils. The neutrophils undergoing cell lysis can be determined by ToPro-3 staining and Attune flow cytometric detection. Gating methodology allows identification of the minimal bacterial number resulting in a ToPro-3 positive neutrophil population.

6.6 Conclusion

S. aureus is a common and successful human pathogen. The evaluation of its multiple virulence mechanisms and resistance to antibiotics brings an urgent challenge of clinical treatment. Neutrophils are the major cellular defence against this organism, yet staphylococcal activities undermine neutrophil immune responses on many levels. In this thesis, a genome-wide library of *S. aureus* mutants was screened for their effects on neutrophil cell death, from which four genes namely *lspA, purB, clpP,* and *pfo* were identified as novel key virulence genes for bacterial regulation of neutrophil immunity. The findings not only reveal novel knowledge of the mechanisms underpinning the host-pathogen interaction between *S. aureus* and human neutrophils, but also provide potential targets for therapeutic development in the future.

References:

ABECK and MEMPEL (1998) *Staphylococcus aureus* colonization in atopic dermatitis and its therapeutic implications.

ALAM, M. T., *et al*. (2014) Dissecting vancomycin-intermediate resistance in *Staphylococcus aureus* using genome-wide association. *Genome Biol Evol,* **6** (5), 1174-85.

ALY, R., *et al*. (1980) Role of teichoic acid in the binding of *Staphylococcus aureus* to nasal epithelial cells. *J Infect Dis,* **141** (4), 463-5.

AMER, A. O. and SWANSON, M. S. (2002) A phagosome of one's own: a microbial guide to life in the macrophage. *Curr Opin Microbiol,* **5** (1), 56-61.

AMULIC, B., *et al*. (2012) Neutrophil function: from mechanisms to disease. *Annu Rev Immunol,* **30**, 459-89.

ANWAR, S., *et al*. (2009) The rise and rise of *Staphylococcus aureus*: laughing in the face of granulocytes. *Clinical and experimental immunology,* **157** (2), 216.

ARIZA, J., *et al*. (1999) Vancomycin in surgical infections due to methicillin-resistant *Staphylococcus aureus* with heterogeneous resistance to vancomycin. In) *Lancet.* Vol. 353. England: pp. 1587-8.

ASLAM, R., *et al*. (2013) Activation of Neutrophils by the Two- Component Leukotoxin LukE/ D from *Staphylococcus aureus*: Proteomic Analysis of the Secretions. *J. Proteome Res.,* **12** (8), 3667-3678.

BABIOR, B. M. (1999) NADPH oxidase: an update. *Blood,* **93** (5), 1464-76.

BAE, T., *et al*. (2008) Generating a collection of insertion mutations in the *Staphylococcus aureus* genome using bursa aurealis. *Methods Mol Biol,* **416**, 103-16.

BAEK, K. T., *et al*. (2014) beta-Lactam resistance in methicillin-resistant *Staphylococcus aureus* USA300 is increased by inactivation of the ClpXP protease. *Antimicrob Agents Chemother,* **58** (8), 4593-603.

BAGGETT, H. C., *et al*. (2003) An outbreak of community-onset methicillin-resistant *Staphylococcus aureus* skin infections in southwestern Alaska. *Infect Control Hosp Epidemiol,* **24** (6), 397-402.

BAGGIOLINI, M. (1984) Phagocytes use oxygen to kill bacteria. *Experientia,* **40** (9), 906-9.

BAINTON, D. F. (1993) Neutrophilic leukocyte granules: from structure to function. *Adv Exp Med Biol,* **336**, 17-33.

BALASUBRAMANIAN, D., *et al*. (2016) *Staphylococcus aureus* Coordinates Leukocidin Expression and Pathogenesis by Sensing Metabolic Fluxes via RpiRc. *MBio,* **7** (3).

BALLARD, T. E., *et al*. (2010) Biological activity of modified and exchanged 2-amino-5-nitrothiazole amide analogues of nitazoxanide. *Bioorg Med Chem Lett,* **20** (12), 3537-9.

BANG, R. L., *et al*. (2002) Septicaemia after burn injury: a comparative study. *Burns,* **28** (8), 746-751.

BARDOEL, B. W. and STRIJP, J. A. (2011) Molecular battle between host and bacterium: recognition in innate immunity. *J Mol Recognit,* **24** (6), 1077-86.

BARDOEL, B. W., *et al*. (2012) Evasion of Toll-like receptor 2 activation by staphylococcal superantigen-like protein 3. *J Mol Med (Berl),* **90** (10), 1109-20.

BARTLETT, A. H., *et al*. (2008) Alpha-toxin facilitates the generation of CXC chemokine gradients and stimulates neutrophil homing in *Staphylococcus aureus* pneumonia. *J Infect Dis,* **198** (10), 1529-35.

BAXTER-GABBARD, K. L. and PATTEE, P. A. (1970) Purine biosynthesis in *Staphylococcus aureus*. *Arch Mikrobiol,* **71** (1), 40-8.

BEASLEY, F. C., *et al*. (2011) *Staphylococcus aureus* transporters Hts, Sir, and Sst capture iron liberated from human transferrin by Staphyloferrin A, Staphyloferrin B, and catecholamine stress hormones, respectively, and contribute to virulence. *Infect Immun,* **79** (6), 2345-55.

BENJAMINI, E. (1988) *Immunology: a short course.* New York: Liss.

BENSON, M. A., *et al*. (2012) Rot and SaeRS cooperate to activate expression of the staphylococcal superantigen-like exoproteins. *J Bacteriol,* **194** (16), 4355-65.

BENTON, B. M., *et al*. (2004) Large-scale identification of genes required for full virulence of *Staphylococcus aureus*. *J Bacteriol,* **186** (24), 8478-89.
BERA, A., *et al*. (2005) Why are pathogenic staphylococci so lysozyme resistant? The peptidoglycan O-acetyltransferase OatA is the major determinant for lysozyme resistance of *Staphylococcus aureus*. *Mol Microbiol,* **55** (3), 778-87.
BERENDS, E. T., *et al*. (2010) Nuclease expression by *Staphylococcus aureus* facilitates escape from neutrophil extracellular traps. *J Innate Immun,* **2** (6), 576-86.
BERUBE, B. J. and BUBECK WARDENBURG, J. (2013) *Staphylococcus aureus* alpha-toxin: nearly a century of intrigue. *Toxins (Basel),* **5** (6), 1140-66.
BESTEBROER, J., *et al*. (2010a) Functional basis for complement evasion by staphylococcal superantigen- like 7. *Cell Microbiol.,* **12** (10), 1506-1516.
BESTEBROER, J., *et al*. (2010b) How microorganisms avoid phagocyte attraction. *FEMS Microbiol Rev,* **34** (3), 395-414.
BESTEBROER, J., *et al*. (2007) Staphylococcal superantigen- like 5 binds PSGL- 1 and inhibits P-selectin- mediated neutrophil rolling. *Blood,* **109** (7), 2936-2943.
BHAKDI, S. and TRANUM-JENSEN, J. (1991) Alpha-toxin of *Staphylococcus aureus*. *Microbiol Rev,* **55** (4), 733-51.
BHATTA, D. R., *et al*. (2016) Association of Panton Valentine Leukocidin (PVL) genes with methicillin resistant *Staphylococcus aureus* (MRSA) in Western Nepal: a matter of concern for community infections (a hospital based prospective study). *BMC Infect Dis,* **16**, 199.
BILL, B. R., *et al*. (2009) A primer for morpholino use in zebrafish. *Zebrafish,* **6** (1), 69-77.
BISWAS, L., *et al*. (2009) Role of the twin-arginine translocation pathway in Staphylococcus. *J Bacteriol,* **191** (19), 5921-9.
BOGOMOLSKI-YAHALOM, V. and MATZNER, Y. (1995) Disorders of neutrophil function. *Blood Rev,* **9** (3), 183-90.
BOLES, B. R. and HORSWILL, A. R. (2008) Agr-mediated dispersal of *Staphylococcus aureus* biofilms. *PLoS Pathog,* **4** (4), e1000052.
BORREGAARD, N. and COWLAND, J. B. (1997) Granules of the human neutrophilic polymorphonuclear leukocyte. *Blood,* **89** (10), 3503-21.
BORREGAARD, N., *et al*. (2007) Neutrophil granules: a library of innate immunity proteins. *Trends Immunol,* **28** (8), 340-5.
BOTS, M. and MEDEMA, J. P. (2006) Granzymes at a glance. *J Cell Sci,* **119** (Pt 24), 5011-4.
BOTTCHER, T. and SIEBER, S. A. (2008) Beta-lactones as specific inhibitors of ClpP attenuate the production of extracellular virulence factors of *Staphylococcus aureus*. *J Am Chem Soc,* **130** (44), 14400-1.
BOTTOMLEY, A. L., *et al*. (2014) *Staphylococcus aureus* DivIB is a peptidoglycan-binding protein that is required for a morphological checkpoint in cell division. *Mol Microbiol*.
BRATTON, D. L. and HENSON, P. M. (2011) Neutrophil clearance: when the party is over, clean-up begins. *Trends Immunol,* **32** (8), 350-7.
BRINKMANN, V., *et al*. (2004) Neutrophil extracellular traps kill bacteria. *Science,* **303** (5663), 1532-5.
BRITTAN, M., *et al*. (2012) A novel subpopulation of monocyte-like cells in the human lung after lipopolysaccharide inhalation. *Eur Respir J,* **40** (1), 206-14.
BRONNER, S., *et al*. (2004) Regulation of virulence determinants in *Staphylococcus aureus*: complexity and applications. *FEMS Microbiol Rev,* **28** (2), 183-200.
BROTZ-OESTERHELT, H., *et al*. (2005) Dysregulation of bacterial proteolytic machinery by a new class of antibiotics. *Nat Med,* **11** (10), 1082-7.
BROWN, E. L., *et al*. (2015) Genome-Wide Association Study of *Staphylococcus aureus* Carriage in a Community-Based Sample of Mexican-Americans in Starr County, Texas. *PLoS One,* **10** (11), e0142130.
BROWN, G. E., *et al*. (2004) Distinct ligand-dependent roles for p38 MAPK in priming and activation of the neutrophil NADPH oxidase. *J Biol Chem,* **279** (26), 27059-68.
BRUMFITT, W. and HAMILTON-MILLER, J. (1989) Methicillin-resistant *Staphylococcus aureus*. *N Engl J Med,* **320** (18), 1188-96.

BUBECK WARDENBURG, J., *et al*. (2008) Panton-Valentine leukocidin is not a virulence determinant in murine models of community-associated methicillin-resistant *Staphylococcus aureus* disease. *J Infect Dis,* **198** (8), 1166-70.
BUBECK WARDENBURG, J., *et al*. (2006) Host defenses against *Staphylococcus aureus* infection require recognition of bacterial lipoproteins. *Proc Natl Acad Sci U S A,* **103** (37), 13831-6.
BURDA, W. N., *et al*. (2014) Investigating the genetic regulation of the ECF sigma factor sigmaS in *Staphylococcus aureus*. *BMC Microbiol,* **14**, 280.
BUTALA, M., *et al*. (2009) The bacterial LexA transcriptional repressor. *Cell Mol Life Sci,* **66** (1), 82-93.
CAO, J., *et al*. (2013) Pneumococcal ClpP modulates the maturation and activation of human dendritic cells: implications for pneumococcal infections. *J Leukoc Biol,* **93** (5), 737-49.
CARRENO PEREZ, L. (1999) Septic arthritis. *Baillieres Best Pract Res Clin Rheumatol,* **13** (1), 37-58.
CASADEVALL, A. and PIROFSKI, L. A. (1999) Host-pathogen interactions: redefining the basic concepts of virulence and pathogenicity. *Infect Immun,* **67** (8), 3703-13.
CASEWELL, M. W. and HILL, R. L. (1986) The carrier state: methicillin-resistant *Staphylococcus aureus*. *J Antimicrob Chemother,* **18 Suppl A**, 1-12.
CHAMBERS, H. F. and DELEO, F. R. (2009) Waves of resistance: *Staphylococcus aureus* in the antibiotic era. *Nat Rev Microbiol,* **7** (9), 629-41.
CHARLES, P. G., *et al*. (2004) Clinical features associated with bacteremia due to heterogeneous vancomycin-intermediate *Staphylococcus aureus*. *Clin Infect Dis,* **38** (3), 448-51.
CHAVAKIS, T., *et al*. (2002) *Staphylococcus aureus* extracellular adherence protein serves as anti-inflammatory factor by inhibiting the recruitment of host leukocytes. *Nat Med,* **8** (7), 687-93.
CHEUNG, A. L., *et al*. (2004) Regulation of virulence determinants in vitro and in vivo in *Staphylococcus aureus*. *FEMS Immunol Med Microbiol,* **40** (1), 1-9.
CHEUNG, G. Y., *et al*. (2011) Role of the accessory gene regulator agr in community-associated methicillin-resistant *Staphylococcus aureus* pathogenesis. *Infect Immun,* **79** (5), 1927-35.
CHOI, K. H. and KIM, K. J. (2009) Applications of transposon-based gene delivery system in bacteria. *J Microbiol Biotechnol,* **19** (3), 217-28.
CHRISTIANSEN, M. T., *et al*. (2014) Genome-wide high-throughput screening to investigate essential genes involved in methicillin-resistant *Staphylococcus aureus* Sequence Type 398 survival. *PLoS One,* **9** (2), e89018.
CHUA, T., *et al*. (2008) Molecular epidemiology of methicillin-resistant *Staphylococcus aureus* bloodstream isolates in urban Detroit. *J Clin Microbiol,* **46** (7), 2345-52.
CHUANG, Y.-Y. and HUANG, Y.-C. (2013) Molecular epidemiology of community-associated meticillin-resistant *Staphylococcus aureus* in Asia. *The Lancet Infectious Diseases,* **13** (8), 698-708.
CLARKE, S. R. and FOSTER, S. J. (2006) Surface adhesins of *Staphylococcus aureus*. *Adv Microb Physiol,* **51**, 187-224.
CLUZEL, M. E., *et al*. (2010) The *Staphylococcus aureus* autoinducer-2 synthase LuxS is regulated by Ser/Thr phosphorylation. *J Bacteriol,* **192** (23), 6295-301.
COHN, M. T., *et al*. (2011) Clp-dependent proteolysis of the LexA N-terminal domain in *Staphylococcus aureus*. *Microbiology,* **157** (Pt 3), 677-84.
CONLON, B. P., *et al*. (2013) Activated ClpP kills persisters and eradicates a chronic biofilm infection. *Nature,* **503** (7476), 365-70.
CRONSTEIN, B. N., *et al*. (1990) The adenosine/neutrophil paradox resolved: human neutrophils possess both A1 and A2 receptors that promote chemotaxis and inhibit O2 generation, respectively. *J Clin Invest,* **85** (4), 1150-7.
CROWHURST, M. O., *et al*. (2002) Developmental biology of zebrafish myeloid cells. *Int J Dev Biol,* **46** (4), 483-92.
CUNNINGHAM, R., *et al*. (1996) Clinical and molecular aspects of the pathogenesis of *Staphylococcus aureus* bone and joint infections. *Journal of medical microbiology,* **44** (3), 157.
DALE, D. C., *et al*. (1998) Effects of granulocyte-macrophage colony-stimulating factor (GM-CSF) on neutrophil kinetics and function in normal human volunteers. *Am J Hematol,* **57** (1), 7-15.

DANG, P. M., *et al*. (1999) Priming of human neutrophil respiratory burst by granulocyte/macrophage colony-stimulating factor (GM-CSF) involves partial phosphorylation of p47(phox). *J Biol Chem,* **274** (29), 20704-8.

DAS, S., *et al*. (2016) Natural mutations in a *Staphylococcus aureus* virulence regulator attenuate cytotoxicity but permit bacteremia and abscess formation. *Proc Natl Acad Sci U S A,* **113** (22), E3101-10.

DAUM, R. S., *et al*. (2002) A novel methicillin-resistance cassette in community-acquired methicillin-resistant *Staphylococcus aureus* isolates of diverse genetic backgrounds. *J Infect Dis,* **186** (9), 1344-7.

DAVID, M. Z. and DAUM, R. S. (2010) Community-associated methicillin-resistant *Staphylococcus aureus*: epidemiology and clinical consequences of an emerging epidemic. *Clin Microbiol Rev,* **23** (3), 616-87.

DE JONG, N. W. M., *et al*. (2017) Immune evasion by a staphylococcal inhibitor of myeloperoxidase. *Proc Natl Acad Sci U S A,* **114** (35), 9439-9444.

DELEO, F. R., *et al*. (2009) Host Defense and Pathogenesis in *Staphylococcus aureus* Infections. *Infect. Dis. Clin. North Am.,* **23** (1), 17-+.

DELEO, F. R., *et al*. (1998) Neutrophils exposed to bacterial lipopolysaccharide upregulate NADPH oxidase assembly. *J Clin Invest,* **101** (2), 455-63.

DESAI, J., *et al*. (2016) PMA and crystal-induced neutrophil extracellular trap formation involves RIPK1-RIPK3-MLKL signaling. *Eur J Immunol,* **46** (1), 223-9.

DHANOA, A., *et al*. (2012) Acute haematogenous community-acquired methicillin-resistant *Staphylococcus aureus* osteomyelitis in an adult: case report and review of literature. *BMC Infect Dis,* **12**, 270.

DIEKEMA, D. J., *et al*. (2001) Survey of infections due to Staphylococcus species: frequency of occurrence and antimicrobial susceptibility of isolates collected in the United States, Canada, Latin America, Europe, and the Western Pacific region for the SENTRY Antimicrobial Surveillance Program, 1997-1999. *Clin Infect Dis,* **32 Suppl 2**, S114-32.

DIEP, B. A., *et al*. (2010) Polymorphonuclear leukocytes mediate *Staphylococcus aureus* Panton-Valentine leukocidin-induced lung inflammation and injury. *Proc Natl Acad Sci U S A,* **107** (12), 5587-92.

DOHERTY, N., *et al*. (2006) Functional analysis of luxS in *Staphylococcus aureus* reveals a role in metabolism but not quorum sensing. *J Bacteriol,* **188** (8), 2885-97.

DOWNEY, G. P., *et al*. (1990) Retention of leukocytes in capillaries: role of cell size and deformability. *J Appl Physiol (1985),* **69** (5), 1767-78.

DUBREUIL, L., *et al*. (1996) In vitro evaluation of activities of nitazoxanide and tizoxanide against anaerobes and aerobic organisms. *Antimicrob Agents Chemother,* **40** (10), 2266-70.

DUMONT, A. L., *et al*. (2013) *Staphylococcus aureus* LukAB cytotoxin kills human neutrophils by targeting the CD11b subunit of the integrin Mac-1. *Proc Natl Acad Sci U S A,* **110** (26), 10794-9.

DURAN, N., *et al*. (2012) Antibiotic resistance genes & susceptibility patterns in staphylococci. *Indian J Med Res,* **135**, 389-96.

EASMON, C. S., *et al*. (1978) Use of lysostaphin to remove cell-adherent staphylococci during in vitro assays of phagocyte function. *British journal of experimental pathology,* **59** (4), 381-385.

EDWARDS, S. (2005) *Biochemistry and physiology of the neutrophil.* Cambridge University Press.

ELLETT, F., *et al*. (2015) Defining the phenotype of neutrophils following reverse migration in zebrafish. *J Leukoc Biol,* **98** (6), 975-81.

ELLIS, T. N. and BEAMAN, B. L. (2004) Interferon-gamma activation of polymorphonuclear neutrophil function. *Immunology,* **112** (1), 2-12.

ENGMAN, J., *et al*. (2012) The YjbH adaptor protein enhances proteolysis of the transcriptional regulator Spx in *Staphylococcus aureus*. *J Bacteriol,* **194** (5), 1186-94.

ERNST, C. M. and PESCHEL, A. (2011) Broad-spectrum antimicrobial peptide resistance by MprF-mediated aminoacylation and flipping of phospholipids. *Mol Microbiol,* **80** (2), 290-9.

ESTIVARIZ, C. F., *et al*. (2007) Emergence of community-associated methicillin resistant *Staphylococcus aureus* in Hawaii, 2001-2003. *J Infect,* **54** (4), 349-57.

FANG, F. C. (2004) Antimicrobial reactive oxygen and nitrogen species: concepts and controversies. *Nat Rev Microbiol,* **2** (10), 820-32.
FARRAND, A. J., *et al*. (2013) Regulation of host hemoglobin binding by the *Staphylococcus aureus* Clp proteolytic system. *J Bacteriol,* **195** (22), 5041-50.
FENG, J., *et al*. (2013) Trapping and proteomic identification of cellular substrates of the ClpP protease in *Staphylococcus aureus*. *J Proteome Res,* **12** (2), 547-58.
FEY, P. D., *et al*. (2013) A genetic resource for rapid and comprehensive phenotype screening of nonessential *Staphylococcus aureus* genes. *MBio,* **4** (1), e00537-12.
FINEGOLD, S. M., *et al*. (2009) Study of the in vitro activities of rifaximin and comparator agents against 536 anaerobic intestinal bacteria from the perspective of potential utility in pathology involving bowel flora. *Antimicrob Agents Chemother,* **53** (1), 281-6.
FINK, S. L. and COOKSON, B. T. (2005) Apoptosis, pyroptosis, and necrosis: mechanistic description of dead and dying eukaryotic cells. *Infect Immun,* **73** (4), 1907-16.
FLANNAGAN, R. S., *et al*. (2015) Antimicrobial Mechanisms of Macrophages and the Immune Evasion Strategies of *Staphylococcus aureus*. *Pathogens,* **4** (4), 826-68.
FLANNAGAN, R. S., *et al*. (2016) Intracellular replication of *Staphylococcus aureus* in mature phagolysosomes in macrophages precedes host cell death, and bacterial escape and dissemination. *Cell Microbiol,* **18** (4), 514-35.
FORSGREN, A. and NORDSTROM, K. (1974) Protein A from *Staphylococcus aureus*: the biological significance of its reaction with IgG. *Ann N Y Acad Sci,* **236** (0), 252-66.
FOSTER, T. J. (2005) Immune evasion by staphylococci. *Nat Rev Microbiol,* **3** (12), 948-58.
FRANCIS, J. S., *et al*. (2005) Severe community-onset pneumonia in healthy adults caused by methicillin-resistant *Staphylococcus aureus* carrying the Panton-Valentine leukocidin genes. *Clin Infect Dis,* **40** (1), 100-7.
FREES, D., *et al*. (2012) New insights into *Staphylococcus aureus* stress tolerance and virulence regulation from an analysis of the role of the ClpP protease in the strains Newman, COL, and SA564. *J Proteome Res,* **11** (1), 95-108.
FREES, D., *et al*. (2004) Clp ATPases are required for stress tolerance, intracellular replication and biofilm formation in *Staphylococcus aureus*. *Mol Microbiol,* **54** (5), 1445-62.
FREES, D., *et al*. (2014) Clp chaperones and proteases are central in stress survival, virulence and antibiotic resistance of *Staphylococcus aureus*. *Int J Med Microbiol,* **304** (2), 142-9.
FREES, D., *et al*. (2003) Alternative roles of ClpX and ClpP in *Staphylococcus aureus* stress tolerance and virulence. *Mol Microbiol,* **48** (6), 1565-78.
FREES, D., *et al*. (2007) Clp ATPases and ClpP proteolytic complexes regulate vital biological processes in low GC, Gram-positive bacteria. *Mol Microbiol,* **63** (5), 1285-95.
FREES, D., *et al*. (2005a) Global virulence regulation in *Staphylococcus aureus*: pinpointing the roles of ClpP and ClpX in the sar/agr regulatory network. *Infect Immun,* **73** (12), 8100-8.
FREES, D., *et al*. (2005b) *Staphylococcus aureus* ClpYQ plays a minor role in stress survival. *Arch Microbiol,* **183** (4), 286-91.
FRYDENLUND MICHELSEN, C., *et al*. (2016) Evolution of metabolic divergence in Pseudomonas aeruginosa during long-term infection facilitates a proto-cooperative interspecies interaction. *Isme j,* **10** (6), 1323-36.
FUCHS, T. A., *et al*. (2007) Novel cell death program leads to neutrophil extracellular traps. *J Cell Biol,* **176** (2), 231-41.
FURDUI, C. and RAGSDALE, S. W. (2000) The role of pyruvate ferredoxin oxidoreductase in pyruvate synthesis during autotrophic growth by the Wood-Ljungdahl pathway. *J Biol Chem,* **275** (37), 28494-9.
FURZE, R. C. and RANKIN, S. M. (2008) Neutrophil mobilization and clearance in the bone marrow. *Immunology,* **125** (3), 281-8.
FYFE, P. K., *et al*. (2010) Structure of *Staphylococcus aureus* adenylo-succinate lyase (PurB) and assessment of its potential as a target for structure-based inhibitor discovery. *Acta Crystallographica Section D: Biological Crystallography,* **66** (Pt 8), 881-888.
GAILLOT, O., *et al*. (2000) The ClpP serine protease is essential for the intracellular parasitism and virulence of Listeria monocytogenes. *Mol Microbiol,* **35** (6), 1286-94.

GAL-MOR, O. and FINLAY, B. B. (2006) Pathogenicity islands: a molecular toolbox for bacterial virulence. *Cell Microbiol,* **8** (11), 1707-19.
GARG, S. K., *et al*. (2009) The YjbH protein of Bacillus subtilis enhances ClpXP-catalyzed proteolysis of Spx. *J Bacteriol,* **191** (4), 1268-77.
GAUPP, R., *et al*. (2012) Staphylococcal response to oxidative stress. *Front Cell Infect Microbiol,* **2**, 33.
GEIGER, T., *et al*. (2008) The virulence regulator Sae of *Staphylococcus aureus*: promoter activities and response to phagocytosis-related signals. *J Bacteriol,* **190** (10), 3419-28.
GEN (2017) Phage Therapy Saves Patient from Drug-Resistant Microbes.) *Genetic Engineering and Biotechnology News.* http://www.genengnews.com/gen-news-highlights/phage-therapy-saves-patient-from-drug-resistant-microbes/81254258.
GIRAUDO, A. T., *et al*. (1994) Characterization of a Tn551-mutant of *Staphylococcus aureus* defective in the production of several exoproteins. *Can J Microbiol,* **40** (8), 677-81.
GLOVER, J. R. and LINDQUIST, S. (1998) Hsp104, Hsp70, and Hsp40: a novel chaperone system that rescues previously aggregated proteins. *Cell,* **94** (1), 73-82.
GOLDBLATT, D. and THRASHER, A. J. (2000) Chronic granulomatous disease. *Clin Exp Immunol,* **122** (1), 1-9.
GOLDENBERG, D. L. (1998) Septic arthritis. *Lancet,* **351** (9097), 197-202.
GONZALEZ-BARCA, E., *et al*. (2001) Predisposing factors and outcome of *Staphylococcus aureus* bacteremia in neutropenic patients with cancer. *Eur J Clin Microbiol Infect Dis,* **20** (2), 117-9.
GOOSENS, V. J., *et al*. (2014) The Tat system of Gram-positive bacteria. *Biochim Biophys Acta,* **1843** (8), 1698-706.
GORDON, R. J. and LOWY, F. D. (2008) Pathogenesis of methicillin-resistant *Staphylococcus aureus* infection. *Clin Infect Dis,* **46 Suppl 5**, S350-9.
GOTTLIEB, D. and SHAW, P. D. (2013) Antibiotics: Volume I Mechanism of Action. In) Springer.
GREENLEE-WACKER, M., *et al*. (2015) How methicillin-resistant *Staphylococcus aureus* evade neutrophil killing. *Curr Opin Hematol,* **22** (1), 30-5.
GRESHAM, H. D., *et al*. (2000) Survival of *Staphylococcus aureus* inside neutrophils contributes to infection. *J Immunol,* **164** (7), 3713-22.
GROSZ, M., *et al*. (2014) Cytoplasmic replication of *Staphylococcus aureus* upon phagosomal escape triggered by phenol-soluble modulin alpha. *Cell Microbiol,* **16** (4), 451-65.
GUERRA, F. E., *et al*. (2017) Epic Immune Battles of History: Neutrophils vs. *Staphylococcus aureus*. *Front Cell Infect Microbiol,* **7**, 286.
GUICHARD, C., *et al*. (2005) Interleukin-8-induced priming of neutrophil oxidative burst requires sequential recruitment of NADPH oxidase components into lipid rafts. *J Biol Chem,* **280** (44), 37021-32.
HAAS, A. (2007) The phagosome: compartment with a license to kill. *Traffic,* **8** (4), 311-30.
HAMASAKI, A., *et al*. (1998) Accelerated neutrophil apoptosis in mice lacking A1-a, a subtype of the bcl-2-related A1 gene. *J Exp Med,* **188** (11), 1985-92.
HAMER, L., *et al*. (2001) Recent advances in large-scale transposon mutagenesis. *Curr Opin Chem Biol,* **5** (1), 67-73.
HAMPTON, M. B., *et al*. (1998) Inside the neutrophil phagosome: oxidants, myeloperoxidase, and bacterial killing. *Blood,* **92** (9), 3007-17.
HART, S. P., *et al*. (2000) Molecular characterization of the surface of apoptotic neutrophils: implications for functional downregulation and recognition by phagocytes. *Cell Death Differ,* **7** (5), 493-503.
HARVIE, E. A. and HUTTENLOCHER, A. (2015) Neutrophils in host defense: new insights from zebrafish. *J Leukoc Biol,* **98** (4), 523-37.
HAYES, F. (2003) Transposon-based strategies for microbial functional genomics and proteomics. *Annu Rev Genet,* **37**, 3-29.
HE, S., *et al*. (2011) Toll-like receptors activate programmed necrosis in macrophages through a receptor-interacting kinase-3-mediated pathway. *Proc Natl Acad Sci U S A,* **108** (50), 20054-9.
HEINEMANN, M., *et al*. (2005) In silico genome-scale reconstruction and validation of the *Staphylococcus aureus* metabolic network. *Biotechnol Bioeng,* **92** (7), 850-64.

HENRY, K. M., *et al*. (2013) Zebrafish as a model for the study of neutrophil biology. *J Leukoc Biol,* **94** (4), 633-42.
HERBERMAN, R. B. (1986) Natural killer cells. *Annu Rev Med,* **37**, 347-52.
HERBERT, S., *et al*. (2007) Molecular basis of resistance to muramidase and cationic antimicrobial peptide activity of lysozyme in staphylococci. *PLoS Pathog.,* **3** (7), 981-994.
HILL, P. C., *et al*. (2001) Prospective study of 424 cases of *Staphylococcus aureus* bacteraemia: determination of factors affecting incidence and mortality. *Intern Med J,* **31** (2), 97-103.
HIRSCH, T., *et al*. (1997) The apoptosis-necrosis paradox. Apoptogenic proteases activated after mitochondrial permeability transition determine the mode of cell death. *Oncogene,* **15** (13), 1573-81.
HOFFMAN, P. S., *et al*. (2007) Antiparasitic drug nitazoxanide inhibits the pyruvate oxidoreductases of Helicobacter pylori, selected anaerobic bacteria and parasites, and Campylobacter jejuni. *Antimicrob Agents Chemother,* **51** (3), 868-76.
HOGAN, S. P., *et al*. (2013) Eosinophils in infection and intestinal immunity. *Curr Opin Gastroenterol,* **29** (1), 7-14.
HORNER, D. S., *et al*. (1999) A single eubacterial origin of eukaryotic pyruvate: ferredoxin oxidoreductase genes: implications for the evolution of anaerobic eukaryotes. *Mol Biol Evol,* **16** (9), 1280-91.
HOWDEN, B. P., *et al*. (2010) Reduced vancomycin susceptibility in *Staphylococcus aureus*, including vancomycin-intermediate and heterogeneous vancomycin-intermediate strains: resistance mechanisms, laboratory detection, and clinical implications. *Clin Microbiol Rev,* **23** (1), 99-139.
HOWDEN, B. P., *et al*. (2006) Isolates with low-level vancomycin resistance associated with persistent methicillin-resistant *Staphylococcus aureus* bacteremia. *Antimicrob Agents Chemother,* **50** (9), 3039-47.
HUSSAIN, M., *et al*. (1982) Mechanism of signal peptide cleavage in the biosynthesis of the major lipoprotein of the Escherichia coli outer membrane. *J Biol Chem,* **257** (9), 5177-82.
IADONATO, S. P. and KATZE, M. G. (2009) Genomics: Hepatitis C virus gets personal. In) *Nature.* Vol. 461. England: pp. 357-8.
IBA, T., *et al*. (2013) Neutrophil cell death in response to infection and its relation to coagulation. *J Intensive Care,* **1** (1), 13.
ISOGAI, S., *et al*. (2001) The vascular anatomy of the developing zebrafish: an atlas of embryonic and early larval development. *Dev Biol,* **230** (2), 278-301.
ITOH, S., *et al*. (2010) Staphylococcal superantigen- like protein 10 (SSL10) binds to human immunoglobulin G (IgG) and inhibits complement activation via the classical pathway. *Mol. Immunol.,* **47** (4), 932-938.
IYER, S. S., *et al*. (2009) Necrotic cells trigger a sterile inflammatory response through the Nlrp3 inflammasome. *Proc Natl Acad Sci U S A,* **106** (48), 20388-93.
JABLONSKA, J. (2014) To NET or not to NET.), American Journal of Immunology.
JEVONS, M. P. (1961) "Celbenin"-resistance staphylococci. *BMJ,* **1**, 124.
JOHANNESSEN, M., *et al*. (2012) Host- and microbe determinants that may influence the success of S. aureus colonization. *Front Cell Infect Microbiol,* **2**, 56.
JOHN CLANCY JR. (1998) *Basic concepts in immunology : a student's survival guide.* New York ; London: New York ; London : McGraw-Hill, Health Professions Division, c1998.
JOHNSTON, P. R., *et al*. (2016) Genomic Signatures of Experimental Adaptation to Antimicrobial Peptides in *Staphylococcus aureus*. *G3 (Bethesda),* **6** (6), 1535-9.
JONGERIUS, I., *et al*. (2010a) Convertase Inhibitory Properties of Staphylococcal Extracellular Complement- binding Protein. *J. Biol. Chem.,* **285** (20), 14973-14979.
JONGERIUS, I., *et al*. (2010b) Staphylococcal complement inhibitor modulates phagocyte responses by dimerization of convertases. *J Immunol,* **184** (1), 420-5.
JONGERIUS, I., *et al*. (2012) *Staphylococcus aureus* Virulence Is Enhanced by Secreted Factors That Block Innate Immune Defenses. *J. Innate Immun.,* **4** (3), 301-311.
JOSEFSSON, E., *et al*. (2001) Protection against experimental *Staphylococcus aureus* arthritis by vaccination with clumping factor A, a novel virulence determinant. *J Infect Dis,* **184** (12), 1572-80.

KACZMAREK, A., *et al*. (2013) Necroptosis: the release of damage-associated molecular patterns and its physiological relevance. *Immunity,* **38** (2), 209-23.
KENNEDY, A. D. and DELEO, F. R. (2009) Neutrophil apoptosis and the resolution of infection. *Immunol Res,* **43** (1-3), 25-61.
KIM, J. and GIBSON, G. (2010) Insights from GWAS into the quantitative genetics of transcription in humans. *Genet Res (Camb),* **92** (5-6), 361-9.
KIM, M. N., *et al*. (2000) Vancomycin-intermediate *Staphylococcus aureus* in Korea. *J Clin Microbiol,* **38** (10), 3879-81.
KIM, N. J., *et al*. (2015) Lipoprotein in the cell wall of *Staphylococcus aureus* is a major inducer of nitric oxide production in murine macrophages. *Mol Immunol,* **65** (1), 17-24.
KING, M. D., *et al*. (2006) Emergence of community-acquired methicillin-resistant *Staphylococcus aureus* USA 300 clone as the predominant cause of skin and soft-tissue infections. *Ann Intern Med,* **144** (5), 309-17.
KIRSTEIN, J., *et al*. (2009) Adapting the machine: adaptor proteins for Hsp100/Clp and AAA+ proteases. *Nat Rev Microbiol,* **7** (8), 589-99.
KITAZUMI, I. and TSUKAHARA, M. (2011) Regulation of DNA fragmentation: the role of caspases and phosphorylation. *Febs j,* **278** (3), 427-41.
KJELDSEN, L., *et al*. (1994) Isolation and characterization of gelatinase granules from human neutrophils. *Blood,* **83** (6), 1640-9.
KLEBANOFF, S. J. (2005) Myeloperoxidase: friend and foe. *Journal of leukocyte biology,* **77** (5), 598.
KLEIN, E., *et al*. (2007) Hospitalizations and deaths caused by methicillin-resistant *Staphylococcus aureus*, United States, 1999-2005. *Emerg Infect Dis,* **13** (12), 1840-6.
KLEMSZ, M. J., *et al*. (1990) The macrophage and B cell-specific transcription factor PU.1 is related to the ets oncogene. *Cell,* **61** (1), 113-24.
KLIONSKY, D. J. (2004) Cell biology: regulated self-cannibalism. In) *Nature.* Vol. 431. England: pp. 31-2.
KLOOS and BANNERMAN (1999) *Manual of Clinical Microbiology*. (Staphylococcus and Micrococcus) ASM Press.
KLUYTMANS, J., *et al*. (1997) Nasal carriage of *Staphylococcus aureus*: epidemiology, underlying mechanisms, and associated risks. *Clin Microbiol Rev,* **10** (3), 505-20.
KOBAYASHI, S. D., *et al*. (2010) Rapid neutrophil destruction following phagocytosis of *Staphylococcus aureus*. *J Innate Immun,* **2** (6), 560-75.
KOBAYASHI, S. D. and DELEO, F. R. (2009) An update on community-associated MRSA virulence. *Curr Opin Pharmacol,* **9** (5), 545-51.
KOBAYASHI, S. D., *et al*. (2015) Pathogenesis of *Staphylococcus aureus* abscesses. *Am J Pathol,* **185** (6), 1518-27.
KOBAYASHI, S. D., *et al*. (2011) Comparative analysis of USA300 virulence determinants in a rabbit model of skin and soft tissue infection. *J Infect Dis,* **204** (6), 937-41.
KOBAYASHI, S. D., *et al*. (2002) Global changes in gene expression by human polymorphonuclear leukocytes during receptor-mediated phagocytosis: cell fate is regulated at the level of gene expression. *Proc Natl Acad Sci U S A,* **99** (10), 6901-6.
KRETSCHMER, D., *et al*. (2010) Human formyl peptide receptor 2 senses highly pathogenic *Staphylococcus aureus*. *Cell Host Microbe,* **7** (6), 463-73.
KUMAR, A., *et al*. (2009) Critically ill patients with 2009 influenza A(H1N1) infection in Canada. *Jama,* **302** (17), 1872-9.
KUROKAWA, K., *et al*. (2009) The Triacylated ATP Binding Cluster Transporter Substrate-binding Lipoprotein of *Staphylococcus aureus* Functions as a Native Ligand for Toll-like Receptor 2. *J Biol Chem,* **284** (13), 8406-11.
KUROKAWA, K., *et al*. (2012) Novel bacterial lipoprotein structures conserved in low-GC content gram-positive bacteria are recognized by Toll-like receptor 2. *J Biol Chem,* **287** (16), 13170-81.
LAARMAN, A. J., *et al*. (2012) *Staphylococcus aureus* Staphopain A inhibits CXCR2-dependent neutrophil activation and chemotaxis. *Embo j,* **31** (17), 3607-19.
LAARMAN, A. J., *et al*. (2011) *Staphylococcus aureus* Metalloprotease Aureolysin Cleaves Complement C3 To Mediate Immune Evasion. *J. Immunol.,* **186** (11), 6445-6453.

LACY, P. (2006) Mechanisms of degranulation in neutrophils. *Allergy Asthma Clin Immunol,* **2** (3), 98-108.
LAM, S. H., *et al*. (2004) Development and maturation of the immune system in zebrafish, Danio rerio: a gene expression profiling, in situ hybridization and immunological study. *Dev Comp Immunol,* **28** (1), 9-28.
LAMBERT, P. A. (2005) Bacterial resistance to antibiotics: modified target sites. *Adv Drug Deliv Rev,* **57** (10), 1471-85.
LAN, L., *et al*. (2010) Golden pigment production and virulence gene expression are affected by metabolisms in *Staphylococcus aureus*. *J Bacteriol,* **192** (12), 3068-77.
LANGONE, J. J. (1982) Protein A of *Staphylococcus aureus* and related immunoglobulin receptors produced by streptococci and pneumonococci. *Advances in immunology,* **32**, 157.
LARSSON, J. T., *et al*. (2007) YjbH is a novel negative effector of the disulphide stress regulator, Spx, in Bacillus subtilis. *Mol Microbiol,* **66** (3), 669-84.
LEE, C. Y., *et al*. (1991) Construction of single-copy integration vectors for *Staphylococcus aureus*. *Gene,* **103** (1), 101-5.
LEE, L. Y. L., *et al*. (2004) Inhibition of complement activation by a secreted *Staphylococcus aureus* protein. *J. Infect. Dis.,* **190** (3), 571-579.
LENTINO, J. R., *et al*. (2008) New antimicrobial agents as therapy for resistant gram-positive cocci. *Eur J Clin Microbiol Infect Dis,* **27** (1), 3-15.
LEY, K., *et al*. (2007) Getting to the site of inflammation: the leukocyte adhesion cascade updated. *Nat Rev Immunol,* **7** (9), 678-89.
LIANG, X., *et al*. (2006) Inactivation of a two-component signal transduction system, SaeRS, eliminates adherence and attenuates virulence of *Staphylococcus aureus*. *Infect Immun,* **74** (8), 4655-65.
LIESCHKE, G. J., *et al*. (2001) Morphologic and functional characterization of granulocytes and macrophages in embryonic and adult zebrafish. *Blood,* **98** (10), 3087-96.
LILES, W. C., *et al*. (1996) Differential expression of Fas (CD95) and Fas ligand on normal human phagocytes: implications for the regulation of apoptosis in neutrophils. *J Exp Med,* **184** (2), 429-40.
LIN, B., *et al*. (2007) Acute phase response in zebrafish upon Aeromonas salmonicida and *Staphylococcus aureus* infection: striking similarities and obvious differences with mammals. *Mol Immunol,* **44** (4), 295-301.
LIPINSKA, U., *et al*. (2011) Panton-Valentine leukocidin does play a role in the early stage of *Staphylococcus aureus* skin infections: a rabbit model. *PLoS One,* **6** (8), e22864.
LIPSKY, B. A. (1997) Osteomyelitis of the foot in diabetic patients. *Clin Infect Dis,* **25** (6), 1318-26.
LIU, C. and CHAMBERS, H. F. (2003) *Staphylococcus aureus* with heterogeneous resistance to vancomycin: epidemiology, clinical significance, and critical assessment of diagnostic methods. *Antimicrob Agents Chemother,* **47** (10), 3040-5.
LIU, C., *et al*. (2008) A population-based study of the incidence and molecular epidemiology of methicillin-resistant *Staphylococcus aureus* disease in San Francisco, 2004-2005. *Clin Infect Dis,* **46** (11), 1637-46.
LIU, G. Y., *et al*. (2005) *Staphylococcus aureus* golden pigment impairs neutrophil killing and promotes virulence through its antioxidant activity. *J. Exp. Med.,* **202** (2), 209-215.
LIU, Q., *et al*. (2017) The ATP-Dependent Protease ClpP Inhibits Biofilm Formation by Regulating Agr and Cell Wall Hydrolase Sle1 in *Staphylococcus aureus*. *Front Cell Infect Microbiol,* **7**, 181.
LOFFLER, B., *et al*. (2010) *Staphylococcus aureus* panton-valentine leukocidin is a very potent cytotoxic factor for human neutrophils. *PLoS Pathog,* **6** (1), e1000715.
LONG, J., *et al*. (2016) Identification of disease-associated pathways in pancreatic cancer by integrating genome-wide association study and gene expression data. *Oncol Lett,* **12** (1), 537-543.
LONGWORTH, D. L. (2001) Microbial drug resistance and the roles of the new antibiotics. *Cleve Clin J Med,* **68** (6), 496-7, 501-2, 504.
LOOD, C., *et al*. (2016) Neutrophil extracellular traps enriched in oxidized mitochondrial DNA are interferogenic and contribute to lupus-like disease. *Nat Med,* **22** (2), 146-53.

LOWY, F. D. (1998) *Staphylococcus aureus* infections - Reply. *N. Engl. J. Med.,* **339** (27), 2026-2027.
LUO, H. R. and LOISON, F. (2008) Constitutive neutrophil apoptosis: mechanisms and regulation. *Am J Hematol,* **83** (4), 288-95.
MAIANSKI, N. A., *et al*. (2004) Functional characterization of mitochondria in neutrophils: a role restricted to apoptosis. *Cell Death Differ,* **11** (2), 143-53.
MALACHOWA, N. and DELEO, F. R. (2010) Mobile genetic elements of *Staphylococcus aureus*. *Cell Mol Life Sci,* **67** (18), 3057-71.
MALACHOWA, N., *et al*. (2012) *Staphylococcus aureus* leukotoxin GH promotes inflammation. *J Infect Dis,* **206** (8), 1185-93.
MALACHOWA, N., *et al*. (2013) *Staphylococcus aureus* leukotoxin GH promotes formation of neutrophil extracellular traps. *J Immunol,* **191** (12), 6022-9.
MALACHOWA, N., *et al*. (2011) Characterization of a *Staphylococcus aureus* Surface Virulence Factor That Promotes Resistance to Oxidative Killing and Infectious Endocarditis. *Infect. Immun.,* **79** (1), 342-352.
MALAWISTA, S. E., *et al*. (1992) Evidence for reactive nitrogen intermediates in killing of staphylococci by human neutrophil cytoplasts. A new microbicidal pathway for polymorphonuclear leukocytes. *J Clin Invest,* **90** (2), 631-6.
MANDELL, G. L. (1975) Catalase, superoxide dismutase, and virulence of *Staphylococcus aureus*. In vitro and in vivo studies with emphasis on staphylococcal-- leukocyte interaction. *The Journal of clinical investigation,* **55** (3), 561.
MANDERS, S. M. (1998) Toxin- mediated streptococcal and staphylococcal disease.) *J. Am. Acad. Dermatol.*
MANI, N., *et al*. (1993) Isolation and characterization of autolysis-defective mutants of *Staphylococcus aureus* created by Tn917-lacZ mutagenesis. *J Bacteriol,* **175** (5), 1493-9.
MANOLIO, T. A. (2010) Genomewide association studies and assessment of the risk of disease. *N Engl J Med,* **363** (2), 166-76.
MARCHESE, A., *et al*. (2000) Heterogeneous vancomycin resistance in methicillin-resistant *Staphylococcus aureus* strains isolated in a large Italian hospital. *J Clin Microbiol,* **38** (2), 866-9.
MARTIN, A., *et al*. (2008) Pore loops of the AAA+ ClpX machine grip substrates to drive translocation and unfolding. *Nat Struct Mol Biol,* **15** (11), 1147-51.
MAZMANIAN, S. K., *et al*. (2001) Sortase-catalysed anchoring of surface proteins to the cell wall of *Staphylococcus aureus*. *Mol Microbiol,* **40** (5), 1049-57.
MCCLINTOCK, B. (1948) *Carnegie Institute of Washington Yearbook.*
MCDOUGAL, L. K., *et al*. (2010) Emergence of resistance among USA300 methicillin-resistant *Staphylococcus aureus* isolates causing invasive disease in the United States. *Antimicrob Agents Chemother,* **54** (9), 3804-11.
MCGANN, L. E., *et al*. (1988) Manifestations of cell damage after freezing and thawing. *Cryobiology,* **25** (3), 178-85.
MCGUINNESS, W. A., *et al*. (2017) Vancomycin Resistance in *Staphylococcus aureus*. *Yale J Biol Med,* **90** (2), 269-281.
MCKERCHER, S. R., *et al*. (1996) Targeted disruption of the PU.1 gene results in multiple hematopoietic abnormalities. *Embo j,* **15** (20), 5647-58.
MCLUCKIE A (2009) In) *Respiratory disease and its management.* New York: Springer, p. 51.
MEDIAVILLA, J. R., *et al*. (2012) Global epidemiology of community-associated methicillin resistant *Staphylococcus aureus* (CA-MRSA). *Curr Opin Microbiol,* **15** (5), 588-95.
MEI, J. M., *et al*. (1997) Identification of *Staphylococcus aureus* virulence genes in a murine model of bacteraemia using signature-tagged mutagenesis. *Mol Microbiol,* **26** (2), 399-407.
MEZA-CERVANTEZ, P., *et al*. (2011) Pyruvate:ferredoxin oxidoreductase (PFO) is a surface-associated cell-binding protein in Trichomonas vaginalis and is involved in trichomonal adherence to host cells. *Microbiology,* **157** (Pt 12), 3469-82.
MICHALIK, S., *et al*. (2012) Life and death of proteins: a case study of glucose-starved *Staphylococcus aureus*. *Mol Cell Proteomics,* **11** (9), 558-70.

MICHEL, A., *et al*. (2006) Global regulatory impact of ClpP protease of *Staphylococcus aureus* on regulons involved in virulence, oxidative stress response, autolysis, and DNA repair. *J Bacteriol,* **188** (16), 5783-96.
MILES, A. A., *et al*. (1938) The estimation of the bactericidal power of the blood. *J Hyg (Lond),* **38** (6), 732-49.
MIOULANE, M., *et al*. (2012) Development of high content imaging methods for cell death detection in human pluripotent stem cell-derived cardiomyocytes. *J Cardiovasc Transl Res,* **5** (5), 593-604.
MISHRA, N. N., *et al*. (2011) Carotenoid- Related Alteration of Cell Membrane Fluidity Impacts *Staphylococcus aureus* Susceptibility to Host Defense Peptides. *Antimicrob. Agents Chemother.,* **55** (2), 526-531.
MONTGOMERY, C. P., *et al*. (2008) Comparison of virulence in community-associated methicillin-resistant *Staphylococcus aureus* pulsotypes USA300 and USA400 in a rat model of pneumonia. *J Infect Dis,* **198** (4), 561-70.
MONTGOMERY, C. P., *et al*. (2010) Importance of the global regulators Agr and SaeRS in the pathogenesis of CA-MRSA USA300 infection. *PLoS One,* **5** (12), e15177.
MOORE, K. L., *et al*. (1995) P-selectin glycoprotein ligand-1 mediates rolling of human neutrophils on P-selectin. *J Cell Biol,* **128** (4), 661-71.
MORGAN, M. J., *et al*. (2008) TNFalpha and reactive oxygen species in necrotic cell death. *Cell Res,* **18** (3), 343-9.
MORGAN, M. S. (2007) Diagnosis and treatment of Panton–Valentine leukocidin (PVL)-associated staphylococcal pneumonia. *International Journal of Antimicrobial Agents,* **30** (4), 289-296.
MOULDING, D. A., *et al*. (2001) BCL-2 family expression in human neutrophils during delayed and accelerated apoptosis. *J Leukoc Biol,* **70** (5), 783-92.
MURPHY, J. M. and VINCE, J. E. (2015) Post-translational control of RIPK3 and MLKL mediated necroptotic cell death. *F1000Res,* **4**.
MURPHY, P. (1976) *The Neutrophil.* Plenum Medical Book Company

New York and London
NAGELKERKE, S. Q., *et al*. (2014) Failure to detect functional neutrophil B helper cells in the human spleen. *PLoS One,* **9** (2), e88377.
NAIMI, T. S., *et al*. (2003) Comparison of community- and health care-associated methicillin-resistant *Staphylococcus aureus* infection. *Jama,* **290** (22), 2976-84.
NAKANO, S., *et al*. (2003) Spx-dependent global transcriptional control is induced by thiol-specific oxidative stress in Bacillus subtilis. *Proc Natl Acad Sci U S A,* **100** (23), 13603-8.
NAKAYAMA, H., *et al*. (2012) Lipoproteins in bacteria: structures and biosynthetic pathways. *Febs j,* **279** (23), 4247-68.
NELSON, C. L., *et al*. (2014) A genome-wide association study of variants associated with acquisition of *Staphylococcus aureus* bacteremia in a healthcare setting. *BMC Infect Dis,* **14**, 83.
NICHOLS, R. L. and RAAD, I. I. (1999) Management of bacterial complications in critically ill patients: surgical wound and catheter-related infections. *Diagnostic Microbiology and Infectious Disease,* **33** (2), 121-130.
NORIS, M. and REMUZZI, G. (2013) Overview of complement activation and regulation. *Semin Nephrol,* **33** (6), 479-92.
NOVICK, R. P. (2003a) Autoinduction and signal transduction in the regulation of staphylococcal virulence. *Mol Microbiol,* **48** (6), 1429-49.
NOVICK, R. P. (2003b) Mobile genetic elements and bacterial toxinoses: the superantigen-encoding pathogenicity islands of *Staphylococcus aureus*. *Plasmid,* **49** (2), 93-105.
NOVICK, R. P., *et al*. (1993) Synthesis of staphylococcal virulence factors is controlled by a regulatory RNA molecule. *Embo j,* **12** (10), 3967-75.
NUNOSHIBA, T., *et al*. (1995) Roles of nitric oxide in inducible resistance of Escherichia coli to activated murine macrophages. *Infect Immun,* **63** (3), 794-8.
NYGAARD, T. K., *et al*. (2010) SaeR binds a consensus sequence within virulence gene promoters to advance USA300 pathogenesis. *J Infect Dis,* **201** (2), 241-54.

OOGAI, Y., *et al*. (2011) Expression of virulence factors by *Staphylococcus aureus* grown in serum. *Appl Environ Microbiol,* **77** (22), 8097-105.
OTTER, J. A. and FRENCH, G. L. (2010) Molecular epidemiology of community-associated meticillin-resistant *Staphylococcus aureus* in Europe. *Lancet Infect Dis,* **10** (4), 227-39.
OTTO, M. (2014) Phenol-soluble modulins. *Int J Med Microbiol,* **304** (2), 164-9.
PALMQVIST, N., *et al*. (2002) Protein A is a virulence factor in *Staphylococcus aureus* arthritis and septic death. *Microb Pathog,* **33** (5), 239-49.
PAPAYANNOPOULOS, V., *et al*. (2010) Neutrophil elastase and myeloperoxidase regulate the formation of neutrophil extracellular traps. *J Cell Biol,* **191** (3), 677-91.
PESCHEL, A., *et al*. (2001) *Staphylococcus aureus* resistance to human defensins and evasion of neutrophil killing via the novel virulence factor MprF is based on modification of membrane lipids with l-lysine. *J Exp Med,* **193** (9), 1067-76.
PFIZER (2007) Zyvox (Linezolid) Datasheet.).
PHE, P. H. E. (2017) *Staphylococcus aureus* (MRSA and

MSSA) bacteraemia mandatory reports

2016/17.).
PHILLIPSON, M., *et al*. (2006) Intraluminal crawling of neutrophils to emigration sites: a molecularly distinct process from adhesion in the recruitment cascade. *J Exp Med,* **203** (12), 2569-75.
PRAJSNAR, T. K., *et al*. (2008) A novel vertebrate model of *Staphylococcus aureus* infection reveals phagocyte-dependent resistance of zebrafish to non-host specialized pathogens. *Cell Microbiol,* **10** (11), 2312-25.
PRAJSNAR, T. K., *et al*. (2012) A privileged intraphagocyte niche is responsible for disseminated infection of *Staphylococcus aureus* in a zebrafish model. *Cell Microbiol,* **14** (10), 1600-19.
PRAT, C., *et al*. (2009) A homolog of formyl peptide receptor-like 1 (FPRL1) inhibitor from *Staphylococcus aureus* (FPRL1 inhibitory protein) that inhibits FPRL1 and FPR. *J Immunol,* **183** (10), 6569-78.
PRINCE, L. R., *et al*. (2012) *Staphylococcus aureus* induces eosinophil cell death mediated by alpha-hemolysin. *PLoS One,* **7** (2), e31506.
QUIE, P. G., *et al*. (1967) In vitro bactericidal capacity of human polymorphonuclear leukocytes: diminished activity in chronic granulomatous disease of childhood. *J Clin Invest,* **46** (4), 668-79.
RAFAI, M., *et al*. (2013) Evolution of a fatal septic arthritis caused by a Panton-Valentine leukocidin (PVL)-producing *Staphylococcus aureus* strain. *Joint Bone Spine,* **80** (5), 525-7.
RATNARAJA, N. V. and HAWKEY, P. M. (2008) Current challenges in treating MRSA: what are the options? *Expert Rev Anti Infect Ther,* **6** (5), 601-18.
RECSEI, P., *et al*. (1986) Regulation of exoprotein gene expression in *Staphylococcus aureus* by agar. *Mol Gen Genet,* **202** (1), 58-61.
RENZONI, A., *et al*. (2009) Identification by genomic and genetic analysis of two new genes playing a key role in intermediate glycopeptide resistance in *Staphylococcus aureus*. *Antimicrob Agents Chemother,* **53** (3), 903-11.
RHODES, J., *et al*. (2005) Interplay of pu.1 and gata1 determines myelo-erythroid progenitor cell fate in zebrafish. *Dev Cell,* **8** (1), 97-108.
RIGBY, K. M. and DELEO, F. R. (2012) Neutrophils in innate host defense against *Staphylococcus aureus* infections. *Semin Immunopathol,* **34** (2), 237-59.
RODRIGUEZ-FERNANDEZ, A., *et al*. (2013) Eosinophil as a protective cell in S. aureus ventilator-associated pneumonia. *Mediators Inflamm,* **2013**, 152943.
ROGER, T. and CALANDRA, T. (2009) TLR2-mediated neutrophil depletion exacerbates bacterial sepsis. *Proc Natl Acad Sci U S A,* **106** (17), 6889-90.
ROOIJAKKERS, S. H., *et al*. (2005a) Immune evasion by a staphylococcal complement inhibitor that acts on C3 convertases. *Nat Immunol,* **6** (9), 920-7.
ROOIJAKKERS, S. H., *et al*. (2005b) Staphylococcal innate immune evasion. *Trends Microbiol,* **13** (12), 596-601.
ROSEN, H. and KLEBANOFF, S. J. (1979) Bactericidal activity of a superoxide anion-generating system. A model for the polymorphonuclear leukocyte. *J Exp Med,* **149** (1), 27-39.

ROSENZWEIG, S. D. and HOLLAND, S. M. (2004) Phagocyte immunodeficiencies and their infections. *J Allergy Clin Immunol,* **113** (4), 620-6.
SABROE, I., *et al*. (2005) The role of Toll-like receptors in the regulation of neutrophil migration, activation, and apoptosis. *Clin Infect Dis,* **41 Suppl 7**, S421-6.
SARALAHTI, A., *et al*. (2014) Adult zebrafish model for pneumococcal pathogenesis. *Dev Comp Immunol,* **42** (2), 345-53.
SASAKI, K., *et al*. (1995) Accumulation and massive cell death of polymorphonuclear neutrophils in the developing bone marrow of the mouse: a histological study. *Acta Anat (Basel),* **153** (2), 111-8.
SAVIJOKI, K., *et al*. (2006) Proteolytic systems of lactic acid bacteria. *Appl Microbiol Biotechnol,* **71** (4), 394-406.
SAWATZKY, D. A., *et al*. (2006) The involvement of the apoptosis-modulating proteins ERK 1/2, Bcl-xL and Bax in the resolution of acute inflammation in vivo. *Am J Pathol,* **168** (1), 33-41.
SCHMALER, M., *et al*. (2010) Staphylococcal lipoproteins and their role in bacterial survival in mice. *Int J Med Microbiol,* **300** (2-3), 155-60.
SCHULZE-OSTHOFF, K., *et al*. (1998) Apoptosis signaling by death receptors. *Eur J Biochem,* **254** (3), 439-59.
SEELEANG, K., *et al*. (2013) Outpatient Management of Skin and Soft Tissue Infections Associated With Community-Associated Methicillin-Resistant *Staphylococcus aureus*: An Evidence-Based Approach. *The Journal for Nurse Practitioners,* **9** (9), 600-605.
SEGAL, A. W. (2005) How neutrophils kill microbes. *Annu Rev Immunol,* **23**, 197-223.
SEGAL, A. W., *et al*. (1980) Kinetics of fusion of the cytoplasmic granules with phagocytic vacuoles in human polymorphonuclear leukocytes. Biochemical and morphological studies. *J Cell Biol,* **85** (1), 42-59.
SEGAL, A. W., *et al*. (1981) The respiratory burst of phagocytic cells is associated with a rise in vacuolar pH. *Nature,* **290** (5805), 406-9.
SHAHMIRZADI, S. V., *et al*. (2016) Evaluation of *Staphylococcus aureus* Lipoproteins: Role in Nutritional Acquisition and Pathogenicity. *Front Microbiol,* **7**, 1404.
SHARFF, K. A., *et al*. (2013) Clinical management of septic arthritis. *Curr Rheumatol Rep,* **15** (6), 332.
SHAW, L. N., *et al*. (2005) Cytoplasmic control of premature activation of a secreted protease zymogen: deletion of staphostatin B (SspC) in *Staphylococcus aureus* 8325-4 yields a profound pleiotropic phenotype. *J Bacteriol,* **187** (5), 1751-62.
SHELEF, M. A., *et al*. (2013) Neutrophil migration: moving from zebrafish models to human autoimmunity. *Immunol Rev,* **256** (1), 269-81.
SHEPPARD, S. K., *et al*. (2013) Genome-wide association study identifies vitamin B5 biosynthesis as a host specificity factor in Campylobacter. *Proc Natl Acad Sci U S A,* **110** (29), 11923-7.
SIBBALD, M. J., *et al*. (2006) Mapping the pathways to staphylococcal pathogenesis by comparative secretomics. *Microbiol Mol Biol Rev,* **70** (3), 755-88.
SIEPRAWSKA-LUPA, M., *et al*. (2004) Degradation of human antimicrobial peptide LL-37 by *Staphylococcus aureus*-derived proteinases. *Antimicrob Agents Chemother,* **48** (12), 4673-9.
SOCHA, A. M., *et al*. (2010) Diversity-oriented synthesis of cyclic acyldepsipeptides leads to the discovery of a potent antibacterial agent. *Bioorg Med Chem,* **18** (20), 7193-202.
SONG, H. O. (2016) Influence of 120 kDa Pyruvate:Ferredoxin Oxidoreductase on Pathogenicity of Trichomonas vaginalis. *Korean J Parasitol,* **54** (1), 71-4.
SOWASH, M. G. and UHLEMANN, A. C. (2014) Community-associated methicillin-resistant *Staphylococcus aureus* case studies. *Methods Mol Biol,* **1085**, 25-69.
SPAAN, A. N., *et al*. (2013a) The staphylococcal toxin Panton-Valentine Leukocidin targets human C5a receptors. *Cell Host Microbe,* **13** (5), 584-94.
SPAAN, A. N., *et al*. (2013b) Neutrophils versus *Staphylococcus aureus*: a biological tug of war. *Annu Rev Microbiol,* **67**, 629-50.
STAPELS, D. A., *et al*. (2014) *Staphylococcus aureus* secretes a unique class of neutrophil serine protease inhibitors. *Proc Natl Acad Sci U S A,* **111** (36), 13187-92.
STARNES, T. W. and HUTTENLOCHER, A. (2012) Neutrophil reverse migration becomes transparent with zebrafish. *Adv Hematol,* **2012**, 398640.

STEFANI, S., *et al*. (2012) Meticillin-resistant *Staphylococcus aureus* (MRSA): global epidemiology and harmonisation of typing methods. *Int J Antimicrob Agents,* **39** (4), 273-82.
STROEHER, U. H., *et al*. (2003) Mutation of luxS of Streptococcus pneumoniae affects virulence in a mouse model. *Infect Immun,* **71** (6), 3206-12.
SUMMERTON, J. and WELLER, D. (1997) Morpholino antisense oligomers: design, preparation, and properties. *Antisense Nucleic Acid Drug Dev,* **7** (3), 187-95.
SUREWAARD, B. G., *et al*. (2013) Staphylococcal alpha-phenol soluble modulins contribute to neutrophil lysis after phagocytosis. *Cell Microbiol,* **15** (8), 1427-37.
SUTCLIFFE, I. C. and RUSSELL, R. R. (1995) Lipoproteins of gram-positive bacteria. *J Bacteriol,* **177** (5), 1123-8.
SUZUKI, M., *et al*. (2016) A genome-wide association study identifies a horizontally transferred bacterial surface adhesin gene associated with antimicrobial resistant strains. *Sci Rep,* **6**, 37811.
SWAIM, L. E., *et al*. (2006) Mycobacterium marinum infection of adult zebrafish causes caseating granulomatous tuberculosis and is moderated by adaptive immunity. *Infect Immun,* **74** (11), 6108-17.
TENG, T. S., *et al*. (2017) Neutrophils and Immunity: From Bactericidal Action to Being Conquered. *J Immunol Res,* **2017**, 9671604.
TENOVER and GAYNES (2000) *Gram-positive pathogens.* Washington, D.C.: Washington, D.C. : ASM Press, c2000.
THAMMAVONGSA, V., *et al*. (2009) *Staphylococcus aureus* synthesizes adenosine to escape host immune responses. *J Exp Med,* **206** (11), 2417-27.
THAMMAVONGSA, V., *et al*. (2015) Staphylococcal manipulation of host immune responses. *Nat Rev Microbiol,* **13** (9), 529-43.
THAMMAVONGSA, V., *et al*. (2013) *Staphylococcus aureus* degrades neutrophil extracellular traps to promote immune cell death. *Science,* **342** (6160), 863-6.
THOENDEL, M., *et al*. (2011) Peptide signaling in the staphylococci. *Chem Rev,* **111** (1), 117-51.
THURLOW, L. R., *et al*. (2011) *Staphylococcus aureus* biofilms prevent macrophage phagocytosis and attenuate inflammation in vivo. *J Immunol,* **186** (11), 6585-96.
THURLOW, L. R., *et al*. (2012) Virulence strategies of the dominant USA300 lineage of community-associated methicillin-resistant *Staphylococcus aureus* (CA-MRSA). *FEMS Immunol Med Microbiol,* **65** (1), 5-22.
TIETZ, A., *et al*. (2005) Transatlantic spread of the USA300 clone of MRSA. In) *N Engl J Med.* Vol. 353. United States: pp. 532-3.
TORRACA, V., *et al*. (2014) Macrophage-pathogen interactions in infectious diseases: new therapeutic insights from the zebrafish host model. *Dis Model Mech,* **7** (7), 785-97.
TRAKULSOMBOON, S., *et al*. (2001) First report of methicillin-resistant *Staphylococcus aureus* with reduced susceptibility to vancomycin in Thailand. *J Clin Microbiol,* **39** (2), 591-5.
TREDE, N. S., *et al*. (2001) Fishing for lymphoid genes. *Trends Immunol,* **22** (6), 302-7.
TRUSCOTT, K. N., *et al*. (2011) Unfolded protein responses in bacteria and mitochondria: a central role for the ClpXP machine. *IUBMB Life,* **63** (11), 955-63.
TSAI, M., *et al*. (2007) Substrate and product complexes of Escherichia coli adenylosuccinate lyase provide new insights into the enzymatic mechanism. *J Mol Biol,* **370** (3), 541-54.
TSIODRAS, S., *et al*. (2001) Linezolid resistance in a clinical isolate of *Staphylococcus aureus*. In) *Lancet.* Vol. 358. England: pp. 207-8.
TSUJI, B. T., *et al*. (2007) Community- and health care-associated methicillin-resistant *Staphylococcus aureus*: a comparison of molecular epidemiology and antimicrobial activities of various agents. *Diagnostic Microbiology and Infectious Disease,* **58** (1), 41-47.
TUAZON, C. U., *et al*. (1975) *Staphylococcus aureus* among insulin-injecting diabetic patients. An increased carrier rate. *Jama,* **231** (12), 1272.
TUAZON, C. U. and SHEAGREN, J. N. (1974) Increased rate of carriage of *Staphylococcus aureus* among narcotic addicts. *J Infect Dis,* **129** (6), 725-7.
VAITKUS, M., *et al*. (2013) Reactive oxygen species in peripheral blood and sputum neutrophils during bacterial and nonbacterial acute exacerbation of chronic obstructive pulmonary disease. *Inflammation,* **36** (6), 1485-93.

VALEVA, A., *et al*. (1997) Transmembrane beta-barrel of staphylococcal alpha-toxin forms in sensitive but not in resistant cells. *Proc Natl Acad Sci U S A,* **94** (21), 11607-11.
VALOUR, F., *et al*. (2013) [*Staphylococcus aureus* broncho-pulmonary infections]. *Rev Pneumol Clin,* **69** (6), 368-82.
VAN DER VAART, M., *et al*. (2012) Pathogen recognition and activation of the innate immune response in zebrafish. *Adv Hematol,* **2012**, 159807.
VARDAKAS, K. Z., *et al*. (2013) Incidence, characteristics, and outcomes of patients with bone and joint infections due to community-associated methicillin-resistant *Staphylococcus aureus*: a systematic review. *Eur J Clin Microbiol Infect Dis,* **32** (6), 711-21.
VEDADI, M., *et al*. (2007) Genome-scale protein expression and structural biology of Plasmodium falciparum and related Apicomplexan organisms. *Mol Biochem Parasitol,* **151** (1), 100-10.
VENDEVILLE, A., *et al*. (2005) Making 'sense' of metabolism: autoinducer-2, LuxS and pathogenic bacteria. *Nat Rev Microbiol,* **3** (5), 383-96.
VENTURA, C. L., *et al*. (2010) Identification of a novel *Staphylococcus aureus* two-component leukotoxin using cell surface proteomics. *PLoS One,* **5** (7), e11634.
VESTERGAARD, M., *et al*. (2016) Genome-Wide Identification of Antimicrobial Intrinsic Resistance Determinants in *Staphylococcus aureus*. *Front Microbiol,* **7**, 2018.
VILHELMSSON, O. and MILLER, K. J. (2002) Synthesis of pyruvate dehydrogenase in *Staphylococcus aureus* is stimulated by osmotic stress. *Appl Environ Microbiol,* **68** (5), 2353-8.
VIRREIRA WINTER, S., *et al*. (2016) Genome-wide CRISPR screen reveals novel host factors required for *Staphylococcus aureus* alpha-hemolysin-mediated toxicity. *Sci Rep,* **6**, 24242.
VON EIFF, C., *et al*. (2003) In vitro activity of recombinant lysostaphin against *Staphylococcus aureus* isolates from anterior nares and blood. *Antimicrobial agents and chemotherapy,* **47** (11), 3613.
VOYICH, J. M., *et al*. (2005) Insights into mechanisms used by *Staphylococcus aureus* to avoid destruction by human neutrophils. *J Immunol,* **175** (6), 3907-19.
VOYICH, J. M., *et al*. (2009) The SaeR/S gene regulatory system is essential for innate immune evasion by *Staphylococcus aureus*. *J Infect Dis,* **199** (11), 1698-706.
WALENKAMP, A. M., *et al*. (2009) Staphylococcal superantigen-like 10 inhibits CXCL12-induced human tumor cell migration. *Neoplasia,* **11** (4), 333-44.
WALPORT, M. J. (2001) Complement. Second of two parts. *N Engl J Med,* **344** (15), 1140-4.
WANG, R., *et al*. (2007) Identification of novel cytolytic peptides as key virulence determinants for community-associated MRSA. *Nat Med,* **13** (12), 1510-4.
WANG, W. K., *et al*. (2009) [Analysis of the molecular epidemiology and distribution of pathogenic bacteria in burn wards of Ruijin Hospital from 2004 to 2006]. *Zhonghua Shao Shang Za Zhi,* **25** (2), 94-7.
WARREN, C. A., *et al*. (2012) Amixicile, a novel inhibitor of pyruvate: ferredoxin oxidoreductase, shows efficacy against Clostridium difficile in a mouse infection model. *Antimicrob Agents Chemother,* **56** (8), 4103-11.
WEISS, E. C., *et al*. (2009) Impact of sarA on daptomycin susceptibility of *Staphylococcus aureus* biofilms in vivo. *Antimicrob Agents Chemother,* **53** (10), 4096-102.
WENZEL, R. P. and PERL, T. M. (1995) The significance of nasal carriage of *Staphylococcus aureus* and the incidence of postoperative wound infection. *J Hosp Infect,* **31** (1), 13-24.
WESTERFIELD, M. (2000) *The zebrafish book: A guide for the laboratory use of zebrafish.*. University of Oregon Press, Eugene.
WONG, S. S., *et al*. (2000) Bacteremia due to *Staphylococcus aureus* with reduced susceptibility to vancomycin. *Diagn Microbiol Infect Dis,* **36** (4), 261-8.
WOODS, I. G., *et al*. (2000) A comparative map of the zebrafish genome. *Genome Res,* **10** (12), 1903-14.
WUNDERINK, R. G. (2013) How Important is Methicillin-Resistant *Staphylococcus aureus* as a Cause of Community-Acquired Pneumonia and What is Best Antimicrobial Therapy? *Infectious Disease Clinics of North America,* **27** (1), 177-188.
XU, L., *et al*. (2006) Role of the luxS quorum-sensing system in biofilm formation and virulence of Staphylococcus epidermidis. *Infect Immun,* **74** (1), 488-96.
YANG, Y., *et al*. (2015) Programmed cell death and its role in inflammation. *Mil Med Res,* **2**, 12.

YARWOOD, J. M., *et al*. (2002) Characterization and expression analysis of *Staphylococcus aureus* pathogenicity island 3. Implications for the evolution of staphylococcal pathogenicity islands. *J Biol Chem,* **277** (15), 13138-47.
YE, F., *et al*. (2016) The development of small-molecule modulators for ClpP protease activity. *Mol Biosyst,* **13** (1), 23-31.
YIPP, B. G., *et al*. (2012) Infection- induced NETosis is a dynamic process involving neutrophil multitasking in vivo. *Nature medicine,* **18** (9), 1386.
YOONG, P. and PIER, G. B. (2012) Immune-activating properties of Panton-Valentine leukocidin improve the outcome in a model of methicillin-resistant *Staphylococcus aureus* pneumonia. *Infect Immun,* **80** (8), 2894-904.
YOUSEFI, S. and SIMON, H. U. (2016) NETosis - Does It Really Represent Nature's "Suicide Bomber"? *Front Immunol,* **7**, 328.
YU, V. L., *et al*. (1986) *Staphylococcus aureus* nasal carriage and infection in patients on hemodialysis. Efficacy of antibiotic prophylaxis. *N Engl J Med,* **315** (2), 91-6.
ZHAO, B. B., *et al*. (2016) ClpP-deletion impairs the virulence of Legionella pneumophila and the optimal translocation of effector proteins. *BMC Microbiol,* **16** (1), 174.
ZHU, F., *et al*. (2015) Role of JAK-STAT signaling in maturation of phagosomes containing *Staphylococcus aureus*. *Sci Rep,* **5**, 14854.